
Electronic Thesis and Dissertation Repository

8-12-2016 12:00 AM

A Long-Term Neuroepigenomic Profile of Prenatal Alcohol Exposure

Benjamin I. Laufer
The University of Western Ontario

Supervisor
Shiva M. Singh
The University of Western Ontario

Graduate Program in Biology

A thesis submitted in partial fulfillment of the requirements for the degree in Doctor of Philosophy

© Benjamin I. Laufer 2016

Follow this and additional works at: <https://ir.lib.uwo.ca/etd>

 Part of the Genetics and Genomics Commons

Recommended Citation

Laufer, Benjamin I., "A Long-Term Neuroepigenomic Profile of Prenatal Alcohol Exposure" (2016).
Electronic Thesis and Dissertation Repository. 3913.
<https://ir.lib.uwo.ca/etd/3913>

This Dissertation/Thesis is brought to you for free and open access by Scholarship@Western. It has been accepted for inclusion in Electronic Thesis and Dissertation Repository by an authorized administrator of Scholarship@Western. For more information, please contact wlsadmin@uwo.ca.

Abstract

Fetal Alcohol Spectrum Disorders (FASD) represent the largest preventable cause of cognitive deficits in the western world. The mechanism(s) of how prenatal alcohol exposure (PAE) results in FASD remain unknown. Towards this end, mouse models of PAE have successfully recreated endophenotypes that are characteristic of FASD. This doctoral thesis examines the long-term epigenomic alterations associated with PAE. I have examined both mice with PAE and human patients with FASD.

In the first set of experiments, mice with PAE and matched controls were raised to adulthood and then their whole brains were examined for alterations to gene expression, non-coding RNA (ncRNA) expression, and DNA methylation. Long-term alterations were observed in genes related to neurodevelopment, cellular signaling, and immune processes. Furthermore, there was an enrichment for alterations to genomically imprinted clusters of ncRNA and genes related to PTEN/PI3K/AKT/mTOR signaling.

In the second set of experiments, buccal epithelial swabs were collected from young children with FASD and matched controls. Children from a discovery cohort were examined for alterations to DNA methylation, which revealed changes to genes involved in neurodevelopment and synaptic signaling as well as hippo signaling. Select candidates (*COLEC11* and *HTT*) were confirmed by sodium bisulfite pyrosequencing. Examination of a replication cohort revealed that while similar pathways are altered, the effect is not identical and that sex and age may alter the methylation profile. A larger group of children, representative of the general population, were then analyzed using a targeted sodium bisulfite next-generation sequencing panel and pyrosequencing. No single gene examined was found to be consistently affected in all FASD children.

Finally, the mouse and human results were compared to identify alterations to shared loci, ontologies, and pathways. The clustered protocadherins, which are involved in generating individual neuronal identity, showed increased DNA methylation in both species. Together, the results suggest that a shared DNA methylation profile related to neurodevelopment is present in both the brains of adult mice and the buccal epithelial swabs of young children with PAE. These results may be used in future functional studies of candidate loci as well as towards the development of much needed diagnostics and precision medicine.

Keywords: Epigenomics, Epigenetics, Fetal Alcohol Spectrum Disorders (FASD), Prenatal Alcohol Exposure, DNA methylation, non-coding RNA (ncRNA), Neurodevelopment, Microarray, Psychiatry, Neuroscience

Co-Authorship

The contents of this thesis contain modified portions of published manuscripts, in which I (B.I.L.) was first author. I contributed to sample collection and preparation, performed the primary experiments and analysis, and wrote the manuscript alongside Dr. Shiva M. Singh.

Chapter 2 contains material from a published manuscript entitled “Long-lasting alterations to DNA methylation and ncRNAs could underlie the effects of fetal alcohol exposure in mice.” This manuscript was published in *Disease Models & Mechanisms* on April 10, 2013 and co-authored by Katarzyna Mantha, Morgan L Kleiber, Eric J Diehl, Sean M F Addison, and Shiva M Singh. B.I.L., K.M., M.L.K. and E.J.D. raised the mice, performed the experimental interventions and extracted the RNA. B.I.L., S.M.F.A., and E.J.D. designed and performed the qPCR experiments. This manuscript was published under an open access CC BY 3.0 license.

Chapters 3 and 4 contain material from a published manuscript, entitled “Associative DNA methylation changes in children with prenatal alcohol exposure.” This manuscript was published in *Epigenomics* on July 16 2015 and co-authored by Joachim Kapalanga, Christina A Castellani, Eric J Diehl, Liying Yan, and Shiva M Singh. The children were diagnosed by J.K. (M.D./Ph.D.) and under his care swabs were collected and matched to controls. Human DNA isolation and purification was done by B.I.L, C.C., and E.J.D. All bioinformatic analysis was done by B.I.L. L.Y. designed and carried out the pyrosequencing assays. J.K. provided intellectual contributions to the writing of the manuscript. This manuscript was published under an open access CC BY-NC-ND 4.0 license and thus permission to use a modified version in this thesis was obtained from the publisher, which is provided in Appendix L.

Epigraph

"We might use the name 'epigenetics' for such studies, thus emphasizing their relation to the concepts, so strongly favourable to the classical theory of epigenesis, which have been reached by the experimental embryologists. We certainly need to remember that between genotype and phenotype, and connecting them to each other, there lies a whole complex of developmental processes. It is convenient to have a name for this complex: 'epigenotype' seems suitable."

- Conrad Hal Waddington (*The Epigenotype. Endeavour*, 1942).

Acknowledgements

I would like to thank my Supervisor, Dr. Shiva Singh, for his mentorship, patience, and support throughout my graduate studies. He has provided me with a number of diverse research, teaching, and communication opportunities that have enabled the success of this thesis and my interest in epigenetics. Furthermore, I would also like to acknowledge the members of the Singh Lab, past and present, for their support and training. I am particularly grateful to Eric Chater-Diehl, Dr. Christina Castellani, Dr. Katarzyna Mantha, Dr. Melkaye Melka, Bonnie Alberry, Aniruddho Chokroborty-Hoque, and Randa Stringer for their support. I would like to thank Dr. Joachim Kapalanga for his informal mentorship and determination, which enabled the clinical collaboration critical to this thesis. I am also thankful to the children and families who participated in this research.

I am appreciative of my advisors Dr. Kathleen Hill and Dr. Anthony Percival-Smith for their guidance throughout the milestones of this thesis. In addition, I would also like to thank David Carter from the London Regional Genomics Centre for his assistance with expression arrays. I am also appreciative of Dr. Liying Yan and the team at EpigenDx for their expertise with next-generation sequencing and insight into biomarker validation. Furthermore, I would like to thank Peter Jozsi and the rest of EpiGenie for their support and encouragement with scientific communication and knowledge.

This thesis also would not have been possible without the support of my family and friends. I am particularly grateful for the love, support, and sacrifices of my wife, Kristin, who has taught me much about writing and life. I would also like to thank my grandparents, Arthur and Loretta Lundy, for their support and encouragement to pursue scientific research. I am also thankful of the support from my in-laws Elaine and Darrin, as well as my brother Joshua, aunt Ellen, cousins Matt and Trevor, and Uncle Jamie. I would further like to thank my friend Ryan Guterman for the scientific comradery throughout the years. I am also appreciative of the long-term support of my friends Michael Weisbrot, Jonathan Smith, David Goldberg, Jordan Novack, Justin Shamis, and Greg Turk. Finally, I would like to thank all the faculty, administrators, and staff in the Department of Biology at the University of Western Ontario who have helped me throughout the years.

Funding Acknowledgements

This work was supported through grants from Natural Sciences and Engineering Research Council of Canada (NSERC) and the Canadian Institute of Health Research (CIHR).

I would like to thank the NSERC for a scholarship through the postgraduate scholarship doctoral (PGS D) program and the government of Ontario for their support through an Ontario Graduate Scholarship (OGS).

Table of Contents

Abstract	II
Keywords	III
Co-Authorship.....	IV
Epigraph.....	V
Acknowledgements.....	VI
Funding Acknowledgements	VII
Table of Contents.....	VIII
List of Tables	XI
Table of Figures	XII
List of Appendices	XIII
List of Abbreviations	XIV
Chapter 1 – Introduction.....	1
1.1 Prenatal Alcohol Exposure	1
1.1.1 PAE Endophenotypes are Associated with Altered Neurodevelopment	2
1.1.2 PAE Alters Short-Term and Long-Term Gene Expression	5
1.2 Epigenetic Mechanisms May Underlie the Altered Gene Expression of PAE.....	8
1.2.1 PAE Alters Histone Post-Translational Modifications	9
1.2.2 PAE Alters Non-Coding RNA Expression	11
1.2.3 PAE Alters DNA Methylation at Specific Genomic Loci	13
1.2.4 PAE May Alter the Epigenetic Landscape of Neurodevelopment	17
1.2.4.1 Genomic Imprinting.....	19
1.2.4.2 Systems Biology Approaches	20
<i>Hypothesis</i>	21
<i>Objectives</i>	21
1.3 References	22
Chapter 2 – Exploration Long-Term Alterations to the Epigenome of a PAE Mouse Model	33
2.1 Overview	33
2.2 Introduction	33
2.3 Materials & Methods	37
2.3.1 Mice	37
2.3.1.1 Chronic Alcohol Treatment of Pregnant Females by Continuous Preference Drinking.....	38
2.3.1.2 Binge Alcohol Treatment of Pregnant Females by Acute Injections	38

2.3.1.3 Tissue Collection and Nucleic Acid Isolation	39
2.3.2 RNA Analysis	41
2.3.2.1 Gene Expression Arrays	41
2.3.2.2 miRNA Expression Arrays	42
2.3.2.3 Quantitative PCR Confirmation.....	43
2.3.2.4 Bioinformatic Analysis of Differentially Expressed Probe Sets....	44
2.3.3 DNA Analysis.....	45
2.3.3.1 DNA Methylation (MeDIP-Chip) Arrays.....	45
2.3.3.2 Bioinformatic Analysis of Differently Methylated Genes.....	47
2.4 Results	48
2.4.1 Differential Gene (mRNA) Expression	48
2.4.2 Differential ncRNA Expression.....	53
2.4.2.1 Reciprocal Differential miRNA and Target Gene Expression	54
2.4.2.2 Confirmations of Differential Expression.....	58
2.4.2.3 Differential ncRNA Expression in All Exposure Paradigms.....	60
2.4.3 Differential DNA Methylation.....	61
2.4.3.1 Gene Families	66
2.4.3.2 CTCF Binding Sites	67
2.5 Discussion.....	75
2.5.1 Imprinted ncRNA Clusters	76
2.5.2 Gene Families	79
2.5.3 Alterations to Cellular Signaling Genes	82
2.5.4 Considerations for Future Research.....	83
2.5.5 Conclusion	84
2.6 References	85

Chapter 3 – Exploration of Differential DNA Methylation in Children with FASD	98
3.1 Overview	98
3.2 Introduction	99
3.3 Materials & Methods	101
3.3.1 Methylation Array.....	103
3.3.2 Pyrosequencing	104
3.3.3 NGS Panel.....	105
3.4 Results	106
3.4.1 Gene Network and Ontologies Associated with FASD	108
3.4.2 The Top Canonical Pathways are Related to Neurodevelopment and Neurotransmission	112
3.4.3 Confirmation of the 450K Array by Pyrosequencing	119
3.4.4 Examination of Select Loci in the General Population.....	121
3.5 Discussion	126
3.5.1 Non-Random Genome-Wide Differential Methylation	126
3.5.2 Comparison of Discovery and Replication Cohorts	128
3.5.3 No Single Gene Examined Identifies FASD	129
3.5.4 Select Functions of Sequenced Genes	131
3.5.5 Considerations for Future Research.....	132

3.5.6 Conclusion	133
3.6 References	134
Chapter 4 – Comparison of PAE Mice and Humans.....	141
4.1 Overview	141
4.2 Introduction	141
4.3 Methods	142
4.4 Results	143
4.4.1 Increased Methylation at the Clustered Protocadherins.....	144
4.5 Discussion.....	148
4.5.1 Functions of the Clustered Protocadherins	148
4.5.2 Conclusion	153
4.3 References	153
Chapter 5 – Discussion.....	158
5.1 Overview	158
5.2 Towards an Inductive Mechanism: PAE Alters Cellular Signaling	158
5.2.1 Alternative Hypotheses	161
5.3 Considerations for Future Experimentation	161
5.4 Conclusions	163
5.5 References	164
Appendices.....	167
<i>Curriculum Vitae</i>	180

List of Tables

Table 2.1. Top differentially-expressed transcripts in CPD adult mouse brains that were annotated with a gene symbol.....	51
Table 2.2. Ontologies and pathways for differentially-expressed genes from CPD adult mouse brains	52
Table 2.3. Updated (2016) analysis of significant differentially expressed mouse miRNAs in CPD adult brains.....	56
Table 2.4. Updated (2016) Partek miRNA target filter analysis for differentially expressed genes and associated miRNAs identified in CPD adult brains	57
Table 2.5. Top ontologies identified by the original (2012) Ingenuity analysis of significantly differentially methylated gene promoters	63
Table 2.6. Updated (2016) analysis of genes in CPD adult brains with the greatest differential DNA methylation.....	72
Table 2.7. Ontologies for the updated (2016) analysis of significant differential DNA methylation in CPD mice.....	73
Table 2.8. Pathways for the updated (2016) analysis of significant differential DNA methylation in CPD mice.....	74
Table 3.1. Clinical features of patients from the discovery and replication cohorts with the diagnosis of FASD	102
Table 3.2. Ontologies for genes with significant differences in CpG methylation from the discovery cohort.....	111
Table 3.3. Pathway analysis for genes with significant differences in CpG methylation from the discovery cohort	113
Table 3.4. Summary of NGS panel results for an average of the same ten FASD and seven control patients from Owen Sound, Ontario that were analyzed across 23 genes.	122
Table 3.5. Summary of pyrosequencing results from children representative of the general population of Owen Sound, Ontario	125
Table 4.1. Nucleotide-specific analysis of CpGs in the protocadherin gene family clusters showing significant alterations to CpG methylation in human buccal epithelial DNA from children of the discovery sample	145
Table 4.2. Tiling-based analysis of promoters from the protocadherin gene clusters showing significant increases in methylation in adult brain tissue from a mouse model of prenatal alcohol exposure	146

List of Figures

Figure 2.1. Flowchart of workflow used to analyze different exposure paradigms.....	40
Figure 2.2. PCA analysis of gene expression arrays from CPD PAE and matched control adult brains.....	49
Figure 2.3. Heatmap of significant ($p < 0.05$) differential gene expression in CPD PAE and matched control adult brains	50
Figure 2.4. A bar graph depicting the quantitation of <i>mmu-mir-679-5p</i> expression in control and CPD PAE adult brains	59
Figure 2.5. Hierarchical clustering of significant differential methylation in CPD PAE adult mouse brains identified by the original (2012) analysis	62
Figure 2.6. Ingenuity pathway analysis of the CDK5 signaling pathway.....	64
Figure 2.7. Ingenuity pathway analysis of the PTEN signaling pathway	65
Figure 2.8. The functional potential of altered CTCF-binding-site methylation after PAE in significant differentially methylated regions identified by the original (2012) analysis	69
Figure 2.9. GeneMANIA network analysis of significant differentially methylated genes containing CTCF-binding sites from the top associative network identified in the original (2012) analysis by Ingenuity Pathway Analysis.....	70
Figure 3.1. Differential DNA methylation in children diagnosed with FASD	107
Figure 3.2. GeneMANIA associative network analysis of genes annotated to differentially methylated CpGs from cheek swabs of the discovery sample.....	109
Figure 3.3. Manhattan plot of human chromosome 5 from the discovery cohort.....	110
Figure 3.4. Genes in the hippo signaling pathway affected by altered CpG methylation in children from the discovery cohort	114
Figure 3.5. Genes in the glutamatergic synapse pathway that were affected by altered CpG methylation in children from the discovery cohort	115
Figure 3.6. Genes in the calcium signaling pathway that were affected by altered CpG methylation in children from the discovery cohort.....	116
Figure 3.7. Genes in the retrograde endocannabinoid signaling pathway that were affected by altered CpG methylation in children from the discovery cohort	117
Figure 3.8. Genes in the serotonergic synapse pathway that were affected by altered CpG methylation in children from the discovery cohort.....	118
Figure 3.9. Pyrosequencing results for <i>COLEC11</i> and <i>HTT</i> in the discovery cohort.....	120
Figure 4.1. Broad profile of increased methylation of clustered protocadherins in children with FASD and PAE mice	147
Figure 4.2. A hypothetical model of gene regulation by CTCF at the clustered protocadherin locus.....	152

List of Appendices

Appendix A: IPA miRNA target filter analysis of CPD PAE adult mouse brains	167
Appendix B: Individual heatmaps of differential miRNA expression generated using hierarchical clustering of the four PAE paradigms	169
Appendix C: Venn diagram of common and unique differentially expressed miRNAs identified by four PAE models	170
Appendix D: Differentially expressed snoRNAs in the <i>Snrpn-Ube3a</i> region identified by miRNA and gene expression arrays in all PAE paradigms	171
Appendix E: Differentially expressed ncRNAs from <i>Dlk1-Dio3</i> and <i>Sfmbt2</i>	172
Appendix F: IPA Legend	173
Appendix G: Profile of FASD patients (first tab) and matched controls (second tab) from the general population of Owen Sound, Ontario	Digital
Appendix H: CpG list, with genomic annotations, for the discovery cohort.....	Digital
Appendix I: Next-generation sequencing panel results for children from the general population of Owen Sound, Ontario	Digital
Appendix J: Pyrosequencing results for children from the general population of Owen Sound, Ontario	Digital
Appendix K: Ethics Approval	176
Appendix L: Journal Copyright Approval	179

List of Abbreviations

5mC	5-Methylcytosine
ADHD	Attention Deficit Hyperactivity Disorder
ARND	Alcohol-Related Neurodevelopmental Disorder
ARVC	Arrhythmogenic right ventricular cardiomyopathy
A ^v y	Agouti Viable Yellow
B6	C57BL/6J
BAC	Blood Alcohol Concentration
BDNF	Brain Derived Neurotrophic Factor
CAMs	Cell Adhesion Molecules
cDNA	Complimentary DNA
.CEL file	Probe intensity data file for Affymetrix arrays
CPD	Continuous Preference Drinking
CpG	CpG Dinucleotide
C _t	Threshold Cycle for qPCR
ddPCR	Droplet Digital Polymerase Chain Reaction
DEP	Differential Enrichment Peak
DMR	Differentially Methylated Region
DNMT	DNA Methyltransferase
dNTP	Deoxyribonucleoside Triphosphate
DSM-5	Diagnostic Statistical Manual of Mental Disorders 5 th Edition
EMT	Epithelial-Mesenchymal Transition
FAS	Fetal Alcohol Syndrome
FASD	Fetal Alcohol Spectrum Disorders
FDR	False Discovery Rate
GD	Gestational Day
GEO	Gene Expression Omnibus
GWAS	Genome-Wide Association Studies
hESC	Human Embryonic Stem Cell
ICM	Inner Cell Mass
ICR	Imprinting Control Region
.idat file	Probe intensity data files for Illumina arrays
lncRNA	Long Non-Coding RNA
MeDIP	Methylated DNA Immunoprecipitation
MeDIP-Chip	Methylated DNA Immunoprecipitation coupled to microarray Chip
miRNA	MicroRNA
MRI	Magnetic Resonance Imaging
mRNA	Messenger mRNA
ncRNA	Non-Coding RNA

ND-PAE	Neurobehavioral Disorder Associated with Prenatal Alcohol Exposure
NGS	Next-Generation Sequencing
PAE	Prenatal Alcohol Exposure
PCB	Polychlorinated Biphenyl
pFAS	Partial Fetal Alcohol Syndrome
PGM	Ion Torrent Personal Genome Machine
PND	Post-Natal Day
PTM	Histone Post-Translational Modification
qPCR	Quantitative reverse transcription Polymerase Chain Reaction
RISC	RNA-Induced Silencing Complex
rRNA	Ribosomal RNA
RT	Reverse Transcription
snoRNA	Small Nucleolar RNA
snRNA	Small Nuclear RNA
sscDNA	Single-Stranded Complimentary DNA
SWAN	Subset-Quantile Array Normalization algorithm
T1	Trimester 1 Human Equivalent; GD8 & GD11
T2	Trimester 2 Human Equivalent; GD14 & GD16
T3	Trimester 3 Human Equivalent; PND 4 & PND7
TEAD	Transcription Enhancer Domain
TEF	Transcriptional Enhancer Factors
tRNA	Transfer RNA
UTR	Untranslated Region
β -value	Ratio of intensities between methylated and unmethylated probes

Chapter 1

Introduction

1.1. Prenatal Alcohol Exposure

Alcohol consumption during pregnancy can result in the development of fetal alcohol spectrum disorders (FASD) (Williams et al. 2015). FASD is an umbrella term for a heterogeneous spectrum of related developmental disorders that are caused by prenatal alcohol exposure (PAE), with the worst possible outcome being fetal alcohol syndrome (FAS) (Lemoine et al. 1968; Jones et al. 1973; Williams et al. 2015). FAS shares commonalities with other psychiatric disorders including growth deficiency and central nervous system impairment. FAS is distinguished from other psychiatric disorders by a history of maternal alcohol consumption during pregnancy and three distinct facial features (Clarren & Smith 1978). First is a smooth philtrum: the vertical groove between the nose and upper lip is flattened. Second is a thin vermillion: a thin upper lip. Third are small palpebral fissures: a reduced width of the eye. However, these facial characteristics used to distinguish FAS and partial FAS (pFAS) do not typically apply to the lower part of the FASD spectrum, which is characterized by neurobehavioral and neuroanatomical alterations without the distinctive facial features.

There are a total of 428 comorbidities related to FASD (Popova et al. 2016). FASD is associated with congenital malformations to the ocular, auditory, skeletal, cardiac, and renal systems. The clinical heterogeneity and uniqueness of each case appears to be driven by the combination of dosage and timing of PAE, other exposures, genetic background, sex, family history of PAE, as well as maternal genotype, nutrition and stress (Kleiber, Diehl, et al. 2014). In Canada, from 2003-2010, ~10% of pregnant women and ~20% of breast feeding women consumed alcohol (Lange et al. 2016). While no official record exists for Canada, FASD is typically diagnosed in only 2-5% of children (May et al. 2014). These numbers are comparable across many alcohol consuming nations and represent a multi-billion dollar public health issue.

The Institute of Medicine (IOM) of the National Academies has four diagnostic categories for the disorders that constitute FASD: FAS, pFAS, alcohol-related neurodevelopmental disorder (ARND), and alcohol-related birth defects (ARBD) (Stratton et al. 1996; Chudley et al. 2005). The latest edition of the diagnostic and statistical manual of mental disorders (DSM-5) now includes the psychiatric diagnosis: Neurobehavioral Disorder Associated with Prenatal Alcohol Exposure (ND-PAE) (American Psychiatric Association 2013). ND-PAE considers the neurobehavioral alterations to be independent from the facial characteristics and is listed in the DSM-5 appendix under “conditions for further study” (Doyle & Mattson 2015).

Endophenotype is a psychiatric genetics concept that deconstructs a complex behavioural phenotype into components with a clearer genetic connection (Gottesman & Gould 2003). The endophenotypes of FASD overlap with other psychiatric disorders, particularly attention deficit hyperactivity disorder (ADHD). While an individual can be diagnosed with the two disorders, they are distinct disorders, and misdiagnosis of one can lead to inappropriate medication and therapy (O’Malley & Nanson 2002; Greenbaum et al. 2009; Peadon & Elliott 2010). Endophenotypes commonly associated with FASD include impairments in cognition, learning, executive function, judgment, attention, and social adaptation (Mattson & Riley 1998; Jirikowic et al. 2008; Green et al. 2014). The molecular mechanisms behind FASD endophenotypes have been difficult to ascertain in humans. However, animal models have greatly aided research into FASD endophenotypes (Gil-Mohapel et al. 2010; Kiecker 2016). The results suggest that FASD endophenotypes are a result of cellular and molecular aberrations to neurodevelopment that are caused by PAE (Resendiz et al. 2014).

1.1.1. PAE Endophenotypes are Associated with Altered Neurodevelopment

Human neurodevelopment is a complex process that takes a relatively long time to produce a mature brain. Once an oocyte is fertilized by a sperm, they form a zygote that undergoes the ~8-week process of embryonic development. During its voyage down the fallopian tube, the zygote undergoes cleavage, which is a series of rapid cell divisions that divide the large cytoplasm of the egg into a solid spherical mass of smaller nucleated cells

known as blastomeres (Gilbert 2013). The spherical structure then begins to form a cavity on the inside and results in a hollow ball of cells known as the blastocyst. The outer cells of the blastocyst form the trophoblast, which is the first embryonic epithelium, and the remaining cells are trapped inside and form the pluripotent inner cell mass (ICM). The blastocyst then arrives in the uterus after four days and implants into the endometrium of the uterine wall after a few more days to begin gastrulation.

During gastrulation the embryo forms three distinct germ layers: endoderm, mesoderm, and ectoderm (Gilbert 2013). The endoderm forms into parts of the digestive system, liver, lungs, and thyroid. The mesoderm forms into a number of muscle types, bone, cartilage, dermis, gonads, circulatory system, and lymphatic system. The ectoderm forms into the surface ectoderm, neural tube, and neural crest. The surface ectoderm forms the epidermis, nails, hair, tooth enamel, parts of the eye, and buccal epithelium. The neural tube forms into the brain, spinal cord, retina, and part of the endocrine system. The neural crest forms into the peripheral nervous system, epinephrine-producing (medulla) cells in the adrenal gland, various pigment cells, and facial bone and cartilage. It also generates connective tissue in the eye, tooth, skin, fat, arteries as well as connective tissue the salivary, lachrymal, thymus, thyroid, and pituitary glands. The diversity of differentiated cell types has led to the neural crest being referred to as the fourth germ layer; however, these stem cells are in fact derived from the neural tube and the diverse fates are determined largely by where they migrate. In later embryonic development and differentiation, a strip of specialized cells in the endoderm known as the notochord induces a portion of the ectoderm to become the neuroectoderm, which is also known as the neuroepithelium (Gilbert 2013). The neuroectoderm then transforms into the neural plate.

During neurulation, the neural plate folds into the neural tube. As neurulation occurs, the neural plate border separates from the neuroectoderm and serves as boundary between the neuroectoderm and surface ectoderm. The neural plate borders, which are peripheral to the neural plate, then fold in on themselves and once connected are known as the neural crest. During this period, the neural tube may fail to close completely and result in neural tube defects. The closing of the neural tube is sensitive to certain environmental conditions with folate (Vitamin B₉) and Vitamin B₁₂ supplementation

greatly reducing the chances of a neural tube defect (Ray et al. 2002). In human PAE pregnancies, ethanol was found to impair the transfer of folate across the placenta (Hutson et al. 2012). Folate and B₁₂ are involved in one-carbon metabolism, which is used to derive the methyl groups of the epigenome and also nucleic acid synthesis (Kobor & Weinberg 2011). After the neural plate closes, it becomes the neural tube. The neural crest cells will then migrate great distances, which leaves the neural tube disconnected from the epidermis. In order to migrate, neural crest cells must undergo an epithelial-mesenchymal transition (EMT). During EMT, epithelial cells undergo morphological change, lose their current cell-to-cell adhesion, and become migratory multipotent mesenchymal stem cells. Inside the neural tube are neural stem cells that will differentiate into neurons and glia. Thus, in addition to the fetal stages of pregnancy, PAE can also alter embryonic development and produce a number of overlapping and distinct clinical outcomes.

Embryonic development represents the first trimester of human pregnancy and results in a fetus just over 1 inch in size that continues to undergo slower cell divisions as it grows and refines existing structures (Gilbert 2013). The developing brain forms intermediate structures and refines a network of synaptic connections throughout the second and third trimester of pregnancy. Notably, throughout fetal development and into young adulthood DNA cytosine methylation in the developing brain continues to reconfigure itself during neurodevelopmental events (Lister et al. 2013). Any of the above developmental processes may be disrupted by PAE.

A single occasion of PAE during the third trimester of pregnancy has been shown to trigger widespread but select acute apoptosis of neurons (Farber et al. 2010) and oligodendrocytes (Creeley et al. 2013) in the fetal macaque brain. Furthermore, PAE induced apoptosis in the fetal macaque brain is comparable to PAE induced apoptosis in the developing rodent brain (Young & Olney 2006). The above observations suggest that PAE causes neurodevelopmental aberrations, which result in life long anomalies associated with FASD. The above conclusion, however, is too general and has provoked more refined studies on the mechanism behind the effect of PAE on neurodevelopment. These mechanistic studies have been greatly aided by more sensitive molecular technologies assessing the effect of PAE at the genomic level. Specifically, such studies

have focused on the effect of PAE on genome-wide gene expression and the epigenome, which are discussed below.

1.1.2. PAE Alters Short-Term and Long-Term Gene Expression

Insight into the effects of alcohol on the developing brain have been assessed using animal models, which typically include rats for neuroscience-based studies and the C57BL/6J (B6) strain of mice for molecular-biology-based studies (Valenzuela et al. 2012; Zhou 2015). The most common *in vivo* PAE paradigm involves injecting acute doses of ethanol during different developmental time points and represents a binge exposure (Kleiber, Diehl, et al. 2014). Studies of PAE in mice have identified differential expression of diverse genes, many of which are involved in development.

Gene expression microarrays have been used to examine PAE in a B6 mouse model with binge injections (3.8 g/kg, twice a day) from gestational days (GD) six to eight (Lee et al. 2004). Craniofacial malformations were observed in both embryos (GD10) and fetuses (GD15). An alteration to “palate, lung, and nasal epithelium clone (*plunc*)”, which is involved in palate closure, was confirmed by polymerase chain reaction (PCR). These findings provided early evidence that PAE results in genome-wide alterations in both embryos and fetuses and that the altered genes are involved in processes related to the morphological abnormalities associated with FASD.

Other studies have used gene expression microarrays to identify PAE induced alterations to genes with functions that include cellular division and proliferation, cell signaling, cell migration, apoptosis, cell-to-cell adhesion, metabolism, and protein synthesis and degradation. In 2004, Gutala *et al.* isolated cortical neurons from GD14 C57BL/6J mouse fetuses and subjected them to 5 days of ethanol treatment *in vivo* (Gutala et al. 2004). They screened 638 genes and identified 56 down-regulated and 10 up-regulated genes. Gene expression associated with “protein synthesis” (ribosome) and “ubiquitin-proteasome” was decreased by alcohol exposure. They also confirmed the genes involved in “ubiquitin-proteasome” by qPCR. Heat shock proteins and members of the PI3K/AKT/mTOR pathway (*mTOR*, *Pten*, and *Marcks*) were also altered. In 2005, Hard *et al.* examined a B6 model of binge injections on GD7 and GD9 and the fetal brains were examined for differential gene expression on GD18 (Hard et al. 2005).

Twenty-five PAE genes were identified, all of which were down-regulated. Notable candidates identified by the authors were *Timp4*, *Bmp15*, *Rnf25*, *Akt1*, *Tulp4*, and *Dexras1*. These identified genes have roles in cellular proliferation, differentiation, signaling, and apoptosis. In 2007, Green *et al.* examined two substrains of C57BL/6 mice and collected embryonic head folds 3 hours after binge injection on GD8 (Green *et al.* 2007). The group observed alterations to 2,906 non-redundant genes, including several hub genes (*Mapk1*, *Ald3a2*, *Cd13*, *Pfkm*, *Tnfrsf1a*, *Rps6*, *Igfl1*, *Egfr*, and *Pten*). There was a significant overall down-regulation of pathways related to the ribosome and proteasome. There was also a significant overall up-regulation of the pathways related to cell adhesion and regulation of actin cytoskeleton. Furthermore, experimentation with a mitochondrial GABA_A receptor antagonist also uncovered a role for *Akt1* and strain-specific effects. Together, the results from Gutala *et al.*, Green *et al.*, and Hard *et al.* suggest that cellular signaling is altered by PAE, particularly the PI3K/AKT/mTOR pathway.

In 2011, Zhou *et al.* examined the effects of ethanol on GD8 B6 whole embryo culture (Zhou, Zhao, et al. 2011). They found that 34 out of 127 (27%) alcohol treated embryos had neural tube defects while only 3 out 139 (2%) controls showed obvious defects. When comparing two array experiments, 87 probe sets were replicated. There were a total of 49 probe sets that had decreased expression, while 38 showed increased expression. The genes were functionally involved in neurodevelopment, chromatin, eye and heart development, retinol metabolism, cell cycle, and cell adhesion. Several genes were also observed to be turned on or off by alcohol exposure. The group also observed *de novo* expression of aldehyde dehydrogenase 1B1 (*Aldh1B1*), which catalyzes the conversion of retinaldehyde to retinoic acid. Retinoic acid is involved in cellular signaling for developmental events.

A number of laboratories have reported on mouse models of PAE based on voluntary and moderate maternal consumption throughout gestation that produce peak blood alcohol concentrations of ~80–120 mg/dl (Allan *et al.* 2003; Boehm *et al.* 2008; Brady *et al.* 2012). Kaminen-Ahola *et al.* examined a B6 maternal voluntary exposure paradigm and found that PAE results in craniofacial changes and growth restriction (Kaminen-Ahola, Ahola, Flatscher-Bader, *et al.* 2010). It was found in this case that PAE

induced growth alterations were not observable prior to birth but were apparent in weanlings. Furthermore, they cross-fostered the weanlings to show that this observation was not the result of altered maternal care by alcohol consuming mothers. Gene expression related to the metabolism of exogenous and endogenous compounds, iron homeostasis, and lipid metabolism was altered in the liver of young PAE mice. In 2014, Dobson *et al.* used qPCR to examine a guinea pig model of voluntary maternal PAE and found it disrupts the expression of genes involved in insulin and insulin-like growth factor (IGF) signaling in the adult prefrontal cortex (Dobson et al. 2014). Insulin signaling is capable of activating the PI3K/AKT/mTOR pathway (Laplante & Sabatini 2009). In 2016 Ramani *et al.* examined a moderate voluntary exposure paradigm and observed that PAE during the first trimester results in the upregulation of mRNA and protein for an astrocytic connexin (*Cx30*), which is involved in forming gap junctions in the hippocampus of young mice (Ramani et al. 2016). Together, these results show that rodents can be used to model a number of PAE paradigms, which include acute binge injections at different developmental time points or variations of a more continuous moderate exposure by voluntary maternal consumption.

The laboratory of Shiva Singh established a B6 maternal continuous preference drinking (CPD) paradigm that resulted in offspring with mild developmental delays, anxiety-related traits, and deficits in learning and memory (Kleiber et al. 2011). Analysis by qPCR revealed a down-regulation of a glutamate receptor (*Grin2c*) and glycine receptor subunit (*Glr1*). This paradigm was extended by evaluating global gene expression changes that occurred in adult brains of CPD PAE mice (Kleiber et al. 2012). The results indicated that alcohol induces subtle but consistent changes to gene expression. Gene enrichment analysis showed overrepresented gene ontology classifications of cellular, embryonic, and nervous system development. A number of the identified genes were previously implicated in FASD-relevant neurobehavioral phenotypes such as cognitive function, anxiety, ADHD, and mood disorders. Ultimately, the above findings suggest that altered gene expression is detectable long after PAE and most likely represents altered gene regulation and a shift in cellular populations for life (Kleiber, Diehl, et al. 2014).

The Singh laboratory has also examined how the variability seen in FASD phenotypes relates to the timing of alcohol exposure. In these experiments a binge exposure paradigm was used, in which B6 mice were exposed to two acute doses of alcohol (5 g/kg of body weight) at neurodevelopmental times representing the human first, second, or third trimester equivalent (Kleiber et al. 2013; Mantha et al. 2014; Kleiber, Laufer, et al. 2014). This method has been previously reported to result in peak blood alcohol concentrations of over 300 mg/dl (for 4–5 hours following injection) and can induce the apoptosis of millions of neurons by both a blockade of NMDA glutamate receptors and excessive activation of GABA_A receptors (Ikonomidou et al. 2007; Wozniak et al. 2004). The first set of experiments utilizing the binge injection models set out to examine physiological, developmental, and behavioural deficits associated with the paradigms examined (Mantha et al. 2013). The results showed that alcohol exposure at any time during gestation causes delays in motor skill and reflex development. Also, the results provided further support for long-term PAE induced deficits in learning and memory, as assessed by the Barnes maze. These same mice were also used to assess changes in the adult brain transcriptome (Kleiber et al. 2013). The results suggested that alcohol disrupts biological processes that are actively occurring at the time of exposure. These include cell proliferation during trimester one, cell migration and differentiation during trimester two, and cellular communication and neurotransmission during trimester three. Furthermore, although alcohol altered a distinct set of genes depending on developmental timing, many of these show interrelatedness and can be associated with one another via ‘hub’ molecules and pathways. However, the regulatory mechanism maintaining the long-term alterations to gene expression remained hypothetical.

1.2. Epigenetic Mechanisms May Underlie the Altered Gene Expression of PAE

In addition to gene expression, PAE alters epigenetic marks (Haycock 2009; Kobor & Weinberg 2011; Basavarajappa & Subbanna 2016). Epigenetic marks maintain gene expression profiles related to development and tissue specificity without altering DNA sequence and are heritable in dividing cells. Epigenetic marks are distinct from transcription factors, however, they influence each other as gene expression is initiated by

transcription factors recruiting RNA polymerase. Epigenetic marks include DNA cytosine methylation (Smith & Meissner 2013), select histone post-translational modifications (Gurard-Levin & Almouzni 2014), and a diverse array of non-coding RNA (ncRNA) species (Pauli et al. 2011; Rinn 2014). These marks enable spatial and temporal control of gene expression by acting together to create distinct states of variation that have unique functions in the brain (Sweatt et al. 2012). While each mammalian cell has a (nearly) identical genome, there are layers of diversity that give each cell type a unique epigenome that is reflective of ontogeny. Epigenetic experimentation has provided invaluable insight into the molecular mechanisms of inheritance and disease that lie outside genetic contribution.

1.2.1. PAE Alters Histone Post-Translational Modifications

There are five types of histone proteins found in the chromatin of mammalian cells: the four core histones (*H2a*, *H2b*, *H3*, and *H4*) and histone *H1*, which is bound to the linker DNA between nucleosomes (Marzluff et al. 2002). Each time a mammalian cell divides, it must rapidly synthesize large amounts of histones. The unique properties of the histone genes are critical for cell cycle regulation (Marzluff et al. 2002). There are approximately 10–20 genes encoding each of the core histone proteins in mammals. The bulk of the replication-dependent histone genes are found in two clusters in both mouse and human (Albig & Doenecke 1997; Albig et al. 1997). The largest cluster is termed *HIST1*, and there is an orthologous *Hist1* cluster on mouse chromosome 13 (Wang et al. 1996). The mouse *Hist1* cluster contains 45 core histone genes with 6 histone H1 genes. A smaller number of histone genes are present in *HIST2* on human chromosome 1, and this cluster is orthologous to the *Hist2* cluster on mouse chromosome 3 (Wang et al. 1996). In addition there is a second small cluster of histone genes on human chromosome 1, termed *HIST3*, and the orthologous *Hist3* cluster is located on mouse chromosome 11 (Marzluff et al. 2002).

A relatively large number of histone post-translational modifications (PTMs) exist (Gurard-Levin & Almouzni 2014) and a number of PTMs may act as epigenetic marks. Multiple PTMs are possible on the same histone. Mono-, di-, and tri- methylations (me1, me2, and me3) and acetylation (ac) are intensely studied PTMs. Histones H2A, H2B, H3,

and H4 represent the core nucleosome subunits. The core subunits are present in duplicate, where the octamer wraps around ~150 bp of DNA and interacts with the linker histone (H1). PTMs typically occur on the exposed N-terminus tail of the histone subunit that is accessible to chromatin modifying machinery. For instance, the exposed lysines (K) at the 4th, 9th, and 27th position in amino acid sequence on Histone H3 (H3K4, H3K9, and H3K27) and H4K20 are relatively well characterized for their function in regulating gene expression. Histones bind to DNA and form chromatin, which also includes DNA methylation and some ncRNAs. PTMs are widely hypothesized to constitute a histone code at a specific locus that encodes gene regulatory information (Jenuwein & Allis 2001). Ultimately, PTMs effect the recruitment of other proteins onto chromatin and can then functionally affect transcription.

Histone PTMs have been shown to be altered by PAE. In 2011, Guo *et al.* examined a rat model of PAE that corresponds to the third trimester of human pregnancy. They found a reduction in a histone acetyltransferase (CREB binding protein) in the developing cerebellum along with a reduction in H3 and H4 acetylation levels (Guo et al. 2011). In 2013, Veazey *et al.* examined the effect of alcohol exposure on GD12.5 B6 cortical neuroepithelial cells maintained as neurosphere cultures (Veazey et al. 2013). The group found that promoters of genes involved in neurodevelopment were under-enriched for H3K4me3 and H3K27me3 after ethanol exposure. Notably, while the group observed large-scale change to chromatin structure, they only observed a few matching alterations to transcription. Together, the above studies demonstrate that more than one histone PTM is altered by PAE.

PAE has also been shown to alter histone PTMs on genes coding for enzymes that establish histone PTMs. Subbanna *et al.* examined a human trimester 3 equivalent mouse model of binge PAE. They observed that PAE increased histone methyltransferase (G9a) activity and lead to an increase in H3K9me2 and H3K27me2 (Subbanna et al. 2013). Later, Subbanna *et al.* found increased H3K14ac in the first exon of *G9a* and also observed that G9a immunoprecipitates with DNA methylation machinery (DNMT3A and MeCP2) (Subbanna et al. 2014). These observations show that PAE alters cooperating epigenetic marks. In 2015, Veazey *et al.* examined *in vitro* and *in vivo* models where it was found that the specific alterations to histone PTMs appear to depend on alcohol

dosage, the specific gene, as well as the time elapsed since alcohol exposure (Veazey et al. 2015). Notable candidates included the *Hox* genes. The predicted regulatory correlation was not observed for individual PTMs and altered gene expression; however, they observed an increase in repressive chromatin modifications that was correlated with significant alterations to the transcripts coding for DNA and histone methyltransferase enzymes. Ultimately, the above studies demonstrate the combinatorial nature of the epigenome and show that epigenetic machinery is also deregulated by PAE. Furthermore, the alterations to histone PTMs may sometimes, but not always, lead to altered gene expression.

1.2.2. PAE Alters Non-Coding RNA Expression

Gene expression is not limited to coding RNA, as ncRNAs represent a variety of RNA species that can be altered by PAE. Small nucleolar RNAs (snoRNA) are a class of RNA that guide the methylation and pseudouridylation of ribosomal RNA (rRNA), transfer RNA (tRNA), and small nuclear RNA (snRNA) (Bachellerie et al. 2002). Also noteworthy are orphan snoRNAs, which have taken on novel functions in alternative splicing, growth, and neurodevelopment (Laufer & Singh 2012).

Another class of ncRNA are microRNAs (miRNA) (Filipowicz et al. 2008). miRNAs are small (~23 bp) endogenous RNA molecules that canonically target the 3' untranslated region (UTR) of messenger RNA (mRNA) and result in post-transcriptional repression (Bartel 2009). The targeting of a mature mammalian miRNA is dependent upon the seed region (six bp; nucleotides 2-7), which is where a nearly perfect match occurs between miRNA and mRNA. Furthermore, several nucleotides thereafter may tolerate some mismatches and hybridize as well. There are thousands of miRNAs in the mammalian genome and ~60% of protein coding genes may be regulated by miRNAs (Friedman et al. 2009).

miRNAs exist in the genome as independent genes, polycistronic gene clusters, or introns. miRNAs are also present in the introns and/or exons of some large non-coding RNAs (lncRNA). miRNAs are processed from a larger pri-miRNA precursor that can have a 5' cap, poly-A tail, and form a secondary structure with a hairpin loop (Filipowicz et al. 2008; Bartel 2009). A Drosha-DGCR8 complex, also known as the microprocessor

complex, processes the pri-miRNA and produces a ~70 bp stem loop known as pre-miRNA. However, introns containing miRNAs do not undergo pri-miRNA processing as their splicing results in pre-miRNA. Exportin-5 recognizes pre-miRNA in the nucleus and exports it to the cytoplasm. Dicer recognizes the pre-miRNA, cleaves the stem loop, and leaves a ~20 bp RNA duplex. Afterwards, one strand (the guide strand) of the duplex is selected as mature RNA, while the other (passenger) strand is either degraded or is selected in some situations to carry out alternative targeting. Mature miRNAs are loaded into the RNA-induced silencing complex (RISC), which is a ribonucleoprotein complex that contains a number of proteins including DICER and AGO. The miRNA loaded RISC complex can then target transcripts, resulting in translational repression or mRNA destabilization. Imperfect matching at the seed region enables a single miRNA to target many genes and a single gene to be targeted by many miRNAs, which allows for the regulation of complex gene expression profiles. A number of miRNAs have been implicated in various abnormalities that often show co-morbidity with FASD, including anxiety, depression, and other psychiatric disorders (O'Connor et al. 2012).

PAE has been shown to alter miRNA expression. In 2007, Sathyan *et al.* examined the effect of alcohol exposure on miRNA expression in GD12.5 B6 cortical neuroepithelial cells maintained as neurosphere cultures (Sathyan et al. 2007). The group found that both high and low ethanol doses alter different miRNAs that influence the cell cycle and apoptosis. One of the altered miRNAs was shown to be regulated by a GABA receptor, while another miRNA is genomically imprinted. Genomically imprinted genes are expressed in a parent-of-origin-specific manner that is based on differential DNA methylation of an imprinting control region (ICR). Thus, the *ex vivo* results of Sathyan *et al.* show that different PAE doses alter distinct miRNAs and that PAE responsive miRNAs are regulated by different mechanisms. In 2009, Wang *et al.* examined miRNA expression in fetal B6 brains exposed to a number of alcohol dosages and observed the deregulation of several miRNAs (Wang et al. 2009). Together the above results demonstrate that PAE induces altered miRNA expression.

Studies of PAE induced miRNA expression have also revealed that the gene expression alterations are dynamic. In 2012, Guo *et al.* examined the effect of a chronic and intermittent exposure on B6 primary cortical neuronal cultures, and observed the

differential expression of 42 miRNAs after 10 days of exposure (Guo et al. 2012). The group also examined the effects of ethanol removal. Five days after removal of the chronic ethanol exposure, they observed a profile of 26 deregulated miRNAs – 20 of which were unique to the removal. The predicted target genes had functions related to transcription, protein phosphorylation, and neurodevelopment. Some of the miRNAs were predicted to target MeCP2, which showed both decreased mRNA and protein levels. These finding suggest that, in addition to the immediate effect of alcohol on the developing fetus, there may also be an alcohol removal effect that alters neurodevelopment as well.

In addition to mice, zebrafish have proved to be a useful model for studying PAE induced alterations to miRNA expression. Soares *et al.* found that ethanol upregulates several miRNAs in embryos with putative targets involved in cell cycle control, apoptosis, and transcription (Soares et al. 2012). Tal *et al.* observed the reciprocal deregulation of miRNAs and predicted target mRNAs, which are involved in brain morphogenesis (Tal et al. 2012). Notably, a knockdown of *mir-9* or *mir-153c* phenocopied the PAE induced alterations to larval and juvenile swimming behaviour. The above zebrafish experiments provide strong evidence that alterations to miRNAs can result in PAE endophenotypes.

Finally, miRNAs themselves may be regulated by other epigenetic marks altered by PAE. In 2013, Pappalardo-Carter *et al.* examined the role of *mir-9* and related target gene expression in zebrafish embryos and mouse cortical neuroepithelial cells maintained as neurosphere cultures (Pappalardo-Carter et al. 2013). The group observed that *mir-9* was suppressed by alcohol and that a *mir-9* knockdown in the zebrafish embryos produced similar craniofacial defects to PAE. Furthermore, there was increased CpG methylation at a *mir-9* locus in the mouse cell line, which suggests an association between alterations to DNA methylation and alterations to miRNA expression.

1.2.3. PAE Alters DNA Methylation at Specific Genomic Loci

One of the most examined mechanisms of the epigenome is DNA methylation: a highly dynamic modification that is used to store additional information on nucleotides. The most widely studied DNA methylation mark is 5-methylcytosine (5mC). During

embryonic development, there are two waves of genome-wide DNA de-methylation (Seisenberger et al. 2013). The first follows the fertilization of the preimplantation embryo, and the second is during the establishment of primordial germ cells in the embryo that will go on to form sperm and oocytes. The first wave of DNA de-methylation retains genomic imprinting, and the second resets it. After the waves of de-methylation, methylation is established *de novo*, maintained across cell division, and also locally modified throughout development as cells become committed to their lineage (Hemberger et al. 2009). DNA methyltransferases (DNMTs) are an enzyme family capable of establishing and maintaining DNA methylation. In vertebrates, DNMTs are involved in establishing methylation at CpG dinucleotides and other sequences in the genome. CpG islands are a regulatory feature composed of greater than 50% GC content and range from 300 to 3000 bp (Gardiner-Garden & Frommer 1987; Fatemi et al. 2005). When methylated, CpG islands typically result in the repression of gene expression and are seen in promoters or the first exon of ~40% of mammalian genes (Fatemi et al. 2005; Brenet et al. 2011). Furthermore, ~70% of human gene promoters have a higher CpG content than is expected when compared to the rest of the genome (Saxonov et al. 2006). Intragenic, or gene body, CpG islands may have a role as alternative tissue-specific promoters (Maunakea et al. 2010). Finally, CpG islands are also mutational hotspots due to the tendency of 5mC to spontaneously undergo deamination and mutate to thymine. Genome-wide scans of CpG sites have revealed that CpG island shores, rather than CpG islands, may be the primary sites of normal tissue-specific differentially methylated regions (DMRs) (Yasui et al. 2007; Irizarry et al. 2009; Doi et al. 2009). CpG island shores are ~250 bp in size, up to 2 kb away from a CpG island, and typically outside of gene promoters. DMRs in CpG island shores often show a strong inverse relationship with gene expression. CpG island shores are associated with developmental genes and are conserved across mice and humans. Additionally, there are CpG island shelves that are located 2-4 kb from a CpG island and also the open sea, which refers to genomic regions that show no significant CpG enrichment (Sandoval et al. 2011). Overall, DNA methylation is a widely used epigenetic mark in mammals and occurs at a number of distinct genomic features.

DNA methylation is the most studied marker for PAE induced epigenomic dysregulation (Haycock 2009). In 1991, Garro *et al.* observed that binge PAE exposure in pregnant mice resulted in global hypomethylation of fetal DNA (Garro et al. 1991). The group also observed that low levels of acetaldehyde, a metabolite of ethanol, were able to interfere with DNA methyltransferase activity *in vitro*. In 1999, Maier *et al.* found that PAE can result in increased methylation and decreased expression of brain-derived neurotrophic factor (*Bdnf*) in the developing olfactory bulb of rats exposed during the equivalent of the first two trimesters of human pregnancy (Maier et al. 1999). Together, the above two studies suggested that PAE alters DNA methylation.

In 2009 Haycock & Ramsay examined the effect of PAE on genomic imprinting in pre-implantation mouse embryos by examining the *H19* differentially methylated region (DMR) (Haycock & Ramsay 2009). They observed that while PAE embryos were severely growth restricted, hypomethylation of the paternal allele at this specific region was only detectable in the placenta. Genomic imprinting is an epigenetic process that utilizes DNA methylation and other marks to enable parent-of-origin specific monoallelic expression of genes related to growth and development. Ouko *et al.* examined the sperm of alcohol-consuming adult human men and found hypomethylation at the imprinted *H19* and *Dlk1-Dio3* DMRs (Ouko et al. 2009). Thus, the above studies suggest that genomic imprinting is deregulated by PAE.

Later in 2009, Liu *et al.* examined the genome-wide effects of ethanol in a B6 whole embryo culture (Liu et al. 2009). Gene expression arrays and methylated DNA immunoprecipitation (MeDIP) arrays (MeDIP-Chip) revealed that genes of promoters with a high CpG content had decreased methylation and increased expression from binge exposure with an enrichment for genes on chromosomes 7, 10, and X. A 10-fold increase of methylation was observed on chromosomes 10 and X in exposed embryos with neural tube defects when compared to those without. The alterations to methylation were seen in a large number of genes associated with olfaction as well as genes involved development, chromatin, and genomic imprinting. The altered methylation was associated with changes in the expression of 84 genes. This study suggests that PAE induced alterations to methylation are not random. The findings also demonstrate that most genes showing

significantly altered methylation do not show significantly altered expression when examined.

A number of studies have examined the mechanism behind PAE induced alterations to DNA methylation. In 2010, Kaminen-Ahola *et al.* used the Agouti viable yellow (A^{vy}) B6 mouse model, which provides a visual phenotype when methylation is altered at a single gene (Kaminen-Ahola, Ahola, Maga, et al. 2010). This revealed that voluntary maternal consumption of 10% alcohol causes hypermethylation. This study showed that PAE at the embryonic stage can result in a long-lasting alteration to DNA methylation. In 2011, Downing *et al.* examined methylation of the imprinted *Igf2* locus in mouse embryos and observed a subtle ~8% decrease to methylation at a single CpG site with associated transcripts showing a -1.5 fold change (Downing et al. 2011). Notably, placing mothers on a methyl-supplemented diet attenuated some of the PAE endophenotypes. Later in 2011, Zhou *et al.* examined the effects of alcohol exposure on rat neural stem cell culture and found altered migration, neuron formation, and growth that was similar in an effect to the DNA methyltransferase inhibitor 5-aza-cytidine (Zhou, Balaraman, et al. 2011). During differentiation, it was found that alcohol exposure prevented the reprogramming of genes related to neurodevelopment, neuronal receptors, and olfaction. The specific sites showing altered methylation were correlated with transcription factors related to neurodevelopment. Overall, these studies link PAE induced differential DNA methylation to birth defects.

Continuous maternal preference drinking also produces offspring with altered DNA methylation. In 2013, Chen *et al.* used immunostaining to visualize altered DNA methylation programming in the developing C57BL/6J mouse hippocampus (Chen et al. 2013). In 2015, Marjonen *et al.* examined a voluntary maternal preference drinking model of PAE and found that early gestational alcohol exposure results in alterations to gene expression in the adolescent post-natal day (PND) 28 hippocampus, bone marrow, and main olfactory epithelium (Marjonen et al. 2015). The group observed gene expression changes related to olfaction, immune response, epigenetics (miRNAs and a histone), and two keratin associated proteins in the hippocampus. Genes showing differential expression belonged to similar families reported by Kleiber *et al.* in 2012, which analyzed some arrays generated for this thesis (Kleiber et al. 2012). Marjonen *et al.* also used

bisulfite sequencing and found alterations to DNA methylation in CpG islands upstream of some of the genes. Furthermore, magnetic resonance imaging (MRI) of post-natal day 60 PAE adult mice revealed an enlargement of the left hippocampus and decreased volume of the left olfactory bulb. While the differential expression in the hippocampus was low and not possible to confirm by quantitative reverse transcription PCR (qPCR), some of the gene expression alterations identified by the gene expression array of the hippocampus were also confirmed in the bone marrow or main olfactory epithelium by qPCR. These observations suggest that differences present in adults with PAE are a long-term result of earlier alterations in embryonic stem cell populations, which differentiate into a number of tissues and maintain some signature of developmental alterations.

DNA methylation alterations induced by PAE are also transmitted transgenerationally. In 2012, Govorko *et al.* examined a rat model of continuous maternal preference drinking from GD7 to GD21. The group examined *Pomc*, a gene that produces multiple peptide hormones, and found that adult (PND60-80) F1 offspring had alterations in the hypothalamus, which is involved in stress reaction (Govorko et al. 2012; Sarkar 2016). The neurons showed increased CpG methylation at the *Pomc* promoter, suppressed gene expression, and a resulting phenotype of altered stress response. Alterations to DNA and histone methyltransferase gene expression levels were also seen. The alterations to the methylation, expression, and function of *Pomc* were also found to be transmitted to both the F2 and F3 generations by the male germ-line with sperm showing alterations to *Pomc* methylation. These findings show that the DNA methylation alterations induced by PAE can transmit not only through mitosis but also meiosis.

1.2.4. PAE May Alter the Epigenetic Landscape of Neurodevelopment

PAE appears to alter a number of epigenetic marks in overlapping and distinct regions. The altered genes are enriched for functions related to cellular fate commitment events that occur during neurodevelopment. Thus, it appears that PAE results not only in immediate toxicity, but also creates distinct epigenotypes that may influence later developmental events. Conrad Waddington proposed the concept of the epigenotype (Waddington 2012), which led to his theory of canalization and the epigenetic landscape

(Waddington 1942; Bird 2007; Reik 2007). The epigenetic landscape is an abstract concept that describes the dynamic epigenomic profiles of stem cells during development. As cells differentiate, they become increasingly committed to certain lineages and are poised (or primed) at the epigenetic level for later events and certain responses (Waddington 1942; Lesch et al. 2013). The brain is highly dependent on the epigenome for neurodevelopmental processes (LaSalle et al. 2013). Developmental trajectories are also sensitive to the environment, where exposures may alter quality of life long after the initial exposure and immediate toxicology (LaSalle 2013). This effect appears to be due to an altered epigenetic programming related to future development that is continuing to exert an effect as well as a shift in vulnerable cell populations. Therefore, early life exposures may continue to exert an effect on adult hippocampal neurogenesis. One third of neurons in the hippocampus are subject to exchange over a lifetime, with annual turnover rate of 1.75% in the renewing fraction of adult humans that is also similar in mice (Spalding et al. 2013). Ultimately, the above suggests that some PAE endophenotypes may be maintained by long-term alterations from the initial exposure.

Studies examining one-carbon metabolism have provided insight into how PAE initiates disruptions to DNA methylation, while also demonstrating the preventable nature of some long-term alterations. Alcohol exposure during embryonic development affects the transfer of folate from the mother to the developing embryo (Hutson et al. 2012). This is of significance to the developing embryo because folate is a methyl donor and essential in establishing and maintaining DNA methylation. The lack of folate has the potential to cause aberrant epigenetic profiles. Treatments that contain methyl donors, such as choline, have been able to attenuate some of the effects of PAE (Zeisel 2011). Of particular interest to this thesis is the observation that co-incubation of alcohol-exposed mouse embryos with folic acid, a synthetic form of folate, was able to prevent altered expression of a miRNA and target gene (Wang et al. 2009). Such results argue that the alcohol-induced molecular cascade might involve DNA methylation. In 2013, Bekdash *et al.* examined the hypothalamus of adult offspring of a voluntary maternal consumption rat model and found a decrease in activating histone and an increase in repressive histone marks and DNA methylation (Bekdash et al. 2013). Furthermore, they observed increased methylation of the *Pomc* promoter and a decrease in *Pomc* mRNA expression. Notably,

these alterations could be attenuated with choline supplementation during PAE. Using the same model in 2014, Gangisetty *et al.* demonstrated a mechanistic role for MeCP2 in altering *Pomc* expression upon PAE (Gangisetty *et al.* 2014). Overall, these studies suggest that altered DNA methylation is mechanistically responsible for some PAE induced differential gene expression and that the prevention, or even potentially the reversal, of these alterations can attenuate some of the endophenotypes.

Given the above observations, it appears that PAE can alter DNA methylation in specific regulatory sequences. For example, CTCF is a highly conserved ubiquitous 11-zinc-finger protein with multiple functions in 3D chromatin organization and gene regulation, including chromatin insulator activity as well as transcriptional activation and repression (Williams & Flavell 2008). CTCF binds to a set of signal sequences that are sensitive to methylation (Filippova 2007) and mediates chromosomal interactions (Ling *et al.* 2006). There are over 100 000 CTCF-binding sites in the mouse genome (Shen *et al.* 2012). CTCF-binding sites involved in the DMR of *H19* have shown significant differential methylation in PAE placental tissue (Haycock & Ramsay 2009) and in the sperm of alcohol-consuming mice (Knezovich & Ramsay 2012). These results argue that the observed affect of PAE on gene expression may be caused by the effect of PAE on DNA methylation at specific regulatory sequences, which include imprinted regions.

1.2.4.1. Genomic Imprinting

A number of studies of PAE have observed methylation changes occurring in genes that are known to be genomically imprinted (Liu *et al.* 2009; Shukla *et al.* 2011; Sittig *et al.* 2011; Dietz *et al.* 2012). Genomic imprinting enables parent-of-origin specific monoallelic expression of a select set of genes that are important in early development, particularly neurodevelopment (Kernohan & Bérubé 2010). These genes are crucial during not only neurodevelopment but also the normal functioning of the brain (Davies *et al.* 2008). Interestingly, ~30% of imprinted genes are hypothesized to be ncRNAs, including miRNAs (Morison *et al.* 2005). The above observations suggest that PAE is best explained as a sequence of events in response to ethanol that may begin with differential methylation of imprinted genes encoding for ncRNAs, which regulate gene expression. For example, moderate and voluntary maternal PAE alters adult levels of a

vesicular glutamate transporter in the mouse hippocampus (Zhang et al. 2015). This glutamate transporter showed increased mRNA levels that were correlated with decreased DNA methylation and increased (activating) H3K4me3 at the transporter promoter. However, while mRNA levels of the transporter were increased, the protein levels were decreased, which suggested post-transcriptional regulation. The discrepancy between mRNA and protein was found to be caused by the increase of an imprinted miRNA from the *Sfmbt2* cluster and further functional experimentation showed that the miRNA binds to the 3'UTR of the transporter mRNA. This observation highlights the complexity of the interactions that shape the epigenetic landscape as well as their potential for disruption by PAE. Ultimately, it appears that the epigenetic landscape is one of the prime mechanism(s) for the long-term deregulation of brain gene expression following PAE. Yet the genome-wide details of this mechanism, particularly DNA methylation and ncRNA, have not been assessed. Also, perhaps more importantly, there remains the possibility that some of the epigenetic alterations observed in animal models are also present in children born with the clinical diagnosis of FASD.

1.2.4.2. Systems Biology Approaches

Given the interactive nature of the epigenetic landscape, single gene approaches do not capture the full complexity of alterations to the epigenome. The genome-wide analyses presented in this thesis make use of systems biology approaches. The genes identified are grouped in three ways. First, gene ontologies allow for genes to be grouped according to annotations of known functions and relationships across three categories: biological process, cellular component, and molecular function. Second, gene lists can also be assembled into associative genetic interaction networks, which are based on gene ontologies and other annotated or computationally predicted relationships. Finally, gene lists can be assembled into canonical protein pathways, which represent a generalized, linear, and well-studied cellular signaling pathway.

Systems biology approaches can be based on the principles of independent component analysis (Lee & Batzoglou 2003). These approaches offer added insight to a series of observations from single genes with low-fold changes and borderline statistical significance by grouping them according to modular functions that show a significant

enrichment. A 1.2-fold change in many genes of a pathway could produce a biologically significant result that is comparable to a 20-fold increase in a single gene (Barabási & Oltvai 2004; Subramanian et al. 2005). Nevertheless, in a network, certain genes serve as hubs where they connect a large number of genes and can also allow for cross-talk between different cellular signaling events. An alteration to a hub can theoretically be more catastrophic than many similar alterations to a number of lesser connected nodes in the network. Overall, systems biology allows for the analysis of complex and large-scale alterations, which are typical of PAE.

Hypothesis: *Alterations to DNA methylation and ncRNA expression are associated with the long-term effect of prenatal alcohol exposure in (i) mice and (ii) humans with FASD.*

Objectives:

1. To examine the differential epigenetic landscape associated with the long-term effects of PAE in adult mouse C57BL/6J brains by comparing to matched controls and assessing alterations in:
 - a. gene expression using the Affymetrix GeneChip® Mouse Gene 1.0 ST array.
 - b. miRNA expression using the Affymetrix GeneChip® miRNA 2.0 array.
 - c. DNA methylation using the NimbleGen MM9 2.1M deluxe promoter array v2.
2. To examine the association of PAE with DNA methylation in buccal swab DNA from children born with a diagnosis of FASD and compare to matched controls using:
 - a. Illumina Infinium HumanMethylation450 BeadChips (450K) to assess genome-wide methylation changes.
 - b. pyrosequencing confirmations of gene-specific CpG methylation differences.
 - c. a targeted NGS bisulfite sequencing panel to confirm gene-specific CpG methylation differences.

Thesis Organization:

The results of this thesis are organized into three chapters. Chapter 2 describes an exploration of long-term alterations in a mouse model. Chapter 3 characterizes alterations

present in young human children with FASD. Chapter 4 presents a comparison of the alterations to DNA methylation in PAE mice and human children.

1.3. References

- Albig, W. & Doenecke, D., 1997. The human histone gene cluster at the D6S105 locus. *Human Genetics*, 101(3), 284–294.
- Albig, W., Kioschis, P., Poustka, A., Meergans, K. & Doenecke, D., 1997. Human histone gene organization: nonregular arrangement within a large cluster. *Genomics*, 40(2), 314–322.
- Allan, A.M., Chynoweth, J., Tyler, L.A. & Caldwell, K.K., 2003. A mouse model of prenatal ethanol exposure using a voluntary drinking paradigm. *Alcoholism: Clinical and Experimental Research*, 27(12), 2009–2016.
- American Psychiatric Association, 2013. *Diagnostic and Statistical Manual of Mental Disorders: DSM-V*,
- Bachellerie, J.P., Cavaillé, J. & Hüttenhofer, A., 2002. The expanding snoRNA world. *Biochimie*, 84(8), 775–790.
- Barabási, A. & Oltvai, Z.N., 2004. Network biology: understanding the cell's functional organization. *Nature Reviews Genetics*, 5(2), 101–113.
- Bartel, D.P., 2009. MicroRNAs: Target Recognition and Regulatory Functions. *Cell*, 136(2), 215–233.
- Basavarajappa, B. & Subbanna, S., 2016. Epigenetic Mechanisms in Developmental Alcohol-Induced Neurobehavioral Deficits. *Brain Sciences*, 6(2), 12.
- Bekdash, R.A., Zhang, C. & Sarkar, D.K., 2013. Gestational choline supplementation normalized fetal alcohol-induced alterations in histone modifications, DNA methylation, and proopiomelanocortin (POMC) gene expression in b-endorphin-producing POMC neurons of the hypothalamus. *Alcoholism: Clinical and Experimental Research*, 37(7), 1133–1142.
- Bird, A., 2007. Perceptions of epigenetics. *Nature*, 447(7143), 396–8.
- Boehm, S.L., Moore, E.M., Walsh, C.D., Gross, C.D., Cavelli, A.M., Gigante, E. & Linsenbardt, D.N., 2008. Using Drinking in the Dark to model prenatal binge-like exposure to ethanol in C57BL/6J mice. *Developmental Psychobiology*, 50(6), 566–578.
- Brady, M.L., Allan, A.M. & Caldwell, K.K., 2012. A Limited Access Mouse Model of Prenatal Alcohol Exposure that Produces Long-Lasting Deficits in Hippocampal-Dependent Learning and Memory. *Alcoholism: Clinical and Experimental Research*,

36(3), 457–466.

Brenet, F., Moh, M., Funk, P., Feierstein, E., Viale, A.J., Soccia, N.D. & Scandura, J.M., 2011. DNA methylation of the first exon is tightly linked to transcriptional silencing. *PLoS ONE*, 6(1), e14524.

Chen, Y., Ozturk, N.C. & Zhou, F.C., 2013. DNA Methylation Program in Developing Hippocampus and Its Alteration by Alcohol. *PLoS ONE*, 8(3), e60503.

Chudley, A.E., Conry, J., Cook, J.L., Loock, C., Rosales, T. & LeBlanc, N., 2005. Fetal alcohol spectrum disorder: Canadian guidelines for diagnosis. *CMAJ*, 172(5 SUPPL.), S1–S21.

Clarren, S.K. & Smith, D.W., 1978. The fetal alcohol syndrome. *N Engl J Med*, 298(19), 1063–1067.

Creeley, C., Dikranian, K., Johnson, S., Farber, N. & Olney, J., 2013. Alcohol-induced apoptosis of oligodendrocytes in the fetal macaque brain. *Acta Neuropathologica Communications*, 1(1), 23.

Davies, W., Isles, A.R., Humby, T. & Wilkinson, L.S., 2008. What are imprinted genes doing in the brain? *Advances in Experimental Medicine and Biology*, 626(4), 62–70.

Dietz, W.H., Masterson, K., Sittig, L.J., Redei, E.E. & Herzing, L.B.K., 2012. Imprinting and expression of Dio3os mirrors Dio3 in rat. *Frontiers in Genetics*, 3, 279.

Dobson, C.C., Thevasundaram, K., Mongillo, D.L., Winterborn, A., Holloway, A.C., Brien, J.F. & Reynolds, J.N., 2014. Chronic prenatal ethanol exposure alters expression of central and peripheral insulin signaling molecules in adult guinea pig offspring. *Alcohol*, 48(7), 687–693.

Doi, A., Park, I.-H., Wen, B., Murakami, P., Aryee, M.J., Irizarry, R., Herb, B., Ladd-Acosta, C., Rho, J., Loewer, S., Miller, J., Schlaeger, T., Daley, G.Q. & Feinberg, A.P., 2009. Differential methylation of tissue- and cancer-specific CpG island shores distinguishes human induced pluripotent stem cells, embryonic stem cells and fibroblasts. *Nature Genetics*, 41(12), 1350–1353.

Downing, C., Johnson, T.E., Larson, C., Leakey, T.I., Siegfried, R.N., Rafferty, T.M. & Cooney, C.A., 2011. Subtle decreases in DNA methylation and gene expression at the mouse Igf2 locus following prenatal alcohol exposure: Effects of a methyl-supplemented diet. *Alcohol*, 45(1), 65–71.

Doyle, L.R. & Mattson, S.N., 2015. Neurobehavioral Disorder Associated with Prenatal Alcohol Exposure (ND-PAE): Review of Evidence and Guidelines for Assessment. *Current Developmental Disorders Reports*, 2(3), 175–186.

Farber, N.B., Creeley, C.E. & Olney, J.W., 2010. Alcohol-induced neuroapoptosis in the fetal macaque brain. *Neurobiology of Disease*, 40(1), 200–206.

- Fatemi, M., Pao, M.M., Jeong, S., Gal-Yam, E.N., Egger, G., Weisenberger, D.J. & Jones, P.A., 2005. Footprinting of mammalian promoters: Use of a CpG DNA methyltransferase revealing nucleosome positions at a single molecule level. *Nucleic Acids Research*, 33(20), e176.
- Filipowicz, W., Bhattacharyya, S.N. & Sonenberg, N., 2008. Mechanisms of post-transcriptional regulation by microRNAs: are the answers in sight? *Nature Reviews Genetics*, 9(2), 102–114.
- Filippova, G.N., 2007. Genetics and Epigenetics of the Multifunctional Protein CTCF. *Current Topics in Developmental Biology*, 80, 337–360.
- Friedman, R.C., Farh, K.K.H., Burge, C.B. & Bartel, D.P., 2009. Most mammalian mRNAs are conserved targets of microRNAs. *Genome Research*, 19(1), 92–105.
- Gangisetty, O., Bekdash, R., Maglakelidze, G. & Sarkar, D.K., 2014. Fetal alcohol exposure alters proopiomelanocortin gene expression and hypothalamic-pituitary-adrenal axis function via increasing MeCP2 expression in the hypothalamus e113228. *PLoS ONE*, 9(11), e113228.
- Gardiner-Garden, M. & Frommer, M., 1987. CpG Islands in vertebrate genomes. *Journal of Molecular Biology*, 196(2), 261–282.
- Garro, a J., McBeth, D.L., Lima, V. & Lieber, C.S., 1991. Ethanol consumption inhibits fetal DNA methylation in mice: implications for the fetal alcohol syndrome. *Alcoholism: Clinical and Experimental Research*, 15(3), 395–398.
- Gil-Mohapel, J., Boehme, F., Kainer, L. & Christie, B.R., 2010. Hippocampal cell loss and neurogenesis after fetal alcohol exposure: Insights from different rodent models. *Brain Research Reviews*, 64(2), 283–303.
- Gilbert, S.F., 2013. *Developmental Biology*, Sinauer Associates.
- Gottesman, I.I. & Gould, T.D., 2003. The endophenotype concept in psychiatry: Etymology and strategic intentions. *American Journal of Psychiatry*, 160(4), 636–645.
- Govorko, D., Bekdash, R.A., Zhang, C. & Sarkar, D.K., 2012. Male germline transmits fetal alcohol adverse effect on hypothalamic proopiomelanocortin gene across generations. *Biological Psychiatry*, 72(5), 378–388.
- Green, C.R., Roane, J., Hewitt, A., Muhajarine, N., Mushquash, C., Sourander, A., Lingley-Pottie, P., McGrath, P. & Reynolds, J.N., 2014. Frequent behavioural challenges in children with fetal alcohol spectrum disorder: A needs-based assessment reported by caregivers and clinicians. *Journal of Population Therapeutics and Clinical Pharmacology*, 21(3), e405–e420.
- Green, M.L., Singh, A. V., Zhang, Y., Nemeth, K.A., Sulik, K.K. & Knudsen, T.B., 2007.

- Reprogramming of genetic networks during initiation of the Fetal Alcohol Syndrome. *Developmental Dynamics*, 236(2), 613–631.
- Greenbaum, R.L., Stevens, S.A., Nash, K., Koren, G. & Rovet, J., 2009. Social cognitive and emotion processing abilities of children with fetal alcohol spectrum disorders: A comparison with attention deficit hyperactivity disorder. *Alcoholism: Clinical and Experimental Research*, 33(10), 1656–1670.
- Guo, W., Crossey, E.L., Zhang, L., Zucca, S., George, O.L., Valenzuela, C.F. & Zhao, X., 2011. Alcohol exposure decreases CREB binding protein expression and histone acetylation in the developing cerebellum. *PLoS ONE*, 6(5), e19351.
- Guo, Y., Chen, Y., Carreon, S. & Qiang, M., 2012. Chronic Intermittent Ethanol Exposure and Its Removal Induce a Different miRNA Expression Pattern in Primary Cortical Neuronal Cultures. *Alcoholism: Clinical and Experimental Research*, 36(6), 1058–1066.
- Gurard-Levin, Z.A. & Almouzni, G., 2014. Histone modifications and a choice of variant: a language that helps the genome express itself. *F1000Prime Reports*, 6(76), 76.
- Gutala, R., Wang, J., Kadapakkam, S., Hwang, Y., Ticku, M. & Li, M.D., 2004. Microarray analysis of ethanol-treated cortical neurons reveals disruption of genes related to the ubiquitin-proteasome pathway and protein synthesis. *Alcoholism, Clinical and Experimental Research*, 28(12), 1779–1788.
- Hard, M.L., Abdolell, M., Robinson, B.H. & Koren, G., 2005. Gene-expression analysis after alcohol exposure in the developing mouse. *Journal of Laboratory and Clinical Medicine*, 145(1), 47–54.
- Haycock, P.C., 2009. Fetal alcohol spectrum disorders: the epigenetic perspective. *Biology of Reproduction*, 81(4), 607–617.
- Haycock, P.C. & Ramsay, M., 2009. Exposure of mouse embryos to ethanol during preimplantation development: effect on DNA methylation in the h19 imprinting control region. *Biology of Reproduction*, 81(4), 618–627.
- Hemberger, M., Dean, W. & Reik, W., 2009. Epigenetic dynamics of stem cells and cell lineage commitment: digging Waddington's canal. *Nature Reviews Molecular Cell Biology*, 10(8), 526–537.
- Hutson, J.R., Stade, B., Lehotay, D.C., Collier, C.P. & Kapur, B.M., 2012. Folic acid transport to the human fetus is decreased in pregnancies with chronic alcohol exposure. *PLoS ONE*, 7(5), e38057.
- Ikonomidou, C., Price, M.T., Stefovská, V. & Ho, F., 2007. Ethanol-Induced Apoptotic Neurodegeneration and Fetal Alcohol Syndrome. *Science*, 1056(2000), 1056–1060.
- Irizarry, R.A., Ladd-Acosta, C., Wen, B., Wu, Z., Montano, C., Onyango, P., Cui, H.,

- Gabo, K., Rongione, M., Webster, M., Ji, H., Potash, J.B., Sabunciyan, S. & Feinberg, A.P., 2009. The human colon cancer methylome shows similar hypo- and hypermethylation at conserved tissue-specific CpG island shores. *Nature Genetics*, 41(2), 178–186.
- Jenuwein, T. & Allis, C.D., 2001. Translating the histone code. *Science*, 293(5532), 1074–1080.
- Jirikowic, T., Olson, H.C. & Kartin, D., 2008. Sensory processing, school performance, and adaptive behavior of young school-age children with fetal alcohol spectrum disorders. *Physical & Occupational Therapy in Pediatrics*, 28(2), 117–136.
- Jones, K.L., Smith, D.W., Ulleland, C.N. & Streissguth, P., 1973. Pattern of malformation in offspring of chronic alcoholic mothers. *Lancet*, 1(7815), 1267–1271.
- Kaminen-Ahola, N., Ahola, A., Flatscher-Bader, T., Wilkins, S.J., Anderson, G.J., Whitelaw, E. & Chong, S., 2010. Postnatal growth restriction and gene expression changes in a mouse model of fetal alcohol syndrome. *Birth Defects Research Part A: Clinical and Molecular Teratology*, 88(10), 818–826.
- Kaminen-Ahola, N., Ahola, A., Maga, M., Mallitt, K.A., Fahey, P., Cox, T.C., Whitelaw, E. & Chong, S., 2010. Maternal ethanol consumption alters the epigenotype and the phenotype of offspring in a mouse model. *PLoS Genetics*, 6(1), e1000811.
- Kernohan, K.D. & Bérubé, N.G., 2010. Genetic and epigenetic dysregulation of imprinted genes in the brain. *Epigenomics*, 2(6), 743–763.
- Kiecker, C., 2016. The chick embryo as a model for the effects of prenatal exposure to alcohol on craniofacial development. *Developmental Biology*.
- Kleiber, M.L., Diehl, E.J., Laufer, B.I., Mantha, K., Chokroborty-Hoque, A., Alberry, B. & Singh, S.M., 2014. Long-term genomic and epigenomic dysregulation as a consequence of prenatal alcohol exposure: A model for fetal alcohol spectrum disorders. *Frontiers in Genetics*, 5, 161.
- Kleiber, M.L., Laufer, B.I., Stringer, R.L. & Singh, S.M., 2014. Third trimester-equivalent ethanol exposure is characterized by an acute cellular stress response and an ontogenetic disruption of genes critical for synaptic establishment and function in mice. *Developmental Neuroscience*, 36(6), 499–519.
- Kleiber, M.L., Laufer, B.I., Wright, E., Diehl, E.J. & Singh, S.M., 2012. Long-term alterations to the brain transcriptome in a maternal voluntary consumption model of fetal alcohol spectrum disorders. *Brain Research*, 1458, 18–33.
- Kleiber, M.L., Mantha, K., Stringer, R.L. & Singh, S.M., 2013. Neurodevelopmental alcohol exposure elicits long-term changes to gene expression that alter distinct molecular pathways dependent on timing of exposure. *Journal of Neurodevelopmental Disorders*, 5(1), 6.

- Kleiber, M.L., Wright, E. & Singh, S.M., 2011. Maternal voluntary drinking in C57BL/6J mice: Advancing a model for fetal alcohol spectrum disorders. *Behavioural Brain Research*, 223(2), 376–387.
- Knezovich, J.G. & Ramsay, M., 2012. The effect of preconception paternal alcohol exposure on epigenetic remodeling of the H19 and Rasgrf1 imprinting control regions in mouse offspring. *Frontiers in Genetics*, 3, 10.
- Kobor, M.S. & Weinberg, J., 2011. Focus on: epigenetics and fetal alcohol spectrum disorders. *Alcohol Res Health*, 34(1), 29–37.
- Lange, S., Quere, M., Shield, K., Rehm, J. & Popova, S., 2016. Alcohol use and self-perceived mental health status among pregnant and breastfeeding women in Canada: A secondary data analysis. *BJOG*, 123(6), 900–909.
- Laplante, M. & Sabatini, D.M., 2009. mTOR signaling at a glance. *Journal of Cell Science*, 122(20), 3589–3594.
- LaSalle, J.M., 2013. Epigenomic strategies at the interface of genetic and environmental risk factors for autism. *Journal of Human Genetics*, 58(7), 396–401.
- LaSalle, J.M., Powell, W.T. & Yasui, D.H., 2013. Epigenetic layers and players underlying neurodevelopment. *Trends in Neurosciences*, 36(8), 460–470.
- Laufer, B.I. & Singh, S.M., 2012. A Macro Role for Imprinted Clusters of MicroRNAs in the Brain. *MicroRNA*, 1(1), 59–64.
- Lee, R. Da, Rhee, G.S., An, S.M., Kim, S.S., Kwack, S.J., Seok, J.H., Chae, S.Y., Park, C.H., Yoon, H.J., Cho, D.H., Kim, H.S. & Park, K.L., 2004. Differential Gene Profiles in Developing Embryo and Fetus After in Utero Exposure To Ethanol. *Journal of Toxicology and Environmental Health, Part A*, 67(23-24), 2073–2084.
- Lee, S.-I. & Batzoglou, S., 2003. Application of independent component analysis to microarrays. *Genome biology*, 4(11), R76.
- Lemoine, P., Harousseau, H., Borteyru, J.P. & Menuet, J.C., 1968. Les enfants de parents alcooliques: Anomalies observees a propos de 127 cas. *Ouest méd*, 21, 476–482.
- Lesch, B.J., Dokshin, G. a, Young, R. a, McCarrey, J.R. & Page, D.C., 2013. A set of genes critical to development is epigenetically poised in mouse germ cells from fetal stages through completion of meiosis. *Proceedings of the National Academy of Sciences of the United States of America*, 110(40), 16061–16066.
- Ling, J.Q., Li, T., Hu, J.F., Vu, T.H., Chen, H.L., Qiu, X.W., Cherry, A.M. & Hoffman, A.R., 2006. CTCF Mediates Interchromosomal Colocalization Between Igf2/H19 and Wsb1/Nfl. *Science*, 312(571), 269–272.
- Lister, R., Mukamel, E. a, Nery, J.R., Urich, M., Puddifoot, C. a, Nicholas, D., Lucero, J.,

- Huang, Y., Dwork, A.J., Schultz, M.D., Yu, M., Heyn, H., Hu, S., Wu, J.C., Rao, A., Esteller, M. & He, C., 2013. Global Epigenomic Reconfiguration During Mammalian Brain Development. *Science*, 341, 629–643.
- Liu, Y., Balaraman, Y., Wang, G., Nephew, K.P. & Zhou, F.C., 2009. Alcohol exposure alters DNA methylation profiles in mouse embryos at early neurulation. *Epigenetics*, 4(7), 500–511.
- Maier, S.E., Cramer, J.A., West, J.R. & Sohrabji, F., 1999. Alcohol exposure during the first two trimesters equivalent alters granule cell number and neurotrophin expression in the developing rat olfactory bulb. *Journal of Neurobiology*, 41(3), 414–423.
- Mantha, K., Kleiber, M.L. & Singh, S.M., 2013. Neurodevelopmental Timing of Ethanol Exposure May Contribute to Observed Heterogeneity of Behavioral Deficits in a Mouse Model of Fetal Alcohol Spectrum Disorder (FASD). *Journal of Behavioral and Brain Science*, 3(1), 85–99.
- Mantha, K., Laufer, B.I. & Singh, S.M., 2014. Molecular changes during neurodevelopment following second-trimester binge ethanol exposure in a mouse model of fetal alcohol spectrum disorder: From immediate effects to long-term adaptation. *Developmental Neuroscience*, 36(1), 29–43.
- Marjonen, H., Sierra, A., Nyman, A., Rogojin, V., Grohn, O., Linden, A.M., Hautaniemi, S. & Kaminen-Ahola, N., 2015. Early maternal alcohol consumption alters hippocampal DNA methylation, gene expression and volume in a mouse model. *PLoS ONE*, 10(5), e0124931.
- Marzluff, W.F., Gongidi, P., Woods, K.R., Jin, J. & Maltais, L.J., 2002. The human and mouse replication-dependent histone genes. *Genomics*, 80(5), 487–498.
- Mattson, S.N. & Riley, E.P., 1998. A review of the neurobehavioral deficits in children with fetal alcohol syndrome or prenatal exposure to alcohol. *Alcoholism: Clinical and Experimental Research*, 22(2), 279–294.
- Maunakea, A.K. et al., 2010. Conserved role of intragenic DNA methylation in regulating alternative promoters. *Nature*, 466(7303), 253–257.
- May, P.A., Baete, A., Russo, J., Elliott, A.J., Blankenship, J., Kalberg, W.O., Buckley, D., Brooks, M., Hasken, J., Abdul-Rahman, O., Adam, M.P., Robinson, L.K., Manning, M. & Hoyme, H.E., 2014. Prevalence and Characteristics of Fetal Alcohol Spectrum Disorders. *Pediatrics*, 134(5), 855–866.
- Morison, I.M., Ramsay, J.P. & Spencer, H.G., 2005. A census of mammalian imprinting. *Trends in Genetics*, 21(8), 457–465.
- O'Connor, R.M., Dinan, T.G. & Cryan, J.F., 2012. Little things on which happiness depends: microRNAs as novel therapeutic targets for the treatment of anxiety and

- depression. *Molecular Psychiatry*, 17(4), 359–376.
- O’Malley, K.D. & Nanson, J., 2002. Clinical implications of a link between fetal alcohol spectrum disorder and attention-deficit hyperactivity disorder. *Canadian Journal of Psychiatry*, 47(4), 349–354.
- Ouko, L. a., Shantikumar, K., Knezovich, J., Haycock, P., Schnugh, D.J. & Ramsay, M., 2009. Effect of Alcohol Consumption on CpG Methylation in the Differentially Methylated Regions of *H19* and *IG-DMR* in Male Gametes-Implications for Fetal Alcohol Spectrum Disorders. *Alcoholism: Clinical and Experimental Research*, 33(9), 1615–1627.
- Pappalardo-Carter, D.L., Balaraman, S., Sathyam, P., Carter, E.S., Chen, W.J.A. & Miranda, R.C., 2013. Suppression and epigenetic regulation of MiR-9 contributes to ethanol teratology: Evidence from zebrafish and murine fetal neural stem cell models. *Alcoholism: Clinical and Experimental Research*, 37(10), 1657–1667.
- Pauli, A., Rinn, J.L. & Schier, A.F., 2011. Non-coding RNAs as regulators of embryogenesis. *Nature Reviews Genetics*, 12(2), 136–149.
- Peadon, E. & Elliott, E.J., 2010. Distinguishing between attention-deficit hyperactivity and fetal alcohol spectrum disorders in children: clinical guidelines. *Neuropsychiatric Disease and Treatment*, 6, 509–515.
- Popova, S., Lange, S., Shield, K., Mihic, A., Chudley, A.E., Mukherjee, R.A.S., Bekmuradov, D. & Rehm, J., 2016. Comorbidity of fetal alcohol spectrum disorder: A systematic review and meta-analysis. *The Lancet*, 387(10022), 978–987.
- Ramani, M., Mylvaganam, S., Krawczyk, M., Wang, L., Zoidl, C., Brien, J., Reynolds, J.N., Kapur, B., Poulter, M.O., Zoidl, G. & Carlen, P.L., 2016. Differential expression of astrocytic connexins in a mouse model of prenatal alcohol exposure. *Neurobiology of Disease*, 91, 83–93.
- Ray, J.G., Meier, C., Vermeulen, M.J., Boss, S., Wyatt, P.R. & Cole, D.E.C., 2002. Association of neural tube defects and folic acid food fortification in Canada. *Lancet*, 360(9350), 2047–2048.
- Reik, W., 2007. Stability and flexibility of epigenetic gene regulation in mammalian development. *Nature*, 447(7143), 425–432.
- Resendiz, M., Mason, S., Lo, C.L. & Zhou, F.C., 2014. Epigenetic regulation of the neural transcriptome and alcohol interference during development. *Frontiers in Genetics*, 5, 285.
- Rinn, J.L., 2014. LncRNAs: Linking RNA to chromatin. *Cold Spring Harbor Perspectives in Biology*, 6(8).
- Sandoval, J., Heyn, H.A., Moran, S., Serra-Musach, J., Pujana, M.A., Bibikova, M. &

- Esteller, M., 2011. Validation of a DNA methylation microarray for 450,000 CpG sites in the human genome. *Epigenetics*, 6(6), 692–702.
- Sarkar, D.K., 2016. Male germline transmits fetal alcohol epigenetic marks for multiple generations: A review. *Addiction Biology*, 21(1), 23–34.
- Sathyan, P., Golden, H.B. & Miranda, R.C., 2007. Competing interactions between micro-RNAs determine neural progenitor survival and proliferation after ethanol exposure: evidence from an ex vivo model of the fetal cerebral cortical neuroepithelium. *The Journal of Neuroscience*, 27(32), 8546–8557.
- Saxonov, S., Berg, P. & Brutlag, D.L., 2006. A genome-wide analysis of CpG dinucleotides in the human genome distinguishes two distinct classes of promoters. *Proceedings of the National Academy of Sciences of the United States of America*, 103(5), 1412–1417.
- Seisenberger, S., Peat, J.R., Hore, T. a, Santos, F., Dean, W. & Reik, W., 2013. Reprogramming DNA methylation in the mammalian life cycle: building and breaking epigenetic barriers. *Philosophical transactions of the Royal Society of London. Series B, Biological sciences*, 368(1609), 20110330.
- Shen, Y., Yue, F., McCleary, D.F., Ye, Z., Edsall, L., Kuan, S., Wagner, U., Dixon, J., Lee, L., Lobanenkov, V. V. & Ren, B., 2012. A map of the cis-regulatory sequences in the mouse genome. *Nature*, 488(7409), 116–120.
- Shukla, P.K., Sittig, L.J., Ullmann, T.M. & Redei, E.E., 2011. Candidate Placental Biomarkers for Intrauterine Alcohol Exposure. *Alcoholism: Clinical and Experimental Research*, 35(3), 559–565.
- Sittig, L.J., Shukla, P.K., Herzing, L.B.K. & Redei, E.E., 2011. Strain-specific vulnerability to alcohol exposure in utero via hippocampal parent-of-origin expression of deiodinase-III. *The FASEB Journal*, 25(7), 2313–2324.
- Smith, Z.D. & Meissner, A., 2013. DNA methylation: roles in mammalian development. *Nature Reviews Genetics*, 14(3), 204–220.
- Soares, A.R., Pereira, P.M., Ferreira, V., Reverendo, M., Simões, J., Bezerra, A.R., Moura, G.R. & Santos, M.A.S., 2012. Ethanol exposure induces upregulation of specific microRNAs in zebrafish embryos. *Toxicological Sciences*, 127(1), 18–28.
- Spalding, K.L., Bergmann, O., Alkass, K., Bernard, S., Salehpour, M., Huttner, H.B., Boström, E., Westerlund, I., Vial, C., Buchholz, B.A., Possnert, G., Mash, D.C., Druid, H. & Frisén, J., 2013. Dynamics of hippocampal neurogenesis in adult humans. *Cell*, 153(6), 1219–1227.
- Stratton, K., Howe, C. & Battaglia, F.C., 1996. *Fetal Alcohol Syndrome: diagnosis, epidemiology, prevention, and treatment*, National Academies Press.

- Subbanna, S., Nagre, N.N., Shivakumar, M., Umapathy, N.S., Psychoyos, D. & Basavarajappa, B.S., 2014. Ethanol induced acetylation of histone at G9a exon1 and G9a-mediated histone H3 dimethylation leads to neurodegeneration in neonatal mice. *Neuroscience*, 258, 422–432.
- Subbanna, S., Shivakumar, M., Umapathy, N.S., Saito, M., Mohan, P.S., Kumar, A., Nixon, R.A., Verin, A.D., Psychoyos, D. & Basavarajappa, B.S., 2013. G9a-mediated histone methylation regulates ethanol-induced neurodegeneration in the neonatal mouse brain. *Neurobiology of Disease*, 54, 475–485.
- Subramanian, A., Tamayo, P., Mootha, V.K., Mukherjee, S., Ebert, B.L., Gillette, M.A., Paulovich, A., Pomeroy, S.L., Golub, T.R., Lander, E.S. & Mesirov, J.P., 2005. Gene set enrichment analysis: A knowledge-based approach for interpreting genome-wide expression profiles. *Proceedings of the National Academy of Sciences*, 102(43), 15545–15550.
- Sweatt, D.J., Meaney, M.J., Nestler, E.J. & Akbarian, S., 2012. *Epigenetic Regulation in the Nervous System: Basic Mechanisms and Clinical Impact*, Academic Press.
- Tal, T.L., Franzosa, J.A., Tilton, S.C., Philbrick, K.A., Iwaniec, U.T., Turner, R.T., Waters, K.M. & Tanguay, R.L., 2012. MicroRNAs control neurobehavioral development and function in zebrafish. *FASEB Journal*, 26(4), 1452–1461.
- Valenzuela, C.F., Morton, R.A., Diaz, M.R. & Topper, L., 2012. Does moderate drinking harm the fetal brain? Insights from animal models. *Trends in Neurosciences*, 35(5), 284–292.
- Veazey, K.J., Carnahan, M.N., Muller, D., Miranda, R.C. & Golding, M.C., 2013. Alcohol-induced epigenetic alterations to developmentally crucial genes regulating neural stemness and differentiation. *Alcoholism: Clinical and Experimental Research*, 37(7), 1111–1122.
- Veazey, K.J., Parnell, S.E., Miranda, R.C. & Golding, M.C., 2015. Dose-dependent alcohol-induced alterations in chromatin structure persist beyond the window of exposure and correlate with fetal alcohol syndrome birth defects. *Epigenetics & Chromatin*, 8(1), 39.
- Waddington, C.H., 1942. Canalization of Development and the Inheritance of Acquired Characters. *Nature*, 150(3811), 563–565.
- Waddington, C.H., 2012. The Epigenotype. 1942. *International Journal of Epidemiology*, 41(1), 10–13.
- Wang, L.L., Zhang, Z., Li, Q., Yang, R., Pei, X., Xu, Y., Wang, J., Zhou, S.-F. & Li, Y., 2009. Ethanol exposure induces differential microRNA and target gene expression and teratogenic effects which can be suppressed by folic acid supplementation. *Human Reproduction*, 24(3), 562–579.

- Wang, Z.F., Krasikov, T., Frey, M.R., Wang, J., Matera, A.G. & Marzluff, W.F., 1996. Characterization of the mouse histone gene cluster on chromosome 13: 45 histone genes in three patches spread over 1Mb. *Genome Research*, 6(8), 688–701.
- Williams, A. & Flavell, R.A., 2008. The role of CTCF in regulating nuclear organization. *The Journal of Experimental Medicine*, 205(4), 747–750.
- Williams, J.F., Smith, V.C. & the COMMITTEE ON SUBSTANCE ABUSE, 2015. Fetal Alcohol Spectrum Disorders. *American Academy of Pediatrics*, 136(5), e1395–1406.
- Wozniak, D.F., Hartman, R.E., Boyle, M.P., Vogt, S.K., Brooks, A.R., Tenkova, T., Young, C., Olney, J.W. & Muglia, L.J., 2004. Apoptotic neurodegeneration induced by ethanol in neonatal mice is associated with profound learning/memory deficits in juveniles followed by progressive functional recovery in adults. *Neurobiology of Disease*, 17(3), 403–414.
- Yasui, D.H., Peddada, S., Bieda, M.C., Vallero, R.O., Hogart, A., Nagarajan, R.P., Thatcher, K.N., Farnham, P.J. & Lasalle, J.M., 2007. Integrated epigenomic analyses of neuronal MeCP2 reveal a role for long-range interaction with active genes. *Proceedings of the National Academy of Sciences of the United States of America*, 104(49), 19416–19421.
- Young, C. & Olney, J.W., 2006. Neuroapoptosis in the infant mouse brain triggered by a transient small increase in blood alcohol concentration. *Neurobiology of Disease*, 22(3), 548–554.
- Zeisel, S.H., 2011. What choline metabolism can tell us about the underlying mechanisms of fetal alcohol spectrum disorders. *Molecular Neurobiology*, 44(3), 185–191.
- Zhang, C.R., Ho, M.-F., Vega, M.C.S., Burne, T.H.J. & Chong, S., 2015. Prenatal ethanol exposure alters adult hippocampal VGLUT2 expression with concomitant changes in promoter DNA methylation, H3K4 trimethylation and miR-467b-5p levels. *Epigenetics & Chromatin*, 8(1), 40.
- Zhou, F.C., 2015. Dissecting FASD through the global transcriptome. *Alcoholism: Clinical and Experimental Research*, 39(3), 408–412.
- Zhou, F.C., Balaraman, Y., Teng, M., Liu, Y., Singh, R.P. & Nephew, K.P., 2011. Alcohol alters DNA methylation patterns and inhibits neural stem cell differentiation. *Alcoholism: Clinical and Experimental Research*, 35(4), 735–746.
- Zhou, F.C., Zhao, Q., Liu, Y., Goodlett, C.R., Liang, T., McClintick, J.N., Edenberg, H.J. & Li, L., 2011. Alteration of gene expression by alcohol exposure at early neurulation. *BMC Genomics*, 12(1), 124.

Chapter 2

Exploration of Long-Term Alterations to the Epigenome of a PAE Mouse Model

2.1 Overview

This chapter examines the mechanisms initiating and maintaining the long-term effect of prenatal alcohol exposure (PAE) in a mouse (C57BL/6J) model of fetal alcohol spectrum disorder (FASD). The results presented include the long-term *in vivo* effects of PAE on brain: 1) Gene Expression, 2) microRNA (miRNA) and small nucleolar RNA (snoRNA) expression, and 3) DNA Cytosine Methylation. The three data sets from different treatment paradigms were integrated to reveal alterations to the epigenetic landscape of the whole brain of adult mice. The results show that PAE causes long-term epigenomic alterations and identify a comprehensive set of affected genes that have been independently implicated in endophenotypes related to Fetal Alcohol Spectrum Disorders (FASD). Ultimately, this chapter highlights an epigenomic hypothesis that may be applied towards understanding the developmental course of the effect of PAE. Most, but not all, of the results included in this chapter are already published in Laufer *et al.* 2013 and some are published in Kleiber *et al.* 2012.

2.2 Introduction

Understanding how PAE results in the development of FASD presents a number of biological as well as ethical challenges. As it stands, most of the relevant experiments cannot be undertaken on humans. In order to address these challenges, the laboratory of Shiva Singh has established a C57BL/6J (B6) mouse model to examine the long-term effects of PAE across a number of exposure paradigms. In the binge exposure paradigms, mice were exposed to ethanol at specific developmental stages to model the first, second, or third trimester of human pregnancy (T1, T2, and T3) (Kleiber et al. 2013; Mantha et al. 2014; Kleiber, Laufer, et al. 2014). It was found that PAE at any time during embryonic/fetal development results in delays to developmental milestones as well as

deficits in learning and memory (Mantha et al. 2013). The aforementioned mice were also reared to adulthood and showed differential brain gene expression in genes related to developmental events disrupted by PAE (Kleiber et al. 2013). The changes to expression were observed primarily in genes involved in cell proliferation (T1), cell differentiation and migration (T2), and neurotransmission and cellular communication (T3) (Kleiber, Diehl, et al. 2014). Thus, PAE primarily alters the expression of genes in a manner that depends on the developmental timing of exposure. While few of the genes were shared across paradigms, a much larger number are associated by gene families, ontologies, ‘hubs’ in associative gene networks, and/or by canonical protein pathways. These results follow Green *et al.* (2007) who found changes in the expression of 2,906 genes in embryonic head folds 3 hours after a single binge injection on gestational day (GD) 8 (Green et al. 2007). There was a significant down-regulation of KEGG pathways related to the ribosome and proteasome and also a significant up-regulation of pathways related to focal adhesion, adherens junction, tight junction, and regulation of actin cytoskeleton. They also observed that PAE altered the expression of a number of hub genes, some of which are involved in the PI3K/AKT/mTOR signaling pathway. Furthermore, Zhou *et al.* examined the effects of ethanol in a whole embryo culture of GD8 B6 mice and found changes in the expression of genes for alcohol metabolism, retinol metabolism, hematopoiesis, neurodevelopment, cell cycle, histones, cell adhesion, homeobox genes, and oncogenes (Zhou, Zhao, et al. 2011).

Chronic and moderate exposures have been examined in a voluntary maternal continuous preference drinking (CPD) paradigm in B6 mice. The resulting PAE mice display relatively mild developmental delays, anxiety-related traits, and deficits in spatial learning (Kleiber et al. 2011). This treatment protocol has been previously shown by others to produce peak maternal blood alcohol concentrations of ~80–120 mg/dl (Allan et al. 2003; Boehm et al. 2008; Brady et al. 2012). The brains of adult PAE mice were also analyzed by gene expression arrays (Kleiber et al. 2012). Genes involved in embryonic and nervous system development showed subtle but consistent changes in expression. Furthermore, some of the genes identified have previously been associated with FASD-relevant endophenotypes. Such genome-wide gene expression results following different PAE paradigms are now common in the literature and pose the next logical question:

What maintains changes in brain gene expression caused by PAE in B6 mice? One of the most logical mechanisms that may account for long-term changes in gene expression are ethanol induced changes to epigenetic marks. Epigenetic marks maintain gene expression profiles without altering DNA sequence and are heritable in dividing cells. Epigenetic marks are involved in gene regulation at two distinct levels. The first occurs at the level of transcription, which is mainly accomplished by chromatin modifications, such as DNA methylation and histone post-translational modifications (Métivier et al. 2008). To this end DNA methylation has become among the most studied of such processes because of the relative ease and effectiveness of analytic technology. Furthermore, the second level of epigenetic regulation may be achieved post-transcriptionally by miRNAs and allows for the fine-tuning of gene expression (Moazed 2009). miRNAs are key regulators of eukaryotic gene expression that act via translational repression and mRNA decay (Friedman et al. 2009). The two aforementioned levels of epigenetic regulation are particularly crucial during embryonic development, where changes to the epigenome are critical in ongoing differentiation (Monk et al. 1987; Howlett & Reik 1991).

It is logical to argue that epigenetic mechanisms may provide the foundation for long-term alterations in gene expression and behavioral outcomes by ethanol's direct effect on epigenetic features, particularly DNA methylation (Garro et al. 1991; Haycock 2009; Kobor & Weinberg 2011). Such a hypothesis is backed by a number of independent and unrelated reports. For example, Liu *et al.* examined a whole embryonic culture of B6 mice at early neurulation (Liu et al. 2009). They observed alterations to methylation in genes involved in development and chromatin organization as well as in genes regulated by genomic imprinting (*Igf2r* and *Ube3a*). Furthermore, Kaminen-Ahola *et al.* examined the Agouti viable yellow (A^{VY}) B6 mouse model and found that continuous maternal preference drinking of 10% alcohol from GD0.5 to GD8.5 results in hypermethylation of the metastable epiallele, as well as postnatal craniofacial and growth defects in congenic PAE siblings. (Kaminen-Ahola et al. 2010). This study demonstrated that PAE during embryogenesis results in a long-term alteration to DNA methylation at a specific locus.

The transcriptional alterations induced by PAE are not limited to protein-coding genes. Interestingly, they also include miRNA expression (Miranda 2012). Sathayan *et al.* examined the effect of alcohol exposure on miRNA expression in GD12.5 B6

neurosphere cultures (Sathyan et al. 2007). It was observed that high and low ethanol doses alter different miRNAs. The target genes were generally involved in apoptosis and the cell cycle. Furthermore, Wang *et al.* showed that PAE induces altered expression of *mir-10a* and its target gene *Hoxa1* (Wang et al. 2009). Co-incubation of alcohol-exposed mouse embryos in folic acid, which is involved in establishing DNA methylation, prevented the alteration to miRNA and target mRNA. Such observations suggest that altered DNA methylation has the potential to directly or indirectly alter the expression of a specific set of miRNAs underlying PAE induced alterations to gene expression.

Genomically imprinted genes typically utilize differential DNA methylation at an imprinting control region (ICR) and studies have observed PAE induced alterations to imprinted genes (Liu et al. 2009; Shukla et al. 2011; Sittig et al. 2011; Dietz et al. 2012). Approximately 30% of genomically imprinted genes are hypothesized to be ncRNAs, including miRNAs (Morison et al. 2005). In the placenta, PAE was shown to induce alterations to DNA methylation at CTCF-binding sites within the differentially methylated region (DMR) of the imprinted gene *H19* (Haycock & Ramsay 2009). Genomic imprinting has been further examined in mouse embryos, where Downing *et al.* observed a ~8% decrease to methylation at a single CpG site in the imprinted *Igf2* DMR (Downing et al. 2011). Furthermore, associated transcripts showed a -1.5 fold change in gene expression. These observations were also extended mechanistically by placing mothers on a methyl-supplemented diet, which ameliorated some of the PAE endophenotypes. The above and related observations in the literature suggest that PAE may alter DNA methylation and thus suppress transcriptional machinery by altering the binding sites of a number of transcription factors. Based on these observations, I hypothesize that large-scale alterations to the epigenome, which may be initiated by PAE, occur in functional sites and maintain the observed long-term alterations to gene expression and behaviour that underlie FASD.

In this chapter, I present comprehensive epigenomic results from four paradigms of PAE. These include continuous preference drinking (CPD) by pregnant B6 mothers as well as injections (binge) during the B6 equivalent of the first (T1), second (T2), or third (T3) trimester of human pregnancy. The results are used to develop a generalized mechanism for alterations to gene expression and behaviour associated with PAE/FASD.

Specifically, the results identify long-term changes in DNA methylation, ncRNA, and mRNAs in the adult brain resulting from multiple PAE paradigms in B6 mice. The results of this chapter ultimately offer novel insights into the mechanisms maintaining FASD endophenotypes and may also be used towards translating rodent model research to human FASD studies.

2.3 Materials & Methods

The methodologies and workflow for the B6 mouse model are overviewed in **Figure 2.1**. The PAE paradigms utilized in this research relied on an established model for CPD (Kleiber et al. 2011) and three established binge injection paradigms (Mantha et al. 2013). The brains of the ethanol exposed and matched control animals were collected on post-natal day (PND) 70.

2.3.1 Mice

Male and female B6 mice were originally obtained from Jackson Laboratories (Bar Harbor, ME) and maintained at the Health Sciences Animal Care Facility at the University of Western Ontario (London, Ontario, Canada). The studies followed Canadian Council of Animal Care guidelines and approved by the Animal Use Subcommittee of the University of Western Ontario (**Appendix K**). All mice were housed in standard cages at 21–24°C with 40–60% humidity at a 14-hour light/10-hour dark cycle with access to food and water *ad libitum*. Virgin females of ~8 weeks of age were time-mated and assessed for pregnancy based on the presence of vaginal plugs (GD0). Pregnant females were transferred to individual cages during gestation. The individual females were exposed to ethanol or control using different treatment paradigms involving binge injections or continuous preference drinking by pregnant females. The resulting offspring were weaned on PND21 and housed in cages with two to four same-sex littermates. Only male offspring were used for all experimentation described in this research.

2.3.1.1 Chronic Alcohol Treatment of Pregnant Females by Continuous Preference Drinking (CPD)

Female mice were placed in individual cages, where they were acclimated to increasing concentrations of ethanol (towards a final of 10%) diluted in water, alongside freely available drinking water, for 2 weeks to establish a stable drinking pattern previously described by Kleiber and Wright (Kleiber et al. 2011; Kleiber et al. 2012). The female mice were then time-mated, where they had only access to water, and once the male was removed the ethanol was replaced to ensure exposure from GD0 to PND10. Control dams had access to water only. Voluntary maternal alcohol consumption and water consumption were measured daily from GD0 to PND10 for each female at 10:00 AM. Resulting pups, both alcohol-exposed and matched controls, were weaned at PND21 and housed in same-sex colony cages of two to four mice until PND70. These mice were raised and assessed by Ben Laufer & Eric Diehl.

2.3.1.2 Binge Alcohol Treatment of Pregnant Females by Acute Injections

The binge exposure models used in this thesis were established by Kleiber and Mantha (Mantha et al. 2013; Kleiber et al. 2013). Pregnant dams were subcutaneously injected with two 2.5 g/kg body weight doses of ethanol in 0.15 M saline (alcohol-treated) spaced 2 hours apart (at 0 hours and 2 hours), or with saline alone (control), at GD8 and GD11 (trimester 1; T1) or GD14 and GD16 (trimester 2; T2) (Ikonomidou et al. 2007; Mantha et al. 2014). Control and alcohol-treated dams were age- and weight-matched. Given that the third trimester human equivalent occurs postnatally in mice (Dobbing & Sand 1979), a binge exposure during this neurodevelopmental period was modeled by treating pups on PND4 and PND7 via subcutaneous injection (trimester 3; T3) (Kleiber, Laufer, et al. 2014). In this model, pups from one litter were matched across treatment groups for sex and weight to control for litter effects. Injections represented two doses of 2.5 g/kg body weight spaced 2 hours apart with matched controls receiving 0.15 M saline. All resulting offspring were weaned on PND21 and housed in cages with two to four

same-sex littermates. T1 & T2 mice were raised by Katarzyna Mantha and the T3 mice were raised by Morgan Kleiber.

2.3.1.3 Tissue Collection and Nucleic Acid Isolation

Alcohol-treated and matched control adult males (PD70) resulting from the four treatment paradigms ($n=12$ per paradigm with six alcohol-exposed and six matched controls) were sacrificed using CO₂ and cervical dislocation. Whole brains were extracted, snap frozen in liquid nitrogen, and stored at -80°C until RNA and DNA isolation. Whole-brain total RNA was isolated from frozen tissues using TRIzol® Reagent (Invitrogen, Carlsbad, CA), purified using the RNeasy® Mini Kit (QIAGEN, Valencia, CA), and quantified using a NanoDrop ND-1000 spectrophotometer (Thermo Fisher Scientific Inc., Wilmington, DE). Total RNA quality was assessed using the Agilent 2001 Bioanalyzer (Agilent Technologies Inc., Palo Alto, CA). Further, whole brain DNA was isolated from the interphase layer of TRIzol using sodium citrate, followed by ethanol precipitation and purification using the QIAamp® DNA Micro Kit (QIAGEN, Valencia, CA). DNA was then quantified using a NanoDrop ND-1000 spectrophotometer (Thermo Fisher Scientific Inc., Wilmington, DE) and all samples had OD260/OD280 nm ratios of 1.8–2.0 and OD260/OD230 nm ratios of 2.0–2.4.

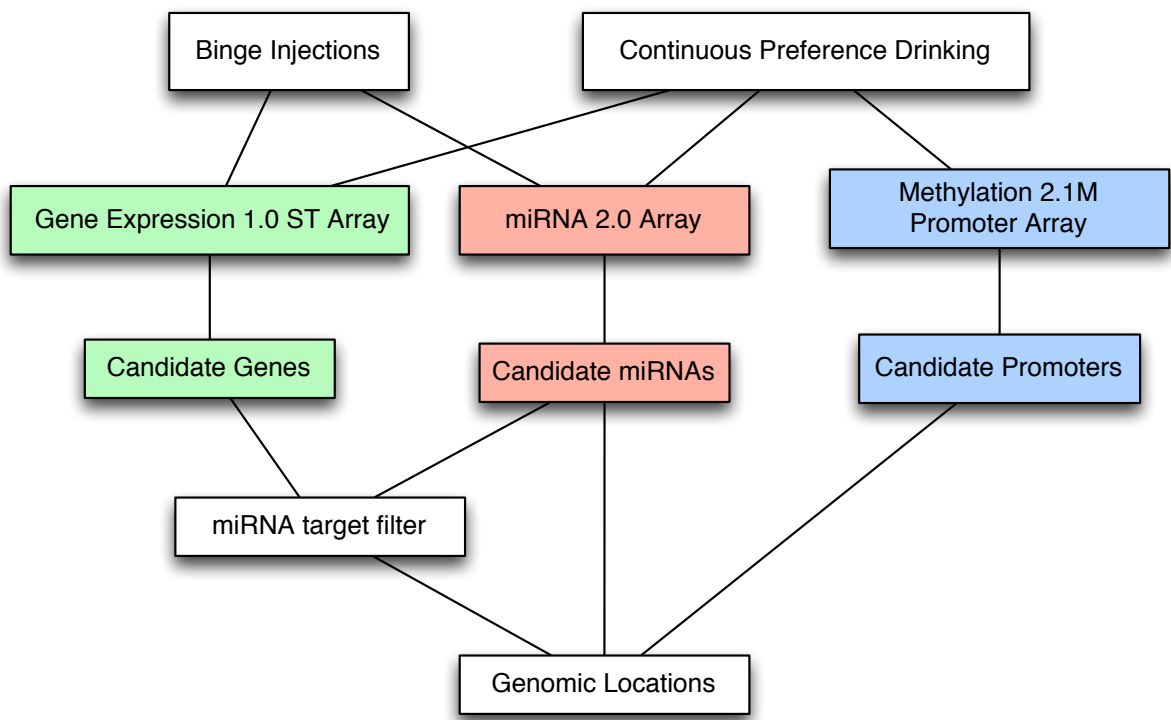


Figure 2.1. Flowchart of workflow used to analyze different exposure paradigms.

2.3.2 RNA Analysis

The RNA studies included in this thesis investigate both coding and non-coding RNAs. These studies relied on RNA isolated from the same mice and were used for hybridization on Affymetrix GeneChip® Mouse Gene 1.0 ST arrays and Affymetrix GeneChip® miRNA 2.0 arrays respectively. The RNA expression analysis primarily examined the CPD PAE paradigm (3 arrays with samples pooled in duplicate); however, the binge injection paradigms were also examined (2 arrays with samples pooled in triplicate).

2.3.2.1 Gene Expression Arrays

Affymetrix gene expression arrays are single channel arrays that have proved useful for the study of ethanol exposure in mice (Kerns & Miles 2008). The Affymetrix GeneChip® Mouse Gene 1.0 ST array (Affymetrix, Santa Clara, CA) consists of 770,317 unique 25-mer perfect match probes that are targeted across 28,853 transcripts, with 1,305 of those being ncRNA, and an average of 27 probes for a gene.

The Affymetrix GeneChip® Mouse Gene 1.0 ST array was used to analyze PAE induced alterations to gene expression. Single-stranded complementary DNA (sscDNA) was prepared from 200 ng of total RNA as per the Ambion WT Expression Kit for Affymetrix GeneChip Whole Transcript WT Expression Arrays (Applied Biosystems, Carlsbad, CA) and the Affymetrix GeneChip WT Terminal Labeling kit and Hybridization User Manual (Affymetrix, Santa Clara, CA). Total RNA was first converted to complementary DNA (cDNA), followed by *in vitro* transcription to make cRNA. By subjecting the cDNA to a cRNA conversion, a biotinylated Uracil analogue is incorporated. The biotin molecules can then be used to attach fluorescent molecules to label the cRNA. Subsequently, 5.5 µg of sscDNA was synthesized, end-labeled, and hybridized for 16 hours at 45°C to Mouse Gene 1.0 ST arrays. GeneChip Fluidics Station 450 performed all liquid handling steps, and GeneChips were scanned with the GeneChip Scanner 3000 7G using the Command Console v1.1 (Affymetrix, Santa Clara, CA). All hybridizations were performed at the London Regional Genomics Centre at the Robarts Research Institute, University of Western Ontario. Probe level (.CEL file) data were

generated using the Affymetrix Command Console v1.1. The .CEL files identify intensities of individual probes.

Probes, which have multiple replicates and target exons, were assembled into probesets that represent single genes. This summarization of the .CEL files was done in Partek Genomics Suite v6.5 (Partek Inc., St Louis, MO) by quantile normalization using the RMA algorithm adjusted for GC content and log₂-transformed (Irizarry et al. 2003). Partek software was then used to determine gene level one-way ANOVA *p*-values and fold changes. All arrays were analyzed by using a 1.2-fold cut-off with a significance threshold of *p*=0.05 to generate a list of genes of interest to be assessed further using bioinformatic analysis of gene ontologies and pathways. The gene expression array results for the T1, T2, T3, and CPD paradigms were deposited within the NCBI GEO database under accessions GSE34469 (T1 & T2), GSE34549 (T3) and GSE34305 (CPD, experiment 2). The data from CPD mice were generated by Ben Laufer, T1 & T2 mice by Katarzyna Mantha, and T3 mice by Morgan Kleiber.

2.3.2.2 miRNA Expression Arrays

The Affymetrix GeneChip® miRNA 2.0 array is based on a similar design as the Affymetrix GeneChip® Mouse Gene 1.0 ST array, and has probes that are 25-mer. However, smaller probes are used if the miRNA is less than 25 bases. The miRNA array targets 722 mouse mature miRNAs, 690 mouse pre-miRNA, and 2,334 small RNAs from humans that include snoRNAs. It also has 9 probes per a probe set for a miRNA. The workflow is also similar to Affymetrix GeneChip® Mouse Gene 1.0 ST arrays.

In order to investigate the effect of PAE on miRNAs, all samples were analyzed at the London Regional Genomics Centre (Robarts Research Institute, London, Ontario) using Affymetrix miRNA 2.0 arrays. Briefly, 1 µg total RNA from each treatment paradigm was labeled using the Flash Tag Biotin HSR kit (Genisphere, Hatfield, PA) and hybridized to Affymetrix miRNA 2.0 arrays for 16 hours at 45°C. Probe level (.CEL file) data were generated using Affymetrix Command Console v1.1. Probes were summarized to gene level data in Partek Genomics Suite v6.6 (Partek Inc., St Louis, MO) by using the RMA algorithm (Irizarry et al. 2003). Partek software was used to determine differences between control and ethanol-treated samples by a one-way ANOVA and corresponding

P-values and fold changes. For each treatment model, the miRNAs present on this array were filtered using stringency criteria of 1.2-fold change ($p<0.05$) and subjected to a hierarchical clustering analysis by using Euclidean distance and average linkage to assess consistency in ethanol response between the arrays of different treatment paradigms. The miRNA expression array results for all treatment protocols were deposited within the NCBI Gene Expression Omnibus (GEO) database under accession GSE34413. Analyses of CPD mice were performed by Ben Laufer, T1 & T2 mice by Katarzyna Mantha and Ben Laufer, and T3 mice by Morgan Kleiber and Ben Laufer.

2.3.2.3 Quantitative PCR Confirmation

The quantitative polymerase chain reaction (qPCR) allows for real-time quantification of DNA amplification by optically measuring fluorescent dyes after laser excitation (Fraga et al. 2008). Taqman® is a methodology that utilizes sequence-specific oligonucleotide probes attached to both a fluorophore and a quencher molecule, which prevents fluorescence. During qPCR, the probe will hybridize to complementary DNA and will then be degraded by Taq polymerase, which releases the fluorophore from the quencher and allows it to be detected after excitation. qPCR technology can also be coupled with reverse transcription (RT) to enable the study of both coding and non-coding RNA expression.

In order to confirm gene expression results, cDNA was reverse transcribed from whole-brain RNA of the CPD paradigm ($n=6$) and matched controls ($n=6$). For mRNA expression, cDNA was created using Applied Biosystems High-Capacity cDNA Reverse Transcription Kit (Foster City, CA) and sequence specific TaqMan™ assays (Foster City, CA), which were used according to the manufacturer's protocol. For miRNA expression, the Applied Biosystems TaqMan™ MicroRNA Reverse Transcription Kit (Foster City, CA), which uses stem-loop reverse transcription primers (Chen et al. 2005), and sequence specific TaqMan™ MicroRNA Assays (Foster City, CA) were used according to the manufacturer's protocol. All TaqMan™ probes were selected using the Applied Biosystems (Carlsbad, CA) search engine to identify previously characterized TaqMan™ assays. *GAPDH* was chosen as an endogenous control for mRNA expression, while *snoRNA 202* was chosen as an endogenous control for miRNA expression (Gao et al.

2010). The target and control reactions were run in separate tubes on the same plate for each sample as per the manufacturer's protocol. Three technical replicates were averaged for both the endogenous control and gene of interest for each sample. qPCR reactions were performed on the Applied Biosystems StepOne™ Real-Time PCR System 2.0 according to the manufacturer's protocol. Fold change was calculated using the $\Delta\Delta Ct$ method (Schmittgen & Livak 2008). The $\Delta\Delta Ct$ method allows for relative quantification of gene expression from qPCR experimentation. C_t is the threshold cycle, which is the PCR cycle where fluorescence exceeds a threshold value. The $\Delta\Delta Ct$ method compares C_t 's for an experimental gene to a reference gene across both the experimental and control group. The results were analyzed using Applied Biosystems DataAssist™ Software v3.0. Statistical significance was assessed by an unpaired Student's *t*-test.

2.3.2.4 Bioinformatic Analysis of Differentially Expressed Probe Sets (mRNAs and miRNAs)

The chromosomal locations for all miRNAs were determined by using miRBase and Ensembl (Flicek et al. 2011; Kozomara & Griffiths-Jones 2011). Genomically imprinted regions were identified by the mouse imprinting catalog (www.mousebook.org).

Data from the CPD paradigm were analyzed through the use of Ingenuity® microRNA target filter [Ingenuity® Systems (www.ingenuity.com)] to generate lists of interactions between genes and miRNAs of interest from the TargetScan Human database (mouse was not available at the time). Results were filtered based on a moderate or high confidence of interaction (Lewis et al. 2005; Vergoulis et al. 2012), brain specificity, and an inverse miRNA to target mRNA expression relationship. miRNAs were filtered based on a 1.15 fold change and a $p<0.3$ cut-off. This analysis is referred to as the original (2012) analysis.

At a later date, updated (2016) annotations and improved software became available for the gene expression and miRNA arrays. These updates offered some improvement and thus were utilized for a re-analysis. Enrichr was used for biological, cellular, and molecular ontologies (Chen et al. 2013). Partek Pathways was used for canonical KEGG pathways. Gene annotations were obtained from UniProt (UniProt-

Consortium 2014). An updated and more stringent (1.2 fold change, $p<0.05$) miRNA target filter analysis was done in Partek using Mouse TargetScan 6.2. This analysis is referred to as the updated (2016) analysis.

2.3.3 DNA Analysis

The DNA studies included in this thesis investigate DNA cytosine methylation. These studies relied on DNA isolated from the same CPD mice used for RNA analysis.

2.3.3.1 DNA Methylation (MeDIP-Chip) Arrays

The DNA methylation analysis of the mice utilized MeDIP-Chip tiling arrays of promoter regions and analyzed the CPD PAE paradigm. The NimbleGen MM9 2.1M deluxe promoter array v2 is a two channel array that contains 2.1 million 50-75mer probes that utilize methylated DNA immunoprecipitation (MeDIP) and a tiling approach to examine DNA methylation. MeDIP involves enriching for 5mC with an antibody to immunoprecipitate ~500 bp fragments with the mark (Weber et al. 2005; Mohn et al. 2009). In MeDIP-Chip, the MeDIP reaction is then coupled to a microarray chip, where the enriched DNA is labelled green with Cy3 and the input sample from before enrichment is labelled red with Cy5. The deluxe promoter array tiles approximately 8.2 kb upstream and 3 kb downstream all 22,425 MM9 mouse gene promoters, 20 kb upstream of 510 mature miRNA transcripts, 16,002 CpG islands, and other biologically relevant sites identified from ENCODE. It also includes positive, negative, and non-CpG control sites. MeDIP-Chip allows for a relative level of methylated DNA enrichment to be analyzed by bioinformatic algorithms, which can determine differentially methylated regions (DMRs). However, MeDIP-Chip does not offer single nucleotide resolution, as the lower detection limit is 2 methylated CpG sites per a DNA fragment. Previous versions of this array have been used successfully in PAE rodents embryos and candidates were confirmed using Sequenom EpiTYPER DNA methylation analysis (Liu et al. 2009; Zhou, Balaraman, et al. 2011).

In order to examine PAE-induced alterations to genome-wide DNA methylation by MeDIP-Chip, equal amounts of brain DNA from two non-littermate males from the CPD paradigm were pooled per biological replicate ($n=3$) to reduce potential litter effects.

All methylated DNA immunoprecipitation (MeDIP), sample labeling, hybridization and processing were performed at Arraystar Inc. (Rockville, MD). Briefly, genomic DNA was sonicated to 200- to 1000-bp fragments followed by immunoprecipitation of methylated DNA using Biomag™ magnetic beads coupled to mouse monoclonal antibody against 5-methylcytidine (Diagenode). The DNA was eluted, whole genome amplified, and purified. The total input and immunoprecipitated DNA were labeled with Cy3- and Cy5-labeled random 9-mers, respectively, and hybridized to the NimbleGen MM9 DNA Methylation 2.1M Deluxe array (Roche NimbleGen Inc., Madison, WI). Scanning was performed with the Axon GenePix 4000B microarray scanner.

Raw data from three arrays were extracted as pair-files by NimbleScan software (Roche NimbleGen Inc.). Median-centering, quantile normalization, and linear smoothing by Bioconductor packages Ringo, limma and MEDME were performed to generate normalized log2-ratio data. From the normalized log2-ratio data, a sliding-window peak-finding algorithm provided by NimbleScan v2.5 (Roche NimbleGen Inc.) was applied to find the enriched peaks with specified parameters (sliding window width: 750 bp; mini probes per peak: 2; maximum spacing between nearby probes within peak: 500 bp). The identified peaks were mapped to genomic features: transcripts and CpG Islands. The MA plots and box-plots were applied to assess the quality of raw data and effect of normalization. A correlation matrix was used to describe correlation among replicate experiments.

To compare differentially enriched regions between ethanol-exposed (E) and matched control (C) mice, the log2-ratio values were averaged and then used to calculate the M' value [$M' = \text{Average}(\log_2 \text{MeDIP}_E/\text{Input}_E) - \text{Average}(\log_2 \text{MeDIP}_C/\text{Input}_C)$] for each probe. The NimbleScan sliding-window peak-finding algorithm (Scacheri et al. 2006) was run on the data to find the differential enrichment peaks (DEPs). The differential enrichment peaks, called by the NimbleScan algorithm, were filtered according to the following criteria: (i) at least one of the two groups had the median value of $\log_2 \text{MeDIP}/\text{Input} \geq 0.3$ and a median value of $M' > 0$ within each peak region; (ii) at least half of the probes in a peak had the median value of coefficient of variability (CV) ≤ 0.8 in both groups within each peak region.

Using an R script, a hierarchical clustering analysis was completed. The probe data matrix was obtained by using PeakScores from DMRs selected by DEP analysis. ‘PeakScore’ is a measure calculated from the *P*-values of the probes within the peak and reflects the significance of the enrichment. This analysis used a ‘PeakScore’ ≥ 2 to define the DEPs by using the NimbleScan sliding-window peak-finding algorithm. The peak score is a $-\log_{10}$ transformed *P*-value, which is the average of the *P*-values for all probes within the peak. Therefore, a ‘PeakScore’ ≥ 2 means the average *P*-value was ≤ 0.01 . This analysis is referred to as the original (2012) analysis.

For the purpose of comparing more directly to the next chapter of this thesis an updated analysis of the methylation data was also later carried out using Partek Genomics Suite Version 6.6. While Partek had gained some capability to analyze the methylation array from raw scans in 2016, it was only under limited support and not fully featured. This analysis is referred to as the updated (2016) analysis.

For the updated (2016) analysis, the 635 nm and 532 nm scans (.pair files) were analyzed in Partek Genomics Suite Version 6.6 and normalized using the default settings for the tiling workflow. An ANOVA was used to analyze each probe and then the model-based analysis of tiling-arrays (MAT) algorithm (Johnson et al. 2006) was used to detect differentially methylated regions (DMRs). The DMRs were then annotated to genes if they occurred in the gene body or were 5000 bp to -3000 bp from the transcriptional start site. The list of genes overlapping DMRs with a MAT *p*-value of <0.005 was used for bioinformatic analysis. The software was not able to produce a proper principle components analysis, heatmaps, or fully present sequence annotations. Thus, the updated (2016) analysis is presented in addition and as complement to the original (2012) analysis.

2.3.3.2 Bioinformatic Analysis of Differently Methylated Genes

For the original (2012) analysis, the top gene promoters identified from the DNA methylation arrays were subjected to Ingenuity Pathway Analysis. The genes corresponding to all previously identified significantly affected promoters were subjected to an Ingenuity Core Analysis. The Ingenuity Knowledge Base (genes only) was used to examine direct and indirect relationships. Results were filtered to consider only molecules

and/or relationships specific to species (mouse, rat, or human) and tissues (nervous system). From the identified ‘Behavior, Neurological Disease, and Psychological Disorders’ network, 30 significantly differentially methylated peaks belonging to different regions of the promoters of hub genes were examined for CTCF-binding sites using the CTCFBS prediction tool (Bao et al. 2008). The genes identified as having CTCF-binding sites were then subjected to a pathway analysis using GeneMANIA (Warde-Farley et al. 2010). Gene annotations were obtained from UniProt (UniProt Consortium 2014). For the updated (2016) analysis, Enrichr (Chen et al. 2013) was used for ontologies and Partek Pathways for canonical pathways.

2.4 Results

2.4.1 Differential Gene (mRNA) Expression

The first set of experiments in this chapter identified alterations to gene expression in CPD PAE brains at PND70 using Affymetrix GeneChip® Mouse Gene 1.0 ST arrays. Principle component analysis (PCA), which examines total signal from the arrays, correctly distinguishes CPD PAE mice from matched controls (**Figure 2.2**). After filtering, there were 783 significantly ($p<0.05$) altered (fold-change cut-off of 1.2) transcripts. A heatmap of the significant alterations distinguishes CPD from matched controls and illustrates that the majority of differentially expressed transcripts are up-regulated by PAE at this level of filtering (**Figure 2.3**). Notably, 456 of the differentially expressed transcripts were ‘housekeeping’ internal control exons and introns that did not have available annotations. Furthermore, 31 of the differentially expressed transcripts were miRNAs and 116 transcripts were largely unannotated expressed sequences identified by consortiums, with most having no predicted protein function. The top differentially expressed transcripts with a gene symbol are presented in **Table 2.1**. The 269 genes annotated with symbols were analyzed with Enrichr for gene ontologies and Partek pathways identified several altered canonical pathways (**Table 2.2**).

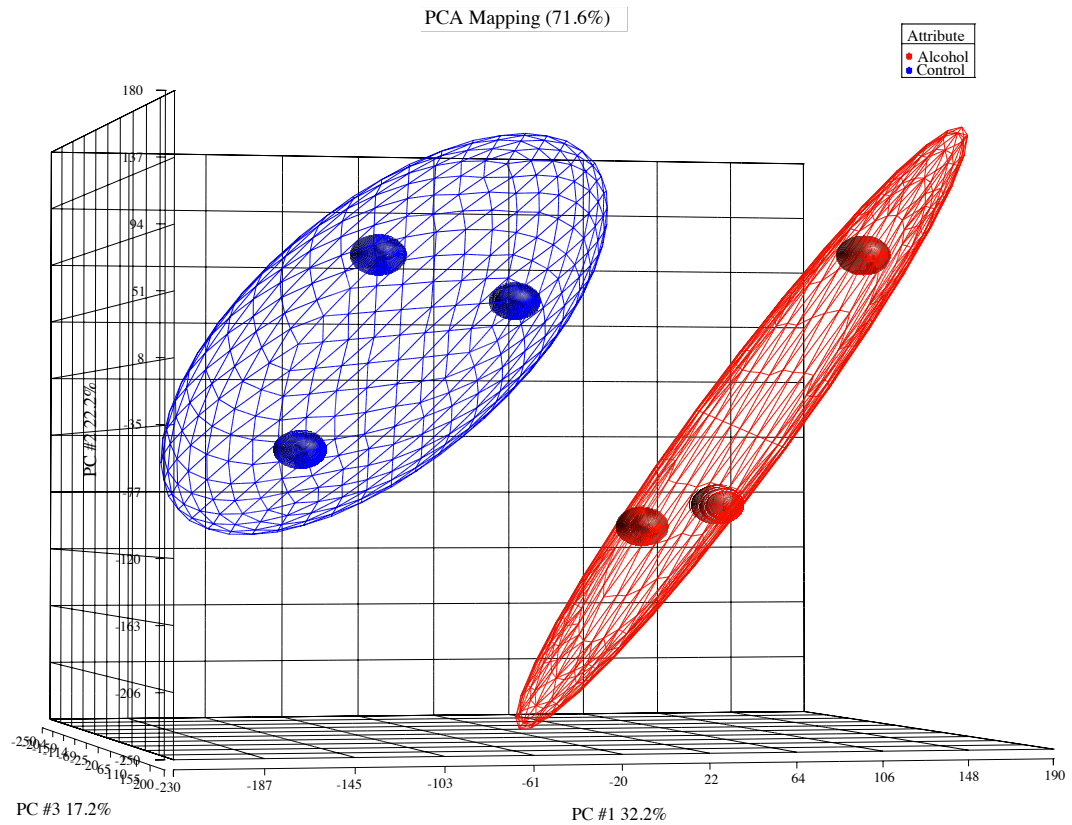


Figure 2.2. PCA analysis of gene expression arrays from CPD PAE (red) and matched control (blue) adult brains. Each point represents a single array and ellipsoids have been placed around groups to allow for visual clustering.

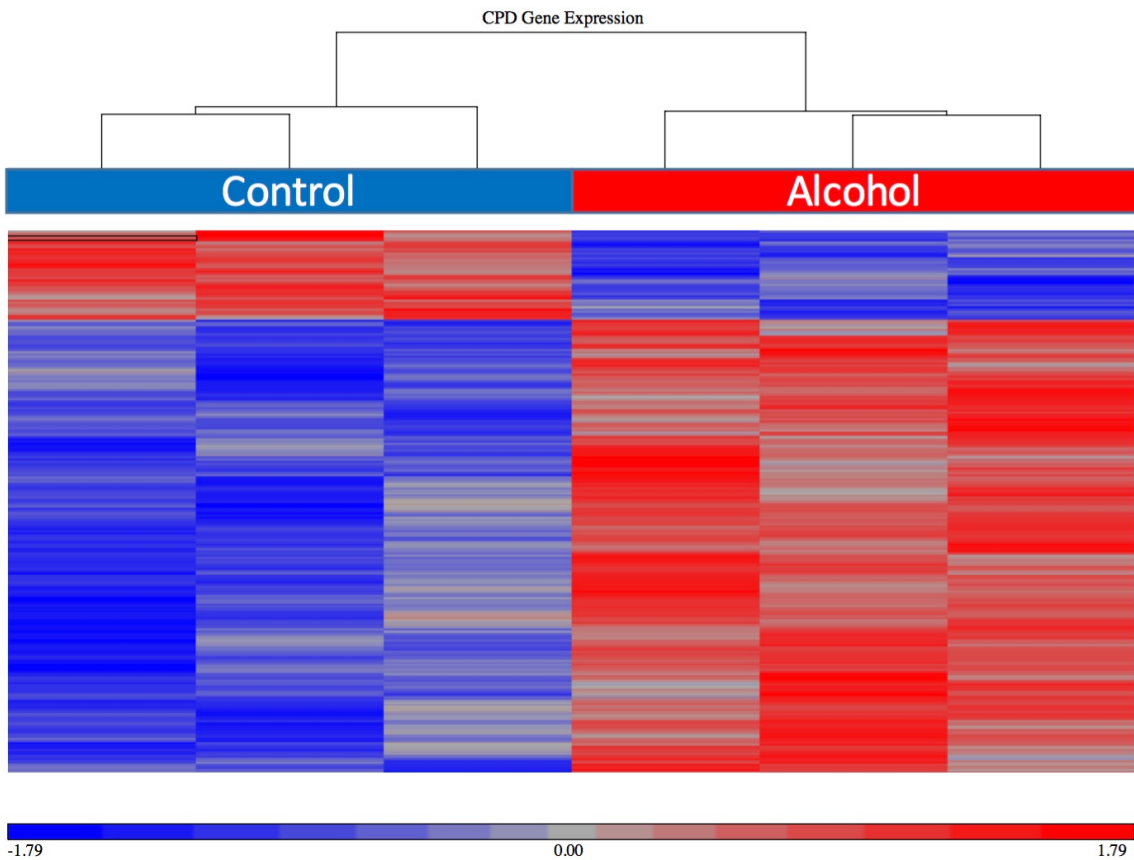


Figure 2.3. Heatmap of significant ($p < 0.05$) differential (fold change cut-off 1.2) gene expression in CPD PAE and matched control adult brains. The expression (intensity) of each gene (probe set) is normalized by being standardized to a mean of 0 and a standard deviation of 1. Genes with no change are displayed with a value of zero (grey), upregulated genes have a positive value (red), and down-regulated genes have negative values (blue).

Table 2.1. Top differentially-expressed transcripts in CPD adult mouse brains that were annotated with a gene symbol.

PAE Upregulated

Fold Change	p-value	Symbol	Gene Name	Gene Function
1.9	0.002	Gm26315	Unknown	Unknown
1.8	0.027	Gm10115	Unknown	Unknown
1.6	0.022	AY512949	Unknown	Unknown
1.6	0.004	Gm16498	Unknown	Unknown
1.6	0.002	Gm22260	Unknown	ncRNA
1.6	0.010	Gm10304	Unknown	Expressed in adult male diencephalon
1.5	0.014	Gm23422	Unknown	ncRNA
1.5	0.038	Gm22951	Unknown	ncRNA
1.5	0.009	9330155M09Rik	Unknown	Expressed in adult male hypothalamus
1.5	0.017	Prp2	Proline rich protein 2	Secreted Protein

PAE Downregulated

Fold Change	p-value	Symbol	Gene Name	Gene Function
-1.4	0.0126	Mrpl46	39S ribosomal protein L46, mitochondrial	Mitochondrial translational regulation
-1.3	0.0386	Prg4	Proteoglycan 4	Skeletal and cartilage development
-1.3	0.0002	Nuak1	NUAK family SNF1-like kinase 1	Cell Adhesion and DNA Damage
-1.3	0.0377	Vmn1r-ps77	Vomeronasal 1 receptor, pseudogene 77	Pheromone receptor pseudogene
-1.3	0.0031	Zfp518a	Zinc finger protein 518A	Transcriptional Regulation
-1.3	0.0427	Ucma	Unique cartilage matrix-associated protein	Skeletal and cartilage development
-1.3	0.0035	Ssna1	Sjogren syndrome nuclear autoantigen 1	Cytoskeleton and Cell Cycle
-1.3	0.0087	Phkg2	Phosphorylase b kinase gamma catalytic chain	Neural and hormonal regulation of glycogen breakdown
-1.3	0.0080	Cldn1	Claudin-1	Cell Adhesion
-1.3	0.0002	Serpingle1	Plasma protease C1 inhibitor	Complement and coagulation cascade [Immune Process]

Table 2.2. Ontologies and pathways for differentially-expressed genes ($p<0.05$, and a fold-change cut-off of 1.2) from CPD adult mouse brains.

Enrichr GO Biological Processes	Overlap	p-value
Regulation of complement activation	3/27	2.6E-04
Regulation of protein activation cascade	3/29	3.2E-04
Dendritic spine morphogenesis	2/8	7.6E-04
Regulation of humoral immune response	3/45	1.1E-03
Regulation of cell communication by electrical coupling	2/10	1.1E-03
Dendritic spine organization	2/13	1.7E-03
Aging	5/204	1.8E-03
Enrichr GO Cellular Location	Overlap	p-value
Extracellular space	15/1120	1.7E-04
Blood microparticle	4/161	7.3E-03
Voltage-gated calcium channel complex	2/38	1.5E-02
Platelet alpha granule lumen	2/48	2.3E-02
Chloride channel complex	2/50	2.4E-02
Outer membrane	3/137	2.8E-02
Serine/threonine protein kinase complex	2/56	3.0E-02
Enrichr GO Molecular Function	Overlap	p-value
Solute:cation antiporter activity	2/28	6.8E-03
Peptidase activator activity	2/37	1.1E-02
Peptidase regulator activity	4/209	1.2E-02
Hormone activity	3/122	1.5E-02
Growth factor binding	3/123	1.5E-02
Nucleotidyltransferase activity	3/140	2.1E-02
Antiporter activity	2/62	2.9E-02
Partek KEGG Pathways	Overlap	p-value
Complement and coagulation cascades	5/71	3.2E-03
Purine metabolism	7/171	9.1E-03
Taste transduction	4/59	9.5E-03
Prion diseases	3/31	1.0E-02
Pyrimidine metabolism	5/99	1.2E-02
Antigen processing and presentation	4/72	1.8E-02
Ribosome	5/133	3.6E-02

Prenatal ethanol induced mRNA (*Pnet-ps*) was the most significant ($p=0.0001$) differentially expressed (1.2 fold increase) gene in the CPD model. *Pnet-ps* was also significantly up-regulated in the T1 model (1.3 fold change, $p=0.003$) (Kleiber et al. 2013). *Pnet-ps* is a pseudogene that appears to be a lncRNA. However, the biological function and genomic properties remain a mystery as there is only one report that used subtractive hybridization, which is a technique able to detect novel transcripts. In that report four transcripts were examined in the neural tube of mouse embryos 1 hour after ethanol treatment (Du & Hamre 2003). While three of the genes detected were previously annotated, one novel transcript (*Pnet-ps*) was detected and showed a seven-fold increase in expression in ethanol-treated embryos. This expression was found to be induced in PAE embryonic brains and also possibly present at a low level in control hearts. In this chapter, both the CPD and T1 models showed a subtler increase; however, the observation demonstrates that a transcript which shows highly increased expression 1 hour after PAE is still altered in the same direction 70 days later in the adult brain.

Trdn was the only protein coding gene to be altered across all exposure paradigms. It showed a significant ($p<0.05$) 1.3, -1.6, -2.2, and 1.2 fold change in the T1, T2, T3, and CPD paradigms respectively. *Trdn* is involved in the release of calcium ions from the sarcoplasmic reticulum, which is a key step in the contraction of cardiac and skeletal muscle (Roux-buisson et al. 2012). Notably, *Trdn* showed a significant ($p<0.05$) 1.5 fold change in PND7 hippocampus from a rat model that was developmentally exposed to a polychlorinated biphenyl (PCB), which acts as a teratogen (Royland & Kodavanti 2008).

2.4.2 Differential ncRNA Expression

The second set of experiments in this chapter identified differences related to ncRNA expression by utilizing Affymetrix GeneChip® miRNA 2.0 arrays and Affymetrix GeneChip® Mouse Gene 1.0 ST arrays. The differential ncRNA expression is represented by two sets of observations. The first set of observations is of the reciprocal differential expression of miRNAs and target genes in CPD PAE mice at PND70. The second set of observations is of miRNA and snoRNA expression in multiple exposure paradigms at PND70. In addition to CPD, binge PAE (injection) at the first (T1), second

(T2) and third (T3) trimester equivalents of human development were analyzed to confirm and expand on the CPD results in the second set of observations. The long-term gene expression alterations from the binge injection models have been compared (Kleiber et al. 2013; Kleiber, Diehl, et al. 2014) and detailed ncRNA expression analysis is available for the T2 (Mantha et al. 2014) and T3 (Stringer et al. 2013; Kleiber, Laufer, et al. 2014) binge exposure paradigms.

2.4.2.1 Reciprocal Differential miRNA and Target Gene Expression

For the original (2012) analysis, IPA's miRNA Target Filter® was used to analyze all possible miRNA and target-gene interactions from the miRNA and gene expression array data sets for the CPD PAE paradigm. The results were filtered based on the confidence of interaction, brain specificity, and an inverse miRNA to target mRNA relationship (**Appendix A**). The miRNA analysis was also updated in 2016 (**Table 2.3**). An updated (2016) target filter analysis was carried in Partek out under more stringent conditions using the mouse-specific TargetScan database and updated annotations for both arrays (**Table 2.4**).

The Partek miRNA target filter revealed two mRNAs (*Slitrk2* and *Otx2*) that had a reciprocal alteration with a shared miRNA (*mir-130b*, 1.2 fold increase) (**Table 2.4**). *Slitrk2* was downregulated (-1.2), whereas one of the IPA target filter predicted miRNAs (*mir-17**) was upregulated (**Appendix A**). *Slitrk2* is expressed in the developing embryo and adult neurons, where it has an inhibitory effect on neurite outgrowth (Aruga & Mikoshiba 2003). *Otx2* was downregulated (-1.3) along with one of its IPA target filter predicted miRNAs (*mir-152*) being upregulated (**Appendix A**). *Otx2* is a homeobox gene that is involved in embryonic head development as well as in the neuroplasticity of GABAergic interneurons in the visual cortex and has been implicated in mood disorders (Acampora et al. 1995; Sabuncian et al. 2007; Sugiyama et al. 2009). Interestingly, both of the above genes are involved in neurodevelopmental processes and were predicted by the Partek target filter to be targeted by a single miRNA.

Aak1 (1.2 fold change, $p=0.007$) showed increased expression, while a number of miRNAs predicted to target it by both IPA and Partek being downregulated (**Table 2.4**

and Appendix A). In the T2 binge PAE model, *Aak1* (1.2 fold change, $p=0.027$) showed an increase in expression and two miRNAs predicted to target it, *mir-10b* (-1.5 fold change, $p=0.002$) *mir-342-5p* (-1.3 fold change, $p=0.025$), showed decreased expression (Mantha et al. 2014; Kleiber, Diehl, et al. 2014). AAK1 is a kinase that regulates clathrin-mediated endocytosis, which is a process that recycles synaptic vesicles at presynaptic terminals (Conner & Schmid 2002; Saheki & De Camilli 2012). Furthermore, AAK1 is a positive regulator of the Notch signaling pathway and directly interacts with an active and membrane-tethered form of Notch that results in part from metalloprotease cleavage by the ADAM gene family (Gupta-Rossi et al. 2011). Other notable candidates identified by the Partek miRNA target filter include *Rnf165* and *Nlrc5* (**Table 2.4**). RNF165 was shown to mediate motor axon extension by BMP-Smad signaling (Kelly et al. 2013). NLRC5 has a role in immune response, where it is a negative regulator of the NF-kappaB and type I interferon signaling pathways (Cui et al. 2010). Finally, both the original (2012) and updated (2016) analysis of altered miRNAs found that *let-7* miRNA(s) were down-regulated (**Table 2.4**). Notably, *let-7* miRNAs promote differentiation over pluripotency and are involved in neurodevelopment (Mayr et al. 2007; Worringer et al. 2014; Ivakhnitskaia et al. 2016)

Table 2.3. Updated (2016) analysis of significant differentially-expressed mouse miRNAs in CPD adult brains ($p<0.05$ and 1.2-fold change cut-off).

miRNA	p-value	Fold Change
<i>mmu-miR-466d-3p</i>	0.023	1.6
<i>mmu-miR-181c</i>	0.040	1.6
<i>hp mmu-mir-686</i>	0.020	1.3
<i>hp mmu-mir-147</i>	0.018	1.3
<i>hp mmu-mir-708</i>	0.044	1.3
<i>hp mmu-mir-28</i>	0.028	1.3
<i>mmu-miR-130b</i>	0.017	1.2
<i>mmu-miR-322*</i>	0.023	1.2
<i>hp mmu-mir-291a</i>	0.015	1.2
<i>hp mmu-mir-146b</i>	0.011	1.2
<i>mmu-miR-151-5p</i>	0.017	1.2
<i>hp mmu-mir-181b-2</i>	0.046	1.2
<i>mmu-miR-291a-5p</i>	0.037	1.2
<i>mmu-miR-669o</i>	0.039	-1.2
<i>hp mmu-mir-491</i>	0.005	-1.2
<i>mmu-miR-27b*</i>	0.010	-1.2
<i>mmu-miR-488</i>	0.048	-1.2
<i>hp mmu-mir-22</i>	0.032	-1.3
<i>hp mmu-mir-707</i>	0.045	-1.3
<i>hp mmu-mir-325</i>	0.046	-1.3
<i>mmu-miR-683</i>	0.002	-1.3
<i>hp mmu-mir-193</i>	0.016	-1.3
<i>mmu-let-7g</i>	0.012	-1.3
<i>hp mmu-mir-340</i>	0.024	-1.3
<i>mmu-let-7f</i>	0.041	-1.3
<i>hp mmu-mir-98</i>	0.001	-1.3
<i>mmu-miR-1306</i>	0.025	-1.3
<i>mmu-miR-146a</i>	0.042	-1.4
<i>mmu-miR-93*</i>	0.007	-1.4
<i>mmu-let-7f*</i>	0.039	-1.4
<i>mmu-miR-122</i>	0.026	-1.5
<i>mmu-miR-150*</i>	0.034	-1.5
<i>mmu-miR-369-5p</i>	0.025	-1.7
<i>mmu-miR-299*</i>	0.029	-1.8

Note: hp = hairpin precursor and * = star

Table 2.4. Updated (2016) Partek miRNA target filter analysis ($p<0.05$ and 1.2-fold change cut-off) of differentially expressed genes and associated miRNAs identified in CPD adult brains.

miRNA	p-value	Fold Change	Gene	p-value	Fold Change
<i>mmu-miR-146a</i>	0.0424	-1.4	<i>Trp53rka</i>	0.0196	1.2
<i>mmu-miR-683</i>	0.0022	-1.3	<i>Aak1</i>	0.0007	1.2
<i>mmu-let-7g</i>	0.0116	-1.3	<i>Aak1</i>	0.0007	1.2
<i>mmu-let-7f</i>	0.0410	-1.3	<i>Aak1</i>	0.0007	1.2
<i>mmu-let-7g</i>	0.0116	-1.3	<i>Nlrc5</i>	0.0103	1.3
<i>mmu-let-7f</i>	0.0410	-1.3	<i>Nlrc5</i>	0.0103	1.3
<i>mmu-miR-130b</i>	0.0170	1.2	<i>Otx2</i>	0.0162	-1.3
<i>mmu-miR-683</i>	0.0022	-1.3	<i>Rnf165</i>	0.0128	1.2
<i>mmu-let-7g</i>	0.0116	-1.3	<i>Rnf165</i>	0.0128	1.2
<i>mmu-let-7f</i>	0.0410	-1.3	<i>Rnf165</i>	0.0128	1.2
<i>mmu-miR-488</i>	0.0476	-1.2	<i>Rnf165</i>	0.0128	1.2
<i>mmu-miR-130b</i>	0.0170	1.2	<i>Slitrk2</i>	0.0002	-1.2

Results were obtained from the 2016 analysis of gene and miRNA expression arrays respectively.

2.4.2.2 Confirmations of Differential Expression

The results observed on the two independent array platforms for the CPD PAE mice were then examined by quantitative PCR (qPCR). Although the qPCR results showed similar fold changes to the arrays for all genes of interest examined (*Pten*, *Nmnat1*, *Slitrk2* and *Otx2*), they were not statistically significant ($p=0.122$, $p=0.129$, $p=0.452$ and $p=0.078$, respectively).

However, it is worth noting that the gene expression and miRNA arrays used were independent platforms that contained different probes for the same snoRNAs and miRNAs. The results showed that some ncRNAs are similarly affected on the two (miRNA and gene expression) arrays. For example, the *MBII-52* snoRNA (*Snord115*) belonging to *Snrpn-Ube3a* is upregulated (**Appendix D**).

Despite difficulties with confirming gene expression, a miRNA identified in the CPD model by the original (2012) IPA analysis was confirmed by qPCR. *mir-679-5p*, which is located in the *Dlk1-Dio3* region, showed a 1.45-fold increase ($p=0.019$) in mice that were treated with ethanol during neurodevelopment via maternal CPD (**Figure 2.4**). The results provide support for the two independent (miRNA and gene expression) array platforms that showed 1.2 ($p=0.03$)- and 1.4 ($p=0.04$)-fold increases, respectively. Notably, this miRNA was not identified as significant in the updated (2016) miRNA analysis.

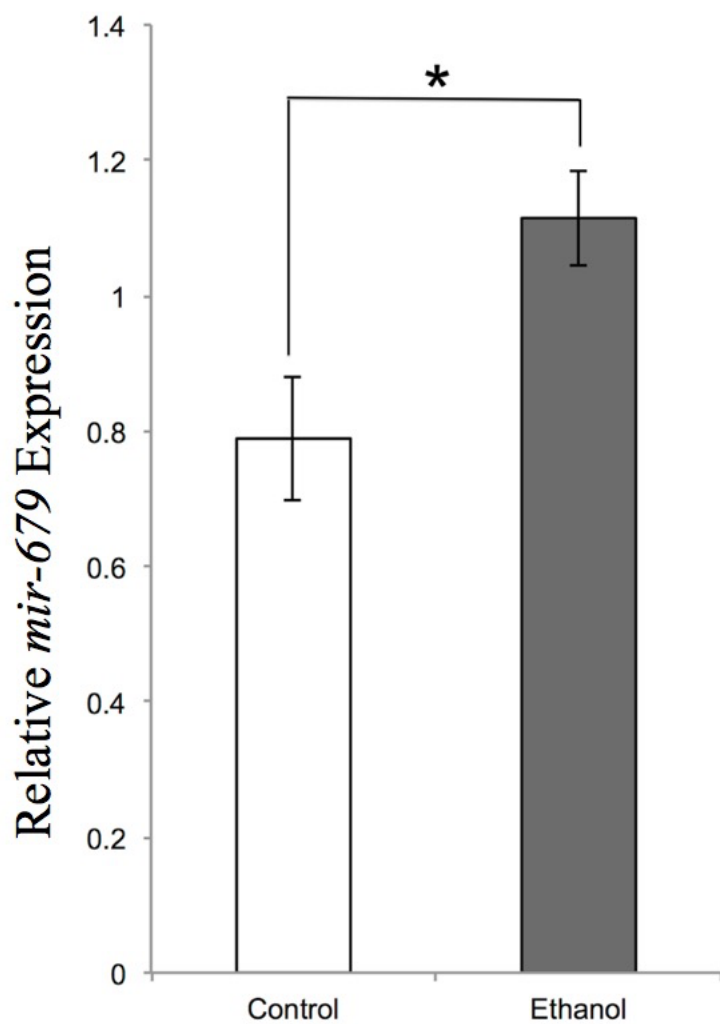


Figure 2.4. A bar graph depicting the quantitation of *mmu-mir-679-5p* expression in control and CPD PAE adult brains. This miRNA was identified in the original (2012) analysis. The y-axis depicts the relative *mir-679* expression normalized to *snoRNA 202*, expressed as a mean \pm s.e.m. of both biological (n=6) and technical (n=3) replicates.
*p<0.05.

2.4.2.3 Differential ncRNA Expression in All Exposure Paradigms

The original (2012) analysis of the mouse miRNA arrays shows that all PAE paradigms resulted in changes to global miRNA expression. The effect of each treatment paradigm was relatively consistent between biological replicates. Consequently, alcohol-treated and matched control ncRNA expression patterns consistently group together when hierarchically clustered (**Appendix B**), however, they do not represent the same transcripts across paradigms.

The pattern of expression between alcohol-exposed and matched control brains is quite distinct. Notably, the miRNAs that were affected were primarily specific to the developmental timing of alcohol treatment (**Appendix C**). Treatment during T1, T2, or T3 resulted in the unique expression for 21/24 (88%), 38/45 (84%) and 60/68 (88%) of the affected miRNAs for each of the three trimesters, respectively. This number for the CPD paradigm was also comparable [28/32 (88%)].

Finally, the altered miRNAs from the four exposure paradigms map to genetically imprinted regions in the mouse genome. Interestingly, 8/32 (25%) of identified miRNA transcripts in the CPD treatment paradigm, 2/24 (8%) in the T1 paradigm, 13/45 (29%) in the T2 paradigm, and 13/68 (19%) in the T3 paradigm mapped to three known imprinted regions of the mouse genome. The genomic locations include the *Snrpn-Ube3a* region of chromosome 7 (**Appendix D**), the *Dikl-Dio3* region of chromosome 12 (**Appendix E**), and the *Sfmbt2* region of mouse chromosome 2 (**Appendix E**).

Ultimately, these results suggest that the long-term changes in ncRNA expression following PAE are subtle and treatment specific, with the relative exception of *Snord115* (*H/MBII-52*).

2.4.3 Differential DNA Methylation

The third experiment in this chapter examines genome-wide as well as specific differences in DNA methylation in CPD PAE adult brains by utilizing NimbleGen MM9 2.1M deluxe promoter arrays (v2).

The original (2012) analysis revealed that the differences across individuals, although variable, show a significant ($p<0.01$) effect of PAE on genome-wide DNA methylation. Upon hierachal clustering analysis, it was observed that experimental and control mice group together according to exposure (**Figure 2.5**). Furthermore, the results reveal significant differentially methylated regions (DMRs) in 6660 regions that are associated with PAE. A total of 16% of transcripts and 18% of the miRNAs that showed significant ($p<0.05$) differential expression (fold change $> \pm 1.2$) also showed significant ($p<0.01$) differential methylation in their gene promoters. Furthermore, ~50% of imprinted regions showed significant differences in methylation.

Next, all the promoters identified were subjected to Ingenuity Pathway Analysis® (IPA®). After filtering, this analysis revealed that a large number of genes associated with cell death as well as nervous system development and function are significantly enriched (**Table 2.5**). An IPA associative genetic interaction network analysis revealed that the ‘Behavior, Neurological Disease, and Psychological Disorders’ network was the most significantly affected network, with an IPA® score of 65. From this network a number of highly connected ‘hub genes’ were identified.

Among the most prominent hub genes was *App*: its promoter is less methylated in the treated mice. Furthermore, the promoters of a set of interacting genes (*Akt1*, *Ghr*, *ApoE*, *Ntrk1*) within this hub are also differentially methylated following PAE. Finally, IPA’s canonical pathway analysis showed that the top two pathways were *Cdk5* signaling ($p=9.01E-7$), with 47/78 molecules affected (**Figure 2.6**), and *Pten* signaling ($p=1.9E-06$), with 54/95 molecules affected (**Figure 2.7**).

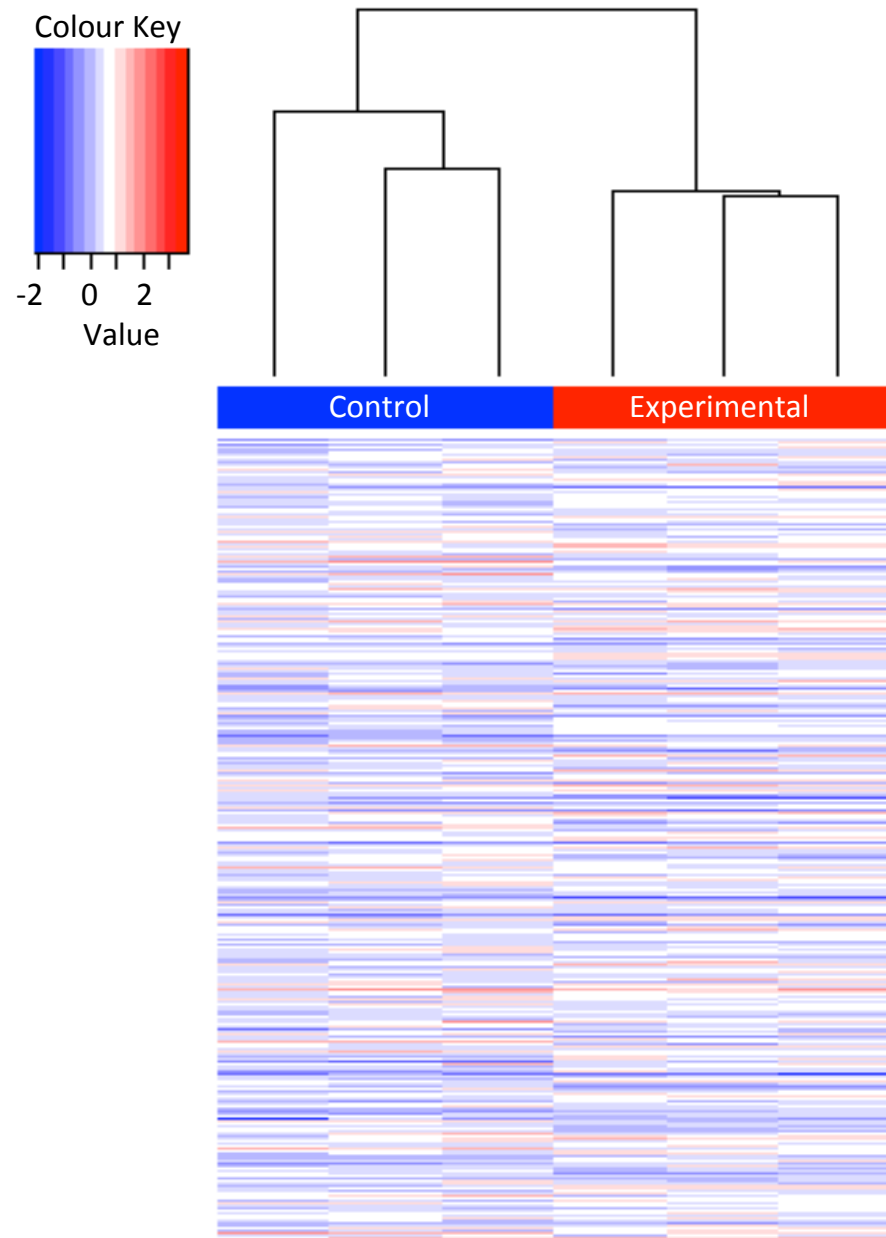


Figure 2.5. Hierarchical clustering of significant ($p<0.01$) differential methylation in CPD PAE adult mouse brains identified by the original (2012) analysis. The heatmap was plotted based on the log2 ratio of probes within the peak regions of each sample.

Table 2.5. Top ontologies identified by the original (2012) Ingenuity analysis of significantly ($p<0.01$) differentially methylated gene promoters.

Molecular and Cellular Functions		
Name	<i>p</i> -value	# Genes
Cell Death	4.06E-04 - 4.97E-02	224
Cellular Development	6.24E-04 - 4.52E-02	166
Cellular Function and Maintenance	9.57E-04 - 4.97E-02	86
Cellular Movement	4.12E-03 - 4.52E-02	41
Cell Signaling	8.43E-03 - 4.97E-02	26
Physiological System Development and Function		
Name	<i>p</i> -value	# Genes
Nervous System Development and Function	3.86E-05 - 4.97E-02	273
Tissue Morphology	1.64E-04 - 4.23E-02	97
Behavior	1.62E-03 - 1.58E-02	24
Embryonic Development	1.23E-02 - 4.23E-02	29
Organismal Development	1.23E-03 - 4.23E-02	25

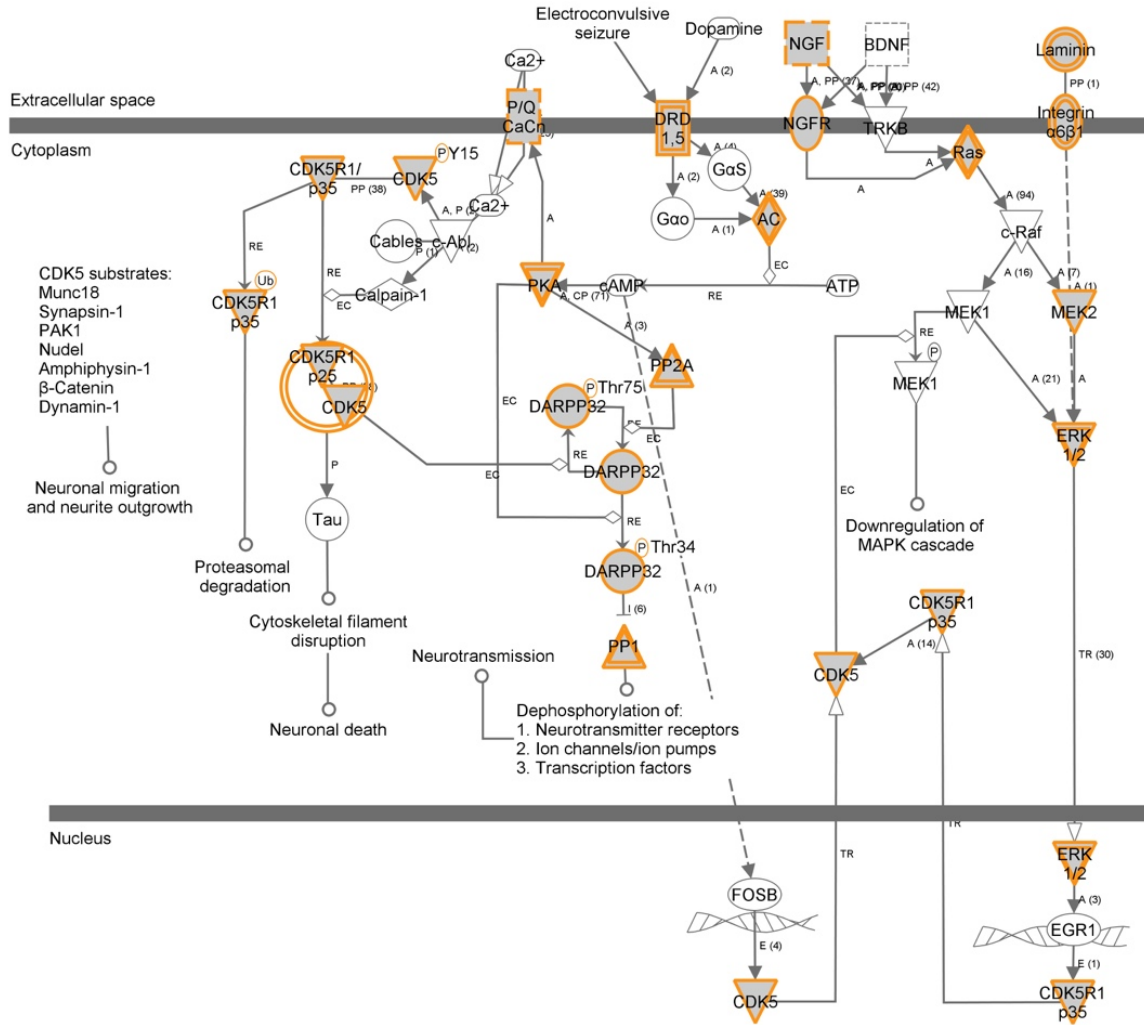


Figure 2.6. Ingenuity pathway analysis of the CDK5 signaling pathway. Genes identified by the original (2012) analysis as showing significant ($p < 0.01$) differential methylation in CPD PAE mice are highlighted. The legend for symbols is in Appendix F.

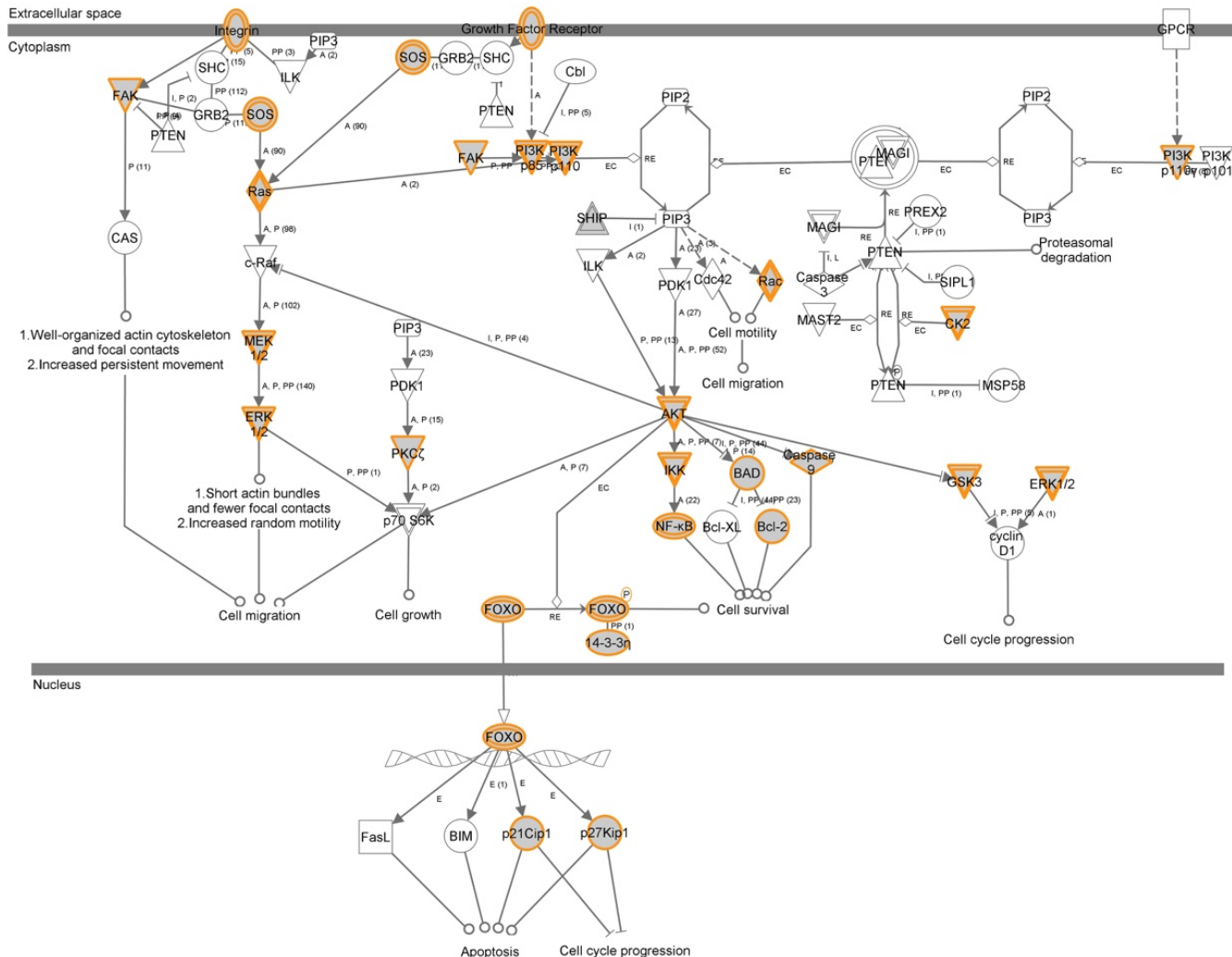


Figure 2.7. Ingenuity pathway analysis of the PTEN signaling pathway. Genes identified by the original (2012) analysis as showing significant ($p<0.01$) differential methylation in CPD PAE mice are highlighted. The legend for symbols is in Appendix F.

In addition to the genome-wide results, ontologies, and pathways, a functional examination of the results was also undertaken. The original (2012) DNA methylation data were integrated with the gene expression data to reveal gene families that showed significant differential methylation and some corresponding alterations in gene expression. Furthermore, an analysis of CTCF binding sites was also carried out on the promoter sequences of a critical gene network identified in the original (2012) analysis.

2.4.3.1 Gene Families

The replication-dependent histone gene clusters showed significant ($p<0.01$) increases in methylation following CPD, including *Hist1h1e*, *Hist1h2aa*, *Hist1h2ak*, *Hist1h2ba*, *Hist1h2be*, *Hist1h2be*, *Hist2h2bb*, *Hist2h3b*, *Hist2h4*, and *Hist3h2ba*. Notably, *Hist1h2ab* showed a significant ($p=0.007$) 1.2 fold decrease in expression in the CPD model. Finally, members of the histone gene family typically showed a similar decrease in expression in all binge exposure paradigms (Kleiber et al. 2013).

Genes from the *HoxA*, *HoxC*, and *HoxD* clusters showed significant ($p<0.01$) decreases in methylation. The genes altered by CPD were *Hoxa3*, *Hoxa4*, *Hoxa6*, *Hoxa7*, *Hoxa13*, *Hoxc8*, *Hoxc13*, *Hoxd1*, *Hoxd3*, *Hoxd8*, and *Hoxd11*. These altered *Hox* genes have promoters with high CpG content. *Hoxc8* showed a significant ($p=0.01$) 1.2 fold increase in expression in the CPD model and *Hoxd10* showed a significant ($p=0.04$) 1.3 fold increase in expression in the T1 model (Kleiber et al. 2013). Significant increases in methylation by PAE were also observed for *Rhox2a*, *Rhox2c*, *Rhox2e*, *Rhox2h*, *Rhox3a*, *Rhox3h*, *Rhox9*, *Rhox10*, and *Rhox11*. These genes have promoters with low to intermediate CpG content. Furthermore, *Rhox1* showed a significant ($p<0.02$) 1.2 fold increase in expression in the CPD model.

In the CPD model, significant ($p<0.01$) alterations to methylation in both directions were seen in *Adam1a*, *Adam1b*, *Adam3*, *Adam4*, *Adam10*, *Adam12*, *Adam23*, *Adam30*, *Adam32*, *Adam33*, *Adamts8*, *Adamts14*, *Adamts15*, *Adamts17*, *Adamtsl2*, *Adamtsl5*, and *Adamtsl5*. *Adamts9* showed a significant ($p<0.008$) 1.2 fold increase in the CPD model and several miRNAs predicted to target it by IPA were significantly ($p<0.05$) down-regulated ~1.2 fold (**Appendix A**). In the T3 model *Adamts9* showed a significant ($p=0.00001$) 1.2 fold decrease, while *Adam9* showed a 1.1 fold decrease and a miRNA

(*mir-26b*) predicted to target it showed a 1.3 fold increase (Kleiber et al. 2013; Kleiber, Diehl, et al. 2014; Kleiber, Laufer, et al. 2014).

The Keratin associated proteins *Krtap4-13*, *Krtap4-16*, *Krtap5-1*, *Krtap5-4*, *Krtap8-2*, *Krtap10-10*, *Krtap26-1*, and *Krtap31-2* showed a significant increase in methylation. *Krtap17-1* showed a significant decrease in methylation. Both *Krtap10-10* and *Krtap31-2* showed a significant ($p<0.03$) 1.2 fold increase in gene expression in the CPD model. Promoters for these genes had low to intermediate CpG content. *Krtap*'s are clusters of genes unique to mammals that are undergoing rapid evolution and are expressed during the terminal differentiation of hair cells (Shimomura & Ito 2005; Wu et al. 2008). Twenty-eight kertain genes, of both the cytoskeletal and cuticular type, showed significant differential methylation that was typically an increase. Keratinocyte differentiation-associated protein (*Krtdap*) also showed a significant increase in methylation. Furthermore, 64 transmembrane (*Tmem*) family genes showed significant ($p<0.01$) altered methylation in the CPD model. Notably, in the CPD model none of the genes with altered methylation showed altered expression. However, *Tmem19*, *Tmem60*, *Tmem150b*, and *Tmem235* showed significant ($p<0.03$) 1.2 fold decreases in expression while *Tmem217* showed a significant ($p<0.02$) 1.2 fold increase in expression. The original (2012) target filter analysis also identified two miRNAs with increased expression that were predicted to target *Tmem19* (**Appendix A**).

2.4.3.2 CTCF Binding Sites

The results included in this chapter suggest that PAE causes significant changes in DNA methylation in the developing brain that last to adulthood (**Figure 2.5**). The DMRs of the original (2012) analysis cover a relatively large number (6610) of gene promoters (6131 unique) that are related to molecular, functional, and phenotypic abnormalities implicated in FASD (**Table 2.5**). The most significant network identified by IPA (score 65) is that of ‘Behavior, Neurological Disease, and Psychological Disorders’, which has a distinct set of ‘hub genes’. Among the most prominent hub genes affected is *App* (amyloid precursor protein), which is a protein that helps direct the migration of neurons during early development (Priller et al. 2006). These results suggest that the hub genes identified (*Akt1*, *Ghr*, *ApoE*, *Ntrk1*) are involved in FASD endophenotypes.

The results also suggest a gene regulatory mechanism underlies some FASD endophenotypes. The alterations in promoter methylation might interfere with transcriptional machinery as demonstrated by the role of differential methylation of *H19* (Hark et al. 2000). Notably, altered methylation was seen in the *H19* promoter, which is involved in CTCF binding and imprinting (**Figure 2.8A**) (Lin et al. 2011). This specific peak has previously been identified as showing significant differential methylation in FASD placental tissue (Haycock & Ramsay 2009). CTCF binds to the *H19/Igf2* ICR in a DNA-methylation-sensitive manner, where it acts as insulator activity for the unmethylated maternal ICR by blocking the *Igf2* promoter from engaging enhancers downstream of *H19* that are shared by *H19* and *Igf2* (**Figure 2.8C**) (Hark et al. 2000). The deletion or mutation of the four CTCF-binding sites within the ICR causes a paternalization of the maternal allele that results in biallelic *Igf2* expression and *H19* repression (Engel et al. 2006).

In addition to the *H19* locus, CTCF binds to DMRs at a number of other imprinted loci. One of these is the secondary DMR of *Gtl2* (*Meg3*) (**Figure 2.7 and Table 2.6**), which also relies on differential methylation at a CTCF-binding site (Nowak et al. 2011) and showed a significant ($p<0.009$) 1.2 fold decrease in expression in the T3 injection paradigm (Kleiber, Laufer, et al. 2014). Given the role of CTCF in imprinted regions implicated in FASD, other important genes that were affected were examined for CTCF binding sites in their promoters. From the ‘Behavior, Neurological Disease, and Psychological Disorders’ network, 30 significantly altered DMRs were examined for CTCF-binding sites using the CTCFBS prediction tool (Bao et al. 2008). Of these 30 regions, 12 (40%) showed sequences that represented predicted CTCF-binding motifs (**Figure 2.7**). Eight of these promoter regions showed increased methylation and four showed decreased methylation. The results on *H19* and *App* are similar to previous research (Liu et al. 2009). However, these results show that the changes are present in adult brain tissue long after PAE. The 12 DMRs with CTCF binding sites were then subjected to a pathway analysis (**Figure 2.9**) using GeneMANIA (Warde-Farley et al. 2010), with the results supporting those of IPA. However, it is worth noting that other methylation-sensitive regulatory proteins are likely to be involved in the altered transcriptomics resulting from PAE.

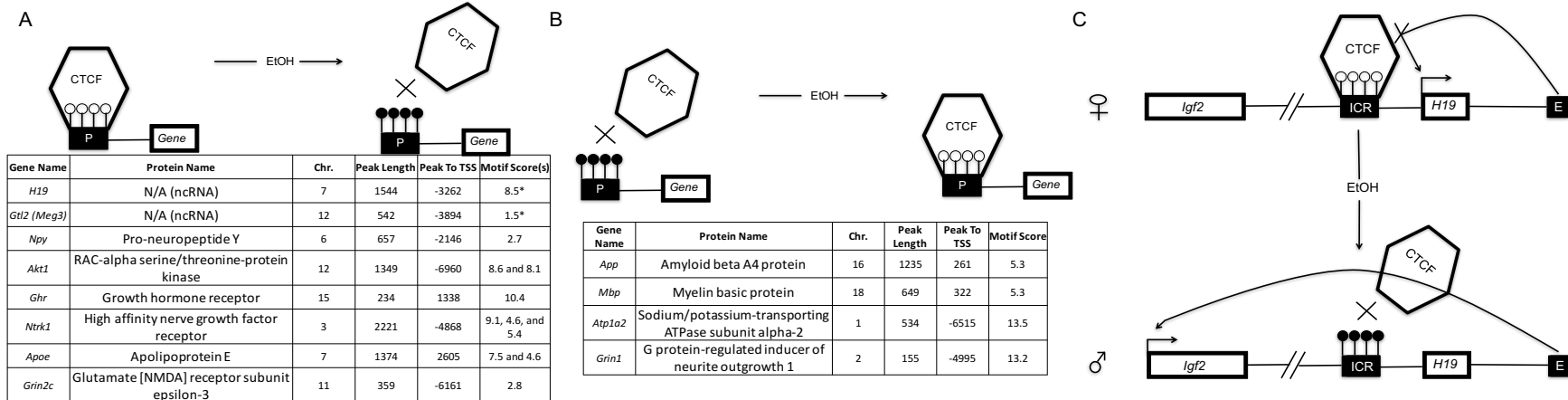


Figure 2.8. The functional potential of altered CTCF-binding-site methylation after PAE in significant ($p<0.01$) differentially methylated regions identified by the original (2012) analysis. Increased (A) and decreased (B) methylation after PAE at select gene promoters ('P') with CTCF sites. (C) Schematic of H19/IGF2 imprinting regulation and the effects of PAE. The black rectangle represents the *H19/Igf2* ICR. On the maternal allele, CTCF binds to the ICR and blocks the *Igf2* promoter from accessing the 3' shared enhancers (E). On the paternal allele, the ICR is methylated and *H19* transcription is repressed. White lollipops represent non-methylated DNA and black lollipops represent methylated DNA.

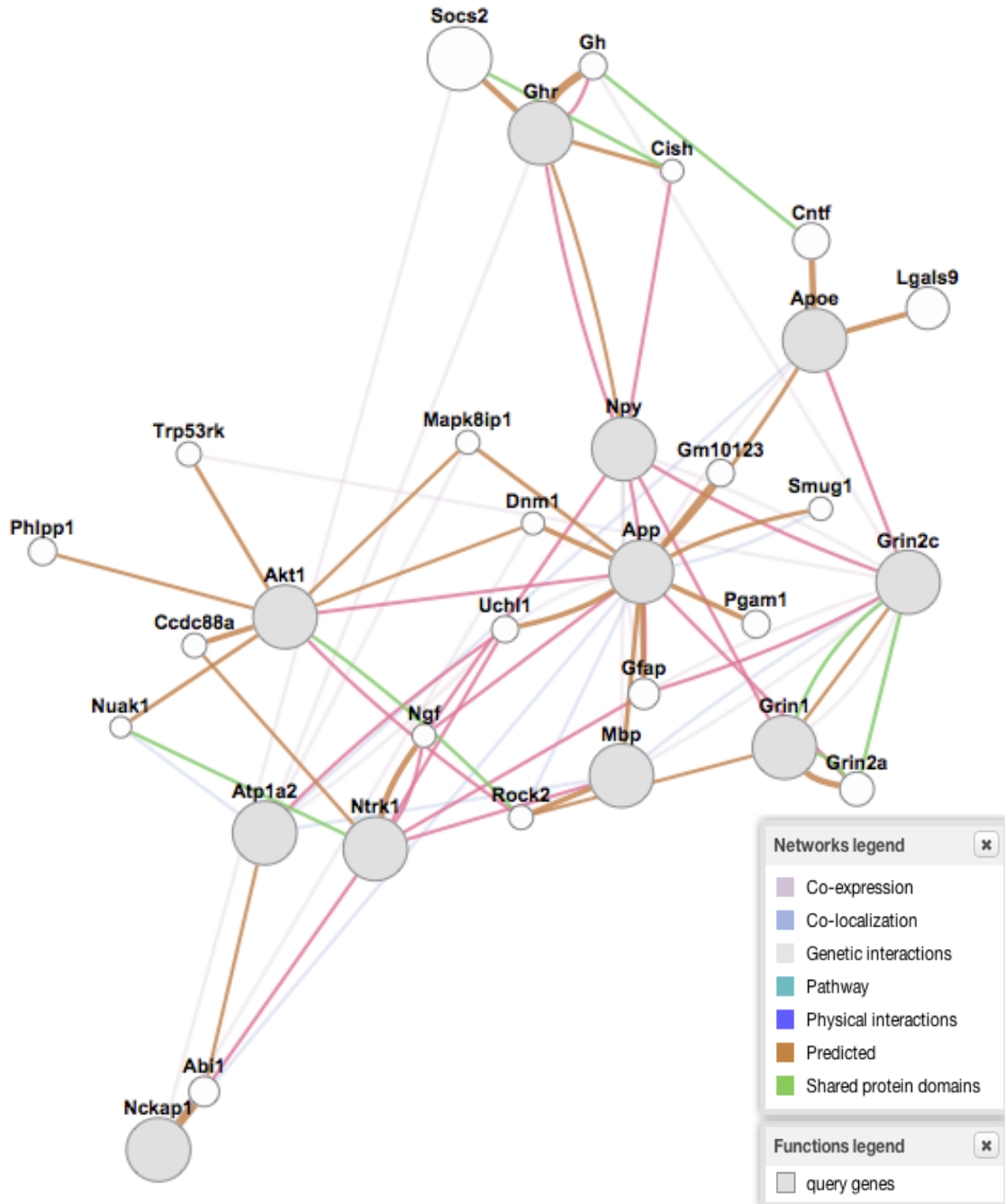


Figure 2.9. GeneMANIA network analysis of significant ($p<0.01$) differentially methylated genes containing CTCF-binding sites from the top associative network identified in the original (2012) analysis by Ingenuity Pathway Analysis (“Behavior, Neurological Disease, and Psychological Disorders”).

Finally, the updated (2016) analysis identified significant ($p<0.005$) alterations to DNA methylation in 4304 gene promoters and/or CpG islands that belonged to 2898 unique annotated genes. The top differentially methylated genes are presented in **Table 2.6**. The analysis also revealed significant ($p<0.002$) alterations in methylation to *Snord11b* and *Ipw*, which are ncRNAs within *Snrpn-Ube3a*. A larger amount of significant alterations were seen in gene ontologies and canonical pathways. The updated ontologies and pathways indicate alterations to ion transport across the membrane, cell-to-cell adhesion events, proliferation and differentiation (cancers) as well as developmental, cellular, immune, and synaptic signaling events (**Tables 2.7 & 2.8**).

Table 2.6. Updated (2016) analysis of genes in CPD adult brains with the greatest differential DNA methylation ($p=0.0001$).

PAE Hypermethylated

Score	Symbol	Gene Name	Gene Function
36	<i>Ntm</i>	Neurotrimin	Cell Adhesion and Neuron Recognition
29	<i>Mroh2a</i>	Maestro heat-like repeat-containing protein family member 2A	Unknown
27	<i>Slc22a5</i>	Solute carrier family 22 member 5	Sodium-ion dependent carnitine transporter
27	<i>Arhgap26</i>	Rho GTPase-activating protein 26	Actin cytoskeleton and nervous system development
25	<i>Bcl11b</i>	B-cell lymphoma/leukemia 11B	Tumor-suppressor
24	<i>Syn3</i>	Synapsin-3	Neurotransmission and synaptogenesis
20	<i>Foxp4</i>	Forkhead box protein P4	Transcriptional repressor
18	<i>Pisd-ps</i>	Phosphatidylserine decarboxylase, pseudogene	Unknown pseudogene
17	<i>Gnas</i>	Guanine nucleotide-binding protein G(s) Alpha Subunit	GPCR signal transduction [Imprinted Gene]
17	<i>Meg3</i>	Maternally expressed 3 [Also known as <i>Gtl2</i>]	lncRNA [Imprinted: <i>Dlk1-Dio3</i>]

PAE Hypomethylated

Score	Symbol	Gene Name	Gene Function
-14	<i>Xiap</i>	X-linked inhibitor of apoptosis	E3 ubiquitin protein ligase [Regulated by <i>Akt1</i>]
-10	<i>Map2k1</i>	Dual specificity mitogen-activated protein kinase kinase 1	MAPK signal transduction
-10	<i>Pmfbp1</i>	Polyamine-modulated factor 1-binding protein 1	Organization of cytoskeleton
-9	<i>Clcn5</i>	H(+)/Cl(-) exchange transporter 5	Proton-coupled chloride transporter
-9	<i>Mir188</i>	MicroRNA 188	Post-transcriptional regulation
-9	<i>Mir532</i>	MicroRNA 523	Post-transcriptional regulation
-9	<i>Eif3e</i>	Eukaryotic translation initiation factor 3 subunit E	Translational regulation
-9	<i>Izumo4</i>	Izumo sperm-egg fusion protein 4	Reproduction [immunoglobulin superfamily protein]
-9	<i>Mob3a</i>	MOB kinase activator 3A	Metal ion binding
-9	<i>Gldc</i>	Glycine dehydrogenase (decarboxylating), mitochondrial	Glycine degradation

Table 2.7. Ontologies for the updated (2016) analysis of significant ($p<0.005$) differential DNA methylation in CPD mice.

Enrichr GO Biological Processes	Overlap	p-value
Calcium ion transmembrane transport	33/128	1.9E-04
Inorganic cation transmembrane transport	82/440	2.5E-04
Response to steroid hormone	71/369	2.9E-04
Response to mechanical stimulus	40/176	4.1E-04
Divalent inorganic cation transport	50/238	4.2E-04
Gland development	47/220	4.5E-04
Divalent metal ion transport	49/234	5.0E-04
Cellular response to lipid	61/315	6.6E-04
Epithelial cell development	27/107	9.2E-04
Regulation of ion transmembrane transport	60/314	9.7E-04
Enrichr GO Cellular Location	Overlap	p-value
Cell-cell junction	65/335	3.6E-04
Postsynaptic membrane	42/195	6.7E-04
Synaptic membrane	46/228	1.3E-03
Cell cortex	22/83	1.4E-03
Integral component of plasma membrane	162/1066	2.1E-03
Contractile fiber part	35/167	2.7E-03
Lamellipodium	25/111	4.7E-03
Centrosome	62/360	5.7E-03
Perinuclear region of cytoplasm	69/411	6.2E-03
Golgi membrane	54/308	7.0E-03
Enrichr GO Molecular Function	Overlap	p-value
Channel activity	85/427	3.9E-05
Passive transmembrane transporter activity	85/427	3.9E-05
Metal ion transmembrane transporter activity	78/400	1.4E-04
Substrate-specific channel activity	79/406	1.4E-04
Inorganic cation transmembrane transporter activity	92/497	1.9E-04
Divalent inorganic cation transmembrane transporter activity	39/154	9.0E-05
Calcium ion transmembrane transporter activity	34/127	1.0E-04
Ion channel activity	76/396	2.7E-04
Cation channel activity	58/285	4.0E-04
Calcium channel activity	28/108	6.2E-04
Gated channel activity	60/323	2.2E-03
RNA polymerase II regulatory region DNA binding	55/288	2.0E-03
SH3 domain binding	28/119	2.1E-03

Table 2.8. Pathways for the updated (2016) analysis of significant ($p<0.005$) differential DNA methylation in CPD mice.

Partek KEGG Pathways	Overlap	p-value
Pathways in cancer	94/234	6.2E-05
Focal adhesion	60/148	1.1E-03
Arrhythmogenic right ventricular cardiomyopathy	26/48	1.5E-03
Melanogenesis	31/70	6.2E-03
Prostate cancer	28/61	6.2E-03
ECM-receptor interaction	27/60	8.7E-03
Renin-angiotensin system	9/11	9.5E-03
Acute myeloid leukemia	19/38	1.2E-02
Calcium signaling pathway	50/136	1.2E-02
TNF signaling pathway	32/78	1.3E-02
Phosphatidylinositol signaling system	25/57	1.4E-02
Glycosphingolipid biosynthesis - globo series	7/8	1.7E-02
Basal cell carcinoma	18/38	2.0E-02
Colorectal cancer	20/44	2.0E-02
HTLV-I infection	69/208	2.2E-02
Regulation of actin cytoskeleton	55/160	2.3E-02
Proteoglycans in cancer	57/167	2.3E-02
Protein digestion and absorption	26/64	2.5E-02
Dilated cardiomyopathy	26/64	2.5E-02
Fc gamma R-mediated phagocytosis	25/61	2.6E-02
Amphetamine addiction	20/47	3.3E-02
Estrogen signaling pathway	27/70	3.6E-02
Adherens junction	22/54	3.7E-02
Endometrial cancer	16/36	4.1E-02
Vasopressin-regulated water reabsorption	14/30	4.1E-02
Hippo signaling pathway	40/115	4.2E-02
Bacterial invasion of epithelial cells	22/55	4.2E-02
Wnt signaling pathway	37/105	4.3E-02
Pertussis	21/52	4.3E-02
Prolactin signaling pathway	21/53	5.0E-02
Osteoclast differentiation	33/93	5.0E-02
Neurotrophin signaling pathway	32/90	5.2E-02
Renal cell carcinoma	19/47	5.3E-02
FoxO signaling pathway	35/101	5.6E-02
Hedgehog signaling pathway	15/35	5.8E-02

2.5 Discussion

The experimentation in this chapter has resulted in a number of observations based on three key experiments (**Figure 2.1**). The first set of experiments are related to gene (mRNA) expression. PAE, an early life exposure, was associated with long-term alterations to the adult brain (**Figures 2.2 & 2.3 and Table 2.1**). Overall, the top up-regulated genes were primarily uncharacterized while the top down-regulated reflected a variety of functions (**Table 2.1**). The genes with long-term alterations share ontologies and pathways related to immune processes, synaptic events, nucleotide metabolism, protein synthesis, ion transport, and the cell membrane (**Table 2.2**). The observation of such long-term alterations to gene expression in adult PAE mice raises two questions. The first question is are they contributing to FASD related behaviours? The results suggest the possibility that some alterations may be playing an active role, but require gene specific functional confirmation. The second question is what is initiating and maintaining the long-term alterations gene expression? To this end, the next two experiments of this chapter tested the hypothesis that miRNAs and DNA methylation are involved in maintaining the long-term alterations and may contain a footprint that is informative of the events initiating these alterations.

In the second set of experiments different ncRNA species were examined. First, the CPD PAE model was examined for reciprocal alterations to the expression of miRNAs and predicted target genes (**Table 2.4**). These results revealed several interactions and aided in the identification of candidate biomarkers by providing additional layers of support for their deregulation (**Figure 2.4**). Second, alterations to ncRNA in the CPD paradigm, which represents moderate exposure were compared to ncRNA alterations in binge exposure paradigms that represent different developmental time points. The results show that PAE by any of the paradigms alters the expression of a number of ncRNAs in the adult brain (**Appendix B**). The results also show that long-term changes in miRNA expression are dependent on the treatment paradigm (**Appendix C**). The exception to this pattern is *Snord115* (*MBII-52*) snoRNA expression, which is affected regardless of the timing of exposure (**Appendix D**). The connection of the ncRNA expression to loci of genomic imprinting then raised the question: are alterations

to methylation responsible for maintaining the long-term alterations to ncRNA and mRNA expression?

In the third set of experiments, long-term alterations to DNA methylation were examined. At the general level, the examination revealed a genome-wide scale of change (**Figure 2.5**). However, the alterations were non-random. The ontologies (**Tables 2.5 & 2.7**) and pathways (**Figures 2.6 & 2.7 and Table 2.8**) altered are related to calcium signaling, ion transport, stem cell signaling, cell adhesion, synaptic events, immune processes, and the cell membrane. The alterations were seen in predicted and known CTCF binding sites (**Figure 2.8**) including those of *H19*, which was previously shown to be deregulated by PAE (Haycock & Ramsay 2009) and provides further evidence for the sensitivity of genomic imprinting to PAE.

Finally, because gene expression, miRNA expression, and DNA methylation were all examined in the CPD paradigm, the different datasets were integrated to observe any biological relationships. Notably, a larger scale of alteration was seen to DNA methylation as compared to gene and ncRNA expression. Furthermore, few genes and ncRNAs showing altered expression also showed altered DNA methylation. This lack of correlation between altered epigenetic marks and transcription has been reported in the literature (Veazey et al. 2015). The lack of correlation presumably reflects on the combinatorial nature of the epigenome, where multiple modifications are needed for effect. Furthermore, the lack of correlation also reflects on the fact that the gene expression tested is from mice in a resting steady state and that differential expression could be seen under other activating conditions (Lussier et al. 2015). However, despite the complexity of the relationship of the epigenome to transcription, three key observations that warrant further examination for both biomarker and therapeutic development have emerged. First, are imprinted clusters of ncRNA, second are select gene clusters, and third is cellular signaling.

2.5.1 Imprinted ncRNA Clusters

Approximately 20% of the miRNAs and some snoRNAs showing differential expression are encoded by one of three imprinted regions of the mouse genome: *Snrpn-Ube3a* (murine 7qC/human 15q11-q13), *Dlk1-Dio3* (murine 12qF1/human 14q32.2), and

Sfmbt2 (murine 2qA1) regions. Genes within these regions displayed differential methylation. The *Sfmbt2*, *Snrpn-Ube3a*, and *Dik1-Dio3* regions are of special interest to PAE because they are also known to affect a range of endophenotypes seen in FASD. These include impaired growth, craniofacial abnormalities, and a range of cognitive and behavioral deficits (May & Gossage 2001). The detailed biological consequences and evolutionary relationship of these imprinted clusters have been previously reviewed (Laufer & Singh 2012); however, their connection to FASD endophenotypes is briefly described below.

Snrpn-Ube3a expresses a neuron-specific polycistronic transcript. The *Snrpn-Ube3a* transcript is processed into two clusters of snoRNAs, *H/MBII-52* (*Snord115*) and *H/MBII-85* (*Snord116*) (de los Santos et al. 2000; Runte et al. 2001; Le Meur et al. 2005) that were deregulated by PAE. This transcript also codes for a number of alternative ncRNA species (Kishore et al. 2010; Bortolin-Cavaille & Cavaille 2012; Falaleeva & Stamm 2012). For example, a long non-coding RNA (lncRNA) transcribed from *Snrpn-Ube3a* undergoes alternative splicing where the introns are processed into *SNORD116* snoRNAs, while the spliced exons form a functional lncRNA (116HG) (Powell, Coulson, Crary, et al. 2013; Powell, Coulson, Gonzales, et al. 2013). 116HG forms a lncRNA cloud that modulates genes involved in circadian rhythm and energy expenditure, which notably includes *mTOR*, (imprinted) *Igf2r*, and *Crebbp*. Notably, *Snord116* and *Ipw*, both of which are in the *Snrpn-Ube3a* locus, showed significant ($p<0.002$) alterations to methylation in the updated (2016) analysis.

Furthermore, the array results from this chapter follow those of Liu *et al.*, who have reported that PAE causes differential methylation at *Ube3a*, which also has an antisense transcript (Liu et al. 2009). The *Snrpn-Ube3a* locus is involved in the classic sister imprinting disorders Prader-Willi syndrome (OMIM: 176270) and Angelman syndrome (OMIM: 105830), both of which display developmental delay and deficits in cognitive function (Knoll et al. 1989; Wagstaff et al. 1992). Interestingly, *H/MBII-52* (*Snord115*) and *H/MBII-85* (*Snord116*), are believed to be key players in these disorders (Buiting 2010; Bieth et al. 2015). Furthermore, overexpression of *Snord115* in a paternal duplication mouse model results in poor social interaction, behavioral inflexibility, abnormal ultrasonic vocalizations, and anxiety (Nakatani et al. 2009). *SNORD115*

changes the alternative splicing of the serotonin receptor *5HTR2C* (Kishore & Stamm 2006; Glatt-Deeley et al. 2010), which is a G-protein coupled receptor involved in calcium signaling (Nakatani et al. 2009). *Snord115* also regulates the splicing of genes (*Dpm2*, *Taf1*, *Ralgps1*, *Pbrm1*, and *Crhrl*) involved in the cell cycle, chromatin modification, and development (Kishore et al. 2010). Further investigation has also revealed that *SNORD115* and *SNORD116* can regulate a large number of genes, as well as modify each other's activity (Falaleeva et al. 2015).

The *Dlk1-Dio3* locus expresses over 40 miRNAs contained in two clusters, including a cluster of snoRNAs that contains *Snord113* and *Snord114* that were deregulated by PAE (**Appendix E**) (Seitz et al. 2004). Notably, *Meg3* (also known as *Gtl2*) showed significant differences in methylation in both the original (2012) and updated (2016) analyses (**Figure 2.8 & Table 2.6**). Altering the dosage of the imprinted genes at the *Dlk1-Dio3* region has also been shown to cause a range of endophenotypes, from growth deficiencies and developmental defects in the embryo and placenta, to defects in adult metabolism and brain function (Rocha et al. 2008). Some of the *Dlk1-Dio3* miRNAs are involved in activity dependent dendritic outgrowth of hippocampal neurons (Fiore et al. 2009). A rat model has also shown that PAE alters the expression of *Dio3* and antisense *Dio3os* in the hippocampus, as well as altering related behaviors and physiology (Sittig et al. 2011; Dietz et al. 2012).

SFMBT2 is a polycomb binding protein that interacts with, or ‘reads’, histones and transcriptionally represses *HOXB13* (Lee et al. 2013). *Sfmbt2* contains a rodent-specific large cluster of miRNAs that has led to it becoming genomically imprinted (Wang et al. 2011). *Sfmbt2* showed decreased methylation in the updated (2016) analysis and its miRNAs were deregulated by PAE (**Appendix E**). Maternal disomy of the *Sfmbt2* region results in fetal and placental growth retardation, whereas paternal disomy was shown to result in normal fetal growth and placental overgrowth (Kuzmin et al. 2008). Recently, another moderate and voluntary maternal PAE paradigm was shown to alter adult levels of a vesicular glutamate transporter in the mouse hippocampus (Zhang et al. 2015). The glutamate transporter showed increased mRNA levels that were correlated with decreased DNA methylation and increased (activating) H3K4me3 at the transporter promoter. Notably, while mRNA (*Slc17a6*) levels of the transporter were increased, the

protein (VGLUT2) levels were decreased by an imprinted miRNA (*miR-467b-5p*) from the *Sfmbt2* cluster, which was functionally confirmed to bind to the transporter mRNA.

Both the *Snrpn-Ube3a* and *Dlk1-Dio3* regions undergo allele-specific chromatin decondensation (or ‘unwinding’) during neuronal maturation (Leung et al. 2009; Leung et al. 2011). These clusters are also shared between mice and humans and expressed in embryo, placenta, and in the adult, in which their expression is confined mostly to the brain (Seitz et al. 2004). The *Snrpn-Ube3a* and *Dlk1-Dio3* regions have also been associated with several neurodevelopmental disorders (Leung et al. 2009). Furthermore, all three imprinted ncRNA clusters contain polycistronic transcripts, with some processed transcripts initially showing similar levels of expression that then change as a result of unequal stability (Seitz et al. 2004; Le Meur et al. 2005; Fiore et al. 2009; Wang et al. 2011).

The observations suggest that PAE might alter the regulation of not only individual miRNAs or snoRNAs, but entire clusters of co-regulated ncRNAs. More importantly, this process could involve differences in DNA methylation as DNA methylation is a functional mark at imprinting control regions. The nature of imprinted ncRNAs creates the potential for an environmentally responsive mechanism in the regulation of neurodevelopmental gene expression. Ultimately, given the observation of upregulated *Snord115* in all four paradigms examined, the confirmation of results across two independent array technologies, and the similar endophenotypes associated with alterations to it, *Snord115* may serve as an ideal candidate for future functional experiments investigating PAE. Thus, the above observations suggest that the similarity and variability in the manifestation of FASD could be in part attributed to the common (*Snord115*) and different ncRNAs and genes affected as a result of variability in exposure.

2.5.2 Gene Families

A number of gene families showed significant differential methylation as well as expression and may contribute to the endophenotypes of FASD. Some of these results are also supported by publications from independent groups. In terms of the histone genes, *Hist1h3b* also showed altered methylation in a whole embryonic culture of C57BL/6J

mice at early neurulation (Liu et al. 2009). The observation of altered methylation and expression observed from this gene family suggests transcriptional repression of histone protein production and, furthermore, a global deregulation of the cell cycle and epigenetic landscape that remains long after PAE.

The *Hox* genes were also deregulated by PAE. In the T2 binge injection model *mir-10b* showed a -1.5 fold change ($p=0.002$) (Mantha et al. 2014). Notably, *mir-10* is located within the *Hox* genes and also targets some of them (Lund 2010). *Hox* genes are a subset of homeobox genes and encode transcription factors that regulate developmental patterning, including in the brain (MacLean & Wilkinson 2010). The only unifying feature of all homeobox genes is that they encode a homeodomain, a motif that binds to specific DNA sequences, proteins, and even some RNAs (Shyu & Wilkinson 2000; Svingen & Tonissen 2006). Homeobox transcription factors have important roles in regulating the differentiation of cells during embryonic development by specifying the spatial positioning of cells and controlling cellular proliferation, apoptosis, cell adhesion, and cell migration (Pearson et al. 2005). Deregulation in the expression of homeobox genes can result in drastic alterations in development and subsequently result in profound changes in the identity of body segments (Duboule 2007; Krumlauf 1994).

At the genomic level, the vertebrate *Hox* gene clusters show a specific organization (Duboule 2007). The four *Hox* clusters of mammals map to distinct chromosomes, are termed *HoxA* through *HoxD*, and contain 9 to 11 protein-coding genes that are transcribed from the same strand (Yekta et al. 2008). In many vertebrates the *Hox* genes are organized on chromosomes in a linear way that matches their expression order along the anterior-posterior axis. Furthermore, the *Hox* clusters are targeted by a number of miRNAs, some of which originate within the *Hox* clusters and have also been implicated in FASD (Yekta et al. 2008; Wang et al. 2009). Over 200 ncRNAs arise from around the *Hox* clusters, including miRNAs and the long non-coding RNA HOTAIR, which is transcribed from *HoxC* and results in repressive H3K27me3 at *HoxD* by recruiting polycomb repressive complex 2 (Rinn et al. 2007). The *Rhox* gene family is a set of homeobox genes clustered on the X chromosome (MacLean et al. 2005). The mouse *Rhox* gene cluster is the largest homeobox gene cluster. Similar to most homeobox genes, *Rhox* genes are expressed during embryonic development (MacLean et al. 2005;

Hogeveen & Sassone-Corsi 2005; Zhan et al. 2005; Daggag et al. 2008). However, unlike most homeobox genes, *Rhox* genes also show high gene expression levels after birth (MacLean et al. 2005). Thus, *Rhox* genes are candidates to control postnatal and adult developmental events, particularly those essential for male and female reproduction. *Rhox5* is the most characterized *Rhox* gene and is regulated by many different stimuli, including differentiation signals, oncogenic signals, and hormones (Kobayashi et al. 2006). Recently, *Rhox5* was demonstrated to be regulated by histone H1 and DNA methylation (Maclean et al. 2011). Furthermore, alcohol dehydrogenase is critical for converting retinol to retinaldehyde, which is competitively inhibited by ethanol, and then later converted to the signaling molecule retinoic acid (Mezey & Holt 1971). As a developmental signaling molecule in mammals, retinoic acid is used to activate the 3' *Hox* genes (Duester 2008). Thus, the *Hox* genes appear to represent a connection between acute alterations to developmental signaling and long-term alterations to the epigenome.

Deregulation of the keratin-associated protein (*Krtap*) gene family was also observed. These results are similar to Marjonen et al., where a similar mouse model was used and a significant ($p=0.04$) 2.1 fold increase in the expression of *Krtap6-1* and a significant ($p=0.004$) 1.7 fold decrease in the expression of *Krtap27-1* was observed (Marjonen et al. 2015). Notably, keratinocytes constitute the vast majority of the epidermis (McGrath et al. 2004). It is tempting to speculate that these alterations in the adult brain may reflect on earlier alterations to developmental stem cell identity during neurulation where neural progenitor cells and the epithelium/epidermis begin to differentiate from each other. This observation may also alternatively or additionally reflect on the possibility of a premature exit from the cell cycle.

Adam (a disintegrin and metalloproteinase) and *Adamts* genes were also deregulated by PAE. These peptidase gene families are involved in cleaving the extra-cellular portions of trans-membrane proteins and stimulate neural crest migration (Prendergast et al. 2012; Kulesa & McLennan 2015). They have a role in cell adhesion and cell signaling as they are used to cleave and thus regulate cell surface molecules, such as Cadherin, Ephrin, EGF, TNF- α , and Notch (Reiss et al. 2005; Alfandari et al. 2009). ADAM10 also processes APP, which is involved in Alzheimer's disease (Haass et al. 2012). Furthermore, *Adam13* has been shown to be required for 3 dimensional cranial

neural crest cell migration and interact with *Cadherin11* (Cousin et al. 2012). Finally, another transmembrane protein family is the *Tmem* gene family, which is relatively uncharacterized and may be representative alterations to cellular signaling.

2.5.3 Alterations to Cellular Signaling Genes

The most significantly altered ($p=9.01E-7$) canonical pathway identified by the 2012 analysis was *Cdk5* signaling, where 60% of the genes involved showed significant differential methylation (Figure 2.6). *Cdk5* signaling is a sensory pathway that is restricted to the nervous systems and plays a critical role in neuronal migration, neuronal differentiation, neurite outgrowth, synaptic vesicle exocytosis and neurotransmission, long-term potentiation, as well as the proteasome, autophagy, and apoptosis (Cheung & Ip 2012). Notably, *Cdk5* signaling has been implicated in neurodegenerative diseases and circadian rhythm (Cheung & Ip 2012; Kwak et al. 2013).

Additionally, 57% of the genes involved in the *Pten* signaling pathway showed significant ($p=1.9E-06$) differential methylation (Figure 2.7). *Pten*, was upregulated (1.38-fold change and $p=2.5E-03$) and the three miRNAs (*mir-369-5p*, *mir-25* and *mir-495*) that were predicted to target it by IPA were downregulated, with *mir-369-5p* belonging to the *Dlk1-Dio3* cluster (Appendix A). This signaling pathway was also identified in the updated (2016) analysis as the phosphatidylinositol signaling system (Table 2.8). PTEN functions as a lipid phosphatase that counteracts the kinase function of phosphatidylinositol-3-kinase (PI3K) and suppresses AKT activation (Maehama & Dixon 1998). *Akt*, which showed a gain of methylation at a predicted CTCF binding-site (Figure 2.8A), is a major mediator of signaling pathways in response to a large spectrum of extracellular stimuli, which include PAE (Hard et al. 2005). Upon its activation in neurons, AKT phosphorylates different substrates, which in turn regulate diverse processes of neuronal development, including morphogenesis, dendritic development, synapse formation and synaptic plasticity, all of which are altered in FASD (Yoshimura et al. 2006). Furthermore, AKT is known to regulate autophagy/lysosome and ubiquitination/proteasome systems, which recycle damaged proteins (Wang et al. 2012; Xu et al. 2015). AKT has been shown to phosphorylate the GABA_A receptor, which increases the number of receptors on the plasma membrane surface, and thus promotes

synaptic plasticity (Wang et al. 2003). Studies in mice with a targeted inactivation of *Pten* in differentiated neurons showed abnormal social interaction and exaggerated responses to sensory stimuli (Kwon et al. 2006). Given the integral role of *Pten* in neurodevelopment, it is no surprise that it has been implicated in the developmental basis of many major psychiatric disorders (Kim et al. 2009) and FASD (Green et al. 2007). Overall, the alterations to all of the above clusters and signaling pathways suggests that there may be a molecular footprint of alterations to developmentally important regions that is sometimes but not always reflected in adult gene expression.

2.5.4 Considerations for Future Research

The research presented in this chapter highlights a number of considerations for future experimentation. The first consideration is the confirmation of alterations to gene expression. Although qPCR is the gold standard for confirmation, the technology used at the time of experimentation contained a limitation related to experiments of this nature. Specifically, it may not be sensitive enough to consistently detect low, but statistically significant, fold changes (<2.0) (Peirson & Butler 2007; Vikalo et al. 2010) that are typical of the fine-tuning nature of miRNAs (Moazed 2009). The results presented in this chapter are similar to Marjonen *et al.*, where a voluntary maternal consumption PAE paradigm revealed alterations to similar gene families. They noted that, “The expression levels of the differentially expressed genes observed in hippocampus were low and impossible to verify by quantitative PCR (TaqMan)” (Marjonen et al. 2015). More recently, the Singh lab has shown that digital droplet PCR (ddPCR), which is a more sensitive technology capable of detecting low fold changes and low copy numbers, can be used to confirm changes not found to be significant by standard qPCR (Chater-Diehl et al. 2016). Therefore, future PAE experimentation would benefit from utilizing ddPCR as a method for confirming some alterations to gene expression.

The second consideration for future research is cell type heterogeneity. In this chapter whole brain homogenate, which contains a number of cell types including neurons and glia, was examined. Therefore, the observed differential gene and ncRNA expression as well as DMRs may represent a combined epigenomic signature of depleted vulnerable cell types as well as specific alterations to the epigenome of surviving cells

(Kleiber, Diehl, et al. 2014). Future experimentation would benefit from single-cell sorting techniques. The third technical consideration for future research is the functional confirmation of predicted miRNA and target mRNA binding. This could be accomplished by *in vitro* luciferase reporter assays (Zhang et al. 2015). The fourth technical consideration is the utility of updating previous bioinformatic analyses. Bioinformatics is a rapidly advancing field and over relatively short periods of time a number of new annotations, algorithms, and software packages become available. Updated or new bioinformatic methods can offer additional insight into previous analyses and allow for a more direct comparison to more recent experiments utilizing the newer methods. However, as the results of this research suggest, a newer analysis does not necessarily invalidate a previous analysis as each bioinformatic method may be better suited for a specific application. Ultimately, with all of the above considerations in mind, there are a number of conclusions that can be drawn from the results of this chapter.

2.5.5 Conclusion

The results of this research demonstrate *in vivo*, long-term, and epigenome-wide alterations in PAE mice. Furthermore, the changes in DNA methylation and ncRNAs may maintain long-term alterations to gene expression following PAE, as the epigenomic changes appear to begin at the time of PAE, where they may then be inherited through successive cell proliferation and differentiation. Thus, the mouse model results presented in this chapter offer the hypothesis that an ontogenetic ‘footprint’ of PAE exists long after exposure (Kleiber et al. 2012) and provides novel evidence that was used to expand it into the epigenetic landscape (Kleiber, Diehl, et al. 2014; Chater-Diehl et al. 2016). The alterations in the epigenome and transcriptome are hypothesized to have arisen in developmentally and/or functionally similar genes in early stem cells (Kleiber, Diehl, et al. 2014; Marjonen et al. 2015). Finally, this footprint may undergo additional modification throughout development and by other environmental exposures.

Ultimately, the results of this research provide a number of candidate genes and pathways for future functional genomics studies and also provide a foundation for human studies. Perhaps more importantly, the epigenomic hypothesis of FASD as proposed may

be applied towards understanding the effect of neurodevelopmental exposures, which includes insight into neurodevelopmental disorders.

Footnote

A modified version of this chapter has been published (Laufer et al. 2013).

2.6 References

- Acampora, D., Mazan, S., Lallemand, Y., Avantaggiato, V., Maury, M., Simeone, A. & Brûlet, P., 1995. Forebrain and midbrain regions are deleted in Otx2^{-/-} mutants due to a defective anterior neuroectoderm specification during gastrulation. *Development*, 121(10), 3279–3290.
- Alfandari, D., McCusker, C. & Cousin, H., 2009. ADAM function in embryogenesis. *Seminars in Cell and Developmental Biology*, 20(2), 153–163.
- Allan, A.M., Chynoweth, J., Tyler, L.A. & Caldwell, K.K., 2003. A mouse model of prenatal ethanol exposure using a voluntary drinking paradigm. *Alcoholism: Clinical and Experimental Research*, 27(12), 2009–2016.
- Aruga, J. & Mikoshiba, K., 2003. Identification and characterization of Slitrk, a novel neuronal transmembrane protein family controlling neurite outgrowth. *Molecular and Cellular Neuroscience*, 24(1), 117–129.
- Bao, L., Zhou, M. & Cui, Y., 2008. CTCFBSDB: A CTCF-binding site database for characterization of vertebrate genomic insulators. *Nucleic Acids Research*, 36, D83–D87.
- Bieth, E., Eddiry, S., Gaston, V., Lorenzini, F., Buffet, A., Conte Auriol, F., Molinas, C., Cailley, D., Rooryck, C., Arveiler, B., Cavaillé, J., Salles, J.P. & Tauber, M., 2015. Highly restricted deletion of the SNORD116 region is implicated in Prader-Willi Syndrome. *European Journal of Human Genetics*, 23(2), 252–255.
- Boehm, S.L., Moore, E.M., Walsh, C.D., Gross, C.D., Cavelli, A.M., Gigante, E. & Linsenbardt, D.N., 2008. Using Drinking in the Dark to model prenatal binge-like exposure to ethanol in C57BL/6J mice. *Developmental Psychobiology*, 50(6), 566–578.
- Bortolin-Cavaille, M.L. & Cavaille, J., 2012. The SNORD115 (H / MBII-52) and SNORD116 (H / MBII-85) gene clusters at the imprinted Prader – Willi locus generate canonical box C / D snoRNAs. *Nucleic Acids Research*, 40(14), 6800–6807.
- Brady, M.L., Allan, A.M. & Caldwell, K.K., 2012. A Limited Access Mouse Model of Prenatal Alcohol Exposure that Produces Long-Lasting Deficits in Hippocampal-

- Dependent Learning and Memory. *Alcoholism: Clinical and Experimental Research*, 36(3), 457–466.
- Buiting, K., 2010. Prader-Willi syndrome and Angelman syndrome. *American Journal of Medical Genetics, Part C: Seminars in Medical Genetics*, 154(3), 365–376.
- Chater-Diehl, E.J., Laufer, B.I., Castellani, C.A., Alberry, B.L. & Singh, S.M., 2016. Alteration of Gene Expression, DNA Methylation, and Histone Methylation in Free Radical Scavenging Networks in Adult Mouse Hippocampus following Fetal Alcohol Exposure. *PloS one*, 11(5), e0154836.
- Chen, C., Ridzon, D.A., Broomer, A.J., Zhou, Z., Lee, D.H., Nguyen, J.T., Barbisin, M., Xu, N.L., Mahuvakar, V.R., Andersen, M.R., Lao, K.Q., Livak, K.J. & Guegler, K.J., 2005. Real-time quantification of microRNAs by stem-loop RT-PCR. *Nucleic Acids Research*, 33(20), e179.
- Chen, E.Y., Tan, C.M., Kou, Y., Duan, Q., Wang, Z., Meirelles, G.V., Clark, N.R. & Ma'ayan, A., 2013. Enrichr: interactive and collaborative HTML5 gene list enrichment analysis tool. *BMC Bioinformatics*, 14(1), 128.
- Cheung, Z.H. & Ip, N.Y., 2012. Cdk5: A multifaceted kinase in neurodegenerative diseases. *Trends in Cell Biology*, 22(3), 169–175.
- Conner, S.D. & Schmid, S.L., 2002. Identification of an adaptor-associated kinase, AAK1, as a regulator of clathrin-mediated endocytosis. *Journal of Cell Biology*, 156(5), 921–929.
- Cousin, H., Abbruzzese, G., McCusker, C. & Alfandari, D., 2012. ADAM13 function is required in the 3 dimensional context of the embryo during cranial neural crest cell migration in *Xenopus laevis*. *Developmental Biology*, 368(2), 335–344.
- Cui, J., Zhu, L., Xia, X., Wang, H.Y., Legras, X., Hong, J., Ji, J., Shen, P., Zheng, S., Chen, Z.J. & Wang, R.F., 2010. NLRC5 Negatively regulates the NF-??B and type I interferon signaling pathways. *Cell*, 141(3), 483–496.
- Daggag, H., Svingen, T., Western, P.S., van den Bergen, J.A., McClive, P.J., Harley, V.R., Koopman, P. & Sinclair, A.H., 2008. The rhox homeobox gene family shows sexually dimorphic and dynamic expression during mouse embryonic gonad development. *Biology of Reproduction*, 79(3), 468–474.
- Dietz, W.H., Masterson, K., Sittig, L.J., Redei, E.E. & Herzing, L.B.K., 2012. Imprinting and expression of Dio3os mirrors Dio3 in rat. *Frontiers in Genetics*, 3, 279.
- Dobbing, J. & Sand, J., 1979. Comparative aspects of the brain growth spurt. *Early Human Development*, 3(1), 379–383.
- Downing, C., Johnson, T.E., Larson, C., Leakey, T.I., Siegfried, R.N., Rafferty, T.M. & Cooney, C.A., 2011. Subtle decreases in DNA methylation and gene expression at

- the mouse Igf2 locus following prenatal alcohol exposure: Effects of a methyl-supplemented diet. *Alcohol*, 45(1), 65–71.
- Du, X. & Hamre, K., 2003. Identity and neuroanatomical localization of messenger RNAs that change expression in the neural tube of mouse embryos within 1 h after ethanol exposure. *Developmental Brain Research*, 144(1), 9–23.
- Duboule, D., 2007. The rise and fall of Hox gene clusters. *Development*, 134(14), 2549–2560.
- Duester, G., 2008. Retinoic Acid Synthesis and Signaling during Early Organogenesis. *Cell*, 134(6), 921–931.
- Engel, N., Thorvaldsen, J.L. & Bartolomei, M.S., 2006. CTCF binding sites promote transcription initiation and prevent DNA methylation on the maternal allele at the imprinted H19/Igf2 locus. *Human Molecular Genetics*, 15(19), 2945–2954.
- Falaleeva, M. & Stamm, S., 2012. Processing of snoRNAs as a new source of regulatory non-coding RNAs. *BioEssays*, 35(1), 46–54.
- Falaleeva, M., Surface, J., Shen, M., de la Grange, P. & Stamm, S., 2015. SNORD116 and SNORD115 change expression of multiple genes and modify each other's activity. *Gene*, 572(2), 266–273.
- Fiore, R., Khudayberdiev, S., Christensen, M., Siegel, G., Flavell, S.W., Kim, T.K., Greenberg, M.E. & Schratt, G., 2009. Mef2-mediated transcription of the miR379-410 cluster regulates activity-dependent dendritogenesis by fine-tuning Pumilio2 protein levels. *The EMBO Journal*, 28(6), 697–710.
- Flicek, P. et al., 2011. Ensembl 2011. *Nucleic Acids Research*, 39, D800–D806.
- Fraga, D., Meulia, T. & Fenster, S., 2008. Real-Time PCR. In *Current Protocols Essential Laboratory Techniques*. John Wiley & Sons, Inc., pp. 1–34.
- Friedman, R.C., Farh, K.K.H., Burge, C.B. & Bartel, D.P., 2009. Most mammalian mRNAs are conserved targets of microRNAs. *Genome Research*, 19(1), 92–105.
- Gao, J., Wang, W.-Y., Mao, Y.-W., Gräff, J., Guan, J.-S., Pan, L., Mak, G., Kim, D., Su, S.C. & Tsai, L.-H., 2010. A novel pathway regulates memory and plasticity via SIRT1 and miR-134. *Nature*, 466(7310), 1105–9.
- Garro, a J., McBeth, D.L., Lima, V. & Lieber, C.S., 1991. Ethanol consumption inhibits fetal DNA methylation in mice: implications for the fetal alcohol syndrome. *Alcoholism: Clinical and Experimental Research*, 15(3), 395–398.
- Glatt-Deeley, H., Bancescu, D.L. & Lalande, M., 2010. Prader-Willi syndrome, Snord115, and Htr2c editing. *Neurogenetics*, 11(1), 143–144.

- Green, M.L., Singh, A. V., Zhang, Y., Nemeth, K.A., Sulik, K.K. & Knudsen, T.B., 2007. Reprogramming of genetic networks during initiation of the Fetal Alcohol Syndrome. *Developmental Dynamics*, 236(2), 613–631.
- Gupta-Rossi, N., Ortica, S., Meas-Yedid, V., Heuss, S., Moretti, J., Olivo-Marin, J.C. & Israël, A., 2011. The adaptor-associated kinase 1, AAK1, is a positive regulator of the notch pathway. *Journal of Biological Chemistry*, 286(21), 18720–18730.
- Haass, C., Kaether, C., Thinakaran, G. & Sisodia, S., 2012. Trafficking and proteolytic processing of APP. *Cold Spring Harbor Perspectives in Medicine*, 2(5), a006270.
- Hard, M.L., Abdolell, M., Robinson, B.H. & Koren, G., 2005. Gene-expression analysis after alcohol exposure in the developing mouse. *Journal of Laboratory and Clinical Medicine*, 145(1), 47–54.
- Hark, A.T., Schoenherr, C.J., Katz, D.J., Ingram, R.S., Levorse, J.M. & Tilghman, S.M., 2000. CTCF mediates methylation-sensitive enhancer-blocking activity at the H19/Igf2 locus. *Nature*, 405(6785), 486–489.
- Haycock, P.C., 2009. Fetal alcohol spectrum disorders: the epigenetic perspective. *Biology of Reproduction*, 81(4), 607–617.
- Haycock, P.C. & Ramsay, M., 2009. Exposure of mouse embryos to ethanol during preimplantation development: effect on DNA methylation in the h19 imprinting control region. *Biology of Reproduction*, 81(4), 618–627.
- Hogeveen, K.N. & Sassone-Corsi, P., 2005. Homeobox galore: When reproduction goes RHOX and roll. *Cell*, 120(3), 287–288.
- Howlett, S.K. & Reik, W., 1991. Methylation levels of maternal and paternal genomes during preimplantation development. *Development*, 113(1), 119–27.
- Ikonomidou, C., Price, M.T., Stefovska, V. & Ho, F., 2007. Ethanol-Induced Apoptotic Neurodegeneration and Fetal Alcohol Syndrome. *Science*, 1056(2000), 1056–1060.
- Irizarry, R.A., Bolstad, B.M., Collin, F., Cope, L.M., Hobbs, B. & Speed, T.P., 2003. Summaries of Affymetrix GeneChip probe level data. *Nucleic acids research*, 31(4), e15.
- Ivakhnitskaia, E., Hamada, K. & Chang, C., 2016. Timing mechanisms in neuronal pathfinding, synaptic reorganization, and neuronal regeneration. *Development Growth and Differentiation*, 58(1), 88–93.
- Johnson, W.E., Li, W., Meyer, C.A., Gottardo, R., Carroll, J.S., Brown, M. & Liu, X.S., 2006. Model-based analysis of tiling-arrays for ChIP-chip. *Proceedings of the National Academy of Sciences*, 103(33), 12457–12462.
- Kaminen-Ahola, N., Ahola, A., Maga, M., Mallitt, K.A., Fahey, P., Cox, T.C., Whitelaw,

- E. & Chong, S., 2010. Maternal ethanol consumption alters the epigenotype and the phenotype of offspring in a mouse model. *PLoS Genetics*, 6(1), e1000811.
- Kelly, C.E., Thymiakou, E., Dixon, J.E., Tanaka, S., Godwin, J. & Episkopou, V., 2013. Rnf165/Ark2C Enhances BMP-Smad Signaling to Mediate Motor Axon Extension. *PLoS Biology*, 11(4), e1001538.
- Kerns, R.T. & Miles, M.F., 2008. Microarray Analysis of Ethanol-Induced Changes in Gene Expression. *Methods in molecular biology*, 447, 395–410.
- Kim, J.Y., Duan, X., Liu, C.Y., Jang, M.H., Guo, J.U., Pow-anpongkul, N., Kang, E., Song, H. & Ming, G. li, 2009. DISC1 Regulates New Neuron Development in the Adult Brain via Modulation of AKT-mTOR Signaling through KIAA1212. *Neuron*, 63(6), 761–773.
- Kishore, S., Khanna, A., Zhang, Z., Hui, J., Balwierz, P.J., Stefan, M., Beach, C., Nicholls, R.D., Zavolan, M. & Stamm, S., 2010. The snoRNA MBII-52 (SNORD 115) is processed into smaller RNAs and regulates alternative splicing. *Human Molecular Genetics*, 19(7), 1153–1164.
- Kishore, S. & Stamm, S., 2006. The snoRNA HBII-52 regulates alternative splicing of the serotonin receptor 2C. *Science*, 311(5758), 230–232.
- Kleiber, M.L., Diehl, E.J., Laufer, B.I., Mantha, K., Chokroverty-Hoque, A., Alberry, B. & Singh, S.M., 2014. Long-term genomic and epigenomic dysregulation as a consequence of prenatal alcohol exposure: A model for fetal alcohol spectrum disorders. *Frontiers in Genetics*, 5, 161.
- Kleiber, M.L., Laufer, B.I., Stringer, R.L. & Singh, S.M., 2014. Third trimester-equivalent ethanol exposure is characterized by an acute cellular stress response and an ontogenetic disruption of genes critical for synaptic establishment and function in mice. *Developmental Neuroscience*, 36(6), 499–519.
- Kleiber, M.L., Laufer, B.I., Wright, E., Diehl, E.J. & Singh, S.M., 2012. Long-term alterations to the brain transcriptome in a maternal voluntary consumption model of fetal alcohol spectrum disorders. *Brain Research*, 1458, 18–33.
- Kleiber, M.L., Mantha, K., Stringer, R.L. & Singh, S.M., 2013. Neurodevelopmental alcohol exposure elicits long-term changes to gene expression that alter distinct molecular pathways dependent on timing of exposure. *Journal of Neurodevelopmental Disorders*, 5(1), 6.
- Kleiber, M.L., Wright, E. & Singh, S.M., 2011. Maternal voluntary drinking in C57BL/6J mice: Advancing a model for fetal alcohol spectrum disorders. *Behavioural Brain Research*, 223(2), 376–387.
- Knoll, J.H., Nicholls, R.D., Magenis, R.E., Graham, J.M., Lalande, M. & Latt, S.A., 1989. Angelman and Prader-Willi syndromes share a common chromosome 15

- deletion but differ in parental origin of the deletion. *American Journal of Medical Genetics*, 32(2), 285–290.
- Kobayashi, S., Isotani, A., Mise, N., Yamamoto, M., Fujihara, Y., Kaseda, K., Nakanishi, T., Ikawa, M., Hamada, H., Abe, K. & Okabe, M., 2006. Comparison of gene expression in male and female mouse blastocysts revealed imprinting of the X-linked gene, RhoX5/Pem, at preimplantation stages. *Current Biology*, 16(2), 166–172.
- Kobor, M.S. & Weinberg, J., 2011. Focus on: epigenetics and fetal alcohol spectrum disorders. *Alcohol Res Health*, 34(1), 29–37.
- Kozomara, A. & Griffiths-Jones, S., 2011. MiRBase: Integrating microRNA annotation and deep-sequencing data. *Nucleic Acids Research*, 39, D152–D157.
- Krumlauf, R., 1994. Hox genes in vertebrate development. *Cell*, 78(2), 191–201.
- Kulesa, P.M. & McLennan, R., 2015. Neural crest migration: trailblazing ahead. *F1000Prime Reports*, 7, 02.
- Kuzmin, A., Han, Z., Golding, M.C., Mann, M.R.W., Latham, K.E. & Varmuza, S., 2008. The Pcg gene Sfmbt2 is paternally expressed in extraembryonic tissues. *Gene Expression Patterns*, 8(2), 107–116.
- Kwak, Y., Jeong, J., Lee, S., Park, Y.U., Lee, S.A., Han, D.H., Kim, J.H., Ohshima, T., Mikoshiba, K., Suh, Y.H., Cho, S. & Park, S.K., 2013. Cyclin-dependent kinase 5 (Cdk5) regulates the function of CLOCK protein by direct phosphorylation. *Journal of Biological Chemistry*, 288(52), 36878–36889.
- Kwon, C.H., Luikart, B.W., Powell, C.M., Zhou, J., Matheny, S.A., Zhang, W., Li, Y., Baker, S.J. & Parada, L.F., 2006. Pten Regulates Neuronal Arborization and Social Interaction in Mice. *Neuron*, 50(3), 377–388.
- Laufer, B.I., Mantha, K., Kleiber, M.L., Diehl, E.J., Addison, S.M.F. & Singh, S.M., 2013. Long-lasting alterations to DNA methylation and ncRNAs could underlie the effects of fetal alcohol exposure in mice. *Disease Models & Mechanisms*, 6(4), 977–992.
- Laufer, B.I. & Singh, S.M., 2012. A Macro Role for Imprinted Clusters of MicroRNAs in the Brain. *MicroRNA*, 1(1), 59–64.
- Lee, K., Na, W., Maeng, J.H., Wu, H. & Ju, B.G., 2013. Regulation of DU145 prostate cancer cell growth by Scm-like with four mbt domains 2. *Journal of Biosciences*, 38(1), 105–112.
- Leung, K.N., Chamberlain, S.J., Lalande, M. & Lasalle, J.M., 2011. Neuronal chromatin dynamics of imprinting in development and disease. *Journal of Cellular Biochemistry*, 112(2), 365–373.

- Leung, K.N., Vallero, R.O., Dubose, A.J., Resnick, J.L. & Lasalle, J.M., 2009. Imprinting regulates mammalian snoRNA-encoding chromatin decondensation and neuronal nucleolar size. *Human Molecular Genetics*, 18(22), 4227–4238.
- Lewis, B.P., Burge, C.B. & Bartel, D.P., 2005. Conserved seed pairing, often flanked by adenosines, indicates that thousands of human genes are microRNA targets. *Cell*, 120(1), 15–20.
- Lin, S., Ferguson-Smith, A.C., Schultz, R.M. & Bartolomei, M.S., 2011. Nonallelic transcriptional roles of CTCF and cohesins at imprinted loci. *Molecular and Cellular Biology*, 31(15), 3094–104.
- Liu, Y., Balaraman, Y., Wang, G., Nephew, K.P. & Zhou, F.C., 2009. Alcohol exposure alters DNA methylation profiles in mouse embryos at early neurulation. *Epigenetics*, 4(7), 500–511.
- de los Santos, T., Schweizer, J., Rees, C. a & Francke, U., 2000. Small evolutionarily conserved RNA, resembling C/D box small nucleolar RNA, is transcribed from PWCR1, a novel imprinted gene in the Prader-Willi deletion region, which is highly expressed in brain. *American Journal of Human Genetics*, 67(5), 1067–1082.
- Lund, A.H., 2010. miR-10 in development and cancer. *Cell Death and Differentiation*, 17(2), 209–214.
- Lussier, A.A., Stepien, K.A., Neumann, S.M., Pavlidis, P., Kobor, M.S. & Weinberg, J., 2015. Prenatal alcohol exposure alters steady-state and activated gene expression in the adult rat brain. *Alcoholism: Clinical and Experimental Research*, 39(2), 251–261.
- Maclean, J.A., Bettegowda, A., Kim, B.J., Lou, C., Yang, S., Bhardwaj, A., Shanker, S., Hu, Z., Fan, Y., Eckardt, S., McLaughlin, K.J., Skoultchi, A.I., Miles, F., Ii, J.A.M. & Wilkinson, M.F., 2011. The Rhox Homeobox Gene Cluster Is Imprinted and Selectively Targeted for Regulation by Histone H1 and DNA Methylation The Rhox Homeobox Gene Cluster Is Imprinted and Selectively Targeted for Regulation by Histone H1 and DNA Methylation. *Molecular and Cellular Biology*, 31(6), 1275–1287.
- MacLean, J.A., Chen, M.A., Wayne, C.M., Bruce, S.R., Rao, M., Meistrich, M.L., Macleod, C. & Wilkinson, M.F., 2005. Rhox: A new homeobox gene cluster. *Cell*, 120(3), 369–382.
- MacLean, J.A. & Wilkinson, M.F., 2010. The Rhox genes. *Reproduction*, 140(2), 195–213.
- Maehama, T. & Dixon, J.E., 1998. The tumor suppressor, PTEN/MMAC1, dephosphorylates the lipid second messenger, phosphatidylinositol 3,4,5-trisphosphate. *Journal of Biological Chemistry*, 273(22), 13375–13378.

- Mantha, K., Kleiber, M.L. & Singh, S.M., 2013. Neurodevelopmental Timing of Ethanol Exposure May Contribute to Observed Heterogeneity of Behavioral Deficits in a Mouse Model of Fetal Alcohol Spectrum Disorder (FASD). *Journal of Behavioral and Brain Science*, 3(1), 85–99.
- Mantha, K., Laufer, B.I. & Singh, S.M., 2014. Molecular changes during neurodevelopment following second-trimester binge ethanol exposure in a mouse model of fetal alcohol spectrum disorder: From immediate effects to long-term adaptation. *Developmental Neuroscience*, 36(1), 29–43.
- Marjonen, H., Sierra, A., Nyman, A., Rogojin, V., Grohn, O., Linden, A.M., Hautaniemi, S. & Kaminen-Ahola, N., 2015. Early maternal alcohol consumption alters hippocampal DNA methylation, gene expression and volume in a mouse model. *PLoS ONE*, 10(5), e0124931.
- May, P.A. & Gossage, J.P., 2001. Estimating the prevalence of fetal alcohol syndrome: A summary. *Alcohol Research & Health*, 25(3), 159–167.
- Mayr, C., Hemann, M.T. & Bartel, D.P., 2007. Disrupting the pairing between let-7 and Hmga2 enhances oncogenic transformation. *Science*, 315(5818), 1576–1579.
- McGrath, J.A., Eady, R.A.J. & Pope, F.M., 2004. Anatomy and Organization of Human Skin. In *Rook's Textbook of Dermatology*. Blackwell Publishing, Inc., pp. 45–128.
- Métivier, R., Gallais, R., Tiffache, C., Le Péron, C., Jurkowska, R.Z., Carmouche, R.P., Ibberson, D., Barath, P., Demay, F., Reid, G., Benes, V., Jeltsch, A., Gannon, F. & Salbert, G., 2008. Cyclical DNA methylation of a transcriptionally active promoter. *Nature*, 452(7183), 45–50.
- Le Meur, E., Watrin, F., Landers, M., Sturny, R., Lalande, M. & Muscatelli, F., 2005. Dynamic developmental regulation of the large non-coding RNA associated with the mouse 7C imprinted chromosomal region. *Developmental Biology*, 286(2), 587–600.
- Mezey, E. & Holt, P.R., 1971. The inhibitory effect of ethanol on retinol oxidation by human liver and cattle retina. *Experimental and Molecular Pathology*, 15(2), 148–156.
- Miranda, R.C., 2012. MicroRNAs and fetal brain development: Implications for ethanol teratology during the second trimester period of neurogenesis. *Frontiers in Genetics*, 3, 77.
- Moazed, D., 2009. Small RNAs in transcriptional gene silencing and genome defence. *Nature*, 457(7228), 413–420.
- Mohn, F., Weber, M., Schübeler, D. & Roloff, T.-C., 2009. Methylated DNA immunoprecipitation (MeDIP). *Methods in molecular biology*, 507, 55–64.
- Monk, M., Boubelik, M. & Lehnert, S., 1987. Temporal and Regional Changes in DNA

- Methylation in the Embryonic, Extraembryonic and Germ-Cell Lineages During Mouse Embryo Development. *Development*, 99(3), 371–382.
- Morison, I.M., Ramsay, J.P. & Spencer, H.G., 2005. A census of mammalian imprinting. *Trends in Genetics*, 21(8), 457–465.
- Nakatani, J. et al., 2009. Abnormal Behavior in a Chromosome- Engineered Mouse Model for Human 15q11-13 Duplication Seen in Autism. *Cell*, 137(7), 1235–1246.
- Nowak, K., Stein, G., Powell, E., He, L.M., Naik, S., Morris, J., Marlow, S. & Davis, T.L., 2011. Establishment of paternal allele-specific DNA methylation at the imprinted mouse Gtl2 locus. *Epigenetics*, 6(8), 1012–1020.
- Pearson, J.C., Lemons, D. & McGinnis, W., 2005. Modulating Hox gene functions during animal body patterning. *Nature Reviews Genetics*, 6(12), 893–904.
- Peirson, S.N. & Butler, J.N., 2007. Quantitative polymerase chain reaction. *Circadian Rhythms: Methods & Protocols*, 362(November), 349–362.
- Powell, W.T., Coulson, R.L., Crary, F.K., Wong, S.S., Ach, R.A., Tsang, P., Yamada, N.A., Yasui, D.H. & LaSalle, J.M., 2013. A Prader-Willi locus lncRNA cloud modulates diurnal genes and energy expenditure. *Human Molecular Genetics*, 22(21), 4318–4328.
- Powell, W.T., Coulson, R.L., Gonzales, M.L., Crary, F.K., Wong, S.S., Adams, S., Ach, R.A., Tsang, P., Yamada, N.A., Yasui, D.H., Chédin, F. & LaSalle, J.M., 2013. R-loop formation at Snord116 mediates topotecan inhibition of Ube3a-antisense and allele-specific chromatin decondensation. *Proceedings of the National Academy of Sciences of the United States of America*, 110(34), 13938–43.
- Prendergast, A., Linbo, T.H., Swarts, T., Ungos, J.M., McGraw, H.F., Krispin, S., Weinstein, B.M. & Raible, D.W., 2012. The metalloproteinase inhibitor Reck is essential for zebrafish DRG development. *Development*, 139(6), 1141–52.
- Priller, C., Bauer, T., Mitteregger, G., Krebs, B., Kretzschmar, H.A. & Herms, J., 2006. Synapse Formation and Function Is Modulated by the Amyloid Precursor Protein. *The Journal of Neuroscience*, 26(27), 7212–7221.
- Reiss, K., Maretzky, T., Ludwig, A., Tousseyn, T., Strooper, B. De, Hartmann, D. & Saftig, P., 2005. ADAM10 cleavage of N-cadherin and regulation of cell–cell adhesion and b-catenin nuclear signalling. *The EMBO Journal*, 24(4), 742–752.
- Rinn, J.L., Kertesz, M., Wang, J.K., Squazzo, S.L., Xu, X., Brugmann, S.A., Goodnough, L.H., Helms, J.A., Farnham, P.J., Segal, E. & Chang, H.Y., 2007. Functional Demarcation of Active and Silent Chromatin Domains in Human HOX Loci by Noncoding RNAs. *Cell*, 129(7), 1311–1323.
- Rocha, S.T. da, Edwards, C.A., Ito, M., Ogata, T. & Ferguson-Smith, A.C., 2008.

- Genomic imprinting at the mammalian Dlk1-Dio3 domain. *Trends in Genetics*, 24(6), 306–316.
- Roux-buisson, N. et al., 2012. Absence of triadin, a protein of the calcium release complex, is responsible for cardiac arrhythmia with sudden death in human. *Human Molecular Genetics*, 21(12), 2759–2767.
- Royland, J.E. & Kodavanti, P.R.S., 2008. Gene expression profiles following exposure to a developmental neurotoxicant, Aroclor 1254: Pathway analysis for possible mode(s) of action. *Toxicology and Applied Pharmacology*, 231(2), 179–196.
- Runte, M., Hüttenhofer, A., Groß, S., Kiefmann, M., Horsthemke, B. & Buiting, K., 2001. The IC-SNURF–SNRPN transcript serves as a host for multiple small nucleolar RNA species and as an antisense RNA for UBE3A. *Human Molecular Genetics*, 10(23), 2687–2700.
- Sabunciyan, S., Yolken, R., Ragan, C.M., Potash, J.B., Nimgaonkar, V.L., Dickerson, F., Llenos, I.C. & Weis, S., 2007. Polymorphisms in the homeobox gene OTX2 may be a risk factor for bipolar disorder. *American Journal of Medical Genetics, Part B: Neuropsychiatric Genetics*, 144(8), 1083–1086.
- Saheki, Y. & De Camilli, P., 2012. Synaptic Vesicle Endocytosis. *Cold Spring Harbor Perspectives in Biology*, 4(9), a005645–a005645.
- Sathyan, P., Golden, H.B. & Miranda, R.C., 2007. Competing interactions between micro-RNAs determine neural progenitor survival and proliferation after ethanol exposure: evidence from an ex vivo model of the fetal cerebral cortical neuroepithelium. *The Journal of Neuroscience*, 27(32), 8546–8557.
- Scacheri, P.C., Crawford, G.E. & Davis, S., 2006. [14] Statistics for ChIP-chip and DNase Hypersensitivity Experiments on NimbleGen Arrays. *Methods in Enzymology*, 411, 270–282.
- Schmittgen, T.D. & Livak, K.J., 2008. Analyzing real-time PCR data by the comparative CT method. *Nature Protocols*, 3(6), 1101–1108.
- Seitz, H., Royo, H., Bortolin, M.L., Lin, S.P., Ferguson-Smith, A.C. & Cavaillé, J., 2004. A large imprinted microRNA gene cluster at the mouse Dlk1-Gtl2 domain. *Genome Research*, 14(9), 1741–1748.
- Shimomura, Y. & Ito, M., 2005. Human Hair Keratin-Associated Proteins. *Journal of Investigative Dermatology Symposium Proceedings*, 251(3), 230–233.
- Shukla, P.K., Sittig, L.J., Ullmann, T.M. & Redei, E.E., 2011. Candidate Placental Biomarkers for Intrauterine Alcohol Exposure. *Alcoholism: Clinical and Experimental Research*, 35(3), 559–565.
- Shyu, A.-B. & Wilkinson, M.F., 2000. The Double Lives of Shutting mRNA Binding

- Proteins. *Cell*, 102(2), 135–138.
- Sittig, L.J., Shukla, P.K., Herzing, L.B.K. & Redei, E.E., 2011. Strain-specific vulnerability to alcohol exposure in utero via hippocampal parent-of-origin expression of deiodinase-III. *The FASEB Journal*, 25(7), 2313–2324.
- Stringer, R.L., Laufer, B.I., Kleiber, M.L. & Singh, S.M., 2013. Reduced expression of brain cannabinoid receptor 1 (Cnr1) is coupled with an increased complementary micro-RNA (miR-26b) in a mouse model of fetal alcohol spectrum disorders. *Clinical Epigenetics*, 5(1), 14.
- Sugiyama, S., Prochiantz, A. & Hensch, T.K., 2009. From brain formation to plasticity: Insights on Otx2 homeoprotein. *Development Growth and Differentiation*, 51(3), 369–377.
- Svingen, T. & Tonissen, K.F., 2006. Hox transcription factors and their elusive mammalian gene targets. *Heredity*, 97(2), 88–96.
- UniProt-Consortium, 2014. Activities at the Universal Protein Resource (UniProt). *Nucleic Acids Research*, 42, D191–D198.
- Veazey, K.J., Parnell, S.E., Miranda, R.C. & Golding, M.C., 2015. Dose-dependent alcohol-induced alterations in chromatin structure persist beyond the window of exposure and correlate with fetal alcohol syndrome birth defects. *Epigenetics & Chromatin*, 8(1), 39.
- Vergoulis, T., Vlachos, I.S., Alexiou, P., Georgakilas, G., Maragkakis, M., Reczko, M., Gerangelos, S., Koziris, N., Theodore, D. & Hatzigeorgiou, A.G., 2012. TarBase 6.0: Capturing the exponential growth of miRNA targets with experimental support. *Nucleic Acids Research*, 40, D222–D229.
- Vikalo, H., Hassibi, B. & Hassibi, A., 2010. Limits of Performance of Quantitative Polymerase Chain Reaction Systems. *IEEE Transactions on Information Theory*, 56(2), 688 –695.
- Wagstaff, J., Knoll, J.H.M., Glatt, K.A., Shugart, Y.Y., Sommer, A. & Lalande, M., 1992. Maternal but not paternal transmission of 15q11-13-linked nondeletion angelman syndrome leads to phenotypic-expression. *Nature Genetics*, 1(4), 291–294.
- Wang, L.L., Zhang, Z., Li, Q., Yang, R., Pei, X., Xu, Y., Wang, J., Zhou, S.-F. & Li, Y., 2009. Ethanol exposure induces differential microRNA and target gene expression and teratogenic effects which can be suppressed by folic acid supplementation. *Human Reproduction*, 24(3), 562–579.
- Wang, Q., Chow, J., Hong, J., Smith, A.F., Moreno, C., Seaby, P., Vrana, P., Miri, K., Tak, J., Chung, E.D., Mastromonaco, G., Caniggia, I. & Varmuza, S., 2011. Recent acquisition of imprinting at the rodent Sfmbt2 locus correlates with insertion of a large block of miRNAs. *BMC genomics*, 12(1), 204.

- Wang, Q., Liu, L., Pei, L., Ju, W., Ahmadian, G., Lu, J., Wang, Y., Liu, F. & Wang, Y.T., 2003. Control of synaptic strength, a novel function of Akt. *Neuron*, 38(6), 915–928.
- Wang, R.C., Wei, Y., An, Z., Zou, Z., Xiao, G., Bhagat, G., White, M., Reichelt, J. & Levine, B., 2012. Akt-mediated regulation of autophagy and tumorigenesis through Beclin 1 phosphorylation. *Science*, 338(6109), 956–959.
- Warde-Farley, D., Donaldson, S.L., Comes, O., Zuberi, K., Badrawi, R., Chao, P., Franz, M., Grouios, C., Kazi, F., Lopes, C.T., Maitland, A., Mostafavi, S., Montojo, J., Shao, Q., Wright, G., Bader, G.D. & Morris, Q., 2010. The GeneMANIA prediction server: Biological network integration for gene prioritization and predicting gene function. *Nucleic Acids Research*, 38, W214–W220.
- Weber, M., Davies, J.J., Wittig, D., Oakeley, E.J., Haase, M., Lam, W.L. & Schübeler, D., 2005. Chromosome-wide and promoter-specific analyses identify sites of differential DNA methylation in normal and transformed human cells. *Nature Genetics*, 37(8), 853–862.
- Worringer, K.A., Rand, T.A., Hayashi, Y., Sami, S., Takahashi, K., Tanabe, K., Narita, M., Srivastava, D. & Yamanaka, S., 2014. The let-7/LIN-41 pathway regulates reprogramming to human induced pluripotent stem cells by controlling expression of prodifferentiation genes. *Cell Stem Cell*, 14(1), 40–52.
- Wu, D.-D., Irwin, D.M. & Zhang, Y.-P., 2008. Molecular evolution of the keratin associated protein gene family in mammals, role in the evolution of mammalian hair. *BMC evolutionary biology*, 8(1), 241.
- Xu, D. et al., 2015. Phosphorylation and activation of ubiquitin-specific protease-14 by Akt regulates the ubiquitin-proteasome system. *eLife*, 4, e10510.
- Yekta, S., Tabin, C.J. & Bartel, D.P., 2008. MicroRNAs in the Hox network: an apparent link to posterior prevalence. *Nature Reviews Genetics*, 9(10), 789–796.
- Yoshimura, T., Arimura, N., Kawano, Y., Kawabata, S., Wang, S. & Kaibuchi, K., 2006. Ras regulates neuronal polarity via the PI3-kinase/Akt/GSK-3 β /CRMP-2 pathway. *Biochemical and Biophysical Research Communications*, 340(1), 62–68.
- Zhan, M., Miura, T., Xu, X. & Rao, M.S., 2005. Conservation and variation of gene regulation in embryonic stem cells assessed by comparative genomics. *Cell Biochemistry and Biophysics*, 43(3), 379–405.
- Zhang, C.R., Ho, M.-F., Vega, M.C.S., Burne, T.H.J. & Chong, S., 2015. Prenatal ethanol exposure alters adult hippocampal VGLUT2 expression with concomitant changes in promoter DNA methylation, H3K4 trimethylation and miR-467b-5p levels. *Epigenetics & Chromatin*, 8(1), 40.
- Zhou, F.C., Balaraman, Y., Teng, M., Liu, Y., Singh, R.P. & Nephew, K.P., 2011. Alcohol alters DNA methylation patterns and inhibits neural stem cell

- differentiation. *Alcoholism: Clinical and Experimental Research*, 35(4), 735–746.
- Zhou, F.C., Zhao, Q., Liu, Y., Goodlett, C.R., Liang, T., McClintick, J.N., Edenberg, H.J. & Li, L., 2011. Alteration of gene expression by alcohol exposure at early neurulation. *BMC Genomics*, 12(1), 124.

Chapter 3

Exploration of Differential DNA Methylation in Children with FASD

3.1. Overview

The results included in chapter 2 show that prenatal alcohol exposure (PAE) in mice involves changes to the DNA methylation of genes implicated in the manifestation of a number of endophenotypes related to fetal alcohol spectrum disorders (FASD). The results suggest that the differential DNA methylation in mice is caused by PAE. Furthermore, the alterations to DNA methylation may maintain changes to gene expression, which are present at adulthood and may result in the lifelong manifestation of some FASD endophenotypes. The experiments included in this chapter examine young children with a diagnosis of FASD whose mothers consumed alcohol during pregnancy. The human experiments had a restriction in that post-mortem brains were not available. Therefore, buccal swabs were utilized as they can be obtained non-invasively from individuals of any age and buccal epithelial cells represent the closest peripheral lineage related to cells incorporated in the brain.

This chapter analyzes data from human samples and characterizes the altered genome-wide CpG methylation profile in buccal swabs from children with FASD as compared to age, sex, and genetic background matched controls. Most, but not all, of these results are published in Laufer *et al.* (2015). The results have revealed a set of candidate genes and pathways that are altered by PAE in children with FASD. Select CpGs from the methylomic profile of the discovery cohort ($n_{\text{FASD}}=5$, $n_{\text{control}}=6$) were further examined in a larger number of children. The results show heterogeneity that is patient specific. As it stands, no single gene is consistently affected in all patients. However, the results do suggest that, as in mice, children with FASD show non-random changes in DNA methylation as compared to matched controls.

3.2. Introduction

The mechanisms of how PAE results in life-long FASD remains a major concern in the medical community. The cause of FASD, PAE, is known (Williams et al. 2015) and theoretically 100% preventable, yet the impact on society remains substantial. Current preventive and ameliorative strategies are complex and ineffective. The best strategy available is an early diagnosis that enables early therapeutic intervention (Paley & O'Connor 2009; Chokrobority-Hoque et al. 2014). A reliable method for early diagnosis of FASD is not yet available and will require understanding the underlying long-term molecular mechanisms. For a variety of reasons, the best insight into FASD has come from studies of animal models. Molecular results from rodent models of PAE have suggested that epigenetic alterations underlie FASD (Kleiber et al. 2014) and have been reproduced in a number of laboratories (Marjonen et al. 2015; Basavarajappa & Subbanna 2016). Unlike mouse model research, reports on the epigenetic profiles of humans with FASD are rather limited.

In 2009, Ouko *et al.* examined the sperm of alcohol consuming adult men and found hypomethylation at the two imprinted regions; *H19* and *DLK1-DIO3* (Ouko et al. 2009). In 2010, Krishnamoorthy *et al.* examined human embryonic stem cells and observed that exposure to low amounts of alcohol altered a nicotinic acetylcholine receptor subunit (CHRNA5), which is linked to the altered expression of GABA and Glutamate (NMDA) receptors (Krishnamoorthy et al. 2010). In 2011, Taléns-Visconti *et al.* examined neural differentiation in neuroepithelial progenitor cells, which were induced from human embryonic stem cells (hESCs), and observed that alcohol alters the survival, differentiation into neurons and glia, and expression of select genes related to these processes (Talens-Visconti et al. 2011).

More recently, Khalid *et al.* examined the transcriptome and methylome of hESCs exposed to alcohol (Khalid et al. 2014). They observed that the expression of genes related to metabolic processes, oxidative stress, and neuronal properties of stem cells were altered. The group also examined differential methylation and observed that undifferentiated cells appear to be more vulnerable to alcohol than their differentiated counterparts, the alterations are wide-spread with distinct regions of hypermethylation, and that not all altered methylation corresponds to altered transcription. The top genes

showing altered methylation were involved in neuroactive ligand–receptor interaction, vascular smooth muscle contraction, calcium signaling pathways, and energy metabolism. Additionally, Halder *et al.* and Mandal *et al.* examined the effect of alcohol on human embryonic carcinoma cells that were induced to undergo neural differentiation (Halder et al. 2015; Mandal et al. 2016). They observed alterations in pathways related to neurodevelopment, cell-signaling (including PI3K/AKT/mTOR), and cell-adhesion.

At the time of this research, two other research groups had published *in vivo* examinations of the association between FASD and DNA methylation at select loci in humans. Lee *et al.* examined a Korean cohort of families, where it was found that there are changes in the unsorted peripheral blood of parents and also the cord blood of FASD children (Lee et al. 2015). There was a significant reduction of methylation to the promoter of a dopamine transporter (*SLC6A3*) in heavy alcohol consuming fathers and their offspring. The *SLC6A3* promoter also showed a significant decrease of promoter methylation in mothers who consumed both moderate and heavy amounts of alcohol. The methylation of a serotonin transporter (*SLC6A4*) promoter was significantly decreased in children from both heavy and moderate alcohol consuming mothers. Methyl CpG binding protein 2 (*MECP2*) showed increased promoter methylation in the offspring of mothers with moderate alcohol consumption. The other human report is by Masemola *et al.*, who examined saliva in a South-African cohort (Masemola et al. 2015). There is elegance to the examination of saliva (buccal epithelial cells) in that the cells share an ontogenetic relationship to neuronal cell types via the ectoderm. The aforementioned study only focused on confirmed cases of FAS, and did not examine FASD, and the differential methylation examined was limited to few selected imprinting control regions (ICRs). Most of the pyrosequenced regions weren't informative but there were significant decreases of methylation in maternal ICRs. KvDMR1 showed a 7.09% decrease in methylation and PEG3 showed a 1.49% decrease.

Taken together, the examinations into human cells shows similarities in alcohol response to the mouse model presented in chapter 2. Also, at the time of this research, no published study on humans had attempted genome-wide DNA methylation scans of patients born with FASD. In this chapter, I will describe the results of experiments on cheek swab DNA methylation from young children diagnosed with FASD as compared to

unaffected (age, sex, and race) matched controls. The results are informative and argue that the effects of PAE on DNA methylation are similar but not identical between the mouse model and human patients. The results suggest that the mouse model used to study the molecular underpinning of PAE is valid. They also show that the analysis of a single gene cannot be used to identify FASD, which demonstrates the heterogeneity of this complex disorder.

3.3. Materials & Methods

The results are primarily based on two cohorts [discovery ($n_{FASD}=5$, $n_{control}=6$) and replication ($n_{FASD}=6$, $n_{control}=6$)] of young children clinically diagnosed with FASD by Dr. J. Kapalanga in Ontario, Canada. All subjects of the discovery cohort had most features of FASD and matched controls showed no sign of the disorders (**Table 3.1A**). The patients were recruited from the same clinic while visiting for annual check-ups or relatively minor non-neurodevelopmental or behavioural problems, which may include asthma, allergies, musculoskeletal problems, or gastrointestinal problems. Following ethical approval and informed consent from parents or guardians, the study subjects contributed cheek swabs for analysis of buccal epithelial DNA. A second cohort of FASD patients (replication cohort) was comprised of a different set of 6 children with FASD and unaffected controls. Although four (E8, E13, E18, E19) of the six patients of the replication cohort were 6 -10 year-old males and not on medication, two were older 7 and 9 year-old females (E7 and E17) and on psychotropic/stimulant medication (**Table 3.1B**). Finally, a third cohort representative of the general population, and consisting in part of the first two cohorts, from Owen Sound, Ontario was also examined (**Appendix G**). This cohort primarily consisted of FASD patients that were much more heterogeneous. The FASD patients and matched controls in the general population cohort were much more variable in terms of age, sex ratio, ancestry, family history of mental illness, as well as other medical conditions and required medication.

Table 3.1. Clinical features of patients from the discovery (A) and replication (B) cohorts with the diagnosis of FASD.

A Discovery Cohort						
Patient ID	E1	E2	E3	E4	E5	E6
Patient (Age) and Sex	(6) M	(6) M	(5) M	(4) M	(3) M	(3) M
Clinical Features						
Developmental delay	X	X	X	X	X	X
Hyperactivity, poor impulse control	X	X	X	X	X	X
Learning disorders	X	X	X			
Short attention span and inattention	X	X		X		
Conduct disorder	X	X	X		X	
Oppositional defiant disorder	X			X	X	
Social difficulties	X			X	X	
Nervousness and anxiety		X	X	X		
Mood disorder	X			X		
Macrocephaly/macrotia		X	X			
Microcephaly/microtia				X	X	
Distinctive facial features	X			X	X	X
Stimulant/Psychotropic Meds	No	No	No	No	No	No

B Replication Cohort						
Patient ID	E7	E8	E13	E17	E18	E19
Patient (Age) and Sex	(7) F	(6) M	(6) M	(9) F	(6) M	(10) M
Clinical Features						
Developmental delay	X	X	X		X	X
Hyperactivity, poor impulse control	X	X	X	X	X	X
Learning disorders	X		X		X	X
Short attention span and inattention	X	X	X	X	X	X
Conduct disorder	X	X	X	X	X	X
Oppositional defiant disorder	X	X	X	X		
Social difficulties	X	X	X			
Nervousness and anxiety	X	X	X			X
Mood disorder			X	X		X
Macrocephaly/macrotia		X				
Microcephaly/microtia						X
Distinctive facial features	X		X			X
Stimulant/Psychotropic Meds	Yes	No	No	Yes	No	No

3.3.1. Methylation Array

The Illumina HumanMethylation450 BeadChip (450K array) is a dual channel SNP genotyping microarray that utilizes sodium bisulfite conversion and a targeted array approach to examine DNA methylation. During sodium bisulfite treatment, cytosine is converted by deamination to uracil, whereas 5-methylcytosine (5mC) is protected from the conversion. During PCR amplification, uracil is paired with adenine and that adenine is later paired thymine. Thus, bisulfite conversion creates a single nucleotide variant that converts cytosine to thymine, whereas 5mC is detected as a cytosine. The 450K array interrogates 485,764 sites at single nucleotide resolution across 99% of RefSeq genes (Bibikova et al. 2011; Sandoval et al. 2011). There is an average of 17 CpG sites per a gene that represent the promoter, 5' UTR, first exon, gene body, and 3' UTR. The 450K array covers 96% of CpG islands and other features, as well as sites based on genome-wide association studies (GWAS). Methylation levels, known as β -values, are determined by comparing the ratio of C to T at the CpG site.

In order to analyze their DNA methylation, individual cheek swabs from FASD and matched control children were used to isolate genomic DNA using the QIAamp DNA Mini Kit following manufacturer's protocol. This DNA was subject to sodium bisulfite modification at The Centre for Applied Genomics (Toronto, Canada). The genome-wide CpG methylation for each subject was assessed using the 450K array, following the manufacturer's protocol. The arrays were scanned using Illumina's GenomeStudio at The Centre for Applied Genomics (Toronto) that generated scan data (.idat files) for each subject used in this analysis.

The .idat files were analyzed using Partek Genomics Suite® Version 6.6. A site based DNA methylation workflow for Illumina BeadArray Methylation was utilized. Pre-processing using both control normalization and background subtraction was performed using Illumina's algorithm to generate β -values. β -values were then normalized, converted to a fold-change and subjected to a one-way ANOVA analysis to identify regions of differential methylation using annotations from Hg18. Custom genome dot plots (also known as Manhattan plots) were generated from the ANOVA results. Different stringencies of genes list were used for hierarchical clustering ($p < 0.005$), gene ontology ($p < 0.005$) analysis using Enrichr (Chen et al. 2013), and bioinformatic pathway

analysis via Partek Pathways ($p < 0.05$). Additional annotations were added to top CpGs using Ensembl (Flieck et al. 2014) (for novel ncRNAs) and Uniprot (UniProt-Consortium 2014) (for protein function and localization). The subset-quantile within array normalization (SWAN) algorithm (Maksimovic et al. 2012; Fortin et al. 2014) from the minifi bioconductor package was used within Partek to allow for the multi-batch analysis (Pidsley et al. 2013).

3.3.2. Pyrosequencing

Pyrosequencing® is a sequencing by synthesis method (Tost & Gut 2007; Nyrén 2007). When a deoxyribonucleoside triphosphate (dNTP) is incorporated a pyrophosphate is released. The pyrophosphate is converted to ATP and used by luciferase to produce light. The nucleotides are added a single base a time, and degraded by apyrase in-between steps. Pyrosequencing enables absolute quantification of methylation levels without depending on normalization to matched controls, and thus is ideal for obtaining methylation in individual cases. While the gold standard for DNA methylation, pyrosequencing is relatively limited by short reads and a high use of resources.

In order to confirm the results of the 450K array, the same bisulfite converted buccal swab DNA from the discovery cohort array was pyrosequenced by EpigenDx on the PSQ96 HS System (Qiagen) following the manufacturer's instructions, using custom assays (www.EpigenDx.com), and a gradient of controls with known methylation levels. This allowed for the quantification of the absolute percent methylation of each CpG using QCpG software (Qiagen) (Lim et al. 2014). The sequencing reads also allowed for the analysis of SNPs known to be within or close to the CpGs of the 450K probes.

For the follow-up into the general population cohort, assays were developed based on performance from the DNA methylation arrays, primarily from the discovery cohort. A number of genes affected in arrays were examined by pyrosequencing. The gene *COLEC11* was selected based on results on the 450K arrays and the NGS panel. *PCDBH18* was selected based on performance on the human arrays and the results in the trimester 3 binge exposure mouse model. *HTT* was selected due to performance on previous DNA methylation arrays and pyrosequencing. Furthermore, a number of CpG

sites located at 12q24.31, 10q26.12, and 2q22.1 were selected based on performance from the NGS panel.

3.3.3. NGS Panel

The Ion Torrent Personal Genome Machine (PGM)TM is a next-generation sequencing (NGS) system that utilizes sequencing by synthesis and detects the release of hydrogen ions from dNTPs during polymerization (Merriman et al. 2012). dNTPs are added one at a time and the released hydrogen ion is detected by an ion sensor. While the Ion Torrent PGM is less accurate than pyrosequencing, it is more resource effective and thus can be used to create custom targeted bisulfite sequencing panels to screen a large number of loci across relatively few samples. Therefore, a subset of the 268 CpGs identified on the arrays were selected for further development on a next generation sequencing (NGS) panel using the Ion Torrent PGM. Thirty of the top performing CpGs from the 450K array were selected as loci for primer design based on the criteria of a greater than 1.5 fold change and a preference against a large number of flanking CpGs. Thirty gene and intragenic sequences +/- 5000 bases were acquired from the Ensembl database or UCSC database. Target regions of each gene were selected based on the methylation array results. The panel design, bisulfite conversion, sequencing, and calculation of methylation values was performed by EpigenDx (Hopkinton, MA).

500 ng human genomic DNA was bisulfite treated using the EZ DNA Methylation Kit (Zymo Research). Multiplex PCR was performed using 0.5 units of TaKaRa EpiTaq HS (Takara Bio) in 2x master mix including primers (EpigenDx) in a 20 μ l reaction. The PCRs were performed using the following protocol: 95°C 15 min; (95°C 30s; 63°C (or 56 °C) 30 s, -1°C; 68°C 30 s) 9x cycles; (95°C 30s; 55°C (or 50°C) 30 s; 68°C 30 s) 36x cycles; 68°C 5 min; 4°C hold. Libraries were prepared using the KAPA Library Preparation Kit (Cat# KK8310) for Ion Torrent and were quantified by real-time PCR using KAPA Library Quantification (KAPA Biosystems). 344 million library molecules were templated using the Ion PGM Template OT2 200 kit and sequenced using an Ion PGMTM Sequencing 200 Kit v2 kit with Ion 316TM and Ion 318TM Chips (Life Technologies) on the Ion Torrent PGM. FASTQ files from the Ion Torrent PGM were aligned to the local database using open source Bismark Bisulfite Read Mapper with the

Bowtie2 alignment algorithm. Methylation levels were calculated in Bismark by dividing the number of methylated reads by the number of total reads, considering all CpG sites covered by a minimum of 30 total reads.

The results presented include a total of 31 target PCRs designed by PyroMark Assay Design Software (Qiagen, Pyrosequencing) for the assessment of the human samples. During design and optimization 23 loci passed quality control for assay design, leaving a total of 67 CpGs for analysis from the Buccal swabs of children. The CpG methylation level was then analyzed using a one-way ANOVA.

3.4. Results

The results suggest that FASD is associated with a profile of differential DNA methylation in buccal swabs. Using a stringent but not false discovery rate (FDR) corrected CpG list ($p<0.005$), genome-wide differential methylation of children with FASD was analyzed in the: **(A)** discovery cohort and **(B)** replication cohort (**Figure 3.1**). In each case, the heatmaps show that children diagnosed with FASD clearly group together and are distinct from matched non-FASD controls. From these arrays a one-way ANOVA was created to generate a list of CpGs and corresponding genes that showed significant differential methylation between FASD children and matched controls (after pre-processing and data normalization). The results of the discovery and replication cohorts were analyzed separately in order to avoid any batch effects. This analysis of the discovery cohort that represented established maternal drinking and relatively uniform manifestation of FASD (developmental delays, hyperactivity/poor impulse control, and mental deficits) identified 268 significantly ($p<0.005$) differentially methylated CpG sites (**Appendix H**). Also notable is the differential methylation of genes that modify the epigenome, such as *EHMT2* ($p=0.0002$), *PRDM6* ($p=0.004$), and *HDCA4* ($p=0.004$).

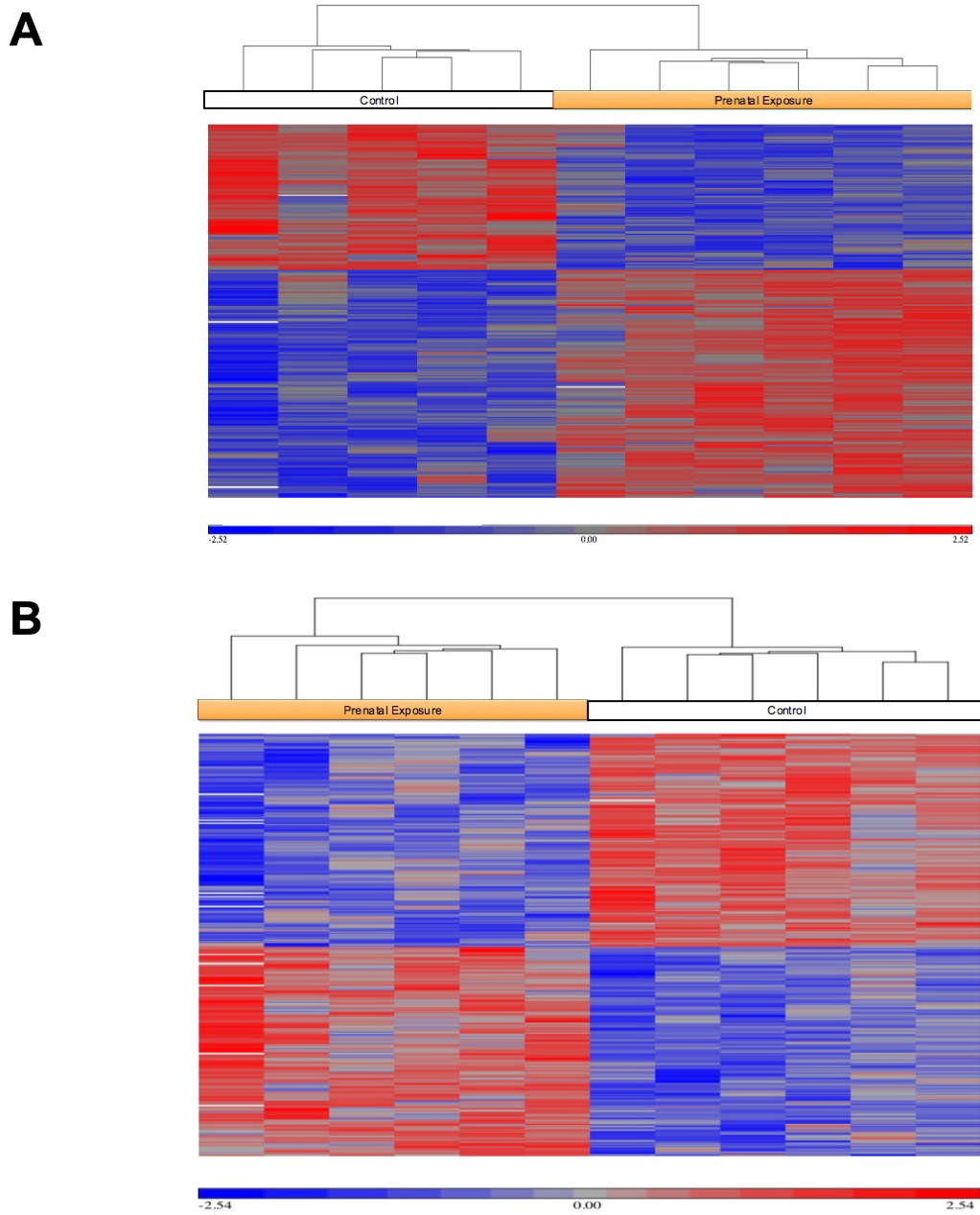


Figure 3.1. Differential DNA methylation in children diagnosed with FASD: **A)** Heatmap of significantly ($p<0.005$) differentially methylated targeted CpG sites generated using hierarchical clustering of standardized β -values from buccal epithelial DNA obtained via swabs from FASD ($n=6$) and matched control ($n=5$) children from the discovery cohort; **B)** Heatmap of significantly ($p<0.005$) differentially methylated targeted CpG sites generated using hierarchical clustering of standardized β -values from buccal epithelial DNA obtained via swab from FASD ($n=6$) and matched control ($n=6$) children from the replication sample.

3.4.1. Gene Network and Ontologies Associated with FASD

Figure 3.2 shows the GeneMANIA network generated from the genes regulated by the 268 CpG sites that showed significantly ($p<0.005$) altered methylation in the discovery cohort. Among other genes it identified 11 sites that regulate the clustered protocadherins genes located on 5q31 (**Figure 3.3**).

Next, the differentially methylated genes from the discovery cohort were used in an analysis towards identification of specific biological processes, functions, and pathways affected as a result of changes in methylation. The results (**Table 3.2**) show that the major biological processes affected include cell adhesion and nervous system development. There are alterations to relevant molecular functions including calcium ion binding and channel activity. The genes code for proteins localized to synaptic vesicles and the cytoskeleton. Notably, alterations to similar ontologies were observed in the gene expression data from the mouse model binge injection paradigms (Kleiber et al. 2013). There were also similar alterations to DNA methylation observed in the continuous preference drinking (CPD) paradigm presented in chapter 2 and those results are compared in chapter 4.

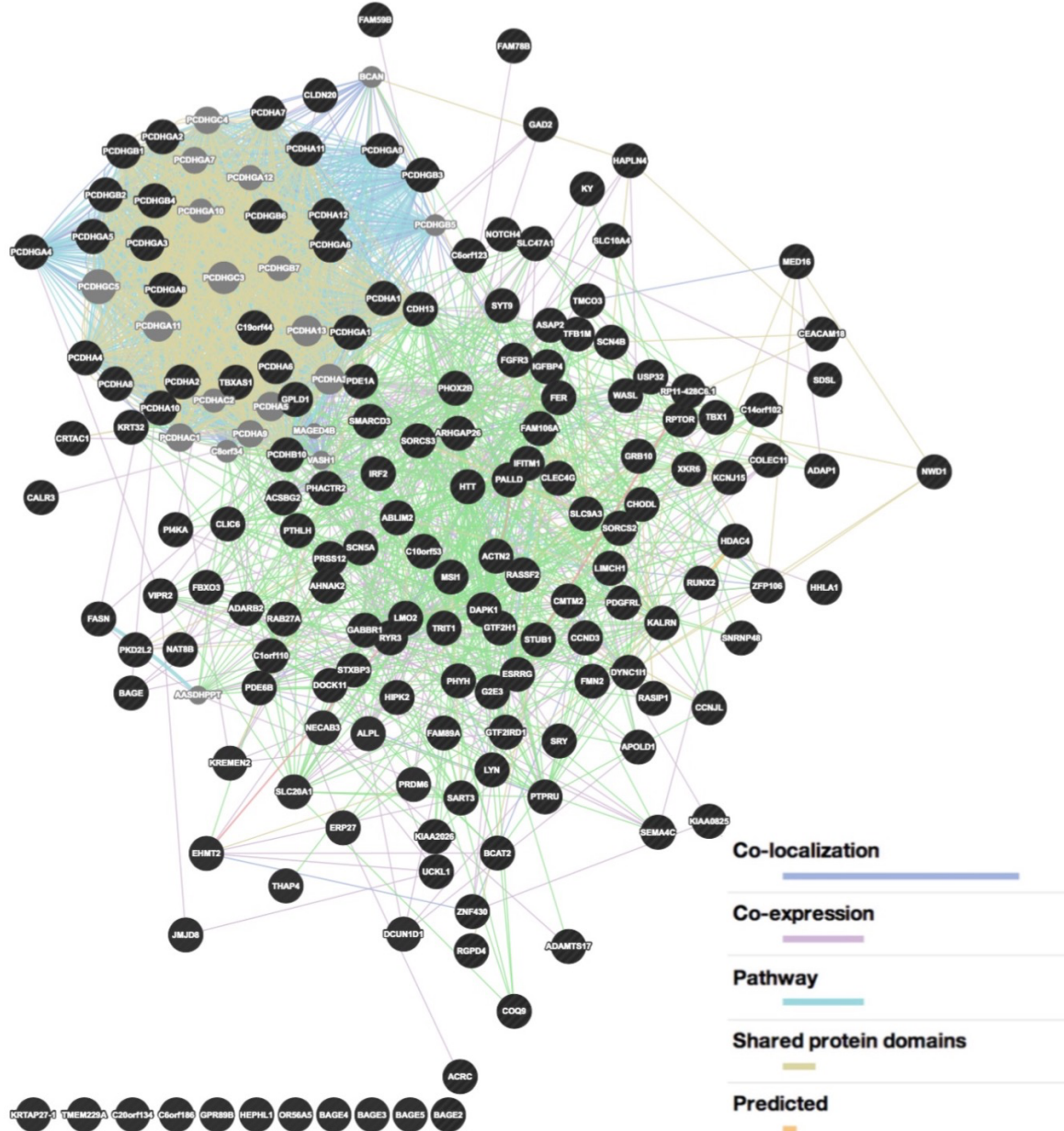


Figure 3.2. GeneMANIA associative network analysis of genes annotated to differentially methylated CpGs ($p < 0.005$) from cheek swabs of the discovery cohort.

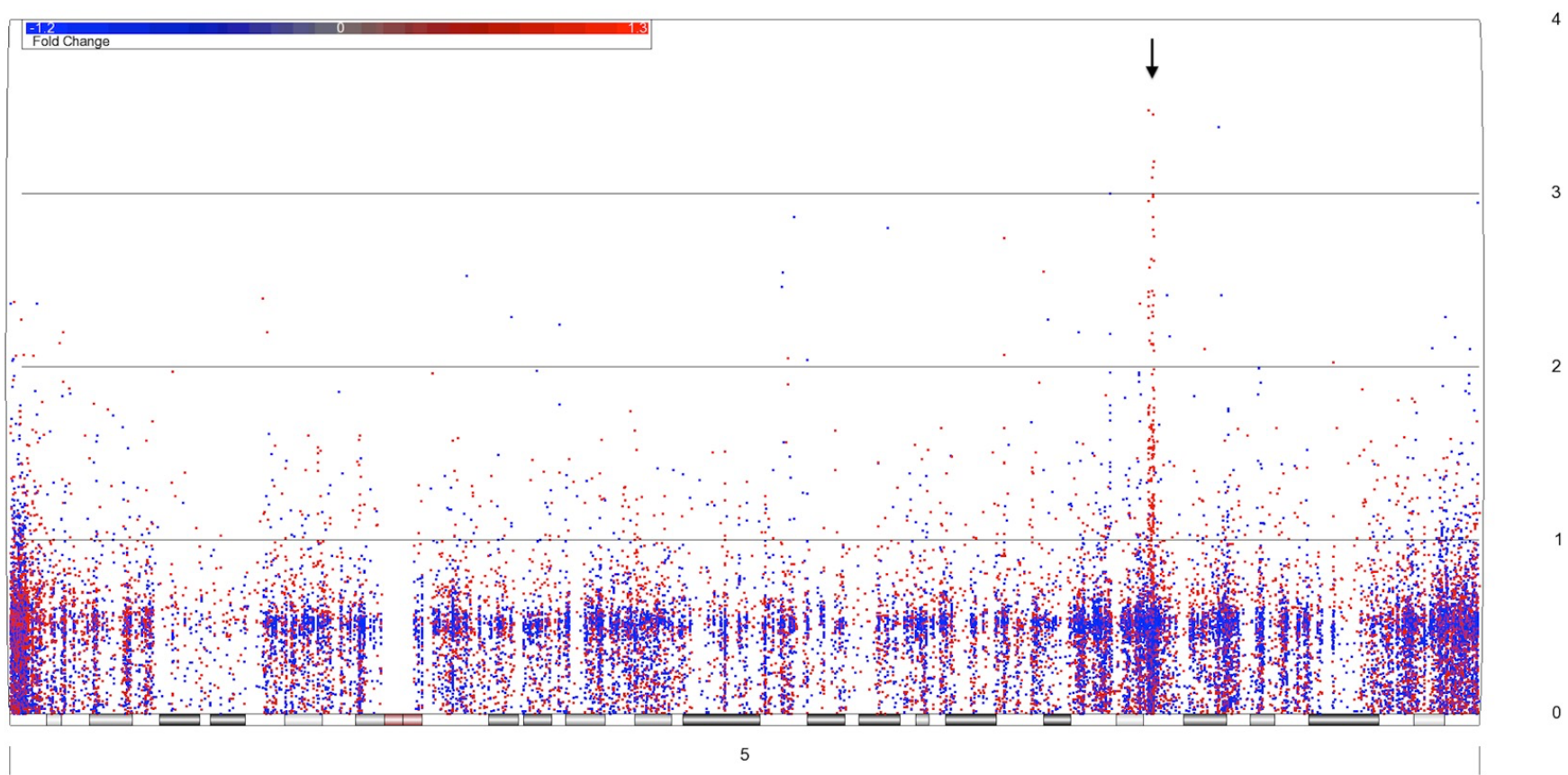


Figure 3.3. Manhattan plot of human chromosome 5 from the discovery cohort. Genomic location is plotted on the x-axis and $-\log_{10}$ (*p*-value) of differential CpG methylation from FAE is on the y-axis (Manhattan plot). Each dot represents a single CpG site. A red dot indicates an increase in methylation and a blue dot indicates a decrease in methylation. A black arrow indicates the clustered protocadherin locus.

Table 3.2. Ontologies for genes with significant ($p<0.005$) differences in CpG methylation from the discovery cohort.

Enrichr GO Biological Processes	Overlap	p-value
Homophilic cell adhesion via plasma membrane adhesion molecules (GO:0007156)	25/142	5.9E-24
Cell-cell adhesion (GO:0098609)	26/191	2.5E-22
Cell-cell adhesion via plasma-membrane adhesion molecules (GO:0098742)	26/190	2.2E-22
Nervous system development (GO:0007399)	12/277	1.0E-05
Replacement ossification (GO:0036075)	4/30	2.3E-04
Endochondral ossification (GO:0001958)	4/30	2.3E-04
Ossification (GO:0001503)	7/116	1.1E-04
Osteoblast development (GO:0002076)	3/19	9.4E-04
Vesicle localization (GO:0051648)	4/51	1.4E-03
Calcium-dependent cell-cell adhesion via plasma membrane cell adhesion molecules (GO:0016339)	3/28	2.6E-03
Enrichr GO Cellular Location	Overlap	p-value
Cytoplasmic vesicle membrane (GO:0030659)	8/229	7.2E-04
Cytoplasmic vesicle part (GO:0044433)	10/363	9.4E-04
Vesicle membrane (GO:0012506)	8/249	1.2E-03
Actin cytoskeleton (GO:0015629)	6/193	5.8E-03
Z disc (GO:0030018)	4/87	6.5E-03
Actin filament (GO:0005884)	3/44	6.6E-03
Voltage-gated sodium channel complex (GO:0001518)	2/15	8.3E-03
Sodium channel complex (GO:0034706)	2/18	1.1E-02
Synaptic vesicle membrane (GO:0030672)	2/22	1.6E-02
Integral component of plasma membrane (GO:0005887)	15/1066	2.9E-02
Enrichr GO Molecular Function	Overlap	p-value
Calcium ion binding (GO:0005509)	34/698	3.3E-15
Solute:proton antiporter activity (GO:0015299)	3/17	8.4E-04
Ion channel binding (GO:0044325)	5/80	1.3E-03
Solute:cation antiporter activity (GO:0015298)	3/28	3.1E-03
Monovalent cation:proton antiporter activity (GO:0005451)	2/10	5.5E-03
3',5'-cyclic-GMP phosphodiesterase activity (GO:0047555)	2/11	6.5E-03
Sodium ion transmembrane transporter activity (GO:0015081)	5/128	8.6E-03
Ligand-dependent nuclear receptor transcription coactivator activity (GO:0030374)	3/46	1.1E-02
Activating transcription factor binding (GO:0033613)	3/53	1.6E-02
Fibroblast growth factor binding (GO:0017134)	2/20	1.8E-02
Monovalent inorganic cation transmembrane transporter activity (GO:0015077)	8/343	1.8E-02
Voltage-gated sodium channel activity (GO:0005248)	2/22	2.0E-02
Cation:cation antiporter activity (GO:0015491)	2/22	2.1E-02

3.4.2. The Top Canonical Pathways are Related to Neurodevelopment and Neurotransmission

The top canonical pathways (**Table 3.3**) of the significantly ($p<0.05$) altered CpGs identified are largely related to neurodevelopment as they are involved in stem cell signaling, synaptic connections, metabolism, and immune processes. Hippo signaling (**Figure 3.4**) had 25 out of 120 genes affected, which was the most significant enrichment ($p=0.0002$) in the pathway analysis. The glutamatergic synapse pathway (**Figure 3.5**) was the top synaptic pathway and showed a significant ($p=0.001$) enrichment with 18 out of 77 genes showing significant (less stringent list, $p<0.05$) alterations to CpG methylation. Furthermore, there was a significant ($p=0.005$) alteration to the calcium signaling pathway (**Figure 3.6**) with 23 out of 102 genes affected. Notably, a number of synaptic pathways were enriched. The retrograde endocannabinoid signaling pathway (**Figure 3.7**) was significantly ($p=0.006$) altered with 16 out of 60 genes affected and the serotonergic synapse pathway (**Figure 3.8**) was significantly ($p=0.009$) altered with 16 out of 63 genes affected.

The pathways presented in detail were selected due to their similarities to results from the mouse model (chapter 2). Also notable is the overlap of the human methylation results with alterations to gene expression observed in the mouse binge injection paradigms (Kleiber et al. 2013). In the trimester 1 exposure paradigm calcium signaling was altered. In the trimester 2 exposure paradigm serotonin receptor signaling was altered. In the trimester 3 exposure paradigm glutamate receptor signaling, retinoic acid-mediated apoptosis, and circadian rhythm signaling were altered. Finally, a role for retrograde endocannabinoid signaling was also seen in the trimester 3 exposure model, where a miRNA and target receptor were reciprocally deregulated (Stringer et al. 2013).

Table 3.3. Pathway analysis for genes with significant ($p<0.05$) differences in CpG methylation from the discovery cohort.

Partek KEGG Pathways	Overlap	p-value
Hippo signaling pathway	25/85	2.0E-04
Other types of O-glycan biosynthesis	8/10	2.9E-04
Phagosome	23/85	9.7E-04
Glutamatergic synapse	18/59	1.1E-03
HTLV-I infection	33/152	2.3E-03
Calcium signaling pathway	23/99	5.1E-03
Retrograde endocannabinoid signaling	16/60	6.2E-03
Viral myocarditis	10/29	7.0E-03
Viral carcinogenesis	23/104	8.4E-03
Serotonergic synapse	16/63	9.2E-03
Axon guidance	17/71	1.2E-02
Allograft rejection	8/22	1.2E-02
Cell adhesion molecules (CAMs)	18/78	1.3E-02
Endocytosis	23/109	1.3E-02
Lysine degradation	9/28	1.5E-02
Graft-versus-host disease	8/23	1.5E-02
Basal cell carcinoma	10/34	1.7E-02
Type I diabetes mellitus	8/24	1.8E-02
Fatty acid metabolism	7/20	2.1E-02
Circadian entrainment	13/53	2.2E-02
Autoimmune thyroid disease	8/27	3.0E-02
Long-term depression	8/28	3.5E-02
Focal adhesion	21/109	3.8E-02
ECM-receptor interaction	11/46	3.9E-02
Dorso-ventral axis formation	5/14	4.7E-02
Cholinergic synapse	14/68	5.5E-02
Apoptosis	10/44	6.1E-02
Arrhythmogenic right ventricular cardiomyopathy (ARVC)	9/38	6.1E-02
Wnt signaling pathway	16/83	6.4E-02

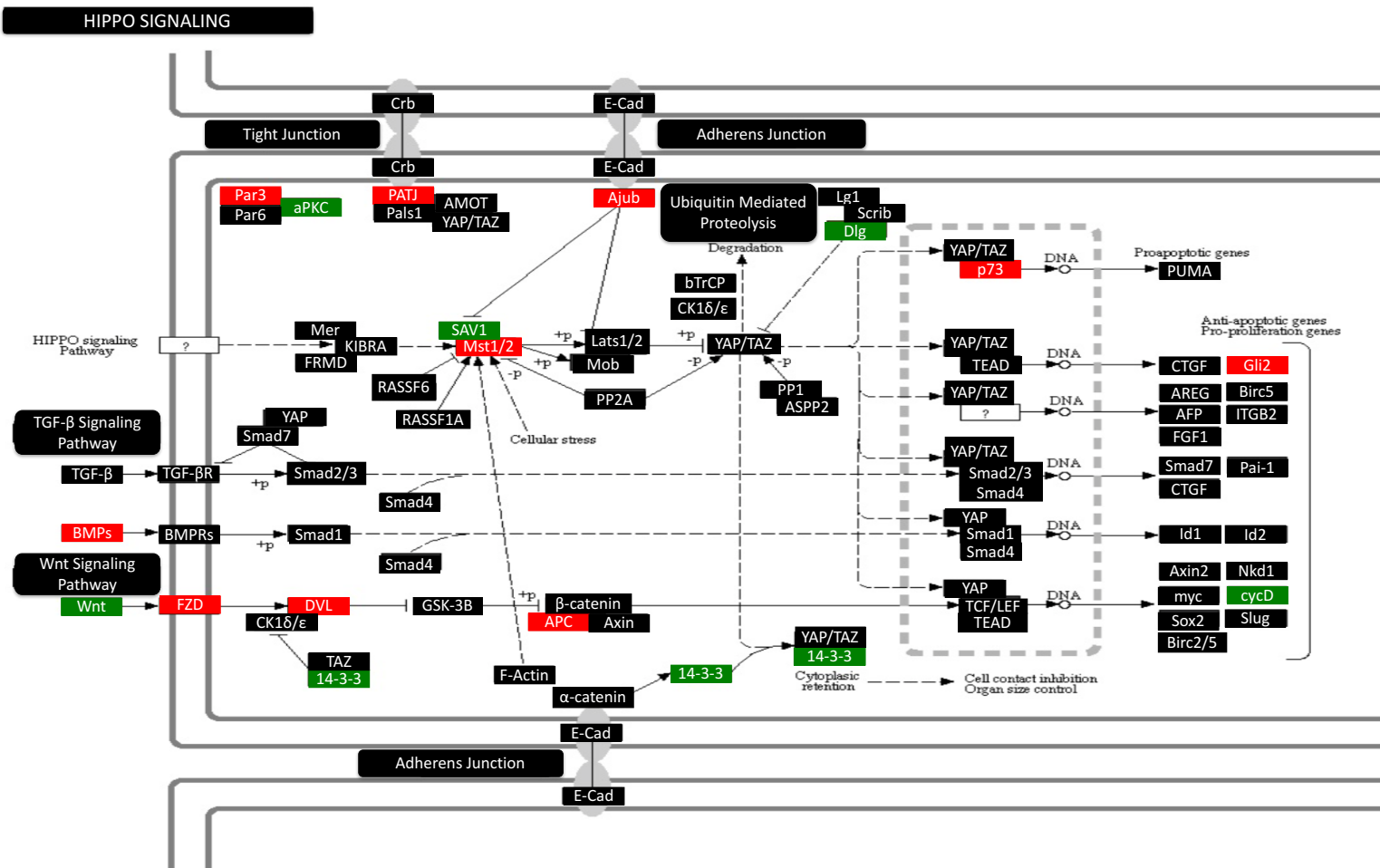


Figure 3.4. Genes in the hippo signaling pathway affected by altered CpG methylation in children from the discovery cohort. Genes were identified and then assembled as protein complexes. Green marks a decrease in methylation and potentially increased gene expression while red indicates an increase in methylation and potentially decreased gene expression.

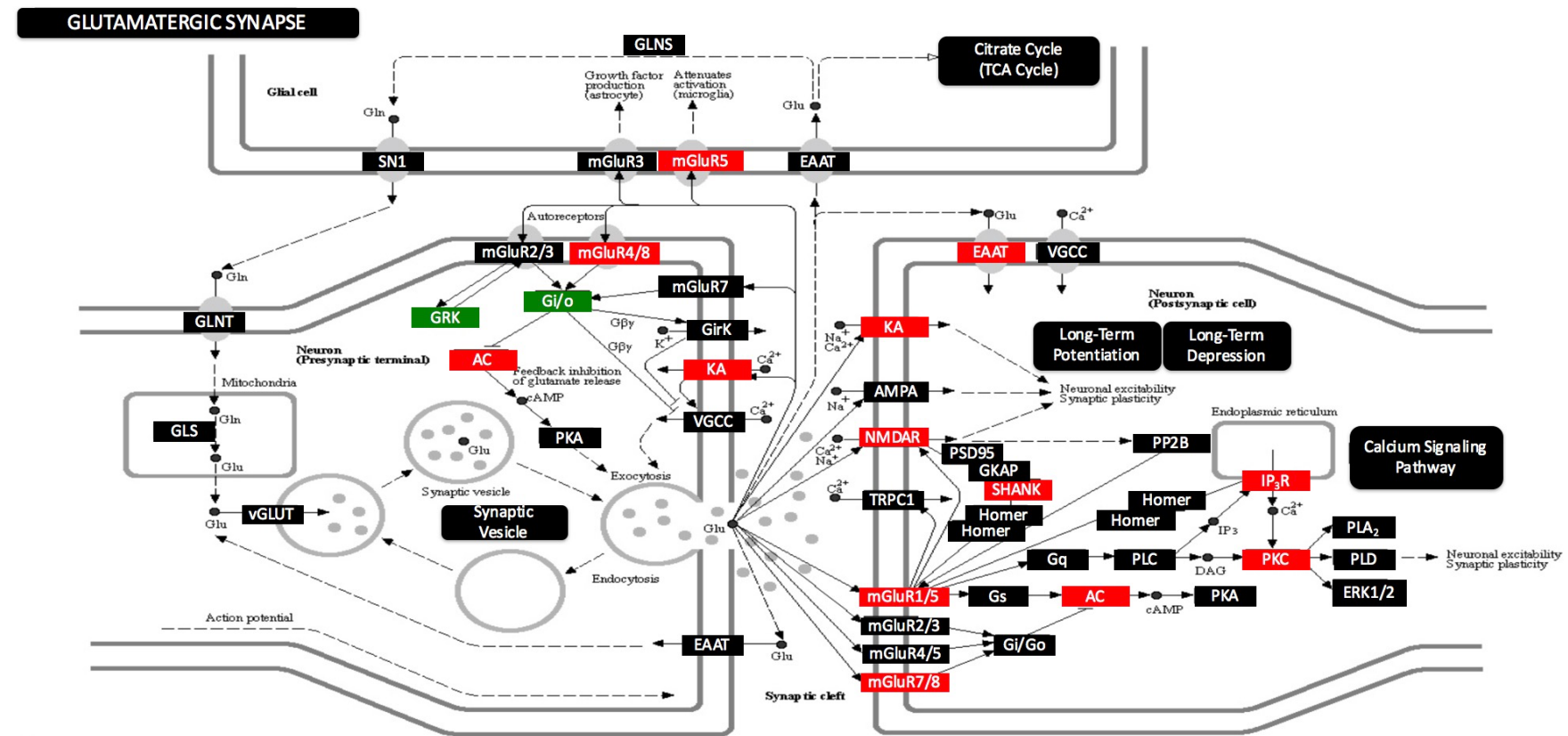


Figure 3.5. Genes in the glutamatergic synapse pathway that were affected by altered CpG methylation in children from the discovery cohort.

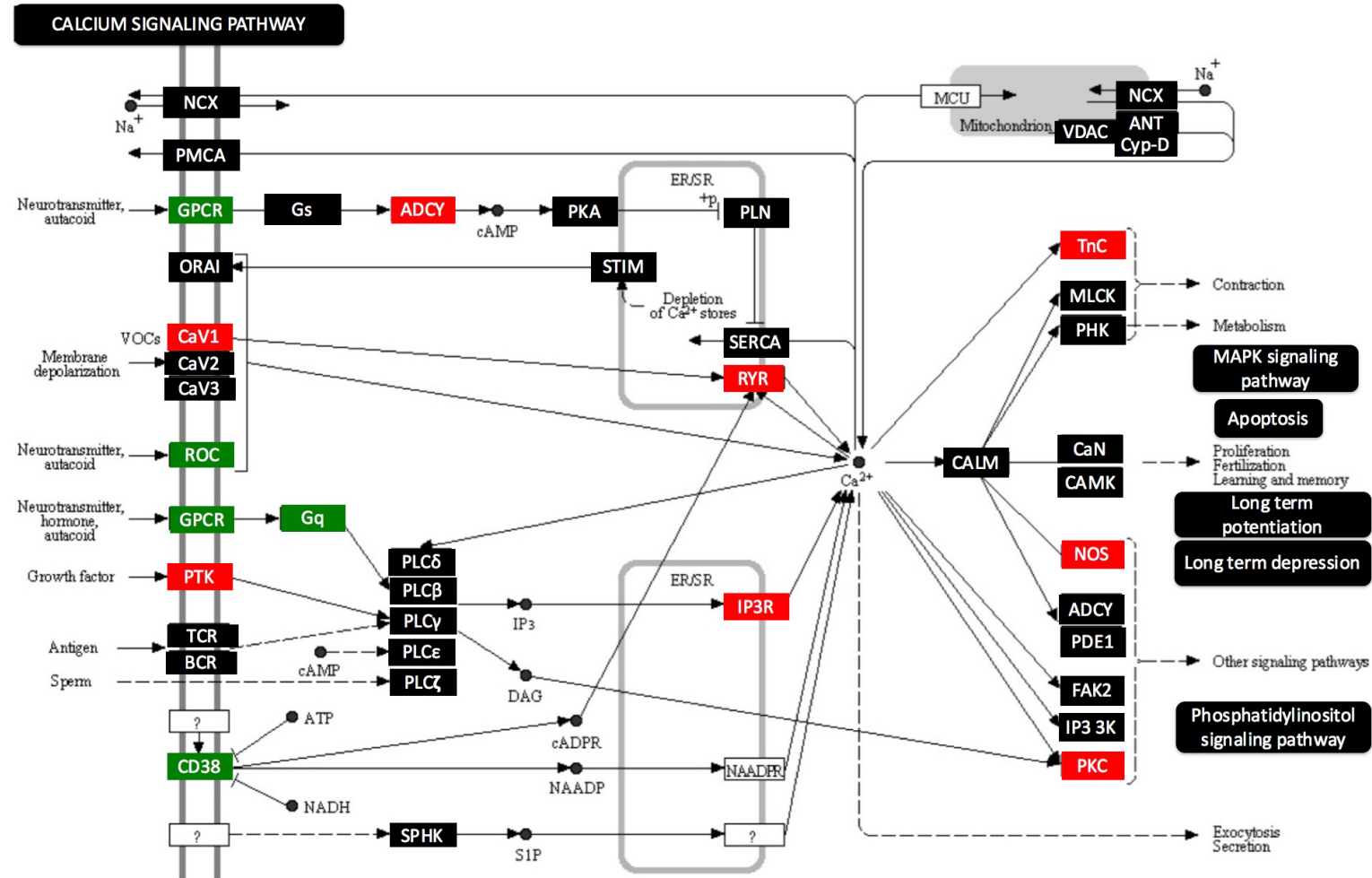
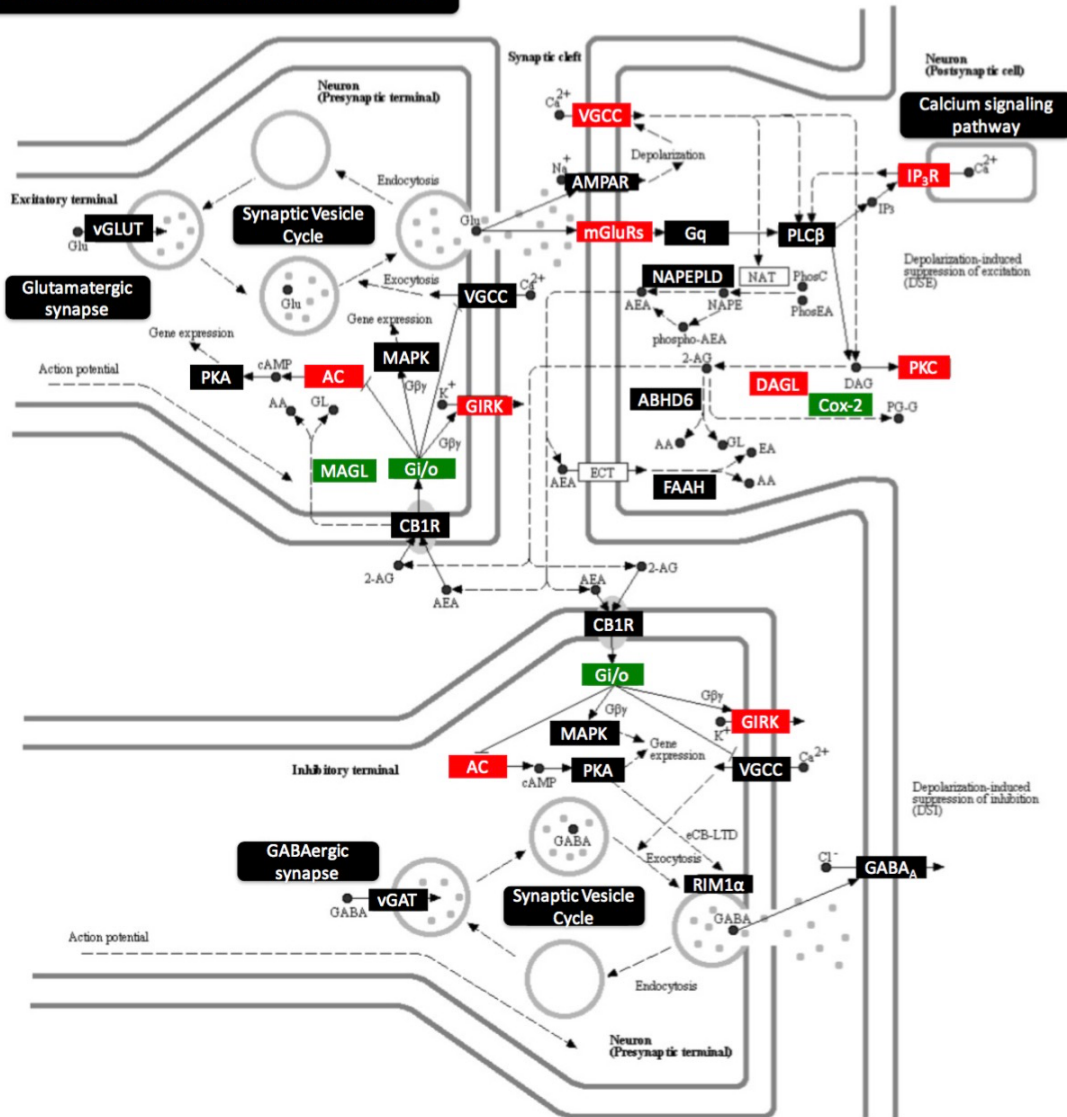


Figure 3.6. Genes in the calcium signaling pathway that were affected by altered CpG methylation in children from the discovery cohort.

RETROGRADE ENDOCANNABINOID SIGNALING



Gene Symbol	Function	CpG ID	p-value	Fold Change	Chromosome	CpG Coordinate
GAD2	Glutamate Metabolism	cg14429209	0.002	1.2	10	26549511
GABBR1	G-Protein Coupled Receptor (GABA)	cg00667298	0.003	1.1	6	29684308
LOC440040	Glutamate Receptor Pseudogene	cg09176539	0.001	1.6	11	49536650

Figure 3.7. Genes in the retrograde endocannabinoid signaling pathway that were affected by altered CpG methylation in children from the discovery cohort. A list of notable CpGs as well as related genes and functions is also presented.

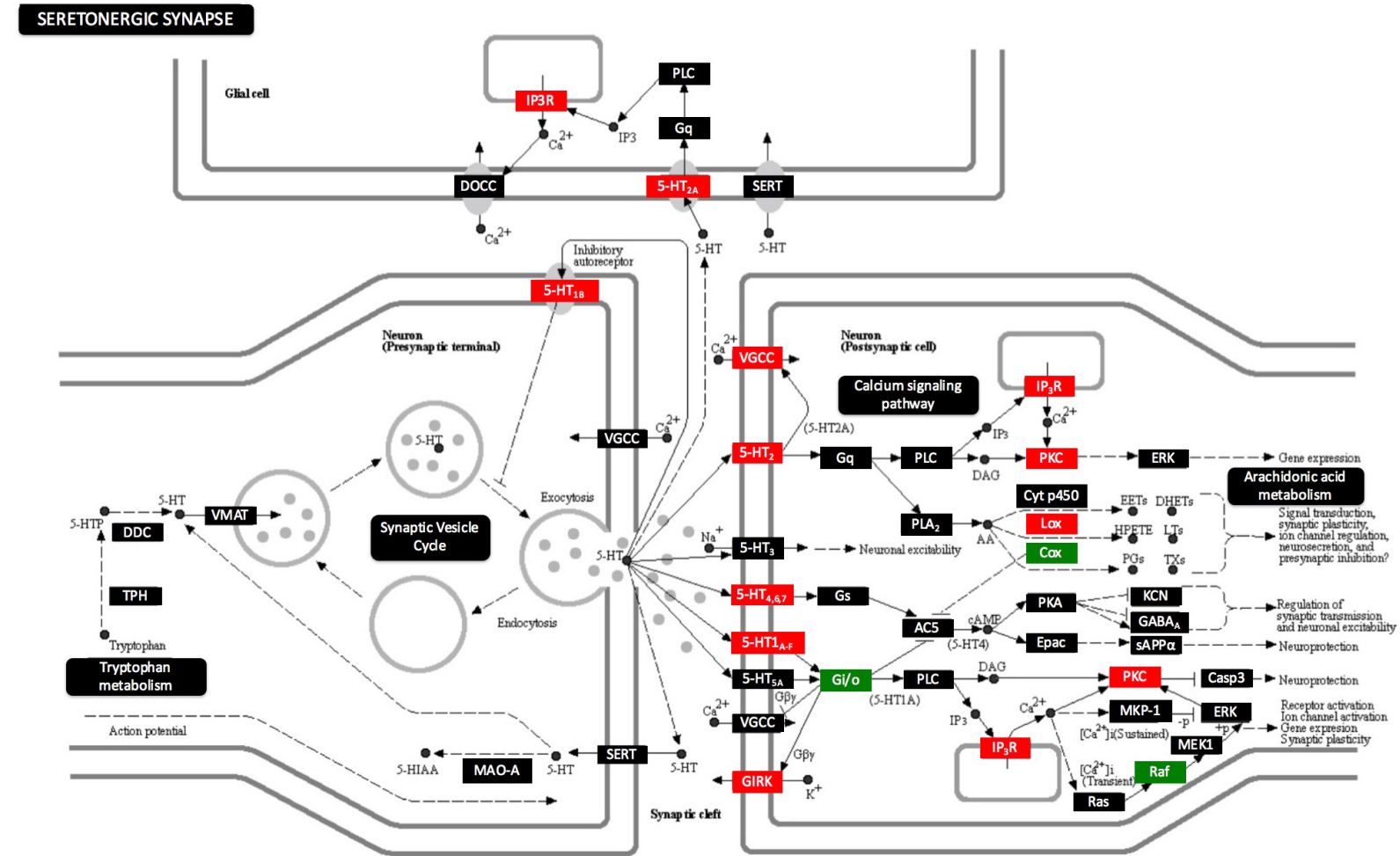


Figure 3.8. Genes in the serotonergic synapse pathway that were affected by altered CpG methylation in children from the discovery cohort.

3.4.3. Confirmation of the 450K Array by Pyrosequencing

Next, microarray results were examined using an independent technology that does not depend on the matched controls for modeling. For this, probes with different performances from the carefully matched discovery cohort were chosen. First, one of two CpGs to pass multiple testing at the FDR filtering level in this relatively small cohort was chosen. The array analysis identified the enhancer of *COLEC11* (FDR $p=1.93\times 10^{-7}$). Pyrosequencing analysis of the affected CpG (cg15730644) in *COLEC11* revealed a significant increase ($p=0.002$) with an average methylation of 94.2% in FASD compared to 79.8% in matched controls (**Figure 3.9A**). It also shows that all children affected with FASD consistently have higher methylation at this CpG site compared to their matched controls. The sequencing run also examined SNP rs182514706 (T>G) and found that it was not present in any members of either the exposed or control groups and thus would not interfere with the confidence in the performance of this probe.

The next probe examined did not pass a FDR cut-off and is more representative of the gene list used for higher level analysis, including heatmaps, ontologies, and pathways. *HTT* (Huntington) is a hub gene involved in neurological disorders and showed a 1.5 fold increase ($p=0.003$) in methylation in FASD patients. In the mouse trimester 3 binge injection paradigm *HTT* showed a significant ($p=0.001$) 23% decrease in gene expression in adult brains. Pyrosequencing analysis of the affected CpG (cg26128129) revealed that the CpG in the enhancer of *HTT* shows a significant increase ($p=0.001$) with an average methylation of 87.6% in FASD and an average of 50.7% in matched controls (**Figure 3.9B**). Interestingly, there is variation among the control samples as compared to the FASD patients. This CpG is known to contain a SNP [rs362313 (C>T)] that causes a loss of the CpG, as well as another SNP near the probe [rs147422679 A>G]; however, pyrosequencing confirmed neither SNP was present in any of the individuals examined. The available results support the suggestion that CpG specific DNA methylation is altered in the cheek swab DNA of children affected with FASD.

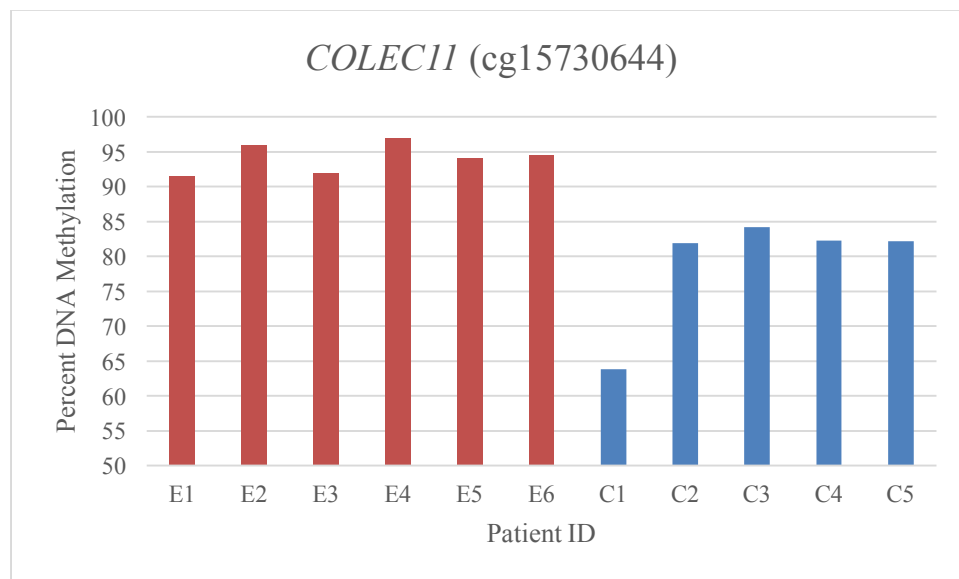
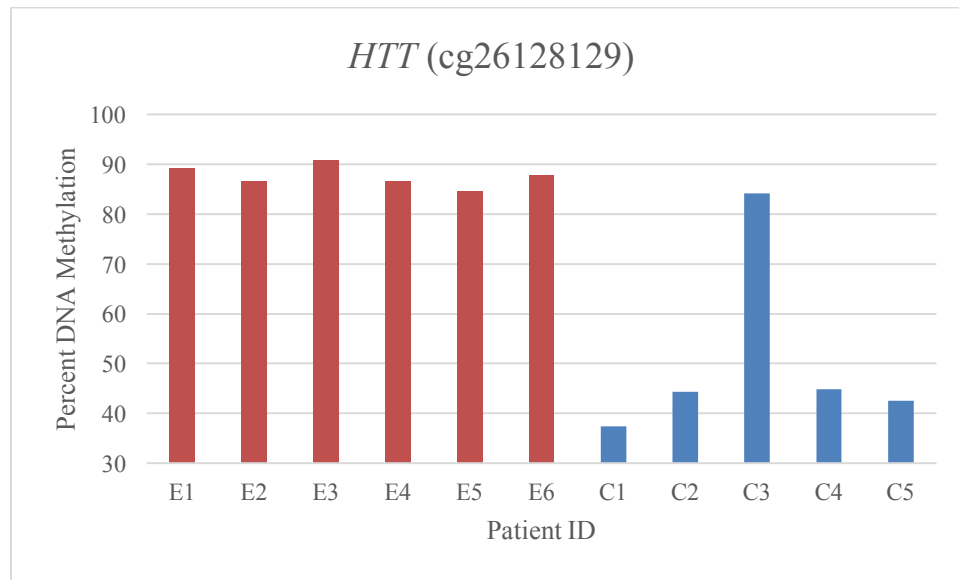
A)**B)**

Figure 3.9. Pyrosequencing results for (A) *COLEC11* and (B) *HTT* in the discovery cohort. Patient ID represents the individuals from the discovery cohort and the metrics represent percent methylation of the CpG from the sample.

3.4.4. Examination of Select Loci in the General Population

An average of 10 FASD and 7 Control patients were analyzed across 23 genes (**Table 3.4 and Appendix I**). Chr12q24.3 showed a significant ($p=0.036$) decrease in methylation (FASD = 2.7 ± 1.2 , Control = 7.4 ± 1.5) at CpG 24, while CpG #26 (cg20313522) showed a trend ($p=0.098$) of decreased methylation (FASD = 2.7 ± 1.3 , Control = 8.5 ± 3.0). *COLEC11* showed a trend ($p=0.056$) of decreased methylation (FASD = 57.5 ± 10.9 , Control = 85.3 ± 5.0) at cg15730644. Chr2q22.1 showed a trend ($p=0.080$) of decreased (FASD = 91.5 ± 1.0 , Control = 87.5 ± 2.0) methylation at CpG 19, while CpG 20 (cg23885472) showed no significant ($p=0.228$) alteration. Chr10q26 showed a trend ($p=0.107$) of increased (FASD = 85.4 ± 4.2 , Control = 71.7 ± 7.3) methylation at cg03697076. The above 4 loci were deemed informative across all individuals and used for follow-up pyrosequencing in more members from the general population. However, pyrosequencing analysis revealed no significant alterations once applied to more individuals (**Table 3.5 and Appendix J**).

Table 3.4. Summary of NGS panel results for an average of the same ten FASD and seven control patients from Owen Sound, Ontario that were analyzed across 23 genes.

Gene Symbol	CpG	Mean FASD	Mean Control	p value
ALPL	CpG#-701	12.3±1.8	13.4±2.0	0.69
	CpG#-700 (cg10487998)	17.9±3.0	14.5±3.5	0.47
AK3L	CpG#95 (cg24049468)	19.6±2.3	21.4±2.6	0.60
Chr1p21.3	CpG#2	10.3±3.2	11.6±5.9	0.84
	CpG#3	49.2±6.2	59.7±7.8	0.30
	CpG#4	40.4±8.4	54.7±8.0	0.24
	CpG#5 (cg21436544)	41.0±5.6	52.8±7.3	0.21
	CpG#6	51.9±5.3	60.2±6.3	0.32
C1orf110	CpG#-68 (cg01450736)	66.7±5.3	71.8±1.9	0.43
	CpG#-67	11.8±6.3	16.4±6.4	0.62
	CpG#-66	83.3±4.4	86.4±1.3	0.55
COLEC11	CpG#602 (cg15730644)	57.5±10.9	85.3±5.0	0.06
	CpG#603	81.5±2.1	83.7±0.9	0.41
	CpG#604 (cg13811808)	90.9±2.2	93.0±0.6	0.46
	CpG#605	88.5±3.0	91.1±1.3	0.48
Chr2q22.1	CpG#19	91.5±1.0	87.5±2.0	0.08
	CpG#20 (cg23885472)	67.9±11.6	47.6±11.3	0.23
LIMCH1	CpG#79 (cg13578194)	18.6±5.1	11.3±3.1	0.26
	CpG#80	43.9±6.3	38.3±3.3	0.47
	CpG#81	61.6±4.3	62.4±3.7	0.90
	CpG#82	45.8±7.8	42.0±4.5	0.69
Chr4q26	CpG#6	60.8±7.4	60.1±4.9	0.94
	CpG#7 (cg04452203)	7.7±0.9	10.2±2.4	0.37
NOTCH4	CpG #68 (cg17351927)	92.8±2.8	95.7±1.1	0.39
RUNX2	CpG#-5 (cg05996042)	34.3±5.1	33.3±6.0	0.91
GRB10	CpG#-322	34.7±2.3	32.0±3.5	0.51

	CpG#-321 (cg10335798)	15.5±1.3	14.2±2.1	0.60
ADARB2	CpG#7041	92.4±1.3	91.3±1.0	0.54
	CpG#7042	93.3±0.9	90.5±2.0	0.18
	CpG#7043	95.2±0.9	94.4±0.5	0.48
	CpG#7044	84.2±1.4	82.9±2.0	0.59
	CpG#7045	86.8±1.1	84.4±2.6	0.40
	CpG#7046	68.0±3.2	68.4±3.0	0.94
	CpG#7047 (cg11270017)	50.7±6.4	53.2±5.6	0.78
PHYH	CpG#70 (cg19018267)	7.1±2.0	4.8±1.0	0.35
	CpG#71	10.2±2.4	11.0±3.4	0.84
	CpG#72	13.4±3.0	13.1±3.6	0.96
	CpG#73	7.2±1.5	5.9±2.0	0.64
	CpG#74	54.3±6.3	55.1±7.1	0.94
Chr10q26	CpG#7 (cg03697076)	85.4±4.2	71.7±7.3	0.11
FBXO3	CpG #-52 (cg05237503)	48.7±11.3	59.3±8.4	0.48
	CpG #-51	90.1±2.8	93.7±0.9	0.27
LMO2	CpG #177 (cg17408637)	18.0±4.7	26.2±5.3	0.28
Chr12p12.3	CpG#7 (cg05694021)	14.4±2.5	16.9±2.9	0.53
Chr12q24.31	CpG#24	2.7±1.2	7.4±1.5	0.04
	CpG#25	0.7±0.4	1.5±1.1	0.53
	CpG#26 c(g20313522)	2.7±1.3	8.5±3.0	0.10
	CpG#27	13.7±4.6	29.5±10.0	0.18
FAM106A	CpG#31	87.8±5.0	85.2±2.8	0.67
	CpG#32 (cg17745575)	45.3±5.0	42.7±4.9	0.71
KRT32	CpG#-6	25.4±3.4	29.6±5.0	0.49
	CpG#-5 (cg25598400)	18.1±3.0	20.9±3.0	0.53
	CpG#-4	68.5±4.5	65.3±6.2	0.68
UCKL1	CpG#481	11.2±2.1	13.2±3.1	0.59
	CpG#482 (cg07507493)	13.9±2.2	14.9±3.7	0.82
	CpG#483	5.0±1.8	3.4±1.2	0.50

	CpG#1	75.4±1.3	76.1±1.3	0.72
	CpG#2	93.8±0.9	93.4±1.3	0.82
KRTAP27-1	CpG#3	95.5±0.4	96.1±0.6	0.38
	CpG#4 (cg05809586)	62.6±10.0	58.6±14.7	0.82
ChrXp11.4	CpG #32 (cg11868078)	11.7±2.9	18.5±4.5	0.21
	CpG #1774	71.9±2.4	77.6±2.9	0.15
	CpG #1775 cg21915313	26.9±1.5	25.5±2.4	0.63
PCDHGA1	CpG #1776	47.5±1.7	51.1±3.3	0.34
	CpG #1777	38.6±1.6	46.0±5.5	0.22
	CpG #1778 (cg01544213)	57.8±2.5	60.8±2.9	0.46
	CpG #1779	30.6±1.0	34.6±2.6	0.18

Table 3.5. Summary of pyrosequencing results from children representative of the general population of Owen Sound, Ontario.

Gene and n	CpG	FASD	Control	p-value
COLEC11 38 FASD 27 Control	CpG#602 (cg1573064)4	87.4±3.2	88.7±1.7	0.38
	CpG#603	60.3±2.3	57.5±2.2	0.20
	CpG#604	78.9±2.3	79.7±1.2	0.39
	CpG#605	77.6±2.2	76.9±1.9	0.40
PCDBH18 8 FASD 4 Control	CpG#-5 (cg27086874)	16±2.2	19.9±5.7	0.23
	CpG#-4	6.4±1.3	6.9±0.9	0.42
	CpG#-3	6.1±1.7	3.6±1.9	0.22
	CpG#-2	9.4±1.6	4.3±2.5	0.06
	CpG#-1	5.4±1.6	5.5±2.8	0.48
HTT 15 FASD 12 Control	CpG#2310 (cg26128129)	75.6±7.7	63.3±6.1	0.12
	CpG#2311	87±1.7	88±0.9	0.33
	CpG#2312	61±3.8	58.9±4.3	0.36
	CpG#2313	27.9±2.6	26.9±4	0.41
12q24.31 11 FASD 8 Control	CpG#26 (cg20313522)	6.3±2.7	9.2±3	0.25
	CpG#27	23.1±6.3	32.9±8.1	0.17
10q26.12 11 FASD 8 Control	CpG#7 (cg03697076)	80.1±4	70±7.8	0.12
2q22.1 11 FASD 8 Control	CpG#19	87.4±1.7	85.2±1.6	0.18
	CpG#20 (cg23885472)	59.2±10.6	52.2±9.6	0.32

Results presented overlap with those from **Figure 3.9.**

3.5. Discussion

The results of the research in this chapter provide a methylomic profile (**Figure 3.1**) of young children with FASD (**Table 3.1**). The genes identified are non-random as they have a number of interactions identified by an associative gene network analysis (**Figure 3.2**).

3.5.1. Non-Random Genome-Wide Differential Methylation

The ontologies (**Table 3.2**) and pathways (**Table 3.3**) identified are related to cellular and synaptic signaling, (neuro)development, immune processes, cell proliferation and differentiation, and also represent non-neuronal tissues such as the heart and kidneys. The analysis of human children has implicated a signaling pathway well-known to be altered by alcohol: the glutamatergic synapse (**Figure 3.5**). The results have also implicated the retrograde endocannabinoid signaling pathway (**Figure 3.7**), which is known to be deregulated by PAE (Basavarajappa 2015). Endocannabinoids are synthesized from the phospholipid membrane and are recognized by receptors that inhibit calcium channels and suppress the release of glutamate or GABA. The serotonergic synapse pathway was also deregulated (**Figure 3.8**). The aforementioned synaptic pathways all utilize calcium signaling (**Figure 3.6**), are specifically relevant to endophenotypes associated with FASD and related mental disabilities, and are an unexpected result of easily obtained buccal swabs.

A novel pathway identified in the results is hippo signaling (**Figure 3.4**). Hippo signaling is known to restrain cell proliferation and promote apoptosis in differentiating epithelial cells (Saucedo & Edgar 2007). While hippo signaling has been primarily studied in *Drosophila melanogaster*, it has been translated to *Mus musculus* and *Homo sapiens* and identified as a highly conserved signaling pathway involved in the control of cell growth, proliferation, and migration as well as apoptosis and organ size control (Wang et al. 2009).

Hippo signaling contains conserved families of signal responsive transcription co-regulators that transduce cytoplasmic signals into a response of transcriptional regulation in the nucleus via kinase cascade (Wang et al. 2009). The hippo signaling components are expressed in many tissues and co-regulate transcriptional enhancer factors [(TEFs) or

transcription enhancer domain (TEAD) factors], runt-domain transcription factors (Runxs), peroxisome proliferator-activated receptor gamma (PPAR- γ), T-box transcription factor 5 (*Tbx5*), and several others. Notably, hippo signaling regulates the growth of niche stem cell precursors (Sarikaya & Extavour 2015) and has recently been linked to chromatin modification by recruiting a histone methyltransferase complex (Oh et al. 2014). It has also been shown to regulate Wnt/ β -Catenin signaling (Varelas et al. 2010).

A transcription factor analysis was also utilized on all the identified genes (Chen et al. 2013). It revealed a significant ($p<0.005$) enrichment for CTCF insulator sites (Kim et al. 2007), which are involved in establishing chromatin domains and boundaries and result in a large-scale nuclear architecture that is specific to cell type. Another transcription factor enriched for was RAD21, which cooperates with pluripotency transcription factors, including CTCF, in the maintenance of embryonic stem cell identity (Nitzsche et al. 2011). CTCF is known to be the master regulator of the clustered protocadherins (Golan-Mashiach et al. 2012; Guo et al. 2012) where it influences complex DNA looping.

The clustered protocadherins are located on 5q31 and showed a concerted increase in methylation (**Figure 3.3**). The protocadherins are trans-membrane proteins with repeats of the cadherin motif or the cadherin extracellular domain (Hirano & Takeichi 2012; Chen & Maniatis 2013). This domain contains a conserved Ca^{2+} binding sequence and the number of extracellular domains may vary across different cadherin molecules. The protocadherins function as cell adhesion molecules with immense isoform diversity that is used to create individual neuronal identities and allow for large-scale network formation via controlling synaptic interactions. An increase in methylation in some, most, or all gene promoters as observed in human FASD patients, is expected to reduce the isoform diversity, thus limiting brain function. The clustered protocadherins were also represented by many of the gene ontologies (**Table 3.2**). They have been implicated in a number of brain disorders with similar endophenotypes to FASD, such as autism spectrum disorders, bipolar disorder, and schizophrenia (Hirano & Takeichi 2012). The molecular functions of the clustered protocadherins are further discussed in chapter 4, where the human observations are compared to the mouse CPD PAE paradigm (chapter 2).

3.5.2. Comparison of Discovery and Replication Cohorts

The replication cohort (**R**) included six patients (3-10 years old) and six matched controls (**Table 3.1B**) and their cheek swab DNA was used to generate genome-wide DNA methylation profiles (**Figure 3.1B**). They were recruited from the same clinic and diagnosed by the same Pediatrician (J. Kapalanga). However, the replication cohort was also much more heterogeneous compared to the discovery cohort with respect to sex, medication exposure, environment, and socioeconomic status. In order to compare the cohorts across batches a different pre-processing algorithm was selected: the subset-quantile within array normalization (SWAN) algorithm (Maksimovic et al. 2012; Fortin et al. 2014) from the minifi (Aryee et al. 2014) bioconductor package. When the two cohorts were pre-processed separately by the Illumina algorithm or together with the SWAN algorithm, they produced genome-wide results that had similarities but were not identical to the discovery cohort. In general, there was decreased significance in the replication cohort and greater levels of variation. Despite these differences, the main similarities between the two cohorts were significant alterations in ontologies related to glutamate and the canonical glutamatergic synapse pathway. Additionally, there was a clustered protocadherin signal on the Manhattan plot, as well as replication of alterations to imprinted regions also seen in the mouse models and the discovery cohort.

Next, the replication cohort was reanalyzed following removal of females and children on medication (**Table 3.1B**; R1 and R4). Also, four controls of the replication cohort were removed to better match age range and medical history. The selected scans were then pre-processed using the Illumina algorithm. Upon removal, the groups cluster much more closely and the signal is almost identical to what was observed in the discovery cohort. Glutamatergic synapses, cell-adhesion, neuroactive ligand receptor interactions, MAPK signaling, axon guidance, and a number of other pathways were all significant ($p<0.005$) even though the ranking of specific pathways varied slightly. The results argue that although DNA methylation is altered in patients with FASD, other factors, including sex, age, and medication history, may affect the final outcome.

An independent group has also replicated some of this research (Laufer et al. 2015). Portales-Casamar *et al.* published an examination of genome-wide DNA methylation patterns in the buccal epithelial cells of a Canadian cohort (Portales-Casamar

et al. 2016). They compared 110 children with FASD to 96 control children between the ages of 5 to 18. In addition to utilizing the 450K array and pyrosequencing, a genotyping array was used to statistically correct for genetic background. Their analysis revealed 658 differentially methylated CpGs with 41 of those showing a >5% change in methylation. They observed an enrichment for genes with functions related to neurodevelopment. Furthermore, there was an increase of methylation in multiple probes from the clustered protocadherins and also alterations to genomically imprinted regions, which included *H19*. Overall, their observations confirm key findings from both the mouse and human results presented in this thesis and expand them to a more diverse cohort.

3.5.3. No Single Gene Examined Identifies FASD

The differential methylation observed was not replicated when examined at select loci in a different cohort more representative of the general population (**Tables 3.4 & 3.5**). While it is possible that the marks examined are simply not informative of PAE, there are also a number alternative possibilities that may account for the lack of replication. First, individual sequencing is a more practical approach for clinical use as a substantial change in methylation level at a biomarker locus would allow for the detection of exposure without the need for carefully matched controls. However, individual sequencing does not have the advantage of normalization of signal across matched samples and reference genes.

These findings highlight the difficulty of expanding from the homogeneity of a small carefully matched group to that of the heterogeneous general population. In the follow-up pyrosequencing and NGS panel, FASD patients were more variable across a number of factors including age, sex, drug exposure, and family history of mental health disorders. The control patients were also in the clinic for a more heterogeneous mixture of acute and chronic medical problems, which involved medication in some cases. Ultimately, given the potential for variation across a number of factors, it appears that each case of FASD may be represented in the epigenome as a complex signature that is altered by other environmental factors. This large amount of heterogeneity would benefit from future experimentation with much larger sample sizes, which would provide added

statistical power. Furthermore, a regression could also be used to dissect the complex environmental interactions that shape the general population.

One possible approach to dissect the heterogeneity of FASD would be to mirror an array discovery approach and machine learning strategy used to detect prenatal exposure to smoking. In this example, the cord blood from 1,062 newborn Norwegian children prenatally exposed to maternal smoking during the second trimester was analyzed on the 450K array, revealing 26 significantly altered CpGs that mapped to 10 genes (Joubert et al. 2012). The genes distinctly altered had functions related to detoxification and development. A separate follow-up study utilized whole blood from an American cohort (of 531 children) that were 3-5 years old and analyzed the same 26 CpGs using machine learning, where they found that 81% of the time they could predict prenatal exposure to smoking (Ladd-Acosta et al. 2016). The above examples suggest that larger sample sizes from interdisciplinary collaborative efforts increase statistical power. However, given that 19% of cases were not identified, there are still limitations to the approach of epigenetic epidemiology and the statistical approaches available need further improvement, in terms of both loci examined and computational analysis, if they are to properly model the heterogeneity of the human population and be used for public health decisions (Ramsay 2015). To further expand on this point, a massive meta-analysis of prenatal exposure to maternal smoking found that even a sustained and heavy exposure results in a 450K profile with only nominal significance when applied to different cohorts of older children with the same heavy prenatal exposure (Joubert et al. 2015). In the same study, moderate exposure to any level of smoking, which made up a larger amount of children, produced a much less distinct profile that wasn't fully explored.

Ultimately, it appears that pyrosequencing of single loci is not suitable for use as a diagnostic of FASD. Methodologies that allow for accurate, rapid, and inexpensive quantification of DNA methylation levels across multiple loci in a single sample will soon emerge. These future technologies could be used to further examine the sites identified, as well as those identified by deeper epigenome wide screens, in a larger number of samples that will allow for the dissection of the interaction of other environmental and inherited variables. The above future improvements and a deeper understanding of natural variation in the methylome may one day enable the possibility of

diagnosing FASD from buccal swabs. Furthermore, this insight into DNA methylation from buccal swabs would be particularly suited for use with other modern diagnostics (Reynolds et al. 2011; Portales-Casamar et al. 2015), such as eye movement recordings (Paolozza, Rasmussen, et al. 2014a; Paolozza, Rasmussen, et al. 2014b; Paolozza et al. 2015), diffusion tensor imaging (Paolozza, Treit, et al. 2014), and/or a robotic virtual reality platform (Williams et al. 2014).

3.5.4. Select Functions of Sequenced Genes

The genes examined by pyrosequencing and the NGS panel have a number of functions that are biologically relevant to PAE. *COLEC11* is involved in fundamental developmental processes and serves as a guidance cue for neural crest cell migration where aberrations are known to produce spectrum disorders with similar endophenotypes to FASD known as 3MC syndrome (Rooryck et al. 2011). This biomarker was one of the strongest performing on the 450K array and was also confirmed by pyrosequencing. In a group of patients with intellectual disability and normal molecular karyotype *COLEC11*, *BLCAP*, *FAM50B*, *SHANK2*, and *GLI2* were identified as showing significant alterations to methylation in peripheral blood by the 450K and confirmed by pyrosequencing (Kolarova et al. 2015). Notably, a marker could not be found for general intellectual disability and thus an individual based approach was taken. The hypermethylation of *COLEC11* was observed and confirmed in a single patient with a thin upper lip vermillion, long flat philtrum, moderate developmental delay, generalized epilepsy, cerebral movement disorder with ataxia, and blepharophimosis. The aforementioned endophenotypes overlap with FASD.

Chr2q22.1 (Chr2:136120695-136120697) is a few kilobases downstream from *CXCR4* (Chr2:136114349-136118165). CXCR-4 is involved in neurogenesis, both developmental and adult, where it has a role in neuronal guidance and is implicated in epilepsy (Bagri et al. 2002). Chr10q26 is inside *WDR11-AS*, the antisense transcript for *WDR11*. *WDR11* is also known as bromodomain and WD repeat-containing protein 2. It is involved in human puberty and in mouse and zebrafish models was found to have a role in developmental neuroepithelial cell migration (Kim et al. 2010). Bromodomains recognize monoacetylated lysine and the WDR domain allows for protein interaction.

Members of this family are typically involved in cell cycle progression, signal transduction, apoptosis, and gene regulation. Chr12q24.31 (Chr12:124774899-124774989) is close to numerous novel lncRNAs and *SCARB1*. *SCARB1* functions as a receptor for high density lipoprotein, its well known for its role in cholesterol homeostasis, and could have a role for membrane and neurosteroid synthesis in neurons of the eye (Provost et al. 2003).

Also, notable is ADARB2 an RNA editing enzyme involved in the post-transcriptional A-to-I modification and is a process. RNA editing results in the recognition of the modified base (Inosine) as a Guanosine by cellular machinery. RNA editing is enriched in the brain at *5htr2c* and *Glur2*, which are serotonin and glutamate receptors that are involved in neurological disorders (Li & Church 2013). In the mouse models, the snoRNA gene families *Snord115* and *Snord116* were markers of PAE in the brain across different exposure dose and timing (Laufer et al. 2013). *SNORD115* is involved in the alternative splicing of *5HTR2C* (Kishore & Stamm 2006). Editing of *Glur2* by *Adar2* alters calcium permeability and is involved in synaptic activity and drug addiction (Lomeli et al. 1994; Schmidt et al. 2014).

3.5.5. Considerations for Future Research

While this research generates a number results, there are also a number of considerations for future studies. Unsorted peripheral tissue contains DNA methylation patterns from a heterogeneous population of cells and is a limitation of studies that use whole blood. Saliva is comprised of both buccal epithelial cells and a variable level of leukocytes and microbes (Aps et al. 2002) that are minimized by using swabs of the cheek pouch as opposed to mouthwashes (Thiede et al. 2000). The above mentioned variations in cellular composition may have the potential to lead to spurious findings in some cases, as alterations can reflect a shift in cell type composition as opposed to specific epigenetic alteration (Souren et al. 2013). However, the buccal epithelium also shares a developmental connection to the brain via the ectoderm and has led to novel insights into the brain as it is an easily accessible peripheral tissue. Interestingly, studies have indicated that the unsorted saliva appears to serve as a better proxy for the psychiatric disorders than unsorted blood (Lowe et al. 2013; Abdolmaleky et al. 2014; Wilmot et al.

2015). While cell type sorting is an ideal standard it is not always practical, particularly in cases where low amounts of DNA available and thus is a limitation to be considered when interpreting the results presented. Furthermore, a study using a similar approach to examine autism spectrum disorders noted that technical inter-array differences accounted for the majority of confounding variation, even after the use of stringent pre-processing algorithms to adjust for batch effects (Berko et al. 2014). The two arrays in this chapter showed a similar outcome and were analyzed separately to minimize the major source of confounding variation.

3.5.6. Conclusion

In this research, it was observed that children (3-6 year olds) with a comprehensive FASD diagnosis and a maternal history of PAE (termed the discovery cohort) have non-random differences in genome-wide DNA methylation. This effect is similar, but not identical, in a replication cohort collected 6 months after. The analysis allowed for the identification of the clustered protocadherins as well as glutamate and hippo signaling proteins as critical molecules. These results may also explain overlaps involving FASD and other neurodevelopmental disorders of unknown etiology. However, these associations were observed in a small sample of carefully matched children and next generation sodium bisulfite sequencing of a larger sample suggests that the selected differences may be influenced by sex, age, medication, and genetic background. Ultimately, the results establish that DNA methylation is affected at specific neurodevelopmental loci in children with FASD but may be altered by other variables.

Thus, despite the potential caveats, the results included have a number of implications. First, the identification of specific loci and pathways, including the clustered protocadherins and hippo signaling, may serve as a foundation for functional genomics studies. Second, with future optimization, the methylomic profile may serve as part of a diagnostic suite that enables early diagnosis and proper application of any corrective therapies, which are most effective for FASD if applied as early as possible during neurodevelopment (Paley & O'Connor 2009; Chokroborty-Hoque et al. 2014). The identified loci may also be utilized towards the development of precision medicine by somatic epigenome editing (Laufer & Singh 2015). Finally, the results of this research

established that a complex epigenomic signature of PAE remains in the saliva of human children.

Footnotes: A substantially modified portion of this chapter has been published (Laufer et al. 2015).

3.6. References

- Abdolmaleky, H.M., Nohesara, S., Ghadirivasfi, M., Lambert, A.W., Ahmadkhaniha, H., Ozturk, S., Wong, C.K., Shafa, R., Mostafavi, A. & Thiagalingam, S., 2014. DNA hypermethylation of serotonin transporter gene promoter in drug naive patients with schizophrenia. *Schizophrenia Research*, 152(2-3), 373–380.
- Aps, J.K.M., Van Den Maagdenberg, K., Delanghe, J.R. & Martens, L.C., 2002. Flow cytometry as a new method to quantify the cellular content of human saliva and its relation to gingivitis. *Clinica Chimica Acta*, 321(1-2), 35–41.
- Aryee, M.J., Jaffe, A.E., Corrada-Bravo, H., Ladd-Acosta, C., Feinberg, A.P., Hansen, K.D. & Irizarry, R.A., 2014. Minfi: A flexible and comprehensive Bioconductor package for the analysis of Infinium DNA methylation microarrays. *Bioinformatics*, 30(10), 1363–1369.
- Bagri, A., Gurney, T., He, X., Zou, Y.-R., Littman, D.R., Tessier-Lavigne, M. & Pleasure, S.J., 2002. The chemokine SDF1 regulates migration of dentate granule cells. *Development*, 129(18), 4249–4260.
- Basavarajappa, B., 2015. Fetal Alcohol Spectrum Disorder: Potential Role of Endocannabinoids Signaling. *Brain Sciences*, 5(4), 456–493.
- Basavarajappa, B. & Subbanna, S., 2016. Epigenetic Mechanisms in Developmental Alcohol-Induced Neurobehavioral Deficits. *Brain Sciences*, 6(2), 12.
- Berko, E.R. et al., 2014. Mosaic Epigenetic Dysregulation of Ectodermal Cells in Autism Spectrum Disorder. *PLoS Genetics*, 10(5), e1004402.
- Bibikova, M., Barnes, B., Tsan, C., Ho, V., Klotzle, B., Le, J.M., Delano, D., Zhang, L., Schroth, G.P., Gunderson, K.L., Fan, J.B. & Shen, R., 2011. High density DNA methylation array with single CpG site resolution. *Genomics*, 98(4), 288–295.
- Chen, E.Y., Tan, C.M., Kou, Y., Duan, Q., Wang, Z., Meirelles, G.V., Clark, N.R. & Ma'ayan, A., 2013. Enrichr: interactive and collaborative HTML5 gene list enrichment analysis tool. *BMC Bioinformatics*, 14(1), 128.
- Chen, W. V & Maniatis, T., 2013. Clustered protocadherins. *Development*, 140(16), 3297–3302.

- Chokroborty-Hoque, A., Alberry, B. & Singh, S.M., 2014. Exploring the complexity of intellectual disability in fetal alcohol spectrum disorders. *Frontiers in Pediatrics*, 2, 90.
- Flicek, P., Amode, M.R., Barrell, D., Beal, K. & onstantinos Billis, Simon Brent, Denise Carvalho-Silva, Peter Clapham, Guy Coates, Stephen Fitzgerald, Laurent Gil, Carlos García Girón, Leo Gordon, Thibaut Hourlier, Sarah Hunt, Nathan Johnson, and S.M.J.S., 2014. Ensembl 2014. *Nucleic Acids Research*, 42, D749–D755.
- Fortin, J.P., Labbe, A., Lemire, M., Zanke, B.W., Hudson, T.J., Fertig, E.J., Greenwood, C.M. & Hansen, K.D., 2014. Functional normalization of 450k methylation array data improves replication in large cancer studies. *Genome Biology*, 15(12), 503.
- Golan-Mashiach, M., Grunspan, M., Emmanuel, R., Gibbs-Bar, L., Dikstein, R. & Shapiro, E., 2012. Identification of CTCF as a master regulator of the clustered protocadherin genes. *Nucleic Acids Research*, 40(8), 3378–3391.
- Guo, Y., Monahan, K., Wu, H., Gertz, J., Varley, K.E., Li, W., Myers, R.M., Maniatis, T. & Wu, Q., 2012. CTCF/cohesin-mediated DNA looping is required for protocadherin α promoter choice. *Proceedings of the National Academy of Sciences of the United States of America*, 109(51), 21081–21086.
- Halder, D., Mandal, C., Lee, B.H., Lee, J.S., Choi, M.R., Chai, J.C., Lee, Y.S., Jung, K.H. & Chai, Y.G., 2015. PCDHB14- and GABRB1-like nervous system developmental genes are altered during early neuronal differentiation of NCCIT cells treated with ethanol. *Human & Experimental Toxicology*, 34(10), 1017–1027.
- Hirano, S. & Takeichi, M., 2012. Cadherins in Brain Morphogenesis and Wiring. *Physiological Reviews*, 92(2), 597–634.
- Joubert, B.R. et al., 2015. DNA Methylation in Newborns and Maternal Smoking in Pregnancy: Genome-wide Consortium Meta-analysis. *American Journal of Human Genetics*, 98(4), 680–696.
- Joubert, B.R., Haberg, S.E., Nilsen, R.M., Wang, X., Vollset, S.E., Murphy, S.K., Huang, Z., Hoyo, C., Midttun, ??ivind, Cupul-Uicab, L.A., Ueland, P.M., Wu, M.C., Nystad, W., Bell, D.A., Peddada, S.D. & London, S.J., 2012. 450K epigenome-wide scan identifies differential DNA methylation in newborns related to maternal smoking during pregnancy. *Environmental Health Perspectives*, 120(10), 1425–1431.
- Khalid, O., Kim, J.J., Kim, H.S., Hoang, M., Tu, T.G., Elie, O., Lee, C., Vu, C., Horvath, S., Spigelman, I. & Kim, Y., 2014. Gene expression signatures affected by alcohol-induced DNA methylomic deregulation in human embryonic stem cells. *Stem Cell Research*, 12(3), 791–806.
- Kim, H.G. et al., 2010. WDR11, a WD protein that interacts with transcription factor EMX1, is mutated in idiopathic hypogonadotropic hypogonadism and Kallmann syndrome. *American Journal of Human Genetics*, 87(4), 465–479.

- Kim, T.H., Abdullaev, Z.K., Smith, A.D., Ching, K.A., Loukinov, D.I., Green, R., Zhang, M.Q., Lobanenkov, V. V. & Ren, B., 2007. Analysis of the Vertebrate Insulator Protein CTCF-Binding Sites in the Human Genome. *Cell*, 128(6), 1231–1245.
- Kishore, S. & Stamm, S., 2006. The snoRNA HBII-52 regulates alternative splicing of the serotonin receptor 2C. *Science*, 311(5758), 230–232.
- Kleiber, M.L., Diehl, E.J., Laufer, B.I., Mantha, K., Chokroverty-Hoque, A., Alberry, B. & Singh, S.M., 2014. Long-term genomic and epigenomic dysregulation as a consequence of prenatal alcohol exposure: A model for fetal alcohol spectrum disorders. *Frontiers in Genetics*, 5, 161.
- Kleiber, M.L., Mantha, K., Stringer, R.L. & Singh, S.M., 2013. Neurodevelopmental alcohol exposure elicits long-term changes to gene expression that alter distinct molecular pathways dependent on timing of exposure. *Journal of Neurodevelopmental Disorders*, 5(1), 6.
- Kolarova, J., Tangen, I., Bens, S., Gillessen-Kaesbach, G., Gutwein, J., Kautza, M., Rydzanicz, M., Stephani, U., Siebert, R., Ammerpohl, O. & Caliebe, A., 2015. Array-based DNA methylation analysis in individuals with developmental delay/intellectual disability and normal molecular karyotype. *European Journal of Medical Genetics*, 58(8), 419–425.
- Krishnamoorthy, M., Gerwe, B.A., Scharer, C.D., Heimburg-Molinaro, J., Gregory, F., Nash, R.J., Arumugham, J., Stewart, B., Stice, S.L. & Nash, R.J., 2010. Low ethanol concentration alters CHRNA5 RNA levels during early human development. *Reproductive Toxicology*, 30(3), 489–492.
- Ladd-Acosta, C., Shu, C., Lee, B.K., Gidaya, N., Singer, A., Schieve, L.A., Schendel, D.E., Jones, N., Daniels, J.L., Windham, G.C., Newschaffer, C.J., Croen, L.A., Feinberg, A.P. & Daniele Fallin, M., 2016. Presence of an epigenetic signature of prenatal cigarette smoke exposure in childhood. *Environmental Research*, 144(Pt A), 139–148.
- Laufer, B.I., Kapalanga, J., Castellani, C.A., Diehl, E.J., Yan, L. & Singh, S.M., 2015. Associative DNA methylation changes in children with prenatal alcohol exposure. *Epigenomics*, 7(8), 1259–1274.
- Laufer, B.I., Mantha, K., Kleiber, M.L., Diehl, E.J., Addison, S.M.F. & Singh, S.M., 2013. Long-lasting alterations to DNA methylation and ncRNAs could underlie the effects of fetal alcohol exposure in mice. *Disease Models & Mechanisms*, 6(4), 977–992.
- Laufer, B.I. & Singh, S.M., 2015. Strategies for precision modulation of gene expression by epigenome editing: an overview. *Epigenetics & Chromatin*, 8(1), 34.
- Lee, B.Y., Park, S.Y., Ryu, H.M., Shin, C.Y., Ko, K.N., Han, J.Y., Koren, G. & Cho, Y.H., 2015. Changes in the Methylation Status of DAT, SERT, and MeCP2 Gene

Promoters in the Blood Cell in Families Exposed to Alcohol During the Periconceptional Period. *Alcoholism: Clinical and Experimental Research*, 39(2), 239–250.

- Li, J.B. & Church, G.M., 2013. Deciphering the functions and regulation of brain-enriched A-to-I RNA editing. *Nature Neuroscience*, 16(11), 1518–1522.
- Lim, A.M., Candiloro, I.L., Wong, N., Collins, M., Do, H., Takano, E.A., Angel, C., Young, R.J., Corry, J., Wiesenfeld, D., Kleid, S., Sigston, E., Lyons, B., Rischin, D., Solomon, B. & Dobrovic, A., 2014. Quantitative methodology is critical for assessing DNA methylation and impacts on correlation with patient outcome. *Clinical Epigenetics*, 6(1), 22.
- Lomeli, H., Mosbacher, J., Melcher, T., Hoger, T., Kuner, T., Monyer, H., Higuchi, M., Bach, A. & Seburg, P., 1994. Control of kinetic properties of AMPA receptor channels by nuclear RNA editing. *Science*, 266(5191), 1709–1713.
- Lowe, R., Gemma, C., Beyan, H., Hawa, M.I., Bazeos, A., Leslie, R.D., Montpetit, A., Rakyan, V.K. & Ramagopalan, S. V., 2013. Buccals are likely to be a more informative surrogate tissue than blood for epigenome-wide association studies. *Epigenetics*, 8(4), 445–454.
- Maksimovic, J., Gordon, L. & Oshlack, A., 2012. SWAN: Subset-quantile within array normalization for illumina infinium HumanMethylation450 BeadChips. *Genome Biology*, 13(6), R44.
- Mandal, C., Kim, S.H., Chai, J.C., Oh, S.M., Lee, Y.S., Jung, K.H. & Chai, Y.G., 2016. RNA sequencing reveals the alteration of the expression of novel genes in ethanol-treated embryoid bodies. *PLoS ONE*, 11(3), e0149976.
- Marjonen, H., Sierra, A., Nyman, A., Rogojin, V., Grohn, O., Linden, A.M., Hautaniemi, S. & Kaminen-Ahola, N., 2015. Early maternal alcohol consumption alters hippocampal DNA methylation, gene expression and volume in a mouse model. *PLoS ONE*, 10(5), e0124931.
- Masemola, M.L., van der Merwe, L., Lombard, Z., Viljoen, D. & Ramsay, M., 2015. Reduced DNA methylation at the PEG3 DMR and KvDMR1 loci in children exposed to alcohol in utero: A South African Fetal Alcohol Syndrome cohort study. *Frontiers in Genetics*, 6, 85.
- Merriman, B., Torrent, I. & Rothberg, J.M., 2012. Progress in Ion Torrent semiconductor chip based sequencing. *Electrophoresis*, 33(23), 3397–3417.
- Nitzsche, A., Paszkowski-Rogacz, M., Matarese, F., Janssen-Megens, E.M., Hubner, N.C., Schulz, H., de Vries, I., Ding, L., Huebner, N., Mann, M., Stunnenberg, H.G. & Buchholz, F., 2011. RAD21 cooperates with pluripotency transcription factors in the maintenance of embryonic stem cell identity. *PLoS ONE*, 6(5), e19470.

- Nyrén, P., 2007. The History of Pyrosequencing. *Pyrosequencing Protocols*, 373, 1–14.
- Oh, H., Slattery, M., Ma, L., White, K.P., Mann, R.S. & Irvine, K.D., 2014. Yorkie Promotes Transcription by Recruiting a Histone Methyltransferase Complex. *Cell Reports*, 8(2), 449–459.
- Ouko, L. a., Shantikumar, K., Knezovich, J., Haycock, P., Schnugh, D.J. & Ramsay, M., 2009. Effect of Alcohol Consumption on CpG Methylation in the Differentially Methylated Regions of *H19* and *IG-DMR* in Male Gametes-Implications for Fetal Alcohol Spectrum Disorders. *Alcoholism: Clinical and Experimental Research*, 33(9), 1615–1627.
- Paley, B. & O'Connor, M.J., 2009. Intervention for individuals with fetal alcohol spectrum disorders: Treatment approaches and case management. *Developmental Disabilities Research Reviews*, 15(3), 258–267.
- Paolozza, A., Munn, R., Munoz, D.P. & Reynolds, J.N., 2015. Eye movements reveal sexually dimorphic deficits in children with fetal alcohol spectrum disorder. *Frontiers in Neuroscience*, 9, 76.
- Paolozza, A., Rasmussen, C., Pei, J., Hanlon-Dearman, A., Nikkel, S.M., Andrew, G., McFarlane, A., Samdup, D. & Reynolds, J.N., 2014a. Deficits in response inhibition correlate with oculomotor control in children with fetal alcohol spectrum disorder and prenatal alcohol exposure. *Behavioural Brain Research*, 259, 97–105.
- Paolozza, A., Rasmussen, C., Pei, J., Hanlon-Dearman, A., Nikkel, S.M., Andrew, G., McFarlane, A., Samdup, D. & Reynolds, J.N., 2014b. Working memory and visuospatial deficits correlate with oculomotor control in children with fetal alcohol spectrum disorder. *Behavioural Brain Research*, 263, 70–79.
- Paolozza, A., Treit, S., Beaulieu, C. & Reynolds, J.N., 2014. Response inhibition deficits in children with Fetal Alcohol Spectrum Disorder: Relationship between diffusion tensor imaging of the corpus callosum and eye movement control. *NeuroImage: Clinical*, 5, 53–61.
- Pidsley, R., Wong, C.C.Y., Volta, M., Lunnon, K., Mill, J. & Schalkwyk, L.C., 2013. A data-driven approach to preprocessing Illumina 450 K methylation array data. *BMC Genomics*, 14, 293.
- Portales-Casamar, E., Lussier, A.A., Jones, M.J., MacIsaac, J.L., Edgar, R.D., Mah, S.M., Barhdadi, A., Provost, S., Lemieux-Perreault, L.-P., Cynader, M.S., Chudley, A.E., Dubé, M.-P., Reynolds, J.N., Pavlidis, P. & Kobor, M.S., 2016. DNA methylation signature of human fetal alcohol spectrum disorder. *Epigenetics & Chromatin*, 9(25), 81–101.
- Portales-Casamar, E., Mah, S.M., MacIsaac, J.L., Barhdadi, A., Provost, S., Dubé, M.-P., Reynolds, J.N., Pavlidis, P. & Kobor, M.S., 2015. DNA methylation changes in fetal alcohol spectrum disorder. *International Journal of Developmental Neuroscience*,

47(Pt A), 126.

- Provost, A.C., Péquignot, M.O., Sainton, K.M., Gadin, S., Sallé, S., Marchant, D., Hales, D.B. & Abitbol, M., 2003. Expression of SR-BI receptor and StAR protein in rat ocular tissues. *Comptes Rendus - Biologies*, 326(9), 841–851.
- Ramsay, M., 2015. Epigenetic epidemiology : is there cause for optimism ? *Epigenomics*, 7(5), 683–685.
- Reynolds, J.N., Weinberg, J., Clarren, S., Beaulieu, C., Rasmussen, C., Kobor, M., Dube, M.P. & Goldowitz, D., 2011. Fetal Alcohol Spectrum Disorders: Gene-Environment Interactions, Predictive Biomarkers, and the Relationship Between Structural Alterations in the Brain and Functional Outcomes. *Seminars in Pediatric Neurology*, 18(1), 49–55.
- Rooryck, C. et al., 2011. Mutations in lectin complement pathway genes COLEC11 and MASP1 cause 3MC syndrome. *Nature Genetics*, 43(3), 197–203.
- Sandoval, J., Heyn, H.A., Moran, S., Serra-Musach, J., Pujana, M.A., Bibikova, M. & Esteller, M., 2011. Validation of a DNA methylation microarray for 450,000 CpG sites in the human genome. *Epigenetics*, 6(6), 692–702.
- Sarikaya, D.P. & Extavour, C.G., 2015. The Hippo pathway regulates homeostatic growth of stem cell niche precursors in the Drosophila ovary. *PLoS Genetics*, 11(2), e1004962.
- Saucedo, L.J. & Edgar, B.A., 2007. Filling out the Hippo pathway. *Nature Reviews Molecular Cell Biology*, 8(8), 613–621.
- Schmidt, H.D., McFarland, K.N., Darnell, S.B., Huizenga, M.N., Sangrey, G.R., Cha, J.-H.J., Pierce, R.C. & Sadri-Vakili, G., 2014. ADAR2-dependent GluA2 editing regulates cocaine seeking. *Molecular Psychiatry*, 20(11), 1460–1466.
- Souren, N.Y.P., Lutsik, P., Gasparoni, G., Tierling, S., Gries, J., Riemenschneider, M., Fryns, J.-P., Derom, C., Zeegers, M.P. & Walter, J., 2013. Adult monozygotic twins discordant for intra-uterine growth have indistinguishable genome-wide DNA methylation profiles. *Genome Biology*, 14(5), R44.
- Stringer, R.L., Laufer, B.I., Kleiber, M.L. & Singh, S.M., 2013. Reduced expression of brain cannabinoid receptor 1 (Cnr1) is coupled with an increased complementary micro-RNA (miR-26b) in a mouse model of fetal alcohol spectrum disorders. *Clinical Epigenetics*, 5(1), 14.
- Talens-Visconti, R., Sanchez-Vera, I., Kostic, J., Perez-Arago, M.A., Erceg, S., Stojkovic, M. & Guerri, C., 2011. Neural differentiation from human embryonic stem cells as a tool to study early brain development and the neuroteratogenic effects of ethanol. *Stem Cells and Development*, 20(2), 327–339.

- Thiede, C., Prange-Krex, G., Freiberg-Richter, J., Bornhäuser, M. & Ehninger, G., 2000. Buccal swabs but not mouthwash samples can be used to obtain pretransplant DNA fingerprints from recipients of allogeneic bone marrow transplants. *Bone Marrow Transplantation*, 25(5), 575–577.
- Tost, J. & Gut, I.G., 2007. DNA methylation analysis by pyrosequencing. *Nature protocols*, 2(9), 2265–2275.
- UniProt-Consortium, 2014. Activities at the Universal Protein Resource (UniProt). *Nucleic Acids Research*, 42, D191–D198.
- Varelas, X., Miller, B.W., Sopko, R., Song, S., Gregorieff, A., Fellouse, F.A., Sakuma, R., Pawson, T., Hunziker, W., Mcneill, H., Wrana, J.L. & Attisano, L., 2010. The Hippo pathway regulates Wnt/beta-catenin signaling. *Developmental Cell*, 18(4), 579–591.
- Wang, K., Degerny, C., Xu, M. & Yang, X.-J., 2009. YAP, TAZ, and Yorkie: a conserved family of signal-responsive transcriptional coregulators in animal development and human disease. *Biochemistry and Cell Biology*, 87(1), 77–91.
- Williams, J.F., Smith, V.C. & the COMMITTEE ON SUBSTANCE ABUSE, 2015. Fetal Alcohol Spectrum Disorders. *American Academy of Pediatrics*, 136(5), e1395–1406.
- Williams, L., Jackson, C.P.T., Choe, N., Pelland, L., Scott, S.H. & Reynolds, J.N., 2014. Sensory-Motor Deficits in Children with Fetal Alcohol Spectrum Disorder Assessed Using a Robotic Virtual Reality Platform. *Alcoholism: Clinical and Experimental Research*, 38(1), 116–125.
- Wilmot, B., Fry, R., Smeester, L., Musser, E.D., Mill, J. & Nigg, J.T., 2015. Methylomic analysis of salivary DNA in childhood ADHD identifies altered DNA methylation in VIPR2. *Journal of Child Psychology and Psychiatry*, 57(2), 152–160.

Chapter 4

Comparison of PAE Mice and Humans

4.1 Overview

The results presented in this thesis represent a number of novel observations. The mouse model (chapter 2) revealed that long-term alterations to DNA methylation as well as non-coding RNA and gene expression are induced by prenatal alcohol exposure (PAE) in the brain. Observations of saliva (chapter 3) show that there is a heterogeneous profile of non-random differential DNA methylation characteristic of young children with Fetal Alcohol Spectrum Disorders (FASD). In this chapter, I highlight that there are some comparable alterations in DNA methylation between the brains of adult male mice and the buccal epithelium of human children. A portion of this chapter has been previously published in Laufer *et al.* 2015. Together, the results of this research suggest that while different genes are altered, a long-term profile exists in diverse cell types with an ontogenetic relationship stemming from the ectoderm. The candidate loci identified in the two species belong to related non-random ontologies and pathways as well as complex epigenetically regulated syntenic loci. The results of this research may be used to guide future functional genomics studies examining the development of FASD following PAE. The novel results are also expected to aid the future development of strategies for early diagnosis and protocols for amelioration.

4.2 Introduction

The mouse model results presented in chapter 2 are in agreement with research using human cells. For example, Khalid *et al.* examined the transcriptome and methylome of human embryonic stem cells (hESCs) exposed to alcohol (Khalid et al. 2014). The top deregulated hub genes were *SCUBE3* and *SLC22A5*, which showed decreased gene expression. Notably, *SLC22A5* was ranked as the 3rd gene showing the highest differential hyper-methylation in the mouse model presented in this thesis. The *SLC22A5* gene codes for a solute carrier protein (OCTN2) that has a role in TGF-β signaling and transports

carnitine, which is involved in transporting fatty acids from the cytosol to the mitochondrial matrix, where they can be used for metabolism (Sonne et al. 2012). *SCUBE3* also codes for a protein that has a number of functions, which include TGF- β signaling and the complement system (Yang et al. 2013). In the analysis of gene expression in the mouse model, the complement system was the top deregulated canonical pathway and also enriched in the gene ontology analysis. Finally, as noted by Khalid *et al.*, the two hub genes identified are expressed in a number of non-neuronal tissues including the heart. These similarities highlight the translational potential of the PAE mouse model, which I used as a comparison point for the observations from human children with FASD.

The experiments involving mice were based on a MeDIP-Chip tiling array that analyzes CpG islands with greater than 2 methylated cytosines per a 50-75 base pair probe, which are then tiled into a larger contiguous sequence to represent a differentially methylated region (DMR) (**Figure 2.7**) (Laufer et al. 2013). For the human analysis, the 450K methylation array was used to analyze alterations to single CpG sites via sodium bisulfite conversion and an (epi)genotyping approach (**Figure 3.1A**) (Laufer et al. 2015). The translational comparison of results allowed for the identification of specific ontologies, pathways, and loci that are concordant between the independent array sets, which may be further developed as robust biomarkers of PAE.

4.3 Methods

The mouse model results are described in chapter 2. Briefly, the updated (2016) methylation analysis was used for the comparison of ontologies and pathways, as this analysis was generated using a workflow more similar to the human results and thus allowed for a more direct comparison. However, the updated analysis is from software with limited support for the array, which did not provide complete genomic location annotations for the tiled sequence, and thus the original (2012) methylation analysis was used for comparative alignment. The analysis of the human observations is described in chapter 3. The observations from the discovery cohort were used for the comparison to mice. Alignment of reference genomes for both species was carried out using the UCSC genome browser (www.genome.ucsc.edu).

4.4 Results

Of the 190 CpGs from the human discovery cohort that were annotated to genes, 36 (19%) overlapped with the 2898 annotated genes identified from the updated 2016 mouse analysis. However, the ontologies and pathways identified in the human discovery cohort (**Tables 3.2 & 3.3**) are similar to those identified in adult PAE mouse brains (**Tables 2.7 & 2.8**) and related to cellular and synaptic signaling, (neuro)development, immune processes, cell proliferation and differentiation, and also represent non-neuronal tissues such as the heart and kidneys. The observations represent a number of diverse ontogenetic events that are altered long after their initial deregulation by PAE. The most common and clearly connected are cellular signaling events related to development and neurotransmission, which are responsive to the external environment. For instance, the top pathway identified in the human results was hippo signaling (**Table 3.3**; 25/85 molecules and $p=0.0002$), which was also altered in the mouse model (**Table 2.8**; 40/115 molecules and $p=0.04$). Calcium signaling was also altered in the children's swabs (**Table 3.3**; 99/475 molecules, $p=0.005$) and mouse brains (**Table 2.8**; 50/136 molecules, $p=0.01$). Calcium signaling has numerous diverse roles, including in neurotransmission, where it contributes to depolarization of the cell membrane and resulting action potentials. Also notable are the only two genes that passed the FDR filtering on the 450K array. Both showed increased methylation, and *AHNAK2* was 1.7 fold ($p=1.93\text{E-}07$) and *COLEC11* was 1.6 fold ($p=6.61\text{E-}08$) (**Appendix D**). *AHNAK2* is a type of giant propeller-like protein linked to calcium channels (Komuro et al. 2004). *COLEC11* encodes a guidance cue for neural crest migration (Rooryck et al. 2011). The CL-K1 protein encoded by *COLEC11* is part of the lectin complement pathway, which functions in complement activation (Wallis et al. 2010), an immune process represented in the ontologies and as the top pathway of mouse gene expression (**Table 2.2**).

The comparison of mouse and human results has enabled the identification of not only ontologies and pathways deregulated by PAE, but also genomic loci. Some genes showing differential methylation in children belonged to genes families with altered methylation in mice [*PHOX2B* ($p=0.0009$), *ADAMTS17* ($p=0.002$), *KRT32* ($p=0.004$), *TMEM229A* ($p=0.004$)]. As another example, complex epigenetically regulated syntenic loci were also identified in both mice and humans. Alterations to imprinted ncRNA from

the *SNRPN-UBE3A* locus [*SNORD116 (HBII-85)* ($p<0.005$) and *SNORD115 (HBII-52)* ($p<0.01$)] were also present in the human buccal DNA, which was the most ubiquitously expressed marker for PAE that was identified in the mouse model chapter of this thesis (**Appendix D**). *SNORD115* changes the alternative splicing of the serotonin receptor *5HTR2C* (Kishore & Stamm 2006; Glatt-Deeley et al. 2010), which is a G-protein coupled receptor involved in calcium signaling (Nakatani et al. 2009). Calcium signaling was deregulated in both the mouse model and human model, and the serotonergic synapse pathway was altered in human children (**Table 3.3**).

4.4.1 Increased Methylation at the Clustered Protocadherins

In both humans with FASD and PAE mice, the clustered protocadherins showed a broad increase in methylation at select regions (**Figure 4.1**). An increase in methylation in some, most, or all gene promoters (**Tables 4.1 & 4.2**) is expected to reduce the isoform diversity, thus restraining brain function. **Table 4.1** contains a list of genes, genomic position, and the functional CpG site that is differentially methylated in the buccal swabs of FASD patients from the discovery cohort as compared to their matched controls. Similarly, **Table 4.2** contains corresponding protocadherin genes that were differentially methylated in adult mouse brains long after PAE. **Figure 4.1A** includes a plot of the raw Illumina β values, which correspond to percent methylation, for significant ($p<0.005$) CpGs in the differentially methylated region of the protocadherin γ cluster of humans and also how they align with alternate transcripts choice. The differential methylation appears to correspond to the first variable exon and preceding promoter of an alternative transcript. Protocadherins are involved in the generation of synaptic complexity in the developing brain and evolved primarily by tandem duplications and divergence. This complex locus contains three clusters (α , β , and γ) of protocadherin gene families that are transcriptionally complex and very similar between humans and mice (**Figure 4.1B**). The clustered protocadherin locus generates comparable transcripts in the two species and has relatively conserved CpG sites. More importantly, a number of the CpG sites/islands are specifically prone to increased methylation following PAE in both species.

Table 4.1. Nucleotide-specific analysis of CpGs in the protocadherin gene family clusters showing significant ($p<0.005$) alterations to CpG methylation in human buccal epithelial DNA from children of the discovery sample.

Family	p-value	CpG ID	CpG Coordinate	Fold Change	Average β
α	2.24E-03	cg03318614	140154796	1.10	0.55
α	4.90E-03	cg16234335	140168303	1.11	0.60
α	4.07E-03	cg25225155	140202437	1.23	0.64
α	4.42E-04	cg15122993	140236606	1.17	0.49
α	3.79E-03	cg13619597	140237001	1.54	0.68
β	1.90E-03	cg27086874	140549040	1.14	0.19
β	1.99E-03	cg05941060	140594004	1.43	0.46
γ	1.37E-03	cg01561869	140704042	1.22	0.29
γ	8.85E-04	cg25657261	140705331	1.34	0.33
γ	6.14E-05	cg24922090	140720687	1.24	0.37
γ	3.24E-03	cg02074191	140731690	1.60	0.46
γ	1.36E-04	cg06757405	140731792	1.35	0.35
γ	4.86E-03	cg26856475	140734108	1.38	0.42
γ	1.08E-03	cg22087053	140734498	1.27	0.35
γ	8.46E-04	cg18297751	140749183	1.31	0.39
γ	4.98E-03	cg24633027	140752470	1.32	0.55
γ	6.18E-04	cg18705909	140754610	1.58	0.45
γ	4.41E-03	cg08854987	140759645	1.26	0.34
γ	4.36E-04	cg21117330	140769634	1.20	0.28
γ	8.56E-04	cg03831054	140769892	1.53	0.48
γ	8.64E-04	cg21915313	140779155	1.50	0.39

Table 4.2. Tiling-based analysis of promoters from the protocadherin gene clusters showing significant ($p<0.01$) increases in methylation in adult brain tissue from a mouse model of prenatal alcohol exposure.

Family	Peak Start	Peak End	Peak Length
α	37090887	37091731	844
α	37099823	37099982	159
α	37100493	37101082	589
α	37120628	37121169	541
α	37121813	37122462	649
α	37128647	37129396	749
α	37148470	37149114	644
α	37153966	37154515	549
α	37159353	37160304	951
α	37166096	37167215	1119
α	37181780	37182430	650
β	37456114	37456763	649
β	37603162	37603321	159
β	37645176	37646223	1047
β	37657621	37657881	260
β	37674825	37674994	169
β	37678546	37679275	729
γ	37828934	37831185	2251
γ	37835333	37836297	964
γ	37840948	37841597	649
γ	37850740	37850974	234
γ	37854441	37854897	456
γ	37868606	37868955	349
γ	37886555	37887889	1334
γ	37892011	37893005	994
γ	37922706	37922835	129

Data based on the original 2012 analysis.

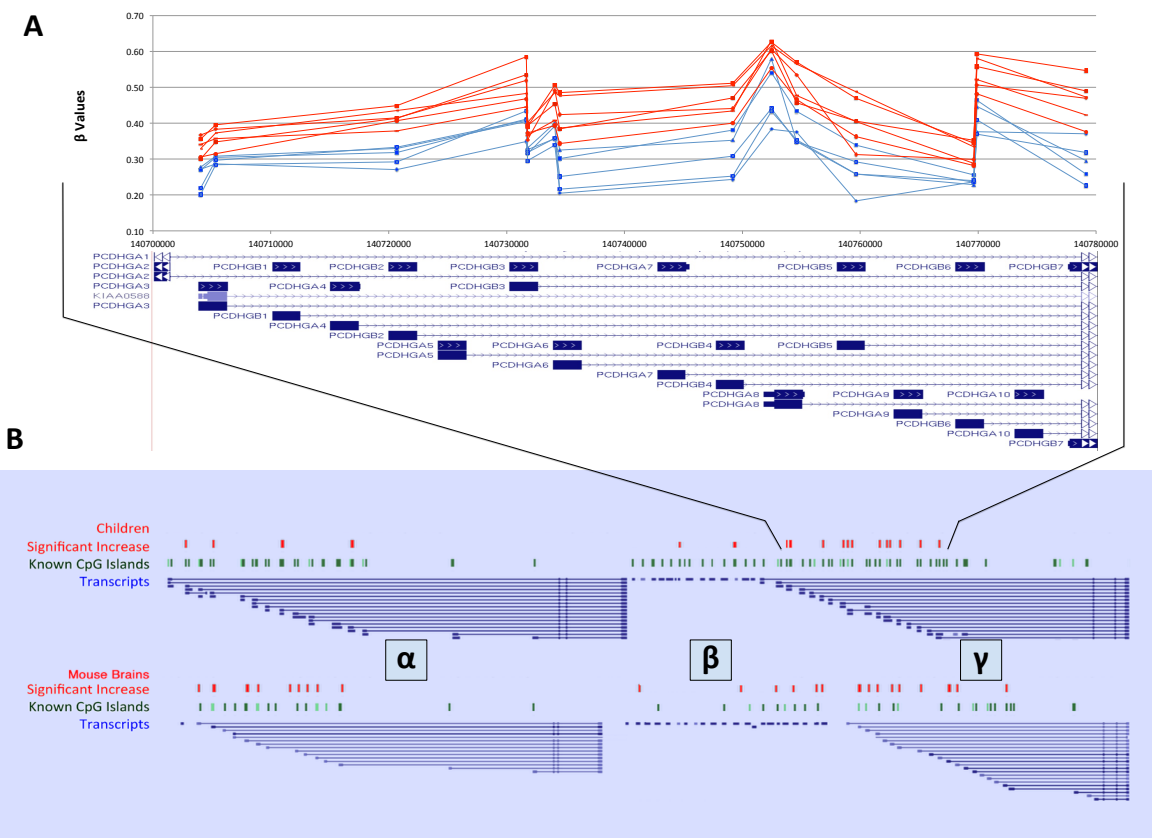


Figure 4.1. Broad profile of increased methylation at the clustered protocadherins in children with FASD and PAE mice: (A) Representative methylation patterns in 14 CpGs of the gamma cluster in the discovery cohort. Red represents children with FASD and blue represents matched controls. (B) Significantly ($p<0.005$) increased methylation in the clustered protocadherin region of patients (red dots), known CpG island (green dots) and potential transcripts (blue lines) along with their similarity to the mouse model ($p<0.01$). Figure is not to scale as non-informative regions have been removed for clarity.

4.5 Discussion

The similarities between mice and humans are striking because the arrays are designed to investigate different regulatory sequences: the mouse arrays are tiled regions of larger change in CpG islands, whereas the human arrays are focused on single CpG sites that could be in a CpG island shore/shelf and up to 2 kilobases away from the corresponding island (Yasui et al. 2007; Irizarry et al. 2009; Doi et al. 2009). Although, some CpG islands are represented on the human array, as exemplified by the clustered protocadherins. Thus, the clustered protocadherin signal is a more direct comparison.

While some of the results may not appear related, most can be connected parsimoniously. For example, the enrichment for cancer pathways is related to developmental events. Many cancers have been redefined as disorders of the epigenome that stem from epigenetic alterations related to stem-cell programming pathways used in development (Feinberg et al. 2006; Feinberg et al. 2016). These results are presumably present due to a larger focus from the research community on cancer rather than development. There are also alterations to genes involved in immune events, which suggest that some alterations may be occurring in glia as well. For instance, microglia induce apoptosis in stressed-but-viable neurons by phagocytosis, which is signaled for by complement components (Brown & Neher 2014). The complement system was implicated in both mouse (**Table 2.2**) and human (*COLEC11*) results, and differential methylation of phagocytosis related genes was observed in both mice (**Table 2.8**) and children (**Table 3.3**). The above example also suggests that the long-term profile informs on not only past alterations to the epigenome, but also active differences in transcription. However, the most striking shared signature was the preferential methylation of the clustered protocadherins, which is similar in mice and children.

4.5.1 Functions of the Clustered Protocadherins

The increased methylation of protocadherin genes from the cheek swab DNA of FASD patients is supported by comparable results in the brains of adult mice prenatally exposed to alcohol (**Figure 4.1B**). These results have the potential to cause a down-regulation of specific gene products depending on the specificity of methylated promoters in neural cells of mice as well as humans. Notably, a number of exposure paradigms in

the previously developed mouse model showed alterations to clustered protocadherin gene expression. *Pcdhb2* was down-regulated (1.2 fold, $p=0.02$) in the voluntary maternal continuous preference drinking (CPD) PAE paradigm. *Pcdhb3* was up-regulated (1.2 fold change, $p=0.005$) in the trimester 1 (T1) binge exposure paradigm, while *Pcdhb7*, *Pcdh15*, *Pcdhb11*, *Pcdhb16*, and *Pcdhb18* were down-regulated (~ 1.3 fold, $p < 0.003$) (Kleiber et al. 2013). In the trimester 3 (T3) exposure paradigm *Pcdhb18* showed a 21% increase after acute exposure and 43% decrease in adult brain gene expression (Kleiber et al. 2013). Furthermore, such changes are expected to affect function because *Pcdhb18* has been demonstrated to control axon growth and arborization in zebrafish (Biswas et al. 2014). Finally, the clustered protocadherins also showed increased histone methylation in the hippocampus of adult PAE mice from the T3 binge exposure paradigm (Chater-Diehl et al. 2016). Both (activating) H3K4me3 and (repressive) H3K27me3 were increased. While the enriched histone post-translational modifications typically act in opposing fashions, this enrichment may also represent bivalent chromatin, which allows for genes silenced in embryonic stem cells to be poised for later activation during differentiation (Bernstein et al. 2006; Vastenhoud & Schier 2012). Finally, some of the clustered protocadherins are proteolytically processed by the metalloprotease ADAM10, which releases an extracellular fragment for signaling (Reiss et al. 2006). *ADAM10* and number of other ADAM(S) genes showed differential methylation in the mouse model. Thus, the mouse models provide further support for the existence of a complex epigenetic signature in the clustered protocadherins that is associated with PAE.

The protocadherins are the largest subgroup of the cadherin gene superfamily of homophilic cell-adhesion proteins (Hirano & Takeichi 2012; Chen & Maniatis 2013). They are primarily expressed in the developing nervous system where they are stochastically involved in a neuronal self-avoidance that allows neurons to interact with the same neuronal subtype but not themselves (Sano et al. 1993). Protocadherins have been observed mediating cell-to-cell interactions in dendrites, axons, synapses, growth cones, and neuronal soma (Kohmura et al. 1998; Wang et al. 2002; Kallenbach et al. 2003; Phillips et al. 2003; Junghans et al. 2008; Lefebvre et al. 2012; Chen et al. 2013). In vertebrates, the majority of protocadherin genes are organized in 3 clusters: α , β , and γ . Intriguingly, the cell specific variation in transcripts created by this locus parallels the

complexity of the immune system. Unlike the immune system, which relies on genetic recombination, the protocadherin complexity is realized by epigenetic mechanisms that parallel the act of recombination via promoter choice and splicing. The transcriptional initiation of the α and γ families is dependent on the methylation status of numerous promoters in the variable regions of the families that end in shared exons. β , on the other hand, does not contain a shared exon and each gene appears to be under the control of its own promoter. The α and γ gene families contain CTCF binding sites that families form a DNA loop structure, which is proposed to bring the isoform specific promoters into the proximity of flanking enhancers and transcriptional machinery (Guo et al. 2012; Golani-Mashiach et al. 2012; Chen & Maniatis 2013; Guo et al. 2015). This allows stochastic expression of several different alternative isoforms from each chromosome, while also enabling both chromosomes to express constitutive isoforms. Thus, it appears that CTCF serves as a master transcription factor for this locus and is used to determine the isoform expression of protocadherins (**Figure 4.2**). Furthermore, stochastic isoform expression from the α cluster is dependent on epigenetic priming by *de novo* methylation patterns established at promoters by *Dnmt3b* during early embryonic stages, which goes on to influence isoform expression in subsequent differentiated cells (Toyoda et al. 2014).

The isoform diversity created by the clustered protocadherins creates a molecular signature on the cell surface of individual neurons that is used to interact in *trans* (Chen et al. 2013). This diversity is accomplished by individual neurons expressing different combinations of the protocadherin isoforms on their cell surface and forms even more diversity by creating multimers (in *cis*). Ultimately, each neuron could have its own unique identity amongst other individuals of the same subtype (Bonn et al. 2007; Schreiner & Weiner 2010). This is believed to be critical for the specific and yet enormous network formation of precise neuronal connections required for neurodevelopment.

The clustered protocadherins function in neurite self-avoidance (Lefebvre et al. 2012), dendritic patterning (Suo et al. 2012), and axonal projection (Katori et al. 2009). Given their essential role underlying neurodevelopment, it comes as no surprise that the protocadherin gene family clusters have been implicated in a number of neurodevelopmental disorders (Kalmady & Venkatasubramanian 2009). Furthermore,

DNA methylation of the clustered protocadherins is known to be environmentally responsive. A broad profile of increases and decreases in DNA methylation, H3K9 acetylation, and gene expression in the hippocampus of the rat revealed that the clustered protocadherins show the largest differential response in adult offspring that received altered maternal care (McGowan et al. 2011). A further comparison to the hippocampus of humans that were abused as children revealed increased methylation in promoters of the clustered protocadherin locus (Suderman et al. 2012). It is notable that the mouse and human results of this thesis displayed a profile more similar to humans who were abused as children, rather than the rodent model of altered maternal care that contained both increases and decreases in methylation. Finally, increased methylation and decreased expression of the γ protocadherins has been observed in fetal Down syndrome cortex (Hajj et al. 2016).

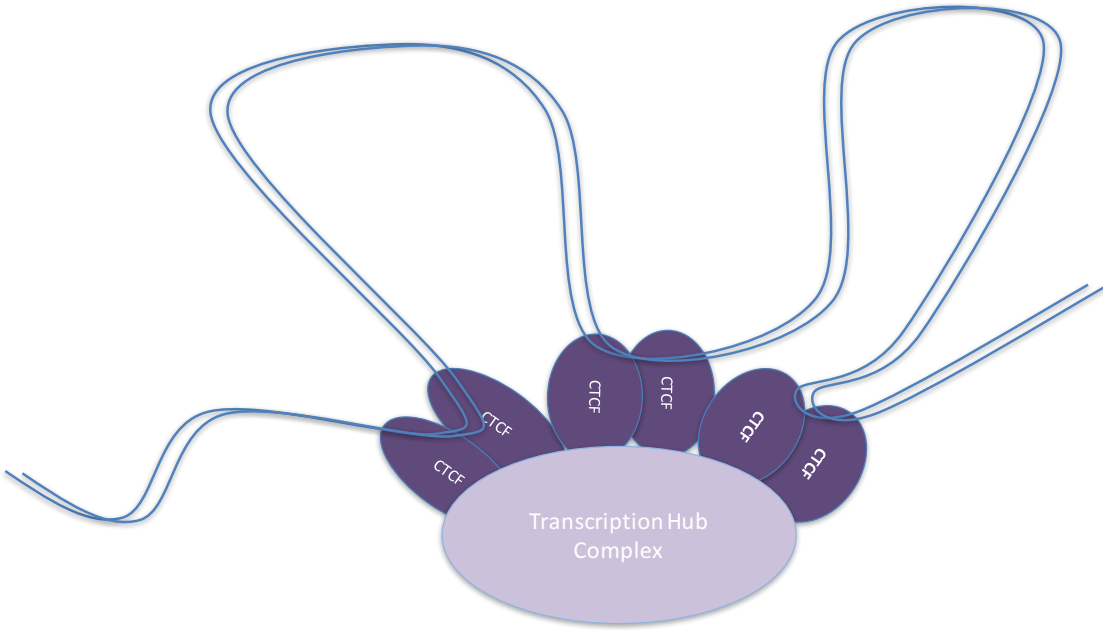


Figure 4.2. A hypothetical model of gene regulation by CTCF at the clustered protocadherin locus. DNA looping mediated by CTCF/Cohesin may regulate gene expression by bringing alternative promoters of select clustered protocadherins into the proximity of enhancers and transcriptional machinery.

4.5.2 Conclusion

The comparison of changes to DNA methylation following PAE shows that there are similarities between the buccal epithelium of children with FASD and the whole brains of PAE adult mice. The similarities typically do not occur in the same genes but are evidenced by alterations to similar ontologies and pathways. These alterations to methylation occur in genes with functions related to cellular and synaptic signaling, (neuro)development, the cell cycle, immune processes, and genomic imprinting (SNORD 115 & SNORD 116). Furthermore, there is a broad profile of increased methylation at the clustered protocadherins in PAE mice and human children. The similarities observed come from functionally diverse tissues that share a stem cell progenitor and suggest an ontogenetic footprint of PAE is maintained by the epigenome. Thus, the findings demonstrate that for translational human studies, rodent models may be used as a reference point to help decipher the complex signature of select life experiences amongst the epigenetic variation that shapes every individual.

Footnote

A modified portion of this chapter has been published (Laufer et al. 2015).

4.6 References

- Bernstein, B.E., Mikkelsen, T.S., Xie, X., Kamal, M., Huebert, D.J., Cuff, J., Fry, B., Meissner, A., Wernig, M., Plath, K., Jaenisch, R., Wagschal, A., Feil, R., Schreiber, S.L. & Lander, E.S., 2006. A Bivalent Chromatin Structure Marks Key Developmental Genes in Embryonic Stem Cells. *Cell*, 125(2), 315–326.
- Biswas, S., Emond, M.R., Duy, P.Q., Hao, L.T., Beattie, C.E. & Jontes, J.D., 2014. Protocadherin-18b interacts with Nap1 to control motor axon growth and arborization in zebrafish. *Molecular Biology of the Cell*, 25(5), 633–42.
- Bonn, S., Seeburg, P.H. & Schwarz, M.K., 2007. Combinatorial expression of alpha- and gamma-protocadherins alters their presenilin-dependent processing. *Molecular and Cellular Biology*, 27(11), 4121–4132.
- Brown, G.C. & Neher, J.J., 2014. Microglial phagocytosis of live neurons. *Nature Reviews Neuroscience*, 15(4), 209–216.
- Chater-Diehl, E.J., Laufer, B.I., Castellani, C.A., Alberry, B.L. & Singh, S.M., 2016. Alteration of Gene Expression, DNA Methylation, and Histone Methylation in Free

Radical Scavenging Networks in Adult Mouse Hippocampus following Fetal Alcohol Exposure. *PLoS one*, 11(5), e0154836.

Chen, W. V., Alvarez, F.J., Lefebvre, J.L., Friedman, B., Nwakeze, C., Geiman, E., Smith, C., Thu, C.A., Tapia, J.C., Tasic, B., Sanes, J.R., Maniatis, T. & Street, O., 2013. Functional Significance of Isoform Diversification in. *Neuron*, 75(3), 402–409.

Chen, W. V & Maniatis, T., 2013. Clustered protocadherins. *Development*, 140(16), 3297–3302.

Doi, A., Park, I.-H., Wen, B., Murakami, P., Aryee, M.J., Irizarry, R., Herb, B., Ladd-Acosta, C., Rho, J., Loewer, S., Miller, J., Schlaeger, T., Daley, G.Q. & Feinberg, A.P., 2009. Differential methylation of tissue- and cancer-specific CpG island shores distinguishes human induced pluripotent stem cells, embryonic stem cells and fibroblasts. *Nature Genetics*, 41(12), 1350–1353.

Feinberg, A.P., Koldobskiy, M.A. & Göndör, A., 2016. Epigenetic modulators, modifiers and mediators in cancer aetiology and progression. *Nature Reviews Genetics*, 17(5), 284–99.

Feinberg, A.P., Ohlsson, R. & Henikoff, S., 2006. The epigenetic progenitor origin of human cancer. *Nature Reviews Genetics*, 7(1), 21–33.

Glatt-Deeley, H., Bancescu, D.L. & Lalande, M., 2010. Prader-Willi syndrome, Snord115, and Htr2c editing. *Neurogenetics*, 11(1), 143–144.

Golan-Mashiach, M., Grunspan, M., Emmanuel, R., Gibbs-Bar, L., Dikstein, R. & Shapiro, E., 2012. Identification of CTCF as a master regulator of the clustered protocadherin genes. *Nucleic Acids Research*, 40(8), 3378–3391.

Guo, Y. et al., 2015. CRISPR Inversion of CTCF Sites Alters Genome Topology and Enhancer/Promoter Function. *Cell*, 162(4), 900–910.

Guo, Y., Monahan, K., Wu, H., Gertz, J., Varley, K.E., Li, W., Myers, R.M., Maniatis, T. & Wu, Q., 2012. CTCF/cohesin-mediated DNA looping is required for protocadherin α promoter choice. *Proceedings of the National Academy of Sciences of the United States of America*, 109(51), 21081–21086.

Hajj, N. El, Dittrich, M., Böck, J., Kraus, T.F.J., Nanda, I., Müller, T., Seidmann, L., Tralau, T., Galetzka, D., Schneider, E. & Haaf, T., 2016. Epigenetic dysregulation in the developing Down syndrome cortex. *Epigenetics*.

Hirano, S. & Takeichi, M., 2012. Cadherins in Brain Morphogenesis and Wiring. *Physiological Reviews*, 92(2), 597–634.

Irizarry, R.A., Ladd-Acosta, C., Wen, B., Wu, Z., Montano, C., Onyango, P., Cui, H., Gabo, K., Rongione, M., Webster, M., Ji, H., Potash, J.B., Sabuncian, S. & Feinberg, A.P., 2009. The human colon cancer methylome shows similar hypo- and

- hypermethylation at conserved tissue-specific CpG island shores. *Nature Genetics*, 41(2), 178–186.
- Junghans, D., Heidenreich, M., Hack, I., Taylor, V., Frotscher, M. & Kemler, R., 2008. Postsynaptic and differential localization to neuronal subtypes of protocadherin beta16 in the mammalian central nervous system. *The European Journal of Neuroscience*, 27(3), 559–571.
- Kallenbach, S., Khantane, S., Carroll, P., Gayet, O., Alonso, S., Henderson, C.E. & Dudley, K., 2003. Changes in subcellular distribution of protocadherin gamma proteins accompany maturation of spinal neurons. *Journal of Neuroscience Research*, 72(5), 549–556.
- Kalmady, S. V. & Venkatasubramanian, G., 2009. Evidence for positive selection on Protocadherin Y gene in Homo sapiens: Implications for schizophrenia. *Schizophrenia Research*, 108(1-3), 299–300.
- Katori, S., Hamada, S., Noguchi, Y., Fukuda, E., Yamamoto, T., Yamamoto, H., Hasegawa, S. & Yagi, T., 2009. Protocadherin-alpha Family Is Required for Serotonergic Projections to Appropriately Innervate Target Brain Areas. *Journal of Neuroscience*, 29(29), 9137–9147.
- Khalid, O., Kim, J.J., Kim, H.S., Hoang, M., Tu, T.G., Elie, O., Lee, C., Vu, C., Horvath, S., Spigelman, I. & Kim, Y., 2014. Gene expression signatures affected by alcohol-induced DNA methylomic deregulation in human embryonic stem cells. *Stem Cell Research*, 12(3), 791–806.
- Kishore, S. & Stamm, S., 2006. The snoRNA HBII-52 regulates alternative splicing of the serotonin receptor 2C. *Science*, 311(5758), 230–232.
- Kleiber, M.L., Mantha, K., Stringer, R.L. & Singh, S.M., 2013. Neurodevelopmental alcohol exposure elicits long-term changes to gene expression that alter distinct molecular pathways dependent on timing of exposure. *Journal of Neurodevelopmental Disorders*, 5(1), 6.
- Kohmura, N., Senzaki, K., Hamada, S., Nobuyuki, K., Yasuda, R., Watanabe, M., Ishii, H., Yasuda, M., Mishina, M. & Yagi, T., 1998. Diversity revealed by a novel family of cadherins expressed in neurons at a synaptic complex. *Neuron*, 20(6), 1137–1151.
- Komuro, A., Masuda, Y., Kobayashi, K., Babbitt, R., Gunel, M., Flavell, R.A. & Marchesi, V.T., 2004. The AHNAKs are a class of giant propeller-like proteins that associate with calcium channel proteins of cardiomyocytes and other cells. *Proceedings of the National Academy of Sciences of the United States of America*, 101(12), 4053–4058.
- Laufer, B.I., Kapalanga, J., Castellani, C.A., Diehl, E.J., Yan, L. & Singh, S.M., 2015. Associative DNA methylation changes in children with prenatal alcohol exposure. *Epigenomics*, 7(8), 1259–1274.

- Laufer, B.I., Mantha, K., Kleiber, M.L., Diehl, E.J., Addison, S.M.F. & Singh, S.M., 2013. Long-lasting alterations to DNA methylation and ncRNAs could underlie the effects of fetal alcohol exposure in mice. *Disease Models & Mechanisms*, 6(4), 977–992.
- Lefebvre, J.L., Kostadinov, D., Chen, W. V., Maniatis, T. & Sanes, J.R., 2012. Protocadherins Mediate Dendritic Self-Avoidance in the Mammalian Nervous System. *Nature*, 488(7412), 517–521.
- McGowan, P.O., Suderman, M., Sasaki, A., Huang, T.C.T., Hallett, M., Meaney, M.J. & Szyf, M., 2011. Broad epigenetic signature of maternal care in the brain of adult rats. *PLoS ONE*, 6(2), e14739.
- Nakatani, J. et al., 2009. Abnormal Behavior in a Chromosome- Engineered Mouse Model for Human 15q11-13 Duplication Seen in Autism. *Cell*, 137(7), 1235–1246.
- Phillips, G.R., Tanaka, H., Frank, M., Elste, A., Fidler, L., Benson, D.L. & Colman, D.R., 2003. Gamma-protocadherins are targeted to subsets of synapses and intracellular organelles in neurons. *The Journal of Neuroscience*, 23(12), 5096–5104.
- Reiss, K., Maretzky, T., Haas, I.G., Schulte, M., Ludwig, A., Frank, M. & Saftig, P., 2006. Regulated ADAM10-dependent ectodomain shedding of γ -protocadherin C3 modulates cell-cell adhesion. *Journal of Biological Chemistry*, 281(31), 21735–21744.
- Rooryck, C. et al., 2011. Mutations in lectin complement pathway genes COLEC11 and MASP1 cause 3MC syndrome. *Nature Genetics*, 43(3), 197–203.
- Sano, K., Tanihara, H., Heimark, R.L., Obata, S., Davidson, M., St John, T., Taketani, S. & Suzuki, S., 1993. Protocadherins: a large family of cadherin-related molecules in central nervous system. *The EMBO Journal*, 12(6), 2249–2256.
- Schreiner, D. & Weiner, J.A., 2010. Combinatorial homophilic interaction between gamma-protocadherin multimers greatly expands the molecular diversity of cell adhesion. *Proceedings of the National Academy of Sciences of the United States of America*, 107(33), 14893–14898.
- Sonne, S., Shekhawat, P.S., Matern, D., Ganapathy, V. & Ignatowicz, L., 2012. Carnitine deficiency in OCTN2^{-/-} newborn mice leads to a severe gut and immune phenotype with widespread atrophy, apoptosis and a pro-inflammatory response. *PLoS ONE*, 7(10), e47729.
- Suderman, M., McGowan, P.O., Sasaki, A., Huang, T.C.T., Hallett, M.T., Meaney, M.J., Turecki, G. & Szyf, M., 2012. Conserved epigenetic sensitivity to early life experience in the rat and human hippocampus. *Proceedings of the National Academy of Sciences*, 109(Supplement 2), 17266–17272.
- Suo, L., Lu, H., Ying, G., Capecchi, M.R. & Wu, Q., 2012. Protocadherin clusters and

- cell adhesion kinase regulate dendrite complexity through Rho GTPase. *Journal of Molecular Cell Biology*, 4(6), 362–376.
- Toyoda, S., Kawaguchi, M., Kobayashi, T., Tarusawa, E., Toyama, T., Okano, M., Oda, M., Nakauchi, H., Yoshimura, Y., Sanbo, M., Hirabayashi, M., Hirayama, T., Hirabayashi, T. & Yagi, T., 2014. Developmental epigenetic modification regulates stochastic expression of clustered Protocadherin genes, generating single neuron diversity. *Neuron*, 82(1), 94–108.
- Vastenhouw, N.L. & Schier, A.F., 2012. Bivalent histone modifications in early embryogenesis. *Current Opinion in Cell Biology*, 24(3), 374–386.
- Wallis, R., Mitchell, D.A., Schmid, R., Schwaebel, W.J. & Keeble, A.H., 2010. Paths reunited: Initiation of the classical and lectin pathways of complement activation. *Immunobiology*, 215(1), 1–11.
- Wang, X., Weiner, J.A., Levi, S., Craig, A.M., Bradley, A. & Sanes, J.R., 2002. Gamma protocadherins are required for survival of spinal interneurons. *Neuron*, 36(5), 843–854.
- Yang, M., Guo, M., Hu, Y. & Jiang, Y., 2013. Scube regulates synovial angiogenesis-related signaling. *Medical Hypotheses*, 81(5), 948–953.
- Yasui, D.H., Peddada, S., Bieda, M.C., Vallero, R.O., Hogart, A., Nagarajan, R.P., Thatcher, K.N., Farnham, P.J. & Lasalle, J.M., 2007. Integrated epigenomic analyses of neuronal MeCP2 reveal a role for long-range interaction with active genes. *Proceedings of the National Academy of Sciences of the United States of America*, 104(49), 19416–19421.

Chapter 5

Discussion

5.1 Overview

The research presented in this thesis has identified differential DNA methylation in prenatal alcohol exposed (PAE) mice (chapter 2) and in children with fetal alcohol spectrum disorders (FASD) (chapter 3). The mouse results revealed alterations to gene and non-coding RNA (ncRNA) expression as well as DNA methylation in adult whole brains. The human observations revealed alterations to DNA methylation from the buccal swabs of children with FASD. When the mouse and human results are compared (chapter 4) they show that many alterations occur in genes involved in the same ontologies and pathways. Furthermore, the comparison of alterations has also allowed for the identification of increased methylation in the clustered protocadherins. In this chapter the results of these studies are synthesized and collectively show that the long-term alterations from PAE represent a ‘footprint’ of cellular signaling events altered at the time of exposure. The results of this thesis also offer a number of considerations for future epigenomic research.

5.2 Towards an Inductive Mechanism: PAE Alters Cellular Signaling

The mechanisms that initiate the altered long-term profile of PAE remain unknown. While the systems biology approaches used in this thesis are suited for discovery, they are not mechanistic and offer only an assessment of the downstream effect. Although the mechanism initiating the long-term profile was not directly examined, the results overlap with literature investigating PAE at the time of exposure.

The pleiotropic effects of ethanol appear to be derived from its ability to alter a number of developmental cellular signaling pathways and a preferential effect on certain multipotent cell types that later undergo coordinated apoptosis (Kiecker 2016). For instance, cell fate and migration depends on signaling pathways with cell surface

receptors that activate downstream transcriptional programming. Examples of these signaling pathways are bone morphogenic protein (BMP)/transforming growth factor- β (TGF β), PI3K/AKT/mTOR, Wnt/ β -catenin, retinoic acid/Hox genes, Delta/Notch, SHH signaling, and MAPK/ERK (Kandel et al. 2000; Lamouille et al. 2014). Notably, members from a number of these pathways have been found to show altered gene expression and epigenetic marks in PAE mice across development (Green et al. 2007; Resendiz et al. 2014). The neural crest is a stem cell population that appears to be particularly impacted by PAE (Smith, Garic, Flentke, et al. 2014). Apoptosis of neural crest cells is driven by elevated reactive oxygen species (ROS) and the binding of alcohol to a G-protein-coupled receptor (GPCR). The activation of GPCRs by ethanol results in the release of phosphoinositol phosphate, which triggers the release of intracellular calcium. This calcium transient prevents β -catenin from activating transcription related to trophic support and cell adhesion, which ultimately results in apoptosis (Smith, Garic, Berres, et al. 2014).

Ethanol acts directly on neurotransmitter system receptors including neuropeptides, amino acids, biogenic amines, and others (Valenzuela et al. 2011; Basavarajappa 2015). Ionotropic receptors are part of a channel pore whereas metabotropic receptors result in signal transduction by secondary messengers and are often GPCRs (Bear et al. 2007). PAE alters a number of neurotransmitter systems but appears to primarily interfere with synaptic signaling involving amino acids and biogenic amines (serotonin and dopamine) (Valenzuela et al. 2011). γ -aminobutyric acid (GABA) is the main inhibitory neurotransmitter, while the amino acid glutamate is the most abundant excitatory neurotransmitter. Ethanol has been shown to directly bind to an allosteric site on the GABA_A receptor, which is an ionotropic receptor for a ligand-gated ion channel, and increases the inhibitory effect (Santhakumar et al. 2007). Ethanol also binds to an allosteric site on the N-methyl-D-aspartate receptor (NMDAR), which is a glutamate receptor subtype, and inhibits excitatory function (Möykkynen & Korpi 2012). Neurotransmitter systems are extensively utilized throughout development. Even before synapses are formed, both glutamate and GABA regulate the migration, proliferation, and differentiation of neural stem cells (Manent & Represa 2007; Valenzuela et al. 2011). Both GABA and glutamate encourage the migration of cortical neurons across the

different layers of a developing embryo's cortex as they pattern it in an inside first, outside last fashion (Luhmann et al. 2015). When GABA or glutamate receptors are activated they trigger calcium transients that remodel the cytoskeleton and result in cellular migration (Luhmann et al. 2015). In neonatal rats, which are the equivalent of the third trimester of human pregnancy, both acute and repeated PAE inhibits the long-term potentiation and thus maturation of GABA_A receptor synapses by temporarily inhibiting L-type voltage-gated calcium channels (Zucca & Valenzuela 2010; Morton & Fernando Valenzuela 2016). These channels result in calcium transients in response to action potentials and are involved in the retrograde release of BDNF (Zucca & Valenzuela 2010; Morton & Fernando Valenzuela 2016). Notably, GABA has an excitatory function that encourages neuronal growth, migration, and synaptogenesis until the end of the rodent equivalent of the third trimester of human pregnancy (Ben-Ari 2002; Valenzuela et al. 2011). Furthermore, glutamate is involved in synaptogenesis and the maturation of neurons (Cline & Haas 2008; Valenzuela et al. 2011). Overall, PAE appears to alter the epigenetic remodeling of embryonic stem cells, neural progenitor cells, and maturing neurons by interfering with a number of cell-adhesion, synaptogenic, and neurotransmission systems (Resendiz et al. 2014). However, PAE also alters other signaling systems upon exposure.

The oxidation of ethanol by alcohol dehydrogenase results in acetaldehyde. Acetaldehyde is more toxic than ethanol and creates an abundance of ROS, which induce oxidative stress (Brocardo et al. 2011). ROS are signaling molecules critical for proper neurodevelopment and a number of cell signaling pathways. One example of a redox sensitive pathway is phosphatidylinositol 3-kinase (PI3K)/AKT/mammalian target of rapamycin (mTOR) signaling, where the antagonist, PTEN, can be inactivated by oxidation (Ostrakhovitch & Semenikhin 2013). The PI3K/AKT/mTOR pathway is an intracellular signaling pathway that regulates the cell cycle and thus proliferation and apoptosis. When activated by growth factors binding to various GPCRs and tyrosine kinase receptors at the cell surface, PI3K phosphorylates phosphatidylinositol on the cell membrane and signals for the activation of AKT. AKT then activates mTOR, inhibits FoxO, and regulates a number of transcription factors to ultimately prevent cell death and promote cell survival (Brunet et al. 2001). However, PTEN inhibits PI3K and therefore

promotes apoptosis. In neural stem cells PI3K/AKT/mTOR promotes cell proliferation, whereas PTEN promotes cell differentiation. Neural stem cells utilize PI3K/AKT/mTOR signaling to carefully balance maintaining a stem cell pool while also providing enough differentiated cells, which can no longer proliferate (Peltier et al. 2007). PI3K/AKT/mTOR signaling is also required for the strengthening of synaptic connections, which is known as long-term potentiation and is the basis for learning and memory (Man et al. 2003; Sui et al. 2008). Overall, the long-term profile of PAE observed in both mice and humans contains many members of the above signaling pathways and suggests that their disruption is maintained as an ‘ontogenetic footprint’.

5.2.1 Alternative Hypotheses

The results suggest that a shared stem cell precursor connects the observations in whole brains and buccal swab DNA. However, there are also a number of possible alternative explanations to the observed footprint. First, the differential epigenomics observed may represent alterations to cell populations as well as alterations to epigenetic marks. This would explain some of the genome-wide alterations, as they could be related to cellular profile; however, the cell line studies reviewed in the introduction of this thesis also establish that genome-wide alterations occur in homogenous populations. Second, not all the observed alterations are connected ontogenetically at the level of the ectoderm. There also appears to be a preferential disturbance of cells dependent on calcium signaling, such as the brain, heart, kidneys, and skeletal structures. Third, and perhaps most likely, is that footprint is a combination of the above possibilities.

5.3 Considerations for Future Experimentation

The field of epigenomics is rapidly advancing, however, as a discipline a number of limitations must be overcome. These challenges are highlighted by the approaches used in this thesis and represent important considerations for future research. They are as follows:

1. **Cell type heterogeneity.** Both the whole brains and the saliva examined contain heterogeneous mixtures of cell types. Thus, the epigenomic signals analyzed represent a mixed profile that may be representative of alterations to a single cell

type or even be heterogeneous within single cells themselves. A deeper understanding this heterogeneity will aid in the knowledge of cell types to be targeted for functional studies, diagnostics, and/or therapeutics.

2. **Whole genome coverage.** The mouse arrays utilized were designed to study CpG islands, specifically promoters, while the human arrays utilized were designed to study individual CpG shores. Future studies would benefit from the use of unbiased designs that allow for the investigation of a number of other features, such as enhancers and gene bodies, or preferentially the whole genome.
3. **Direct comparisons.** This research made use of adult mouse whole brains and buccal swabs from children. To allow for a more direct comparison, future research would benefit from also examining buccal cells in mice and human post-mortem brains. This additional characterization would provide a reference point to identify which alterations are tissue specific and which are species specific.
4. **Integrated analysis.** This thesis has demonstrated the utility of genome-wide scans for both gene expression and DNA methylation in identifying candidate genes. Approaches examining a number of epigenetic marks alongside gene expression would help prioritize candidates.
5. **Larger sample sizes.** The results of this thesis are limited by sample size and genetic diversity. An increase in both would increase statistical power.
6. **A developmental reference epigenome.** The epigenome appears to create more variation than the genome alone. Therefore, an understanding of the extent of this variation across tissues would allow for the determination of modifications that are inherited, stochastic, and/or environmentally induced.
7. **Functional confirmation of candidate loci.** While systems biology based approaches are suited for discovery, they also require functional confirmation experiments to show causation of a candidate in producing an endophenotype. Functional experiments could be carried out by epigenome editing with CRISPR/Cas9 biotechnology (Day 2014; Laufer & Singh 2015). First, mouse models without PAE would be used to establish causation by recreating key marks, which include differential methylation in imprinting control regions for *Snrpn-Ube3a* and *Dlk1-Dio3* as well as the clustered protocadherins, *Colec11*, and

Htt. Then, a series of experiments could be carried with the opposite effector that targets the same regions in PAE mice. These causative confirmation experiments could be used to develop therapeutic interventions for FASD patients that are based on somatic epigenome editing of the brain (once the technology is developed for the clinic).

5.4 Conclusions

The results of this thesis present a number of conclusions, which are derived from observations in adult PAE mice and human children with FASD. The similarities come from functionally diverse tissues that are derived from a common stem cell progenitor.

The analysis of adult PAE mice shows that:

1. PAE results in long-term alterations to gene and ncRNA expression as well as DNA methylation in the adult brain.
2. While genome-wide, the alterations to the epigenome are non-random and occur in:
 - Imprinted clusters of ncRNA: *Snrpn-Ube3a* and *Dlk1-Dio3*.
 - Functional sites of genes related to neurodevelopment, stem cell signaling, and immune processes.
3. Chronic and moderate PAE or acute and binge PAE at any time point in pregnancy distinctly alters the epigenome.

The observations in children with FASD reveal that:

1. DNA from buccal swabs of children with FASD contains a genome-wide DNA methylation signature related to neurodevelopment, which distinguishes children with FASD from matched controls.
2. Targeted sequencing of a select gene does not identify FASD in a random child from the general population.

The comparison of adult PAE mice to human children with FASD shows that:

1. The alterations to methylation occur in functionally related genes and pathways; however, the specific genes altered are generally not identical.
2. The clustered protocadherins display a large-scale increase in methylation in both PAE mice and humans.

In conclusion, the results of this thesis provide foundational evidence for the long-term effects of gene-by-environment interactions. They suggest that deregulation of the epigenome can be inherited across cell divisions and maintain long-term alterations that originate from developmental exposures. The results also suggest that non-invasively obtained buccal swab DNA contains a signature of neurodevelopmental exposure in humans. Furthermore, the results demonstrate that rodent models may be used as a reference point when analyzing the complexities of the human epigenome. Aside from the relevance of the results to FASD, the results also provide insight into basic biological principles. Chromatin is a dynamic molecule that enables a static linear sequence of DNA to maintain a molecular memory of developmental events and form distinct tissues. Disruption of this programming by adverse environmental experiences can result not only in immediate consequences to the exposed stem cells but may also be inherited across cell division and maintained in resulting differentiated cells. As the epigenome is more dynamic than the genome, therapeutic treatment of disorders through novel epigenetic avenues represents a frontier in personalized medicine.

5.5 References

- Basavarajappa, B., 2015. Fetal Alcohol Spectrum Disorder: Potential Role of Endocannabinoids Signaling. *Brain Sciences*, 5(4), 456–493.
- Bear, M.F., Connors, B.W. & Paradiso, M.A., 2007. *Neuroscience: Exploring the Brain*, Lippincott Williams & Wilkins.
- Ben-Ari, Y., 2002. Excitatory actions of gaba during development: the nature of the nurture. *Nature Reviews Neuroscience*, 3(9), 728–739.
- Brocardo, P.S., Gil-Mohapel, J. & Christie, B.R., 2011. The role of oxidative stress in fetal alcohol spectrum disorders. *Brain Research Reviews*, 67(1-2), 209–225.
- Brunet, A., Datta, S.R. & Greenberg, M.E., 2001. Transcription-dependent and -independent control of neuronal survival by the PI3K-Akt signaling pathway. *Current Opinion in Neurobiology*, 11(3), 297–305.
- Cline, H. & Haas, K., 2008. The regulation of dendritic arbor development and plasticity by glutamatergic synaptic input: a review of the synaptotrophic hypothesis. *The Journal of Physiology*, 586(6), 1509–1517.
- Day, J.J., 2014. New Approaches to Manipulate the Epigenome. *Dialogues in Clinical Neuroscience*, 16(3), 345–357.

- Green, M.L., Singh, A. V., Zhang, Y., Nemeth, K.A., Sulik, K.K. & Knudsen, T.B., 2007. Reprogramming of genetic networks during initiation of the Fetal Alcohol Syndrome. *Developmental Dynamics*, 236(2), 613–631.
- Kandel, E.R., Schwartz, J.H. & Jessell, T.M., 2000. *Principles of Neural Science*, McGraw-Hill New York.
- Kiecker, C., 2016. The chick embryo as a model for the effects of prenatal exposure to alcohol on craniofacial development. *Developmental Biology*.
- Lamouille, S., Xu, J. & Deryck, R., 2014. Molecular mechanisms of epithelial–mesenchymal transition. *Nature Reviews Molecular Cell Biology*, 15(3), 178–196.
- Laufer, B.I. & Singh, S.M., 2015. Strategies for precision modulation of gene expression by epigenome editing: an overview. *Epigenetics & Chromatin*, 8(1), 34.
- Luhmann, H.J., Fukuda, A. & Kilb, W., 2015. Control of cortical neuronal migration by glutamate and GABA. *Frontiers in Cellular Neuroscience*, 9, 4.
- Man, H.Y., Wang, Q., Lu, W.Y., Ju, W., Ahmadian, G., Liu, L., D’Souza, S., Wong, T.P., Taghibiglou, C., Lu, J., Becker, L.E., Pei, L., Liu, F., Wymann, M.P., MacDonald, J.F. & Wang, Y.T., 2003. Activation of PI3-kinase is required for AMPA receptor insertion during LTP of mEPSCs in cultured hippocampal neurons. *Neuron*, 38(4), 611–624.
- Manent, J.B. & Represa, A., 2007. Neurotransmitters and brain maturation: early paracrine actions of GABA and glutamate modulate neuronal migration. *The Neuroscientist*, 13(3), 268–279.
- Morton, R.A. & Fernando Valenzuela, C., 2016. Further characterization of the effect of ethanol on voltage-gated Ca²⁺ channel function in developing CA3 hippocampal pyramidal neurons. *Brain Research*, 1633, 19–26.
- Möykynen, T. & Korpi, E.R., 2012. Acute effects of ethanol on glutamate receptors. *Basic & Clinical Pharmacology & Toxicology*, 111(1), 4–13.
- Ostrakhovitch, E.A. & Semenikhin, O.A., 2013. The role of redox environment in neurogenic development. *Archives of Biochemistry and Biophysics*, 534(1-2), 44–54.
- Peltier, J., O’Neill, A. & Schaffer, D. V., 2007. PI3K/Akt and CREB regulate adult neural hippocampal progenitor proliferation and differentiation. *Developmental Neurobiology*, 67(10), 1348–1361.
- Resendiz, M., Mason, S., Lo, C.L. & Zhou, F.C., 2014. Epigenetic regulation of the neural transcriptome and alcohol interference during development. *Frontiers in Genetics*, 5, 285.
- Santhakumar, V., Wallner, M. & Otis, T.S., 2007. Ethanol acts directly on extrasynaptic

- subtypes of GABAA receptors to increase tonic inhibition. *Alcohol*, 41(3), 211–221.
- Smith, S.M., Garic, A., Berres, M.E. & Flentke, G.R., 2014. Genomic factors that shape craniofacial outcome and neural crest vulnerability in FASD. *Frontiers in Genetics*, 5, 224.
- Smith, S.M., Garic, A., Flentke, G.R. & Berres, M.E., 2014. Neural crest development in fetal alcohol syndrome. *Birth Defects Research Part C - Embryo Today: Reviews*, 102(3), 210–220.
- Sui, L., Wang, J. & Li, B.-M., 2008. Role of the phosphoinositide 3-kinase-Akt-mammalian target of the rapamycin signaling pathway in long-term potentiation and trace fear conditioning memory in rat medial prefrontal cortex. *Learning & Memory*, 15(10), 762–776.
- Valenzuela, C.F., Puglia, M.P. & Zucca, S., 2011. Focus on: neurotransmitter systems. *Alcohol Research & Health*, 34(1), 106–120.
- Zucca, S. & Valenzuela, C.F., 2010. Low concentrations of alcohol inhibit BDNF-dependent GABAergic plasticity via L-type Ca²⁺ channel inhibition in developing CA3 hippocampal pyramidal neurons. *The Journal of Neuroscience*, 30(19), 6776–6781.

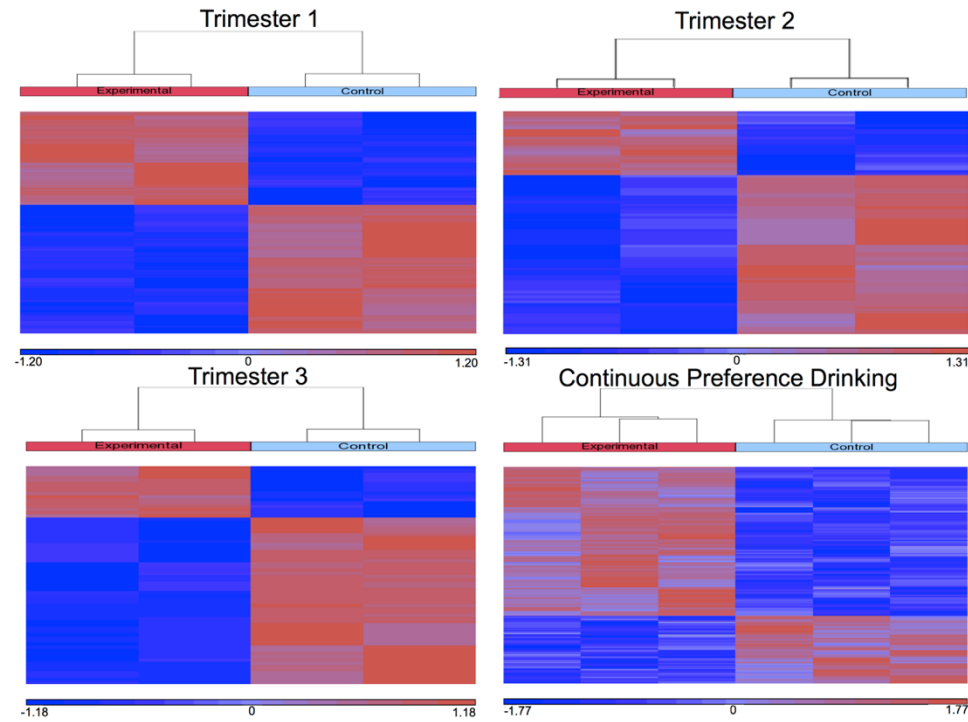
Appendix A – IPA® miRNA target filter analysis of CPD PAE adult mouse brains.

miRNA	Fold Change	Gene	Fold Change
<i>let-7d*</i>	-1.5	<i>Aak1</i>	1.2
<i>mir-124*</i>	-1.3	<i>Aak1</i>	1.2
<i>mir-133b</i>	-1.4	<i>Aak1</i>	1.2
<i>mir-369-5p</i>	-1.3	<i>Aak1</i>	1.2
<i>mir-25</i>	-1.2	<i>Aak1</i>	1.2
<i>mir-27a</i>	-1.4	<i>Aak1</i>	1.2
<i>mir-495</i>	-1.2	<i>Aak1</i>	1.2
<i>mir-331-3p</i>	-1.2	<i>Aak1</i>	1.2
<i>mir-34b-3p</i>	-1.3	<i>Aak1</i>	1.2
<i>mir-500</i>	-1.3	<i>Aak1</i>	1.2
<i>mir-124*</i>	-1.3	<i>Adamts9</i>	1.2
<i>mir-369-5p</i>	-1.3	<i>Adamts9</i>	1.2
<i>mir-25</i>	-1.2	<i>Adamts9</i>	1.2
<i>mir-30a*</i>	-1.3	<i>Adamts9</i>	1.2
<i>mir-495</i>	-1.2	<i>Adamts9</i>	1.2
<i>mir-34b-3p</i>	-1.3	<i>Adamts9</i>	1.2
<i>mir-362-5p</i>	-1.2	<i>Adamts9</i>	1.2
<i>mir-489</i>	1.2	<i>Ankrd49</i>	-1.2
<i>mir-124*</i>	-1.3	<i>Cspp1</i>	1.3
<i>mir-369-5p</i>	-1.3	<i>Cspp1</i>	1.3
<i>mir-495</i>	-1.2	<i>Cspp1</i>	1.3
<i>mir-340-5p</i>	1.2	<i>Ddit4l</i>	-1.3
<i>mir-200a*</i>	1.2	<i>Ddit4l</i>	-1.3
<i>mir-27a</i>	-1.4	<i>Dnajc13</i>	1.3
<i>mir-30a*</i>	-1.3	<i>Dnajc13</i>	1.3
<i>mir-200a*</i>	1.2	<i>Eapp</i>	-1.2
<i>mir-369-5p</i>	-1.3	<i>Ephb1</i>	1.3
<i>mir-495</i>	-1.2	<i>Ephb1</i>	1.3
<i>mir-369-5p</i>	1.3	<i>Fam155a</i>	1.3
<i>mir-30a*</i>	-1.3	<i>Fam155a</i>	1.3
<i>mir-124*</i>	-1.3	<i>Gpatch8</i>	1.2
<i>mir-15a*</i>	-1.2	<i>Gpatch8</i>	1.2
<i>mir-369-5p</i>	-1.3	<i>Gpatch8</i>	1.2
<i>mir-199b*</i>	-1.2	<i>Gpatch8</i>	1.2
<i>mir-25</i>	-1.2	<i>Gpatch8</i>	1.2
<i>let-7d*</i>	-1.5	<i>Hmga2</i>	1.2
<i>mir-15a*</i>	-1.2	<i>Hmga2</i>	1.2

<i>mir-369-5p</i>	-1.3	<i>Hmga2</i>	1.2
<i>mir-25</i>	-1.2	<i>Hmga2</i>	1.2
<i>mir-146b</i>	1.2	<i>Nuak1</i>	-1.3
<i>mir-19b</i>	1.4	<i>Nuak1</i>	-1.3
<i>mir-151-5p</i>	1.2	<i>Nuak1</i>	-1.3
<i>mir-152</i>	1.2	<i>Otx2</i>	-1.3
<i>mir-369-5p</i>	-1.3	<i>Pten</i>	1.4
<i>mir-25</i>	-1.2	<i>Pten</i>	1.4
<i>mir-495</i>	-1.2	<i>Pten</i>	1.4
<i>mir-743a</i>	1.3	<i>Rps27l</i>	-1.2
<i>mir-15a*</i>	-1.2	<i>Slc24a1</i>	1.2
<i>mir-27a</i>	-1.4	<i>Slc24a1</i>	1.2
<i>mir-17*</i>	1.5	<i>Slitrk2</i>	-1.2
<i>mir-17*</i>	1.5	<i>Tbc1d17</i>	-1.3
<i>mir-146b</i>	1.2	<i>Tmem19</i>	-1.2
<i>mir-340-5p</i>	1.2	<i>Tmem19</i>	-1.2
<i>mir-369-5p</i>	-1.3	<i>Trdn</i>	1.2
<i>mir-30a*</i>	-1.3	<i>Trdn</i>	1.2
<i>mir-495</i>	-1.2	<i>Trdn</i>	1.2
<i>mir-369-5p</i>	-1.3	<i>Ypell</i>	1.2
<i>mir-199b*</i>	-1.2	<i>Ypell</i>	1.2
<i>mir-27a</i>	-1.4	<i>Ypell</i>	1.2

Results were obtained from gene and miRNA expression arrays respectively. They are filtered based on confidence of interaction, brain specificity, and an inverse miRNA ($p<0.3$, fold change 1.15) to target mRNA ($p<0.05$, fold change 1.2) relationship.

Appendix B – Individual heatmaps of differential miRNA expression generated using hierarchical clustering of the four PAE paradigms ($p<0.05$ and 1.2-fold change cut-off). Experimental mice are labelled red and control mice are labelled blue.



Appendix C – Venn diagram of common and unique differentially expressed miRNAs identified by four PAE models ($p<0.05$ and 1.2-fold change cut-off).



Appendix D – Differentially expressed snoRNAs in the *Snrpn-Ube3a* region (chromosome 7) identified by miRNA and gene expression arrays in all PAE paradigms ($p<0.05$ and 1.2-fold change cut-off).

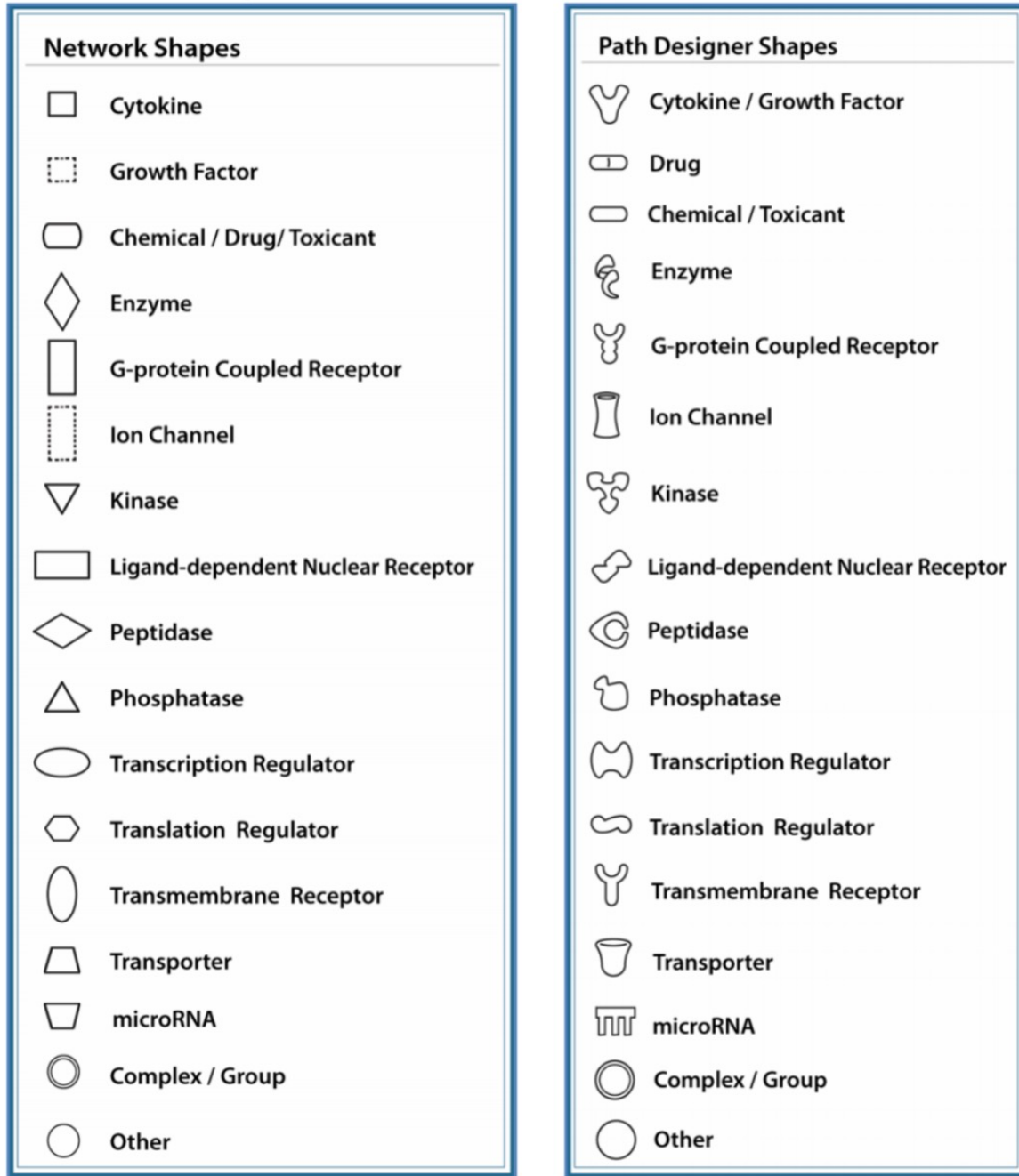
Snrpn-Ube3a		CPD			Trimester 1			Trimester 2			Trimester 3		
miRNA array		ID	FC	<i>p</i>	ID	FC	<i>p</i>	ID	FC	<i>p</i>	ID	FC	<i>p</i>
	No Significant ncRNAs	HBII-52-48	1.2	0.049	HBII-52-2	1.2	0.044	HBII-52-15	1.5	0.001			
		HBII-85-7	-1.3	0.037	HBII-85-22	-1.3	0.001	HBII-85-29	1.4	0.026			
		HBII-85-23	-1.8	0.050	HBII-85-26	-1.2	0.039						
		HBII-85-24	-1.4	0.039									
		HBII-85-28	-1.4	0.009									
Expression Array	Ensembl ID	FC	<i>p</i>	Ensembl ID	FC	<i>p</i>				Ensembl ID	FC	<i>p</i>	
MBII-52	ENSMUST00000101805	1.4	0.019	ENSMUST00000097244	1.4	0.009	*No Significant ncRNAs*			ENSMUST00000102015	1.5	0.003	
	ENSMUST00000101980	1.2	0.003	ENSMUST00000101805	1.2	0.050				ENSMUST00000102017	1.3	0.017	
	ENSMUST00000101860	1.3	0.035	ENSMUST00000101861	1.2	0.050				ENSMUST00000102028	1.6	0.001	
	ENSMUST00000101803	1.2	0.002	ENSMUST00000101896	1.3	0.004				ENSMUST00000102037	1.4	0.025	
	ENSMUST00000097244	1.3	0.0003	ENSMUST00000101917	1.3	0.017				ENSMUST00000102046	1.3	0.022	
	ENSMUST00000101917	1.2	0.038	ENSMUST00000101935	1.3	0.017							
	ENSMUST00000101951	1.3	0.017	ENSMUST00000101935	1.5	0.029							
	ENSMUST00000101896	1.2	0.0002	ENSMUST00000101980	1.3	0.028							
	ENSMUST00000101932	1.2	0.0002	ENSMUST00000102037	1.3	0.038							
	ENSMUST00000101816	1.4	0.004										

Appendix E – Differentially expressed ncRNAs from *Dlk1-Dio3* and *Sfmbt2* ($p<0.05$ and 1.2-fold change cut-off). A) Dysregulated ncRNAs from the *Dlk1-Dio3* region (chromosome 12) identified by miRNA and gene expression arrays in all PAE paradigms. **B)** Dysregulated imprinted miRNAs encoded in the *Sfmbt2* region (chromosome 2) identified by miRNA expression arrays in all PAE paradigms.

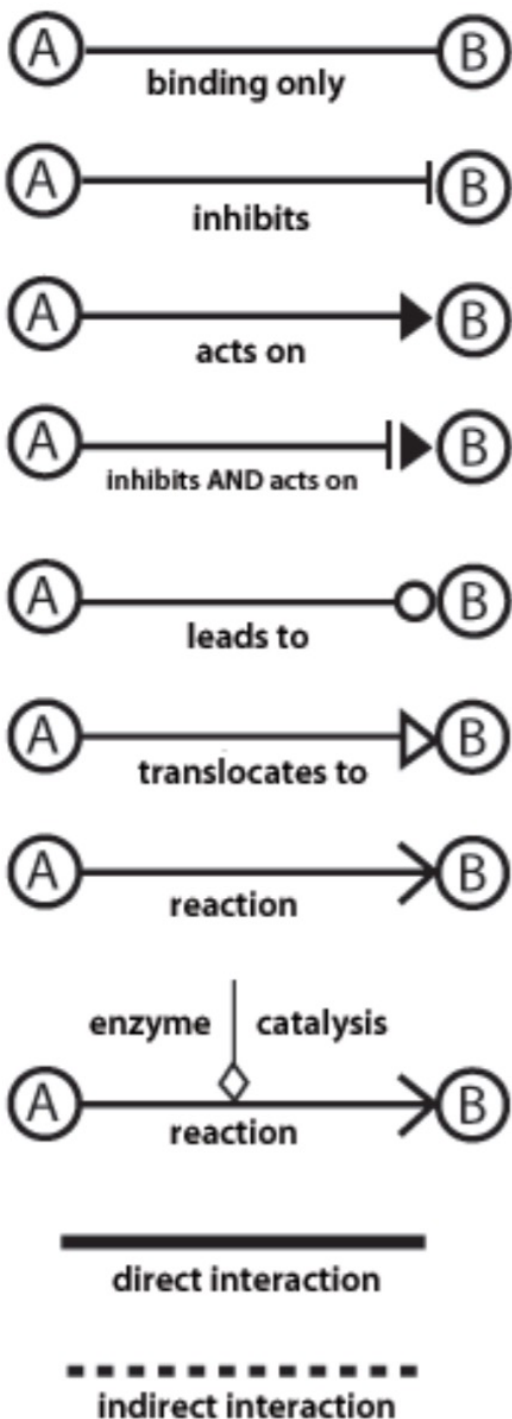
A)	Dlk1-Dio3			CPD			Trimester 1			Trimester 2			Trimester 3		
	miRNA array	ID	FC	<i>p</i>	ID	FC	<i>p</i>	ID	FC	<i>p</i>	ID	FC	<i>p</i>		
		miR-679	1.2	0.03	miR-665	1.2	0.05	miR-666-5p	-1.2	0.003	miR-665	-1.2	0.03		
		miR-300	-1.3	0.05				miR-369-5p	1.3	0.003	miR-434-3p	1.2	0.01		
								hp_mmu-mir-300	1.3	0.021	miR-376b	-1.7	0.04		
								hp_mmu-mir-379	-1.2	0.031	miR-544	-1.3	0.02		
										hp_mmu-mir-485	-1.3	0.04			
Expression Array	Ensembl ID	FC	<i>p</i>								Ensembl ID	FC	<i>p</i>		
SNORD 113	ENSMUST00000082745	1.3	0.02	*No Significant ncRNAs*			*No Significant ncRNAs*			ENSMUST00000082553	-1.5	0.01			
	ENSMUST00000082553	1.3	0.02							ENSMUST00000082611	-1.5	0.01			
	ENSMUST00000082611	1.3	0.02							ENSMUST00000082786	1.6	0.04			
	ENSMUST00000082786	1.2	0.04							ENSMUST00000082792	-1.3	0.00			

B)	Sfmbt2			CPD			Trimester 1			Trimester 2			Trimester 3		
	miRNA array	ID	FC	<i>p</i>	ID	FC	<i>p</i>	ID	FC	<i>p</i>	ID	FC	<i>p</i>		
		miR-466f-3p	1.4	0.02	hp_mmu-mir-669j	1.72	0.002	miR-466b-3p	-1.4	0.04	miR-467b	1.3	0.04		
		miR-467c	-1.2	0.01				miR-669a	-1.8	0.05	miR-467a-1*	-1.3	0.04		
		miR-467a*	1.9	0.01				miR-466e-3p	-1.5	0.0002	hp_mmu-mir-297c	-1.3	0.037		
		miR-466c-3p	1.2	0.003				miR-466c-3p	-1.9	0.03	hp_mmu-mir-466e	-1.7	0.034		
		miR-669h-3p	1.6	0.01				hp_mmu-mir-297b	-1.4	0.03	hp_mmu-mir-466f-2	-1.6	0.05		
		hp_mmu-mir-466h	1.3	0.03				hp_mmu-mir-297c	-1.6	0.02	hp_mmu-mir-466h	-1.6	0.03		
								hp_mmu-mir-466e	-1.3	0.03	hp_mmu-mir-669j	-1.4	0.0002		
								hp_mmu-mir-466f-2	-1.3	0.05	hp_mmu-mir-669m-1	-1.4	0.02		
								hp_mmu-mir-669d	-2.1	0.03					

Appendix F – Ingenuity Pathway Analysis Legend



Relationships



Note: "Acts on" and "inhibits" edges
may also include a binding event.

Relationship Labels

- A Activation**
- B Binding**
- C Causes/Leads to**
- CC Chemical-Chemical interaction**
- CP Chemical-Protein interaction**
- E Expression (includes metabolism/ synthesis for chemicals)**
- EC Enzyme Catalysis**
- I Inhibition**
- L ProteoLysis (includes degradation for Chemicals)**
- LO Localization**
- M Biochemical Modification**
- MB Group/complex Membership**
- P Phosphorylation/Dephosphorylation**
- PD Protein-DNA binding**
- PP Protein-Protein binding**
- PR Protein-RNA binding**
- RB Regulation of Binding**
- RE Reaction**
- RR RNA-RNA Binding**
- T Transcription**
- TR Translocation**

Appendix K – Ethical Approval

Mouse



Nov.1, 2010

*This is the 3rd Renewal of this protocol

*A Full Protocol submission will be required in 2011

Dear Dr. Singh

Your Animal Use Protocol form entitled:

Genetic Regulatory Mechanisms: Genes Determining Ethanol Preference in Mice

has had its yearly renewal approved by the Animal Use Subcommittee.

This approval is valid from **Nov.1, 2010** to **Oct.31, 2011**

The protocol number for this project remains as **2007-059**

1. This number must be indicated when ordering animals for this project.
2. Animals for other projects may not be ordered under this number.
3. If no number appears please contact this office when grant approval is received.
If the application for funding is not successful and you wish to proceed with the project, request that an internal scientific peer review be performed by the Animal Use Subcommittee office.
4. Purchases of animals other than through this system must be cleared through the ACVS office. Health certificates will be required.

REQUIREMENTS/COMMENTS

Please ensure that individual(s) performing procedures on live animals, as described in this protocol, are familiar with the contents of this document.

The holder of this *Animal Use Protocol* is responsible to ensure that all associated safety components (biosafety, radiation safety, general laboratory safety) comply with institutional safety standards and have received all necessary approvals. Please consult directly with your institutional safety officers.

c.c. M. Kleiber, W. Lagerwerf

The University of Western Ontario

Animal Use Subcommittee / University Council on Animal Care
Health Sciences Centre, • London, Ontario • CANADA – N6A 5C1
PH: 519-661-2111 ext. 86770 • FL 519-661-2028 • www.uwo.ca/animal



2007-059-10::5:

AUP Number: 2007-059-10

AUP Title: Genetic Regulatory Mechanisms: Genes Determining Ethanol Preference in Mice

Approval Date: 10/27/2011

The YEARLY RENEWAL to Animal Use Protocol (AUP) 2007-059-10 has been approved.

1. This AUP number must be indicated when ordering animals for this project.
2. Animals for other projects may not be ordered under this AUP number.
3. Purchases of animals other than through this system must be cleared through the ACVS office. Health certificates will be required.

REQUIREMENTS/COMMENTS

Please ensure that individual(s) performing procedures on live animals, as described in this protocol, are familiar with the contents of this document.

The holder of this Animal Use Protocol is responsible to ensure that all associated safety components (biosafety, radiation safety, general laboratory safety) comply with institutional safety standards and have received all necessary approvals. Please consult directly with your institutional safety officers.

Submitted by: Kinchlea, Will D
on behalf of the Animal Use Subcommittee

The University of Western Ontario
Animal Use Subcommittee / University Council on Animal Care
Health Sciences Centre • London, Ontario • CANADA N6A 5C1
PH: 519-661-2111 ext. 86768 • FL 519-661-2028

Human



November 20th, 2014

Dr. Joachim Kapalanga M.D. PhD
Department of Paediatrics
Grey Bruce Health Services

RE: Identifying epigenetic biomarkers ("molecular footprints") of prenatal alcohol exposure in children affected with Fetal Alcohol Spectrum Disorder.

The Grey Bruce Health Services Ethics Committee approved our participation in the above named study at a meeting held on November 20th, 2014

Under FDA regulations, this approval will last only one year. If the study extends beyond one year, you must request re-approval for the next year at least three weeks prior to November 20th, 2015.

FDA requires you to notify this Committee of any new advertisements or recruiting material, change of Investigator, Study Coordinator or site location, serious adverse events, amendments or changes in the protocol, significant protocol deviations, patient death or termination of the study. Please note that you must submit all protocol amendments and/or advertising to the Committee, prior to implementing the amendments and or advertisements.

The Grey Bruce Health Services Ethics Committee complies with and is constituted in accordance with the requirements of: TCPS2 – 2nd edition of the Tri-Council Policy Statement: Ethical Conduct for Research Involving Humans; the International Conference on Harmonization of Good Clinical Practices (ICH GCP); Part C Division 5 of the Food & Drug Regulations of Health Canada; and the provisions of the Ontario Personal Health Information Protection Act 2004 and its applicable regulations. The Grey Bruce Health Services Ethics committee is also in compliance with the regulations of the Food & Drug Administration as described in 21 CFR parts 50 & 56.

Sonja Glass
Chair, Ethics Committee
Grey Bruce Health Services

Mr. Bernie Hartung
Chair, Clinical Research Advisory Group
Grey Bruce Health Services

Cc: Heather Daye, Manager Health Records
Sue Snowdon, Manager Women and Child Care

Appendix L – Journal Copyright Approval

From: Georgia Patey
Subject: RE: Permission to Use Copyrighted Material in a Doctoral Thesis
Date: January 22, 2016 at 10:14 AM
To: Benjamin Laufer

GP

Dear Dr Laufer,

I confirm that the arrangements detailed in your below email meet with the approval of FSG, and we grant you permission to use a modified version of your pre-production manuscript '*Associative DNA methylation changes in children with prenatal alcohol exposure*' (Epigenomics, doi:10.2217/epi.15.60, Future Medicine, 2015) in your thesis. We understand and accept all of the terms of use outlined in your email.

With my best wishes,
Georgia Patey
Commissioning Editor
Future Medicine

part of future science group

From: Benjamin Laufer
Sent: 22 January 2016 14:55
To: Georgia Patey
Subject: Permission to Use Copyrighted Material in a Doctoral Thesis

Dear Editor,

I am a University of Western Ontario graduate student completing my Doctoral thesis entitled "Neurodevelopmental epigenetic footprints from prenatal alcohol exposure". My thesis will be available in full-text on the internet for reference, study and / or copy. Except in situations where a thesis is under embargo or restriction, the electronic version will be accessible through the Western Libraries web pages, the Library's web catalogue, and also through web search engines. I will also be granting Library and Archives Canada and ProQuest/UMI a non-exclusive license to reproduce, loan, distribute, or sell single copies of my thesis by any means and in any form or format. These rights will in no way restrict republication of the material in any other form by you or by others authorized by you.

I would like permission to allow the inclusion of a modified pre-production version of the following in my thesis: *Associative DNA methylation changes in children with prenatal alcohol exposure*, Epigenomics, doi:10.2217/epi.15.60, Future Medicine, 2015.

The material will be attributed through a citation.

Please confirm in writing or by email that these arrangements meet with your approval.

Sincerely,

Benjamin Laufer

Curriculum Vitae
Benjamin I. Laufer

Current Position:

Ph.D. Candidate, Molecular Genetics
Supervisor: Dr. Shiva M. Singh
The University of Western Ontario

Comprehensive Exam (2013) Topics: Microarrays, Neuroplasticity, and Cellular Signaling

Degrees Earned:

B.Sc. (Honors Specialization in Genetics), The University of Western Ontario, 2010

Graduate Courses:

- Epigenetics
- Genetic Variation
- Biology of Aging
- Advances in Epigenetics

Teaching Experience:

Biology 4582: Investigative Techniques in Genetics. *Fall and Winter 2010-2015.*

- Guest lectures included: 1) Epigenetics, 2) Epigenetic Techniques, 3) Microarrays, 4) Personal Genomics, and 5) CRISPR/Cas9 Biotechnology

Biology 3595A: Advanced Genetics. *Fall 2016.*

- Guest lectures included 1) Epigenetics, 2) Personal Genomics, and 3) Workshops on interpreting scientific literature

Biology 2581B: Genetics. *Winter 2016.*

Academic Honors and Awards:

Name	Year(s)	Value (CAD)
Canadian Institute of Health Research (CIHR) Post-Doctoral Fellowship Award	2016 - 2019	\$150,000 (\$50,000/year)
Natural Sciences and Engineering Research Council of Canada (NSERC) Postgraduate Scholarship Doctoral (PGS D)	2012-2015	\$63,000 (\$21,000/year)
National FASD Poster Competition Winner (FACE)	2013	\$200
NIAAA Travel Award (for ICPG)	2012	\$2,000
Ontario Graduate Scholarship (Masters)	2011	\$15,000
First Place Oral Presentation at the Biology Graduate Research Forum (BGRF)	2011	N/A
Graduated with Distinction and Western Scholar's	2010	N/A
Dean's Honor List	2006-2010	N/A
Jeanette Holden Post-Secondary Entrance Scholarships for Siblings of Students with ASD (Undergraduate)	2006	\$1,000

Departmental and University Service

- Society of Graduate Students (SOGS) Bursary Committee Member. 2010-2015.
- Undergraduate Thesis Advisory Committee Member. 2013-2014.
- Biology Graduate Research Forum Web Organizer. 2012.

Publications (Sorted by authorship and then chronology):

Laufer, BI., and Singh, SM. (2015). Strategies for precision modulation of gene expression by epigenome editing: An overview. *Epigenetics & Chromatin*.

Laufer, BI., Kapalanga, J., Castellani, CA., Diehl, EJ., Yan, L., and Singh, SM. (2015). Associative DNA methylation changes in children with prenatal alcohol exposure. *Epigenomics*.

Laufer, BI., Diehl, EJ., and Singh, SM. (2013). Neurodevelopmental epigenetic etiologies: insights from studies on mouse models of fetal alcohol spectrum disorders. *Epigenomics*.

Laufer, BI., Mantha, K., Kleiber, ML., Diehl, EJ., Addison, SMF., and Singh, SM. (2013). Long lasting alterations to DNA methylation and ncRNAs may underlie the effects of fetal alcohol exposure. *Disease Models & Mechanisms*.

Laufer, BI., and Singh, SM. (2012). A Macro Role for Imprinted Clusters of MicroRNAs in the Brain. *MicroRNA*.

Chater-Diehl, EJ., **Laufer, BI.**, Castellani, CA., Alberry, BL., Singh, SM. (2016). Alteration of Gene Expression, DNA Methylation, and Histone Methylation in Free Radical Scavenging Networks in Adult Mouse Hippocampus following Fetal Alcohol Exposure. *PLOS ONE*.

Castellani, CA., **Laufer, BI.**, Melka, MG., Diehl, EJ., O'Reilly, R., and Singh, SM. (2015). DNA methylation differences in monozygotic twin pairs discordant for schizophrenia identifies psychosis related genes and networks. *BMC Medical Genomics*.

Kleiber, ML., **Laufer, BI.**, Stringer, R., and Singh, SM. (2014). Third Trimester-Equivalent Ethanol Exposure Is Characterized by an Acute Cellular Stress Response and an Ontogenetic Disruption of Genes Critical for Synaptic Establishment and Function in Mice. *Developmental Neuroscience*.

Singh, SM., **Laufer, BI.**, and Kapalanga, J. (2014). Fetal alcohol and the right to be born healthy.... *Frontiers in Genetics*.

Mantha, K., **Laufer, BI.**, and Singh, SM. (2014). Molecular changes during neurodevelopment following second-trimester binge ethanol exposure in a mouse model of fetal alcohol spectrum disorder: from immediate effects to long-term adaptation. *Developmental Neuroscience*.

Melka, MG., **Laufer, BI.**, Castellani, CA. Rajakumar, RN., O'Reilly, R., and Singh, SM. (2014). The effects of olanzapine on genome-wide DNA methylation in the hippocampus and cerebellum. *Clinical Epigenetics*.

Stringer, R., **Laufer, BI.**, Kleiber, M., Singh, SM. (2013). Reduced expression of brain cannabinoid receptor 1 (Cnr1) is coupled with an increased complementary micro-RNA (miR-26b) in a mouse model of fetal alcohol spectrum disorders. *Clinical Epigenetics*.

Kleiber, ML., **Laufer, BI.**, Wright, E., Diehl, EJ., and Singh, SM. (2012). Long-term alterations to the brain transcriptome in a maternal voluntary consumption model of fetal alcohol spectrum disorders. *Brain Res.*

Castellani*, CA., Melka*, MG., Diehl, EJ., **Laufer, BI.**, O'Reilly, R., and Singh, SM. (2015). DNA methylation in psychosis: insights into etiology and treatment. *Epigenomics*.

Kleiber, ML., Diehl, EJ., **Laufer, BI.**, Mantha, K., Chokroboray-Hoque, A., Alberry, B., and Singh, SM. (2014). Long-term genomic and epigenomic dysregulation as a consequence of prenatal alcohol exposure: a model for fetal alcohol spectrum disorders. *Frontiers in Genetics*.

Melka, MG., A Castellani, CA. **Laufer, BI.**, Rajakumar, RN., O'Reilly, R., and Singh, SM. (2013). Olanzapine induced DNA methylation changes support the dopamine hypothesis of psychosis. *Journal of Molecular Psychiatry*.

Anderson-Schmidt H, Beltcheva O, Brandon MD, Byrne EM, Diehl EJ, Duncan L, Gonzalez SD, Hannon E, Kantojarvi K, Karagiannidis I, Kos MZ, Kotyuk E, **Laufer BI.**, Mantha K, McGregor NW, Meier S, Nieratschker V, Spiers H, Squassina A, Thakur GA, Tiwari Y, Viswanath B, Way MJ, Wong CCP, O'Shea A, DeLisi LE. (2013). Selected Rapporteur Summaries From the XX World Congress of Psychiatric Genetics, Hamburg, Germany, October 14–18, 2012. *American Journal of Medical Genetics Part B: Neuropsychiatric Genetics*.

Conference Presentations:

Laufer, BI., Kapalanga J, Diehl, EJ., Kleiber, ML., Chokroboray-Hoque, A., Alberry BLJ., Mantha, K., and Singh, SM. A Neuroepigenomic Model of the Fetal Alcohol Exposure Spectrum. American Society of Human Genetics (ASHG). 18 October, 2014, San Diego, California, USA. *Invited Poster Presentation*.

Laufer BI, Kapalanga J, Diehl EJ, Mantha K, Kleiber ML, Chokroboray-Hoque A, Alberry BLJ, Koren G, Singh SM. Translating epigenetic alterations in a mouse model to humans. The Fetal Alcohol Canadian Expertise (FACE) Research Association. September 7, 2013, St. John's, Newfoundland and Labrador, Canada. *First Place Invited Poster Presentation (\$200 Prize)*

Laufer, BI., Mantha, K., Kleiber, ML., Diehl, EJ., Addisson, SMF., and Singh, SM Alterations in genomically imprinted miRNA and snoRNA clusters in a mouse model of

Fetal Alcohol Spectrum Disorders (FASD). American Society of Human Genetics (ASHG). 9 November, 2012, San Francisco, California, USA. *Invited Oral Presentation.*

Laufer, BI., Mantha, K., Kleiber, ML., Diehl, EJ., Addisson, SMF., and Singh, SM. Alterations in genomically imprinted miRNA and snoRNA clusters in a mouse model of Fetal Alcohol Spectrum Disorders (FASD). World Conference of Psychiatric Genetics (WCPG). 15 October, 2012, Hamburg, Germany. *Invited Poster Presentation.*

Laufer, BI., Mantha, K., Kleiber, ML., Diehl, EJ., Addisson, SMF., and Singh, SM. Alterations in genomically imprinted miRNA and snoRNA clusters in a mouse model of Fetal Alcohol Spectrum Disorders (FASD). Mouse Molecular Genetics Conference. 4 October, 2012, Pacific Grove, California, USA. *Invited Oral Presentation.*

Laufer, BI. Epigenetics: The Bridge Between Nature and Nurture. Western Research Forum. 27 March, 2012, London, Canada. *Invited Oral Presentation.*

Laufer, BI., Diehl, E., Kleiber, M., Janus, K., Wright, E., and Singh, S. Disruption of Imprinted Regions in a Mouse Model of Fetal Alcohol Spectrum Disorders (FASD). Biology Graduate Research Forum. 22 October, 2011, London, Canada. *Invited Oral Presentation.*

Laufer, BI., Diehl, E., Kleiber, M., Janus, K., Wright, E., and Singh, S. Disruption of Imprinted Regions in a Mouse Model of Fetal Alcohol Spectrum Disorders (FASD). 12th International Congress on Human Genetics and the 61st Annual Meeting of the American Society of Human Genetics. 11-15 October, 2011, Montreal, Canada. *Invited Poster Presentation.*

Scientific Communities:

- American Society of Human Genetics (ASHG)
- Genetics Society of America (GSA)
- The International Society of Psychiatric Genetics (ICPG)
- Fetal Alcohol Canadian Expertise (FACE)

Peer Review Experience:

- Translational Psychiatry (Nature Publishing Group)
- Brain, Behaviour, and Immunity (Elsevier)

Research Mentorship:

Sean Addison. September 2011 – April 2012. Undergraduate Thesis Student. Thesis entitled: *The role of microRNA in maintaining long-term neural gene dysregulation in a mouse model of fetal alcohol exposure.*

Randa Stringer. September 2012– April 2013. Undergraduate Scholar’s Elective Student. Manuscript entitled: *Reduced expression of brain cannabinoid receptor I (Cnrl) is coupled with an increased complementary micro-RNA (miR-26b) in a mouse model of fetal alcohol spectrum disorders.*